MICRORNA AND MESSENGER RNA INTERACTIONS IN OVARIAN CANCER

A Dissertation
Presented to
The Academic Faculty

by

Shubin W. Shahab

In Partial Fulfillment
of the Requirements for the Degree
Doctor of Philosophy in Biology in the
School of Biology

Georgia Institute of Technology
August, 2011

MICRORNA AND MESSENGER RNA INTERACTIONS IN OVARIAN CANCER

Approved by:

Dr. John F. McDonald, Advisor
School of Biology
Georgia Institute of Technology

Dr. Yuhong Fan
School of Biology
Georgia Institute of Technology

Dr. Alfred H. Merrill, Jr.
School of Biology
Georgia Institute of Technology

Dr. Philip J. Santangelo
Department of Biomedical Engineering
Georgia Institute of Technology

Dr. I. King Jordan
School of Biology
Georgia Institute of Technology

Date Approved: May 17, 2011

To my family…

ACKNOWLEDGEMENTS

Firstly I would like to thank my thesis advisor Dr. McDonald, who has supported and supervised my research work and guided me for the last 4 years. Without his advice and support I would not be able to accomplish my research goals. He has not only mentored my current research but also helped shape my scientific philosophy and for this I will be forever grateful. I would also like to thank my committee members Drs. Al Merrill, King Jordan, Yuhong Fan and Philip Santangelo who have taken the time out of their busy schedules to meet with me multiple times, write me exam questions, read and critique my proposal and guide me throughout this endeavor.

I am also really grateful to all members of the McDonald lab who have supported me during my time at Georgia Tech. I would specifically like to express my gratitude to Dr. DeEtte Walker for her kindness and motherly affection and help with proofreading manuscripts. Special thanks go to Dr. Erin Dickerson for her guidance, training and help with proofreading my drafts. My gratitude also goes to Drs. Nathan Bowen, Roman Mezencev, Lilya Matyunina and Lijuan Wang for their advice, suggestions, contributions to my thesis and active guidance with my projects. I would be amiss if I don't acknowledge the contributions of all my co-graduate students, especially Vinay Mittal, Chris Hill, Gaurav Arora, Andrew Huang, Neda Jabbari and Loukia Lili for their emotional support and help with my work. I would also like to acknowledge the other members of our group, as well as the undergraduate students who were not involved with my project but have helped me immensely by critiquing my presentations during our lab meetings, or through their contributions in maintaining the lab.

On a personal note, I would like to thank my family and friends. Firstly I would like to thank my amazing mother, without whose guidance, affection and countless sacrifices I would not be here. I would also like to thank my father for his advice and for always being a role model. My thanks also go to my brother and sister-in-law who have given me emotional support and inspiration when I really needed it. I thank the rest of my family members and my friends in the United States and all over the globe who have encouraged me through these years. Finally I would like to acknowledge my wonderful wife who has encouraged me to reach this goal, proof-read most of the chapters and still managed to find the time to make me dinner, manage our social and financial responsibilities and start a small business. Without her constant support, encouragement and love I would not have made it through this.

Thank you all!

TABLE OF CONTENTS

LIST OF TABLES

LIST OF FIGURES

LIST OF SYMBOLS AND ABBREVIATIONS

AGO	Argonaute
AMO	Anti-miRNA Oligonucleotides
Avg	Average
BLAST	Basic Local Alignment Search Tool
BLASTN	Nucleotide BLAST
Ca	Carcinoma
CAGR	Cancer Associated Genomic Regions
cDNA	Complementary Deoxyribonucleic Acid
CEPI	Cancer Epithelial (cells)
Cerv	Cervix
ChIP-seq	Chromatin Immunoprecipitation and Sequencing
CLIP-seq	Cross-linking Immunoprecipitation and Sequencing
cRNA	Complementary Ribonucleic Acid
DEGs	Differentially Expressed Genes
DNA	Deoxyribonucleic Acid
DSMA	Decision Site for Microarray Analysis
dsRNA	Double Stranded Ribonucleic Acid
EGFR	Epidermal Growth Factor Receptor
eIF4F	Eukaryotic Initiation Factor 4F
EMT	Epithelial-to-Mesenchymal Transition
ENCODE	Encyclopedia of Deoxyribonucleic Acid Elements
Endo	Endometrium

EOC	Epithelial Ovarian Cancer
EX	Exon
FDR	False Discovery Rate
GCOS	Gene Chip Operating System
GEO	Gene Expression Omnibus
GO	Gene Ontology
GTPase	Guanosine Triphosphatase
HEK293	Human Embryonic Kidney 293
HIOSE	Human Immortalized Ovarian Surface Epithelium
hnRNP	Heterogeneous Nuclear Ribonucleoprotein
Hx	History
IC	Inversely Correlated
ID	Identity
IN	Intron
kb	Kilobases
LCM	Laser Capture Micro-dissection
LR	Log Ratio
M	MiRanda
MIAME	Minimum Information About Microarray Experiment
miRISC	MicroRNA Induced Silencing Complex
miRNA	MicroRNA
miR-NC	Negative Control MicroRNA
mRNA	Messenger RNA

NC	No Change
NCBI	National Center for Biotechnology Information
NF-κB	Nuclear Factor Kappa-light-chain-enhancer of Activated B Cells
nt	Nucleotide
ORF	Open Reading Frame
OSE	Ovarian Surface Epithelial (cells)
Ov	Ovary
p53	Tumor Protein p53
PABP	Poly(A) Binding Protein
PBS	Phosphate Buffered Saline
PC	Positively Correlated
Pol	Polymerase
Pre-miRNA	Precursor MicroRNA
Pri-miRNA	Primary MicroRNA
PRKRA	Protein Kinase, Interferon Inducible dsRNA Activator
PT	PicTar
qPCR	Quantitative (real-time) Polymerase Chain Reaction
REST	Relative Expression Software Tool
RISC	RNA Induced Silencing Complex
RNA	Ribonucleic Acid
RNAi	Ribonucleic Acid Interference
RNAse	Ribonuclease
RNU6B	U6B Small Nucleolar Ribonucleic Acid

RPMI	Roswell Park Memorial Institute Medium
SAM	Statistical Analysis of Microarray
SFRS1/SF2/ASF	Splicing Factor, Serine/Arginine Rich 1
siNC	Negative Control Short Interfering RNA
siRNA	Short Interfering Ribonucleic Acid
snoRNA	Small Nucleolar Ribonucleic Acid
TRBP	Trans-Activation Responsive (TAR) RNA Binding Protein
tRNA	Transfer Ribonucleic Acid
TS	TargetScanS/TargetScan
UCSC	University of California at Santa Cruz
UTR	Untranslated Region

SUMMARY

MicroRNAs (miRNAs) are a recently identified class of short regulatory RNAs involved in a diverse array of cellular processes in mammals. Aberrant expression of miRNAs can lead to the development of several diseases including cancers. Mammalian miRNAs regulate the expression of target genes by binding to partially complementary sites usually located in the 3'UTR of target mRNAs (Bartel, 2009). With rare exceptions, this leads to a decrease in translation followed by destabilization and degradation of the mRNA (Fabian et al., 2010). As a result of this targeted degradation, development of miRNAs as targets for gene therapy has garnered increasing interest. Because transfection with a single miRNA can lead to global changes in gene expression (Baek et al., 2008; Lim et al., 2005; Selbach et al., 2008), identifying the mechanisms and also the broad implications of such large scale perturbations must be addressed before miRNAs can make the transition into the clinical setting.

To address these issues, we assessed miRNAs and mRNAs in epithelial ovarian cancer using high throughput microarray and computational analysis, pathway enrichment, network building, statistical analysis, and experimental evidence. The results of our study indicate that *in vitro* based models of miRNA function are inadequate to explain the effects of changes in expression of miRNAs *in vivo*. Specifically, we found that the direct regulatory action of miRNAs on target mRNAs can induce a series of indirect effects including regulation of trans-regulatory genes and other miRNAs. These indirect effects can initiate a cascade of down-stream effects resulting in feed-back loops that can mask direct effects of miRNA regulation. Interestingly, the indirect effects

appear not to be random but functionally coordinated suggesting that miRNAs may have particular value in the treatment of cancer from the systems perspective.

Research Advance 1. Using a combination of genome-wide miRNA and mRNA profiles in ovarian cancer samples collected from patients and cell lines, we studied the nature of miRNA-mRNA interactions at the molecular level. Microarray analysis demonstrated that nine miRNAs are significantly up-regulated and three miRNAs are significantly down-regulated between patients' samples from ovarian cancer epithelial cells (CEPI) and normal ovarian surface epithelial (OSE) cells. While current models of miRNA regulation suggest a pattern of inverse correlation between miRNAs and their cognate targets, our analysis of mRNA profiles from the same cancer samples showed that only ~11 % of predicted targets of each miRNA are inversely correlated. This finding was reaffirmed by using predictions from multiple computational algorithms as well as experimentally validated targets from miRNA transfection experiments. These data suggest the current model of miRNA regulation may be inadequate to address the complex nature of these interactions *in vivo*.

Research Advance 2. To begin to systemically dissect the mechanisms of genome-wide consequences of miRNA over-expression, parallel transfection experiments using different miRNAs were carried out in the ovarian cancer cell line, HEY. The off-target effects of the miRNAs were studied in a therapeutic framework by targeting the EGFR oncogene. Transfection of each miRNA affects hundreds of genes in addition to EGFR, but less than 20 % of these genes are predicted targets of the miRNAs. Network analysis of the differentially expressed genes suggests miRNAs may target hub genes that in turn modulate the expression of multiple downstream transcripts. Enrichment analysis

of target and off-target genes demonstrates significant over-representation of genes belonging to pathways specific for cancer and development, which is consistent with functional specialization of miRNAs. In addition, miRNAs were found to modulate the levels of other miRNAs suggesting a new layer of regulation for these small RNAs. Computational and experimental evidence is presented in support of mechanisms that may explain this phenomenon.

CHAPTER 1

INTRODUCTION

Background

Epithelial ovarian cancer is the leading cause of gynecologic cancer-related mortality and the 5th most deadly cancer in women in the United States (Jemal et al., 2008). Because most cases of ovarian cancer are diagnosed at an advanced stage (stage III or IV) where long-term treatment responses are low, the 5-year survival rate stands at less than 30% (www.seer.cancer.gov, SEER, 2009). Thus, understanding the biology of ovarian cancer development and progression is critical to improving the outcome of ovarian cancer patients.

MicroRNAs (miRNAs) are a class of short (~22 nucleotides) regulatory RNA molecules that modulate gene expression and translation in unicellular and multicellular organisms. In recent years miRNAs have emerged as regulators of several critical processes and are often expressed at altered levels in many cancers including ovarian cancer (Li et al., 2010; van Jaarsveld et al., 2010). While they may have initially evolved as a mechanism of cellular defense against viruses (Shabalina and Koonin, 2008), mammalian miRNAs are now known to be involved in such diverse processes as the regulation of development, differentiation, inflammation, apoptosis, and cell proliferation (Bartel, 2004; Chang and Mendell, 2007). In cancer, up-regulation or down-regulation of miRNAs has been shown to be causally linked with oncogenesis, progression, metastasis, and can be potentially used in diagnosis, prognosis and therapy (Garofalo and Croce, 2011; Lee and Dutta, 2009).

MiRNAs were identified within a few years of the discovery of RNA silencing (Napoli et al., 1990). While studying the temporal regulation of *C. elegans* development a small RNA from the locus '*lin-4*' was found to block the translation of *lin-14* mRNA in a developmentally specific pattern by binding to complementary sites on the 3' untranslated region (3' UTR) of the mRNA (Lee et al., 1993; Wightman et al., 1993). While initially thought to be limited to *C. elegans*, it was later realized that these small RNAs belong to a novel class of regulatory RNAs conserved in vertebrates, invertebrates and plants (Lagos-Quintana et al., 2001; Lau et al., 2001; Lee and Ambros, 2001; Pasquinelli et al., 2000; Reinhart et al., 2002). Aberrant miRNA expression was first linked to human disease when researchers demonstrated that a frequently deleted chromosomal locus in patients with a type of B-cell leukemia harbors genes encoding the miRNAs miR-15 and miR-16 (Calin et al., 2002). These small RNAs have since been implicated in the development of many other types of cancers (Lee and Dutta, 2009) as well as different types of neurological and cardiovascular diseases (Bushati and Cohen, 2007; Chang and Mendell, 2007; Couzin, 2008). Recent studies also suggest that miRNAs are critically intertwined with ovarian tumorigenesis, progression and therapy resistance (Li et al., 2010; van Jaarsveld et al., 2010). This chapter gives a brief introduction to miRNAs by describing what is known about their synthesis and maturation, their mechanism of target recognition and regulation, their involvement with ovarian cancer, and finally the potential for their clinical applications.

Biogenesis of miRNAs

The synthesis of miRNA is a multistep process that begins inside the nucleus. It is estimated that about 50 % of miRNAs are located within introns and occasionally exons of coding or non-coding genes, while the rest are located in intergenic regions (Rearick et al., 2010). Synthesis is usually carried out by RNA Pol II (Lee et al., 2004) and occasionally Pol III (Borchert et al., 2006) from both autonomous promoters and promoters of other genes (Fujita and Iba, 2008; Ozsolak et al., 2008; Zhou et al., 2007). The transcript synthesized at the first step can be anywhere from hundreds of bases to many kilobases (kb) in length (Saini et al., 2007). This primary miRNA (pri-miRNA) transcript is usually polyadenylated, 5' capped, and can undergo splicing like messenger RNA (Bracht et al., 2004; Cai et al., 2004; Cullen, 2004). The pri-miRNA is subsequently cleaved into a shorter stem loop structure called the pre-miRNA by the RNAse III enzyme Drosha (RNASEN) with the help of its dsRNA binding partner called DGCR8 in humans or Pasha in Drosophila (Denli et al., 2004; Gregory et al., 2004). While additional cofactors may be involved, DGCR8/Pasha is a minimal requirement for Drosha activity. One exceptional group of miRNAs encoded from introns of genes, called "mirtrons," can be processed by the splicing machinery directly into pre-miRNA independently of Drosha (Berezikov et al., 2007). The pre-miRNA is typically 70-90 nucleotides (nts) in length and forms a hairpin like loop, which is then exported out of the nucleus by the nuclear export protein Exportin-5 and its cofactor Ran GTPase (Yi et al., 2003). Once in the cytoplasm, the pre-miRNA is subject to further processing where the loop region is cleaved off by another RNAse III enzyme Dicer (Bernstein et al., 2001), and its RNA binding partner TAR RNA binding protein (TRBP) and/or PRKRA (Haase et al., 2005). At the end of this step, a ~22 base pair duplex is formed containing the

mature miRNA and its partner strand designated miRNA*, which exists at lower steady state levels. More often the more stable miRNA strand is incorporated into the miRNA induced silencing complex (RISC/miRISC), which also includes other proteins essential for complex formation (e.g., TRBP). This incorporated strand is believed to be thermodynamically favored due to less hydrogen bonding at the 5'end and/or other sequence features (Hu et al., 2009). However, in some cases both strands can participate in the process of regulation (Yang et al., 2011).

Regulation of miRNA levels

Transcriptional regulation of miRNA synthesis shares common themes with mRNA transcriptional regulation. Like oncogenes and tumor suppressor genes, miRNA expression in cancer can often be deregulated by translocation as miRNA genes are frequently located in cancer associated genomic regions (CAGR; Calin and Croce, 2006b). MiRNA promoters can also be under the regulation of transcription factors like p53 (Feng et al., 2011), NF-κB (Mott et al., 2010; Pacifico et al., 2010; Wang et al., 2010; Zhou et al., 2009), as well as cell type specific factors like PU.1, REST or MEF2 (Davis-Dusenbery and Hata, 2010). These transcription factors have all been implicated in cancer development and progression (Goh et al., 2011; He and Karin, 2011; Majumder, 2006; Marks et al., 2001; Somervaille and Cleary, 2006) and are often aberrantly expressed in cancers. Epigenetic mechanisms including DNA methylation and histone modifications also reconfigure miRNA promoter regions and can lead to altered miRNA profiles in cancer. Zhang et al. (2008) reported that up to ~36 % of miRNAs down-regulated in late-stage epithelial ovarian cancer were under epigenetic regulation.

Another mechanism of regulation of miRNA transcription involves feedback loops. MiRNAs can regulate their own transcription through single negative or double negative feedback loops with transcription factors (Krol et al., 2010).

As miRNA synthesis is a multistep complex process, regulation can occur at every step of biogenesis (Pawlicki and Steitz, 2010). In addition to the battery of proteins that are required for miRNA maturation, recent work has shown that a multitude of accessory proteins also facilitate the process. This is exemplified by the involvement of the LIN-28 protein in the maturation of let-7 family miRNAs. LIN-28 can bind to the terminal loop of pri-let-7 molecules and block Drosha activity (Newman et al., 2008) or to pre-let-7 and block its maturation by interfering with Dicer (Lehrbach et al., 2009). This regulatory system is highly conserved across evolution and may play an essential role in let-7 mediated self-renewal of stem cells, development, and cancer (Viswanathan et al., 2008). Other examples of auxiliary factors include DEAD-box RNA helicase interacting proteins, hnRNPs, splicing regulators SF2/ASF, KSRP, etc. that can also modulate miRNA processing by interacting with Dicer and Drosha (Table 1.1; Davis-Dusenbery and Hata, 2010; Krol et al., 2010).

Recent studies (Bail et al., 2010; Katoh et al., 2009) have shown that the stability of miRNAs can be differentially regulated. Bail and colleagues showed that some miRNAs decay faster than others in HEK293 cells when transcription is blocked. They further demonstrated that the stability of one of these miRNAs, miR-382, was dependent on seven nucleotides at its 3' terminal end. Therefore, in addition to the transcriptional regulation of miRNA synthesis and post-transcriptional regulation of miRNA processing, there is also differential regulation of mature miRNA stability.

Table 1.1. Proteins that affect miRNA processing/transcription. A partial list of proteins that act as co-factors or transcription factors and take part in miRNA synthesis or maturation.

Protein ID	Regulatory step	Regulatory role	Reference
ARS2	Primary Transcript synthesis	Stabilizes and helps delivery of capped pri-miR-21, pri-miR-155, pri-let-7 to the miRNA processing complex (Drosha)	(Gruber et al., 2009; Sabin et al., 2009)
p68/p72 helicases	Drosha processing	Components of microprocessor that act to stimulate pri-miRNA processing	(Fukuda et al., 2007)
Smad-p68 complex	Drosha processing	Induces pre-miR-21, enhances Drosha processing	(Davis et al., 2008)
SNIP1	Drosha processing	Increases association of Drosha with pri-miRNAs	(Yu et al., 2008)
SF2/ASF	Drosha processing	Promotes pri-miR-7 maturation by facilitating Drosha cleavage	(Wu et al., 2010a)
hnRNPA1	Drosha processing	Facilitates Drosha processing of pri-miR-18a by interacting with its loop region	(Michlewski et al., 2008)
KSRP	Dicer and Drosha processing	Binds to primary and pre-miRNAs and optimizes positioning and/or recruitment of microRNA processing complexes	(Trabucchi et al., 2009)
ERα-p68/p72	Drosha processing	Inhibits Drosha processing of miRNAs	(Yamagata et al., 2009)
NF90-NF45	Drosha processing	Binds to stem loop of primary miRNAs and prevents DGCR8 binding	(Sakamoto et al., 2009)
Drosha	Drosha processing	Negative feedback by regulating DGCR8 levels	(Han et al., 2009)

Table 1.1 (continued)

Protein ID	Regulatory step	Regulatory role	Reference
LIN-28/LIN-28B	Drosha and Dicer processing	Binds to terminal loop of primary transcript of let-7 family miRNAs and blocks Drosha. Also inhibits Dicer processing by inducing uridylation of pre-let-7.	(Heo et al., 2008; Viswanathan et al., 2008)
ADAR1/ADAR2	Pri-miRNA or Pre-miRNA	Adenosine deaminases edit pri-miRNA or pre-miRNA and affect the accumulation of mature miRNA by affecting cleavage by Dicer/Drosha, export, etc.	(Heale et al., 2009; Kawahara et al., 2008; Kawahara et al., 2007)
c-Myc	Pri-miRNA transcription	Demonstrated to induce (miR-17~92 cluster) or inhibit (let-7, miR-15-16, miR-34a etc.) miRNA transcription	(Chang et al., 2008; O'Donnell et al., 2005)
p53 (TP53)	Pri-miRNA transcription	Induces the transcription of miR-34a and miR-34b/c	(He et al., 2007a; Raver-Shapira et al., 2007)
DNMT1, DNMT3b	Pri-miRNA transcription	Epigenetically modify miRNA loci to modify transcription	(Han et al., 2007)
Tudor-SN	Pri-miRNA stability	Degrades edited pri-miRNAs	(Scadden, 2005)
GLD-2	miRNA stability	Adds Adenosine to 3' end of miR-122 to increase stability in liver	(Katoh et al., 2009)

Principles of target recognition by miRNAs

The principles of miRNA target recognition are complex and a matter of intense research. One early observation from experimental and computational analysis lead to the conclusion that Watson-Crick complementarity between the binding region on the mRNA (e.g., 3'UTR in mammals) and a consecutive stretch of 6-8 nucleotides, called the "seed,"

near the 5' terminal end of the miRNA, is the most important requirement (Bartel, 2009). Complementarity at the 3' end of the molecule is much less stringent, but it may contribute to the overall stability and specificity of the miRNA:mRNA interaction (Brennecke et al., 2005). The central region of the miRNA:mRNA pair usually contains a bulge, the size and location of which may contribute to the efficiency of target repression (Kiriakidou et al., 2004; Ye et al., 2008). Sequence composition flanking the seed (e.g., an A across position 1, A or C across position 9) may also influence the efficacy of the miRNA (Bartel, 2009). Additional factors such as local sequence context (e.g. presence of AU rich elements in the UTR), RNA folding and accessibility of the site may also contribute to effective repression (Bartel, 2009; Didiano and Hobert, 2008). Finally, interaction of multiple miRNAs with the same transcript, distance between binding sites and length of the 3'UTR have also been shown to be important factors for miRNA repression (Doench and Sharp, 2004; Hon and Zhang, 2007; Wu et al., 2010b).

Several target prediction programs have been developed to help identify miRNA targets based on some of the observations from experimental systems already mentioned. Different programs score their putative targets differently, and often there is little overlap between the targets predicted by the programs. Despite this inconsistency, three of the prediction programs using three different approaches (miRanda, TargetScanS and PicTar) have been shown to have the highest sensitivity of identifying experimentally validated targets (Birney et al., 2007). TargetScanS (Friedman et al., 2009; Grimson et al., 2007; Lewis et al., 2005) considers factors including seed region complementarity, local sequence context, 3' compensatory pairing, and conservation of target sites for predicting miRNA targets. PicTar (Chen and Rajewsky, 2006; Grun et al., 2005; Krek et al., 2005;

Lall et al., 2006) uses conservation, seed complementarity, folding energy, presence of multiple sites, and a hidden Markov model (HMM) likelihood score to identify miRNA targets. Predictions from PicTar and TargetScanS usually overlap better with one another than predictions from other algorithms (Rajewsky, 2006). MiRanda (Betel et al., 2010; Betel et al., 2008; Enright et al., 2003; John et al., 2004) scores target sites mainly through consideration of alignment score, RNA folding energy, and sequence conservation. Recently, the predictions of miRanda were improved significantly by adding a support vector regression analysis (mirSVR) to remove false positive predictions for each miRNA-mRNA pair (Betel et al., 2010; based on the version of miRanda at the Memorial Sloan-Kettering cancer center). This change may result in better overlap between the miRanda predictions and predictions from TargetScanS and PicTar, although this is yet to be demonstrated. MiRanda-mirSVR and PicTar also take into account the possibility of multiple miRNAs interacting with the 3' UTR (Betel et al., 2010; Krek et al., 2005), which most other target prediction programs still ignore. While some recent studies suggest that animal miRNA sites may occasionally be located in the 5'UTR or even the ORF (Duursma et al., 2008; Elcheva et al., 2009; Forman et al., 2008; Henke et al., 2008; Jopling et al., 2005; Lal et al., 2008; Moretti et al., 2010; Orom et al., 2008; Tay et al., 2008; Tsai et al., 2009) the vast majority of target sites are typically located in the 3'UTR, most likely due to steric hindrance from the translational machinery (Gu et al., 2009). Because of this, most prediction algorithms do not include the 5' UTR and ORF regions in their analysis, although a few *in silico* approaches have considered these non-canonical sites (e.g., Stark et al., 2007). Because the early versions of miRanda, TargetScanS and PicTar prediction programs suffered from high false

positive prediction rates (Table 1.2; Min and Yoon, 2010) a combination of two or more prediction programs was recommended for predictions (Sethupathy et al., 2006). However, with the expanding knowledge of miRNA biology, the latest versions of these prediction programs have incorporated new features, which have significantly improved their predictive power. The new generation target prediction methods using support vector machines (SVM; e.g., mirSVR for miRanda) or similar machine learning approaches may be better able to take into account the multitude of factors contributing to targeting efficacy and produce better target predictions as we learn more about the complex nature of miRNA-target interactions.

Table 1.2. False positive rates of first generation target prediction methods. Estimated false positive rates of early versions of the three major miRNA target prediction algorithms miRanda, TargetScan and PicTar.

Target Prediction Method	Estimated False Positive Rate (%)*
miRanda	24-39
TargetScan	22-31
PicTar	~30

*Source: (Martin et al., 2007); these estimates are based on early versions of these prediction algorithms and these numbers may have changed since recent updates.

Cellular components and mechanisms of miRNA regulation

In mammals, miRNA interaction with the 3'UTR usually causes repression of translation and/or mRNA destabilization. This process is thought to be initiated when the miRNA associated RISC binds to the target mRNA and subsequently leads to translational inhibition and shuttling of the target to cytoplasmic foci called 'P-bodies' or processing bodies (also called GW bodies; Fabian et al., 2010). P-bodies contain proteins

like GW182, CCR4-NOT1 deadenylase complex, decapping enzyme complex DCP1-DCP2, and 5'-3' exonuclease XRN1, that help in degrading the mRNA and further inhibit translation (Parker and Sheth, 2007).While there are examples of translational inhibition without detectable changes in mRNA levels (Olsen and Ambros, 1999; Wightman et al., 1993), recent studies indicate a high correlation between changes in levels of mRNA and protein from miRNA repression (Baek et al., 2008). MiRNA mediated mRNA destabilization may even be the predominant mechanism in mammals (Guo et al., 2010). As a result, these recent results suggest that measuring global mRNA changes is useful and informative for studying miRNA effects.

MiRNA mediated translational inhibition can occur pre- or post-initiation. In one model of pre-initiation translational repression, the miRNA-RISC complex interferes with the eIF4F-5'cap recognition and recruitment of the 40S ribosomal subunit (Fabian et al., 2010) which are both required steps for translation initiation. Alternatively, miRNAs may prevent recruitment of the 60S subunit (Chendrimada et al., 2007; Wang et al., 2008). Recognition of the 5'cap might involve the Argonaute (AGO) proteins (Kiriakidou et al., 2007), which are essential components of the RISC. Some reports suggest translational inhibition may also depend on the poly(A) tail (Wakiyama et al., 2007), possibly because the poly(A) binding protein (PABP) helps in translation initiation by interacting with components of the eIF4F complex. This may also explain why translational inhibition is thought to occur coupled with mRNA deadenylation. The post-initiation model of translational inhibition proposes regulation occurs by ribosome drop-off at the elongation step of translation (Maroney et al., 2006; Nottrott et al., 2006; Petersen et al., 2006). However there is still no consistent model of how this might take

place (Fabian et al., 2010). Most existing evidence supports the model of translational inhibition at the pre-initiation step.

MRNA destabilization by miRNA usually begins by removal of the poly(A) tail. This is followed by either degradation from the 3' end by a 3'-5' exonuclease or by removal of the 5' cap and degradation by a 5'-3' exonuclease (Xrn1; Eulalio et al., 2008; Fabian et al., 2009; Fabian et al., 2010). Repression by transcript destabilization requires recruitment of the GW182, PABP and the Argonaute (AGO) proteins (Tritschler et al., 2010). Deadenylation is initiated when GW182 recruits the CCR4-NOT1 deadenylase complex (Behm-Ansmant et al., 2006). This may involve GW182 C-terminus interacting with PABP. Deadenylation of the mRNA may occur independently of translational repression (Fabian et al., 2009; Wakiyama et al., 2007). Decapping at the 5' end involves the decapping complex DCP1-DCP2 and other proteins that act as decapping enhancers. Many of these proteins are enriched in P-bodies suggesting the involvement of these cytoplasmic bodies in repression (Fillman and Lykke-Andersen, 2005). However, whether P-bodies are causes or consequences of miRNA repression is still unresolved.

Whether mRNA destabilization or translational repression occurs first is currently debated. Recently Djuranovic et al. (2011) argued that translation inhibition coupled with deadenylation precedes mRNA decay. Degradation of the transcript leads to a consolidation of the initial transient repression of translation. However, the authors acknowledge that without more experimental and kinetic studies it is impossible to know with conviction which is the triggering event in miRNA mediated repression.

In rare instances, miRNAs can also induce translation and even transcription. Translational activation was demonstrated in quiescent cells under serum starvation

conditions (Vasudevan et al., 2007). In one case, translation was activated from a previously repressed mRNA by releasing it from P-body and recruitment of ribosome (Bhattacharyya et al., 2006). In another case, translation was activated when the miRNA targeted the 5'UTR region of ribosomal protein encoding mRNAs (Orom et al., 2008). Another miRNA, miR-373, was shown to bind to promoter regions of cold-shock domain-containing protein 2 (CSDC2) and E-cadherin to induce transcription of mRNA for these genes (Place et al., 2008). These studies suggest regulation by miRNAs is complex and may depend on the cellular state, location of target sites on the specific gene, the specific miRNA, or other unknown factors.

MiRNAs in ovarian cancer

As miRNAs can regulate the expression of oncogenes and tumor suppressor genes, disruption of miRNA expression can potentially lead to cancers. MiRNA genes have also been mapped to chromosomal regions frequently amplified, deleted or translocated in tumors (Calin et al., 2004). Many miRNA promoters have been postulated to be under transcriptional regulation through genetic or epigenetic mechanisms, which often go awry in cancer. Consequently, aberrant miRNA expression has been associated with various types of cancers (Calin and Croce, 2006b; Farazi et al., 2011; Garofalo and Croce, 2011).

In ovarian cancer, multiple studies have reported that miRNAs show altered expression patterns in cancer cells compared to normal cells of the ovary (Table 1.3; Dahiya et al., 2008; Iorio et al., 2007; Nam et al., 2008; Wyman et al., 2009; Yang et al., 2008; Zhang et al., 2008) [for a recent list of miRNAs associated with ovarian cancer see

(van Jaarsveld et al., 2010)]. However, there is little overlap between the results of these studies, which may be partly explained by the source of the samples used (Li et al., 2010; Zorn et al., 2003). In some cases, human immortalized ovarian surface epithelial (HIOSE) cells were used as controls while in others, cultured cancer cell lines or whole ovaries were used for sampling. Despite these discrepancies, aberrant expressions of some miRNAs have been found repeatedly across multiple studies. These included down-regulation of members of the let-7 family (let-7a-g/i, miR-98 and miR-202) and up-regulation of members of the miR-200 family (miR-141, miR-200a/b/c and miR-429; Li et al., 2010; van Jaarsveld et al., 2010). The let-7 family of miRNAs has been implicated in regulating development, self-renewal, and cancer (Peter, 2009) and the miR-200 family has been shown to be involved in regulating epithelial-to-mesenchymal transition (EMT), a process central to metastasis of cancer cells. The involvement of these two miRNA families in ovarian cancer may suggest that these miRNAs are regulating key processes that are important in ovarian cancer development and progression. Unlike other cancers, epithelial ovarian cancer (EOC) is believed to progress from a less differentiated state to a well-differentiated state in that EOC cells resemble committed epithelial cells more than uncommitted surface epithelial (OSE) cells (Auersperg et al., 2001; Naora, 2007). This is consistent with the finding that miR-200 family members are often up-regulated in EOC cells and expressed in low levels in the OSE cells. It is possible that crosstalk exists between the miR-200 and let-7 families (Peter, 2009) and this interplay may regulate the progression of EOC from the normal to malignant and from the malignant to the metastatic states. Other miRNAs shown to play important roles in EOC include miR-9 and miR-199a, which participate in regulating the NF-κB pathway, miR-

214, which has been shown to regulate PTEN/PI3K pathway, the miR-34 family miRNAs regulated by p53, and the hypoxia responsive miRNA, miR-210 (Mezzanzanica et al., 2010; van Jaarsveld et al., 2010). Thus, the altered expression of these miRNAs may help push the ovarian epithelial cells into malignancy, contribute to metastatic progression, and even lead to the development of resistance to current cytotoxic therapies.

Table 1.3. Comparison of previous studies for miRNA expression profiling in ovarian cancer. Comparison of a number of previous studies for miRNA expression profiling in ovarian cancer in terms of their selection of tissue/cell samples and the profiling method used.

Reference	Control group	Sample Group	Profiling method
Dahiya et al., 2008	Surface epithelial cells (HOSE-B) immortalized with E6 and E7 papillomavirus	Ovarian cancer cell lines, fresh frozen ovarian biopsies	miRCURY LNA miRNA microarray
Eitan et al., 2009	Formalin fixed paraffin embedded (FFPE) tumor sample from patient with stage I EOC	Formalin fixed paraffin embedded (FFPE) tumor sample from patient with stage III EOC	Custom miRNA microarray
Gallagher et al., 2009	Normal whole ovary	Fresh frozen primary serous ovarian adenocarcinoma specimens	TaqMan miRNA qPCR
Iorio et al., 2007	Normal ovarian tissue specimens	Epithelial Ovarian cancer tissues and cell lines	Custom miRNA microarray
Laios et al., 2008	Primary ovarian tissue specimens	Recurrent ovarian tissue specimens	TaqMan miRNA assay (qPCR)
Lee et al., 2009	Normal fallopian tube samples	Fresh frozen serous ovarian tumor samples	Ambion miRNA microarray

Table 1.3 (continued)

Reference	Control group	Sample Group	Profiling method
Nam et al., 2008	Normal ovarian tissue specimens (pooled RNA from 8 samples)	Primary ovarian tumor specimens	mirVana miRNA microarray
Wyman et al., 2009	Cultured ovarian surface epithelial cells	Fresh frozen epithelial ovarian tumor specimens	Transcriptome (454) sequencing
Yang et al., 2008	HIOSE cell lines	Primary serous ovarian carcinoma specimens	Custom miRNA microarray
Zhang et al., 2008	Immortalized ovarian surface epithelia (IOSE); also low-grade tumor biopsies	Epithelial ovarian cancer cell lines; also high-grade tumor biopsies	Custom miRNA microarray

Clinical uses of miRNAs

MiRNAs are capable of interacting with multiple target genes (Borgdorff et al., 2010). In cancer and other diseases, miRNA levels are often altered and many have been implicated in the regulation of critical pathways involved in cell cycle, EMT, and self renewal. Inhibiting or over-expressing miRNAs (Garofalo and Croce, 2011) can therefore potentially serve to restore the pre-disease states. This has prompted intense research in academia and industry to explore avenues of developing miRNA-based treatments. Several clinical trials are currently underway to investigate this potential (Wahid et al., 2010). While delivery is still the biggest challenge of RNA based therapeutics, additional challenges of miRNA therapy include identifying all the targets of a miRNA while avoiding false positives and understanding/predicting the unintended phenotypic consequences of affecting off-target genes.

Despite these challenges, some recent studies have achieved exciting results that demonstrate the potential for therapeutic use of miRNAs in cancers (Furuta et al., 2010; Kota et al., 2009; Trang et al., 2011; Tsuda et al., 2006). In these studies, miRNA mimics or miRNA expression vectors were used to reduce cancer cell growth *ex vivo* and in some cases *in vivo* (Kota et al., 2009; Trang et al., 2011). Several strategies have been devised to decrease the amounts of oncogenic miRNAs. These include using antisense oligonucleotides called "anti-miRNA oligonucleotides (AMOs)" or "Antagomirs" that bind to the miRNA and prevent it from interacting with target mRNA (Krutzfeldt et al., 2005). A similar oligonucleotide based approach called "miR-mask" or "target protector" interferes with the miRNA by pairing with the target site, thus making the site inaccessible to the miRNA (Choi et al., 2007; Xiao et al., 2007). Another strategy employs aptly named "miRNA sponges," synthetic mRNA constructs with multiple miRNA binding sites that isolate miRNAs from their endogenous binding sites (Ebert et al., 2007). Small molecule inhibitors that decrease the biogenesis of miRNAs are also being developed (Gumireddy et al., 2008). These and other similar approaches may bring the promise of miRNA therapy to the clinic in the near future.

MiRNAs can also serve as diagnostic and prognostic markers in several cancers. Since miRNAs are differentially expressed in many cancers, it is possible to use miRNA expression signatures for diagnostic purposes (Lu et al., 2005). In particular, miRNAs can be reliably detected in serum even in some early stage cancers (Hausler et al., 2010; Zhang et al., 2010; Zhao et al., 2010). Recent studies have also demonstrated that miRNA profiles have the ability to help discern prognostic indicators such as higher grade versus lower grade tumor subtypes (Brase et al., 2011; Catto et al., 2009) and also distinguish

between tumor stages (Eitan et al., 2009). As miRNAs are shorter than typical mRNAs, they are significantly more stable to RNA degrading insults (Jung et al., 2010) and consequently provide more reliable and consistent signature profiles than mRNA. There are also reports suggesting high miRNA stability in plasma samples (Mitchell et al., 2008). Thus, in addition to being a promising mode of therapeutic intervention, there is significant potential for miRNA based signatures for disease diagnosis and prognosis.

Mechanisms of miRNA-mRNA interactions in ovarian tumors

As discussed above, previous studies have established that miRNA levels often correlate with ovarian cancer development and progression (Dahiya et al., 2008; Eitan et al., 2009; Iorio et al., 2007; Laios et al., 2008; Nam et al., 2008; Yang et al., 2008; Zhang et al., 2008). However, the effects of miRNA expression profile changes on global mRNA expression have not been studied in detail in ovarian cells. We will address some of the limitations of the current model of miRNA-target interactions *in vivo* and discuss the different mechanisms used by miRNAs to regulate mRNA levels in ovarian cancer cells. Both ovarian tumor patient samples and established cell culture models were used to investigate the complex nature of these interactions. The direct and indirect effects of miRNAs on mRNA expression were investigated using a combination of target prediction algorithms, pathway and network analysis. In addition we describe a novel regulatory mechanism used by miRNAs that may help explain the downstream effects of miRNA over-expression.

In CHAPTER 2 we discuss the relationship between changes in global miRNA and mRNA levels in ovarian tumor cells compared to normal surface epithelial cells. As

there is little overlap between the miRNA profiles in ovarian cancer identified in previous analyses (see "MiRNAs in ovarian cancer"), in this study we used epithelial cells collected by brushing the surface of the ovary as controls and cancer cells isolated using laser capture micro-dissection on tumor specimens to obtain the most appropriate control and sample population of cells. The miRNA and mRNA expression profiles from these samples were then used to test the expected model of inverse correlation between miRNAs and target mRNAs predicted using three different currently available *in silico* target prediction tools. This analysis revealed that only ~11 % of predicted targets were inversely correlated with their regulating miRNAs as expected, while the majority of targets demonstrated non-significant changes in expression. To ensure that the conclusions drawn from predictions made *in silico* were consistent with data from experimental observations, miRNA transfection experiments were carried out in ovarian tumor cell lines and a set of experimentally verified targets of these transfected miRNAs were identified. Using these verified targets, the analysis was repeated and again a low fraction of these targets were inversely correlated *in vivo*. Together these results suggest that current models of miRNA regulation are inadequate to explain the nature of miRNA-mRNA interactions *in vivo*.

In CHAPTER 3 we investigated the nature of miRNA-mRNA interactions further in a transfection model using an established ovarian cancer cell line. We studied the effect of miRNAs on genome-wide mRNA expression in detail by analyzing the global mRNA expression profile following the transfection of miRNAs. To study these genome-wide effects in a therapeutic context, we considered the off-target effects after miRNA targeted knock-down of an ovarian cancer oncogene, EGFR. The analysis demonstrated

that the miRNAs altered the expression of hundreds of genes in addition to down-regulating EGFR. Less than 20 % of these off-target genes could be attributed to predicted direct miRNA targets, while the rest were indirect downstream effects. Network analysis demonstrated that many of these downstream genes may be regulated by 'hub genes' which were directly or indirectly regulated by the miRNAs. Pathway enrichment analysis of differentially expressed genes suggested a pattern of functional specialization for each miRNA which supports the hypothesis that the downstream off-target effects were not random. These results suggest that while direct targets and indirect downstream effects result in hundreds of altered genes following miRNA transfection, these may ultimately alter signature pathways associated with each miRNA.

In the fourth chapter we discuss a hitherto overlooked effect of miRNA over-expression which ultimately leads to the global disruption of hundreds of transcripts. Using microarray analysis of miRNAs, we demonstrated that a miRNA may regulate the expression of other miRNAs. We present evidence in support of putative mechanisms for this regulation, which may occur by miRNAs targeting transcripts that harbor other miRNAs, or through indirectly regulating transcription factors and/or other regulatory proteins. Specifically, in this study we propose a mechanism by which miR-7 regulates miRNAs through the NF-κB transcription factor. We computationally identified significant number of the differentially expressed miRNAs with proximity to NF-κB binding sites (Birney et al., 2007) and demonstrated that experimental siRNA knock-down of the RELA component of NF-κB resulted in altered miRNA expression. We identified a second mechanism which could lead to miR-7 affecting miRNA levels by regulating the levels of the splicing factor SF2, which, in turn, may regulate miRNAs

(Wu et al., 2010a). We also found additional evidence supporting this hypothesis by mapping binding sites for SF2 (Sanford et al., 2009) on the primary transcripts of several of the differentially expressed miRNAs. These data are consistent with miRNAs regulating the levels of other miRNAs by a multitude of mechanisms which may ultimately serve as an additional trigger for their genome-wide off-target effects.

CHAPTER 2

EVIDENCE FOR THE COMPLEXITY OF MICRORNA-MEDIATED REGULATION IN OVARIAN CANCER: A SYSTEMS APPROACH

Abstract

MicroRNAs (miRNAs) are short (~22 nucleotides) regulatory RNAs that can modulate gene expression and are aberrantly expressed in many diseases including cancer. Previous studies have shown that miRNAs inhibit the translation and facilitate the degradation of their targeted messenger RNAs (mRNAs) making them attractive candidates for use in cancer therapy. However, the potential clinical utility of miRNAs in cancer therapy rests heavily upon our ability to understand and accurately predict the consequences of fluctuations in levels of miRNAs within the context of complex tumor cells. To evaluate the predictive power of current models, levels of miRNAs and their targeted mRNAs were measured in laser captured micro-dissected (LCM) ovarian cancer epithelial cells (CEPI) and compared with levels present in ovarian surface epithelial cells (OSE). We found that the predicted inverse correlation between changes in levels of miRNAs and levels of their mRNA targets held for only ~11 % of predicted target mRNAs. We demonstrate that this low inverse correlation between changes in levels of miRNAs and their target mRNAs *in vivo* is not merely an artifact of inaccurate miRNA target predictions. Our findings underscore the complexities of miRNA-mediated regulation *in vivo* and the inadequacy of current models to accurately predict the molecular consequences of fluctuations in levels of miRNAs within the complex context of tumor cells.

Introduction

MicroRNAs (miRNAs) are members of an abundant class of small (~22 nts) regulatory RNAs believed to play significant roles in a variety of biological processes and diseases in both plants and animals (Bartel, 2004). Of recent interest, is the possible contribution of aberrantly expressed miRNAs to cancer initiation and development (Calin and Croce, 2006a; Esquela-Kerscher and Slack, 2006). Numerous *in vitro* studies have demonstrated that miRNAs are capable of inhibiting the translation and/or facilitating the degradation (Bartel, 2009; Pillai et al., 2007; Tang et al., 2008b; Valencia-Sanchez et al., 2006) of their targeted mRNAs making them attractive candidates for potential use in cancer therapy (Hammond, 2006; Tong and Nemunaitis, 2008). However, the potential clinical utility of miRNAs in cancer therapy rests heavily upon our ability to understand and accurately predict the consequences of fluctuations in levels of miRNAs within the context of tumor cells *in vivo*. The general expectation that changes in levels of miRNAs will be inversely correlated (IC) with changes in levels of their mRNA targets (Nam et al., 2009; Ruike et al., 2008; Sood et al., 2006; Wang and Li, 2009; Xin et al., 2009) has yet to be conclusively tested within the context of tumor cells *in vivo.* For example, previous independent estimates of relative miRNA levels in ovarian cancers vs. controls often have been inconsistent, possibly due to differences in sample type (*e.g.*, bulk tissue samples vs. micro-dissected cells, etc.), biological variability among different cancer sub-types and individual patient samples (*e.g.*, Dahiya et al., 2008; Iorio et al., 2007; Nam et al., 2008; Wyman et al., 2009; Yang et al., 2008; Zhang et al., 2006) or due to inaccuracies in the prediction of the mRNA targets (Min and Yoon, 2010; Saito and Saetrom, 2010).

In an effort to reduce variation that may obscure biologically significant trends, we have conducted microarray (Affymetrix) analyses of miRNAs and mRNAs from the same ovarian cancer epithelial (CEPI) cells isolated from patient samples by laser capture micro-dissection (LCM). We monitored differences in levels of miRNA expression between CEPI and ovarian surface epithelial (OSE) cells (collected from ovaries of normal patients) with expression levels of their putative mRNA targets as determined by various prediction algorithms and by experimental validation. While ovarian cancers may arise from either the fimbrial epithelium of the oviduct or OSE, it has recently been shown that both classes of cells are part of a transitional epithelium of common origin and thus either may serve as a precursor to CEPI (Auersperg, 2011). Since OSE can be harvested from the surface of ovaries with minimal contamination, they were selected as appropriate controls in our study.

We found that only ~11 % of mRNA targets displaying significant ($p < 0.005$) changes in levels of expression in CEPI relative to normal were IC with changes in levels of their regulating miRNAs ($p < 0.01$). The levels of the majority (~79 %) of target mRNAs were unchanged in CEPI while the rest (~10 %) of the mRNA targets displayed changes in levels positively correlated (PC) with their respective regulating miRNAs. We conclude that the low predictability of miRNA regulatory effects in CEPI isolated from patient samples is attributable to the complexity of miRNA function *in vivo*.

Results

The majority of miRNAs differentially expressed in CEPI relative to OSE are up-regulated.

Hierarchical clustering of the expression profiles of miRNAs detected on the miRChip (Asuragen Inc, Austin, TX) was performed on three CEPI and three OSE patient samples. The miRChip contains a total of 13,349 probes including 467 annotated human miRNAs (Sanger miRBase V9.2; Griffiths-Jones, 2004; Griffiths-Jones et al., 2006; Griffiths-Jones et al., 2008), 455 miRNAs annotated in various other species and 12,894 (exploratory) probes of predicted, but as yet not validated/annotated miRNAs. Using a threshold of 2-fold or greater change, 42 miRNA probes were found to be differentially expressed ($p < 0.01$) between our cancer and control samples. Of these, 33 were up-regulated and 9 down-regulated in the CEPI relative to OSE, including 12 previously annotated human miRNAs (9 up-regulated and 3 down-regulated). A heat map of the 42 differentially expressed miRNA probes is presented in Figure 2.1A (the miRNA sequences of these 42 probes, $\log_2$ difference between CEPI and OSE, and p-values from t-test are provided in Table A.1). To independently test the validity of the differential miRNA expression patterns determined by microarray, we conducted measurements of miRNA levels using quantitative real-time polymerase chain reaction (qPCR). Five (*miR-141, miR-429, miR-205, miR-383 and miR-320*) of the 12 previously annotated human miRNAs shown to be differentially expressed by microarray were selected for qPCR analysis in three cancer and three control samples. The qPCR results confirmed the differences detected in the microarray study (Figure 2.1B).

A

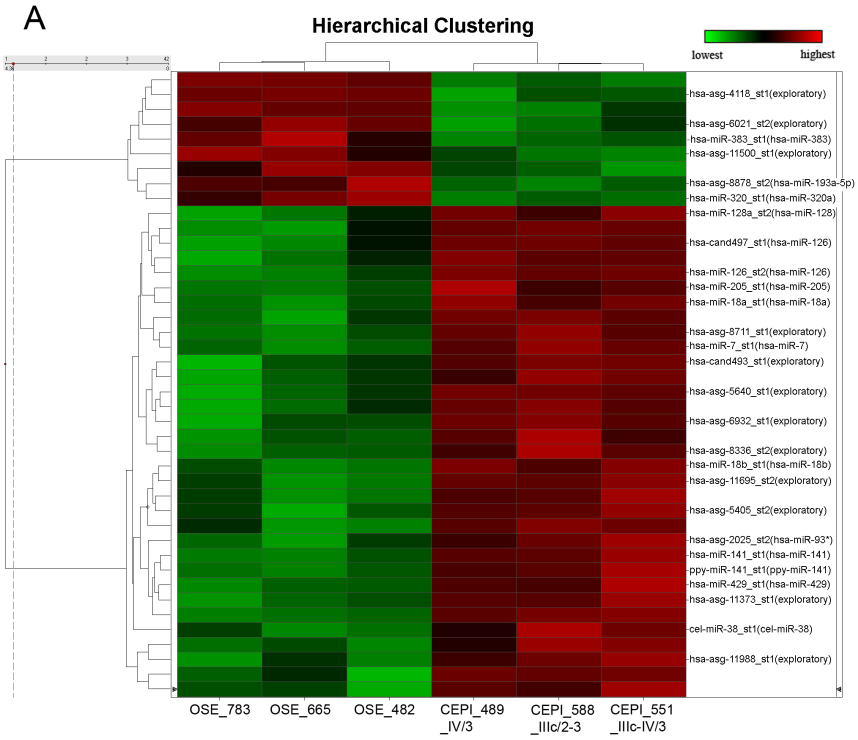

B

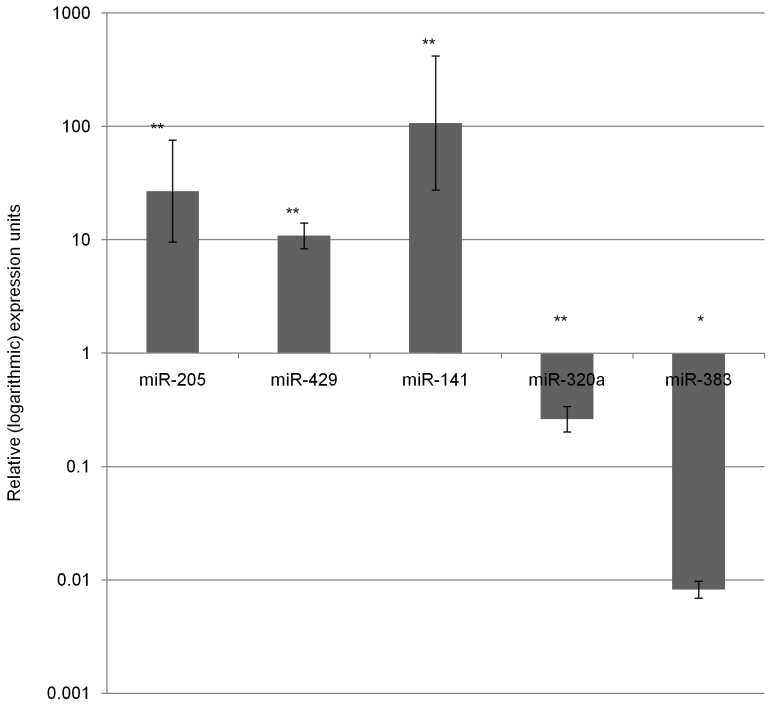

	miR-205	miR-429	miR-141	miR-320	miR-383
Relative expression	26.9479446	10.85574375	107.3344956	0.262251573	0.008215287
SEM	1.496268448	0.375527114	1.960683019	0.372356421	0.250425248

Figure 2.1. Differentially expressed miRNAs in CEPI relative to OSE. (A) Hierarchical clustering of normal and cancer patient samples ($p < 0.01$, fold change ≥ 2). The dendogram on the left shows that the probes cluster into 2 groups corresponding to the up-regulated and down-regulated miRNAs differentially expressed between normal and cancer. The cancer stage/grade of each of the CEPI samples is also provided. IDs of selected probes are given on the right (including the annotated human miRNAs, see Table A.1 for a complete list). Key: hsa-miR-x: annotated human miRNAs; hsa-asg/cand-x: predicted candidate human miRNAs; ppy-: *Pongo pygmaeus* miRNA; cel-: *C. elegans* miRNA. (B) Confirmation of expression patterns for selected miRNAs by qPCR. The relative expression of each miRNA in logarithmic units in cells from three cancer patients is shown compared to cells from three normal ovaries after normalization to RNU6B ($\Delta\Delta$Ct method). These were found to be statistically significant by Relative Expression Software Tool (REST®) by a randomization method. Randomization was performed 5000 times. Consistent with the microarray results, miR-141, miR-205 and miR-429 were confirmed to be significantly up-regulated in cancer, while miR-320 and miR-383 were found to be significantly down-regulated. Error bars represent standard error of the mean. ** $p < 0.01$; * $p < 0.05$

In contrast to some earlier studies (Dahiya et al., 2008; Iorio et al., 2007; Nam et al., 2008; Yang et al., 2008; Zhang et al., 2006), our results indicate that the majority of miRNAs displaying significant differences in levels of expression between CEPI and OSE are up-regulated in ovarian cancer. The basis of this discrepancy is unknown but may be due to differences in sample type (e.g., bulk tissue samples vs. micro-dissected cells, etc.) and/or biological variability among individual patient samples. Our finding that the majority of miRNAs are up-regulated in ovarian cancer is consistent with the fact that miRNA targets are significantly enriched (hypergeometric distribution, $p < 0.05$) among mRNAs down-regulated in our cancer samples, while up-regulated genes have relatively few miRNA targets (Figures 2.2 and 2.3; see also Table A.2). A possible biological explanation of why miRNAs are up-regulated in EOC may lie in the fact that in contrast to other cancers (da Costa, 2001; Diaz-Cano, 2008), the transition from OSE

to CEPI is postulated to involve changes from a less differentiated to a more differentiated state (Auersperg et al., 2001; Naora, 2007; Scully et al., 2004).

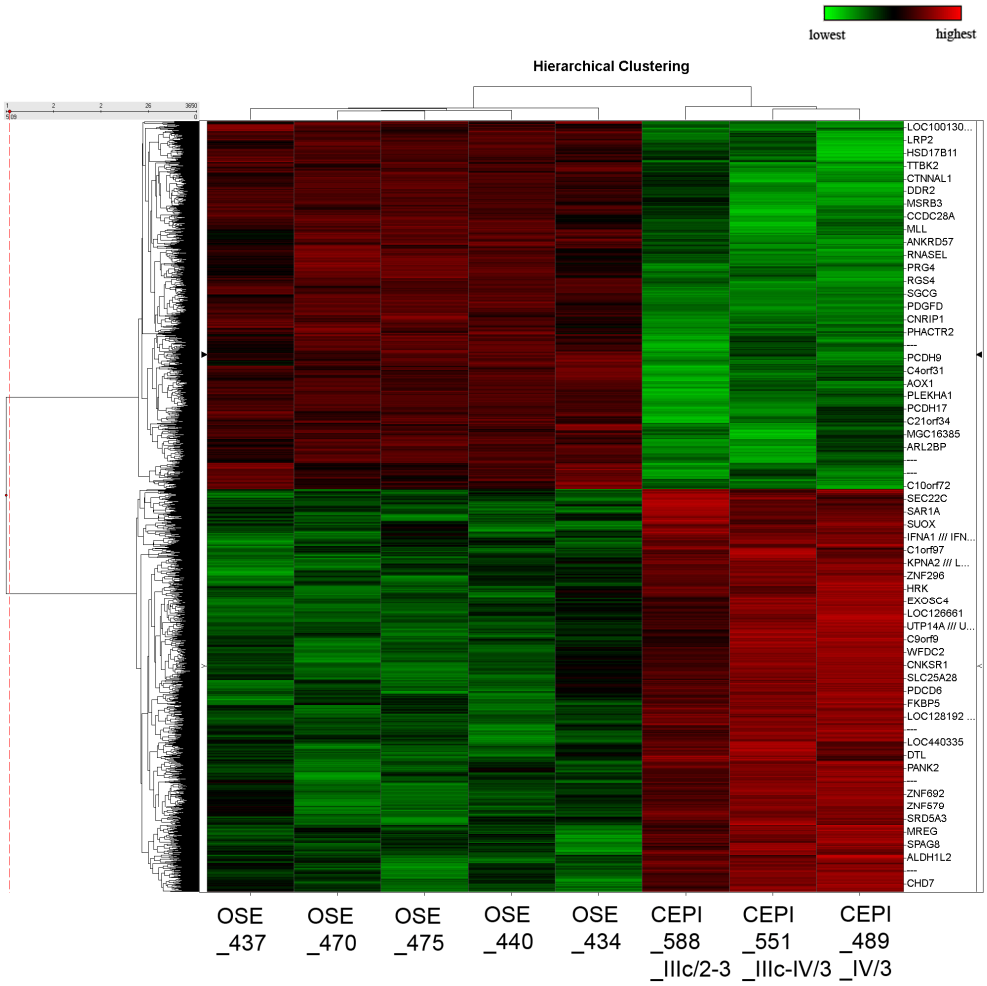

Figure 2.2: Differentially expressed mRNAs between CEPI and OSE. Hierarchical clustering of CEPI samples and OSE samples based on the differentially expressed genes. The ~3650 probesets correspond to ~2700 unique gene symbols and were selected based on p-value <0.005, fold change ≥2, and Affymetrix "Present" call in at least 1 sample. The dendogram on the left clusters the up-regulated genes and down-regulated genes into 2 groups and the number of genes in each of these classes are approximately equal. Gene symbols corresponding to representative differentially expressed probesets are shown on the right (See Table A.2 for listing of all differentially expressed probesets).

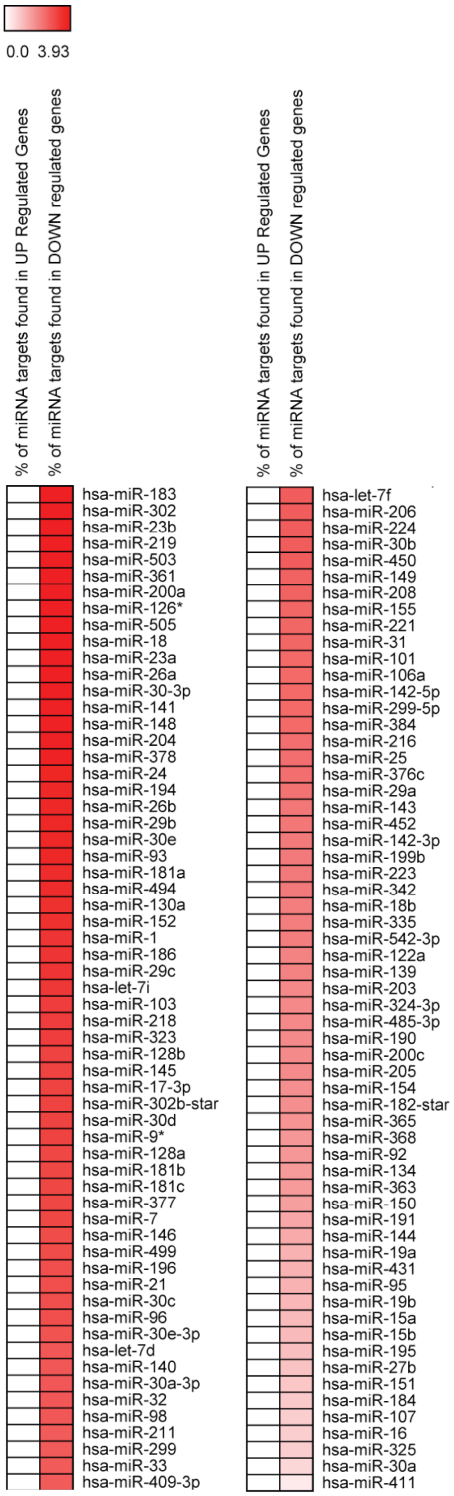

Figure 2.3: Overlap between differentially expressed genes in ovarian cancer and miRNA target genes. Genomica was used to calculate significant (false discovery rate corrected $p < 0.05$) gene set overlaps between genes differentially expressed in the

ovarian cancer data set and gene sets containing targets of individual miRNAs. This is analogous to a "GO" (gene ontology) enrichment analysis (the miRNA identities are the "ontologies" in this case). The coloring represents the percentage (%) of genes within the cancer data set that overlap with the individual miRNA target gene set listed on the right. The miRNAs listed here include differentially expressed miRNAs found in our microarray experiment as well as additional miRNAs predicted using Genomica.

Among the 12 previously annotated miRNAs displaying a significant change in levels in the CEPI samples, miR-205, miR-141, and miR-429 are all significantly up-regulated consistent with previous studies linking these miRNAs with the maintenance of cells in the differentiated epithelial state (Gregory et al., 2008). Of the miRNAs that are down-regulated in CEPI relative to OSE, miR-320 and miR-383 are located in regions associated with frequent DNA copy number losses in ovarian cancer (Zhang et al., 2006). miR-320 previously has been identified as an inhibitor of lung carcinoma proliferation (Schaar et al., 2009). Its down-regulation in CEPI suggests that it may act as a tumor suppressor in ovarian cancers as well.

Only ~11 % of the predicted mRNA targets of miRNAs differentially expressed between the CEPI and OSE display the expected inverse pattern of change in gene expression.

Previous studies have established that human miRNAs repress gene expression by pairing with complementary sequences located within the 3' untranslated regions (3' UTR) of targeted mRNAs resulting in translational repression and mRNA degradation (Tang et al., 2008b; Valencia-Sanchez et al., 2006). Based on these findings, changes in the expression levels of miRNAs are generally predicted to be inversely correlated with

changes in the expression levels of their targeted mRNAs (Nam et al., 2009; Ruike et al., 2008; Sood et al., 2006; Wang and Li, 2009; Xin et al., 2009). To test this hypothesis in the context of cells isolated from patient samples, we compared changes in the levels of the previously annotated human miRNAs with levels of their predicted target mRNAs in our CEPI samples relative to the OSE controls. The putative mRNA targets of these previously annotated human miRNAs were initially identified using the miRanda algorithm (Betel et al., 2008; Enright et al., 2003; John et al., 2004). The results indicate that only ~11 % of the changes in mRNA expression between CEPI and OSE were inversely correlated (IC) with the observed changes in miRNA levels (Tables 2.1 and A.3). Earlier studies of levels of miRNAs and their targeted mRNAs in a series of cell lines reported similar findings (Blower et al., 2007; Guimbellot et al., 2009; Wang and Li, 2009). The expression of the majority (No Change, NC: ~79 %) of the predicted mRNA targets was not significantly different ($p > 0.005$ and/or fold change < 2) between the CEPI and OSE samples, while ~10 % of the targeted mRNAs displayed changes positively correlated (PC) with their putatively regulating miRNAs.

Table 2.1. Summary values of IC, PC and NC targets in CEPI vs. OSE using miRanda. MiRNA targets that were differentially expressed between CEPI and OSE based on t-test $p < 0.005$ and fold change of at least 2 were classified as being IC or PC with their regulating miRNAs (while target genes that do not meet the above criteria are classified as NC). Total number of targets from miRanda algorithm present after removing probesets with "Absent" calls in all samples is shown along with fraction of IC, PC and NC targets for each miRNA. On average, 78.6 % of the target mRNAs are "No Change", or do not change significantly with miRNAs, 11.2 % are "inversely correlated" and 10.3 % are "positively correlated" with miRNAs.

miRNA	Total Targets (miRanda)	Inversely Correlated Targets (%)	No Change (%)	Positively Correlated Targets (%)
miR-7	2363	10.62	79.94	9.44
miR-18a	1738	11.10	79.86	9.03
miR-18b	1710	11.40	79.24	9.36
miR-126	84	14.29	75.00	10.71
miR-128	2691	11.82	79.23	8.96
miR-141	3074	13.53	77.91	8.56
miR-205	2268	13.49	78.31	8.20
miR-429	3316	13.48	78.62	7.90
miR-93*	2252.00	13.14	77.00	9.86
Average (for up-regulated miRNAs)	2166.22	12.54	78.34	9.11
miR-383	2118	9.02	78.80	12.18
miR-320a	3073	8.30	79.08	12.63
miR-193a-5p	1216	12.01	78.45	9.54
Average (for down-regulated miRNAs)	2135.67	9.77	78.78	11.45
Average (for Up and Down)	2150.94	11.16	78.56	10.28

Table 2.2. Summary values of IC, PC and NC targets using TargetScan. MiRNA targets that were differentially expressed between CEPI and OSE based on t-test $p < 0.005$ and fold change of at least 2 were classified as being IC or PC with their regulating miRNAs (while target genes that do not meet the above criteria are classified as NC). Total number of targets from TargetScan algorithm present after removing probesets with "Absent" calls in all samples is shown along with fraction of IC, PC and NC targets for each of the 12 annotated miRNAs. On average, 79.3 % of the target mRNAs are NC, 10.4 % are inversely correlated and 10.3 % are positively correlated with miRNAs.

miRNA	Total Targets (TargetScan)	Inversely Correlated Targets (%)	No Change (%)	Positively Correlated Targets (%)
miR-7	272	13.24	78.68	8.09
miR-18a	177	15.82	79.66	4.52
miR-18b	177	15.82	79.66	4.52
miR-126	15	0	80	20

Table 2.2 (continued)

miRNA	Total Targets (TargetScan)	Inversely Correlated Targets (%)	No Change (%)	Positively Correlated Targets (%)
miR-128	671	12.97	77.94	9.09
miR-141	471	14.65	76.01	9.34
miR-205	262	16.03	74.81	9.16
miR-429	736	14.13	78.4	7.47
miR-93* (Custom)	248.00	13.71	77.02	9.27
Average (for up-regulated miRNAs)	336.56	12.93	78.02	9.05
miR-383	95	3.16	84.21	12.63
miR-320a	468	7.26	79.49	13.25
miR-193a-5p	69	13.04	78.26	8.7
Average (for down-regulated miRNAs)	210.67	7.82	80.65	11.53
Average (for Up and Down)	273.61	10.37	79.34	10.29

Table 2.3. Summary values of IC, PC and NC targets using PicTar. MiRNA targets that were differentially expressed between CEPI and OSE based on t-test $p < 0.005$ and fold change of at least 2 were classified as being IC or PC with their regulating miRNAs (while target genes that do not meet the above criteria are classified as NC). Total number of targets from PicTar algorithm present after removing probesets with "Absent" calls in all samples is shown along with fraction of IC, PC and NC targets for each of the 12 annotated miRNAs. On average, 80.5 % of the target mRNAs are in the NC group, 9.4 % are in the IC group and 10.1 % are in the PC group.

miRNA	Total Targets (PicTar)	Inversely Correlated Targets (%)	No Change (%)	Positively Correlated Targets (%)
miR-7	235	9.79	79.57	10.64
miR-18a	126	15.87	75.40	8.73
miR-18b	127	17.32	74.02	8.66
miR-126	12	0.00	100.00	0.00
miR-128	485	13.20	77.53	9.28
miR-141	767	13.43	77.18	9.39
miR-205	223	12.56	77.58	9.87

Table 2.3 (continued)

miRNA	Total Targets (PicTar)	Inversely Correlated Targets (%)	No Change (%)	Positively Correlated Targets (%)
Average (for up-regulated miRNAs)	282.14	11.74	80.18	8.08
miR-383	61	1.64	78.69	19.67
miR-320a	377	6.10	81.70	12.20
miR-193a-5p	149	8.05	79.87	12.08
Average (for down-regulated miRNAs)	263	7.08	80.78	12.14
Average (for Up and Down)	272.57	9.41	80.48	10.11

To determine if the unexpectedly low percentage of IC changes may be a computational artifact of our use of the miRanda algorithm to predict targeted mRNAs, we repeated the analysis independently using the PicTar (www.pictar.org) and TargetScan (www.targetscan.org) miRNA target prediction algorithms. In both instances, the results were consistent with our original finding that only a minority of the changes in mRNA expression between CEPI and OSE are inversely correlated (IC) with the observed changes in miRNA levels (PicTar: IC 9.4 % , PC 10.1 %, NC 80.5 %; TargetScan: IC 10.4 %, PC 10.3 %, NC 79.3 %; see Tables 2.2 and 2.3). To increase the stringency of target predictions, we reanalyzed the data using only miRNA targets that were commonly predicted by all three algorithms (intersection). We found that by overlapping the three independent prediction algorithms, each miRNA had fewer predicted targets, yet using these commonly predicted targets, only ~7 % of the mRNA changes between CEPI and OSE were found to be inversely correlated (IC) with the observed changes in miRNA levels (Table 2.4). We also analyzed our data using

intersections of predictions from two algorithms at a time (miRanda+TargetScan, miRanda+PicTar, and PicTar+TargetScan), and again we found that changes in levels of only 6-9 % of the predicted mRNA targets were inversely correlated with changes in miRNA levels (Tables 2.5, 2.6 and 2.7).

Table 2.4. Summary values of IC, PC and NC targets in CEPI vs. OSE using overlap of miRanda, TargetScan and PicTar target predictions. MiRNA targets that were differentially expressed between CEPI and OSE based on t-test p <0.005 and fold change of at least 2 were classified as being IC or PC with their regulating miRNAs (while target genes that do not meet the above criteria are classified as NC). Total number of targets from the intersection (M_TS_PT) of miRanda (M), TargetScan (TS) and PicTar (PT) predictions present after removing probesets with "Absent" calls in all samples is shown along with fraction of IC, PC and NC targets for each miRNA. On average, 76.7 % of the target mRNAs are "No Change", or do not change significantly with miRNAs, 6.8 % are "inversely correlated" and 16.5 % are "positively correlated" with miRNAs.

miRNA	Total Targets (M_TS_PT)	Inversely Correlated Targets (%)	No Change (%)	Positively Correlated Targets (%)
miR-7	105	10.48	84.76	4.76
miR-18a	59	13.56	83.05	3.39
miR-18b	59	13.56	83.05	3.39
miR-126	2	0.00	100.00	0.00
miR-128	237	11.81	79.75	8.44
miR-141	177	15.82	74.58	9.60
miR-205	73	21.92	67.12	10.96
Average (for up-regulated miRNAs)	101.71	12.45	81.76	5.79
miR-383	15	0.00	80.00	20.00
miR-320a	112	3.57	84.82	11.61
miR-193a-5p	2	0.00	50.00	50.00
Average (for down-regulated miRNAs)	43.00	1.19	71.61	27.20
Average (for Up and Down)	72.36	6.82	76.68	16.50

Table 2.5. Summary values of IC, PC and NC targets using overlap of miRanda and TargetScan predictions. MiRNA targets that were differentially expressed between CEPI and OSE based on t-test p <0.005 and fold change of at least 2 were classified as being IC or PC with their regulating miRNAs (while target genes that do not meet the above criteria are classified as NC). Total number of targets from the overlap of miRanda (M) and TargetScan (TS) algorithms present after removing probesets with "Absent" calls in all samples is shown along with fraction of IC, PC and NC targets for each of the 12 annotated miRNAs. On average, 79.2 % of the target mRNAs are in the NC group, 9 % are in the IC group and 11.8 % are in the PC group.

miRNA	Total Targets (M_TS)	Inversely Correlated Targets (%)	No Change (%)	Positively Correlated Targets (%)
miR-7	212	12.26	79.72	8.02
miR-18a	136	13.97	80.88	5.15
miR-18b	135	14.07	80.74	5.19
miR-126	6	0.00	83.33	16.67
miR-128	447	13.20	78.75	8.05
miR-141	383	14.88	75.20	9.92
miR-205	199	22.11	69.35	8.54
miR-429	620	14.68	78.06	7.26
miR-93*(Custom)	163	15.34	77.30	7.36
Average (for up-regulated miRNAs)	255.67	13.39	78.15	8.46
miR-383	73	2.74	80.82	16.44
miR-320a	342	6.43	79.53	14.04
miR-193a-5p	52	15.38	73.08	11.54
Average (for down-regulated miRNAs)	155.67	4.59	80.18	15.24
Average (for Up and Down)	205.67	8.99	79.16	11.85

Table 2.6. Summary values of IC, PC and NC targets using overlap of miRanda and PicTar predictions. MiRNA targets that were differentially expressed between CEPI and OSE based on t-test p <0.005 and fold change of at least 2 were classified as being IC or PC with their regulating miRNAs (while target genes that do not meet the above criteria are classified as NC). Total number of targets from the overlap of miRanda (M) and PicTar (PT) algorithms present after removing probesets with "Absent" calls in all samples is shown along with fraction of IC, PC and NC targets for each of the 12

annotated miRNAs. On average, 78.3 % of the target mRNAs are in the NC group, 8.6 % are in the IC group and 13.1 % are in the PC group.

miRNA	Total Targets (M_PT)	Inversely Correlated Targets (%)	No Change (%)	Positively Correlated Targets (%)
miR-7	162	9.88	83.33	6.79
miR-18a	84	16.67	75.00	8.33
miR-18b	86	18.60	73.26	8.14
miR-126	3	0.00	100.00	0.00
miR-128	332	12.95	79.52	7.53
miR-141	388	16.75	75.26	7.99
miR-205	150	17.33	73.33	9.33
Average (for up-regulated miRNAs)	172.14	13.17	79.96	6.87
miR-383	41	0.00	73.17	26.83
miR-320a	256	6.25	80.08	13.67
miR-193a-5p	17	5.88	76.47	17.65
Average (for down-regulated miRNAs)	104.67	4.04	76.57	19.38
Average (for Up and Down)	138.40	8.61	78.27	13.13

Experimental validation is currently considered the most stringent method to validate miRNA targets (Kuhn et al., 2008; Thomas et al., 2010). Thus, to further test the possibility that the low inverse correlation between changes in miRNA levels and target mRNAs observed in the tissue samples was merely a reflection of the limited accuracy of target prediction algorithms, we conducted a series of transfection experiments using two miRNAs that were significantly up-regulated in CEPI (miR-7 and miR-128) to identify experimentally validated targets of these miRNAs in CEPI.

Table 2.7. Summary values of IC, PC and NC targets using overlap of TargetScan and PicTar predictions. MiRNA targets that were differentially expressed between CEPI and OSE based on t-test p <0.005 and fold change of at least 2 were classified as being IC or PC with their regulating miRNAs (while target genes that do not meet the above criteria are classified as NC). Total number of targets from the overlap of TargetScan (TS) and PicTar (PT) algorithms present after removing probesets with "Absent" calls in all samples is shown along with fraction of IC, PC and NC targets for each of the 12 annotated miRNAs. On average, 76.8 % of the target mRNAs are in the NC group, 6.4 % are in the IC group and 16.7 % are in the PC group.

miRNA	Total Targets (TS_PT)	Inversely Correlated Targets (%)	No Change (%)	Positively Correlated Targets (%)
miR-7	123.00	11.38	81.30	7.32
miR-18	72.00	15.28	81.94	2.78
miR-126	6.00	0.00	100.00	0.00
miR-128	326.00	12.58	76.99	10.43
miR-141	210.00	14.76	75.24	10.00
miR-205	93.00	17.20	69.89	12.90
Average (for up-regulated miRNAs)	138.33	11.87	80.89	7.24
miR-383	17.00	0.00	82.35	17.65
miR-320a	129.00	3.10	86.05	10.85
miR-193a-5p	2.00	0.00	50.00	50.00
Average (for down-regulated miRNAs)	49.33	1.03	72.80	26.17
Average (for Up and Down)	93.83	6.45	76.85	16.70

A series of independent transfection experiments was carried out with miR-7, miR-128 and a matched set of negative control miRNAs in a well-established EOC cell line (HEY; Buick et al., 1985). Total RNA was collected from cells 48 hrs after transfection and the relative levels of mRNAs present were determined by Affymetrix microarray analyses (HG-U133 Plus 2.0; Tables A.4 and A.5).

Table 2.8. Summary values of IC, PC and NC targets in transfection experiments using miRanda, TargetScan and PicTar target predictions. MiRNA targets that were differentially expressed between miR-7 or miR-128 transfected cells compared to negative control miRNA transfected cells, based on fold change of at least 1.4 and false discovery rate threshold of 5 % were classified as being IC or PC with their regulating miRNAs (while target genes that do not meet the above criteria are classified as NC). Total number of targets from miRanda (M), TargetScan (TS) and PicTar (PT) or their intersections (two at time and all three) present after removing probesets with "Absent" calls in all samples is shown along with fraction of IC, PC and NC targets for each miRNA.

miRNA_prediction algorithm	Total Targets	Inversely Correlated Targets (%)	No Change (%)	Positively Correlated Targets (%)
	miR-7 transfection			
miR-7_M	2432	7.98	91.24	0.78
miR-7_TS	259	23.55	75.29	1.16
miR-7_PT	238	16.39	83.19	0.42
miR-7_M_TS	234	20.51	78.63	0.85
miR-7_PT_TS	118	22.88	77.12	0
miR-7_M_PT	159	20.75	79.24	0
miR-7_M_TS_PT	99	23.23	76.77	0
	miR-128 transfection			
miR-128_M	2744	9.55	79.15	11.30
miR-128_TS	654	16.36	73.85	9.79
miR-128_PT	441	15.19	74.60	10.20
miR-128_M_TS	449	20.04	72.83	7.13
miR-128_TS_PT	301	16.94	73.75	9.30
miR-128_M_PT	306	17.32	74.18	8.50
miR-128_TS_M_PT	221	19.91	73.30	6.79

Table 2.9. Summary values of IC, PC and NC mRNAs in CEPI vs. OSE for miR-7 and miR-128 using "experimentally validated" targets only. Targets that were predicted by miRanda (M), TargetScan (TS), PicTar (PT) or any combination of the three programs and were down-regulated (FDR <5 %, fold change ≤-1.4) in miR-7 transfection or in miR-128 transfection were assumed to be experimentally validated targets. The direction of change of these same targets in CEPI vs. OSE were then used to calculate IC, NC and PC fractions using a p-value <0.005 and a fold change of at least 2 in the tissue microarray data.

miRNA_prediction algorithm	Total Targets	Inversely Correlated Targets (%)	No Change (%)	Positively Correlated Targets (%)
miR-7_M	180	12.22	80.56	7.22
miR-7_TS	60	6.67	88.33	5
miR-7_PT	37	0	91.89	8.11
miR-7_M_TS	47	6.38	87.23	6.38
miR-7_PT_TS	27	0	96.30	3.70
miR-7_PT_M	33	0	90.91	9.09
miR-7_M_TS_PT	23	0	95.65	4.35
Average for miR-7 (all methods)	58.14	3.61	90.12	6.26
miR-128_M	252	11.90	74.60	13.49
miR-128_TS	103	10.68	75.73	13.59
miR128_PT	63	17.46	69.84	12.70
miR-128_M_TS	87	12.64	72.41	14.94
miR-128_PT_TS	49	16.33	69.39	14.29
miR-128_M_PT	52	11.54	75	13.46
miR-128_M_PT_TS	43	11.63	72.09	16.28
Average for miR-128 (all methods)	92.71	13.17	72.73	14.11
Average (overall)	75.43	8.39	81.42	10.19

Consistent with the results from CEPI tissue samples, only a minority of predicted mRNA targets were found to be significantly reduced (IC) after miR-7 or miR-128 transfection (Table 2.8). The predicted mRNA targets that were significantly down-regulated in these transfection experiments were taken as "experimentally validated" mRNA targets of miR-7 and miR-128 respectively. Using only these targets, we reanalyzed the microarray data from the tissue samples and found that only ~8 % (range 0-18 %) of the "experimentally validated" mRNA targets displayed changes in expression IC with changes in miR-7 and miR-128 expression in CEPI (Table 2.9). Collectively our results indicate that the low inverse correlation between changes in levels in miRNAs and their target mRNAs *in vivo* is not merely an artifact of inaccurate

target predictions but rather a reflection of the complexity of miRNA function in cancer cells.

Discussion and Conclusion

It is well known that genes and their mRNA products are subject to a vast array of regulatory controls. The relative contribution of malfunctions in these controls to the onset and progression of diseases, such as cancer, can be varied and complex (Pardee, 2006). MiRNAs and other small non-coding RNAs recently have been shown to be important regulators of gene expression, and disruption of miRNA expression has been implicated in many diseases including cancer (Esquela-Kerscher and Slack, 2006; Lee and Dutta, 2009; Ventura and Jacks, 2009; Visone and Croce, 2009; Wiemer, 2007). While it is well established that miRNAs can serve as useful biomarkers for the diagnosis and staging of a variety of human cancers (e.g., Bartels and Tsongalis, 2009; Calin and Croce, 2006a; Lu et al., 2005), the manner and extent to which miRNAs contribute to the processes underlying cancer is only beginning to be understood (Calin and Croce, 2006a; Lee and Dutta, 2009). For example, the regulatory function of miRNAs was initially believed to operate exclusively at the translational level (Lee et al., 1993; Wightman et al., 1993), but more recent findings have demonstrated that these small regulating RNAs also play a role in the modulation of mRNA stability and that these two modes of control may be inter-related (Djuranovic et al., 2011; Valencia-Sanchez et al., 2006).

Extensive *in vitro* and *in vivo* studies previously have demonstrated that human miRNAs can repress gene expression by pairing with sequences located within the 3' untranslated regions of targeted messenger RNAs (mRNAs) resulting in translational repression and subsequent mRNA degradation (Bartel, 2004; Tang et al., 2008b;

Valencia-Sanchez et al., 2006). Thus far there are few examples of miRNAs increasing the transcription or translation of target genes (Place et al., 2008; Vasudevan et al., 2007), resulting in positive correlations between miRNAs and target mRNAs. Therefore, a generally held expectation is that changes in the expression levels of mRNAs will be inversely correlated with changes in the levels of their targeting miRNAs (Ritchie et al., 2009). However, the fact that individual miRNAs may target multiple mRNAs and that individual mRNAs may be targeted by multiple miRNAs creates the potential for a complex network of interactions in cancer cells replete with a variety of positive and negative feedback loops (Aguda et al., 2008; Volinia et al., 2010). The extent to which these complexities may mitigate our ability to accurately predict the function of miRNAs within the context of cancer cells has relevance to the proposed use of miRNAs in cancer therapy.

The purpose of the current study was to systematically evaluate the extent to which the regulatory consequence of changes in miRNA levels in tumors can be predicted from current models of miRNA function. The fact that prior efforts to obtain expression profiles of miRNAs and their mRNA targets were typically carried out on samples obtained from different patients and/or from mixed (bulk) tissues have contributed to inconsistent findings (e.g., Dahiya et al., 2008; Iorio et al., 2007; Nam et al., 2008; Wyman et al., 2009; Yang et al., 2008; Zhang et al., 2006). In an effort to reduce experimental variation, we assayed changes in levels of miRNA and their targeted mRNAs in ovarian cancer cells isolated from the same patients by LCM. Our results indicate that only ~11 % of the changes in levels of mRNAs are IC with changes in levels of their regulating miRNAs in the same ovarian cancer (CEPI) cells. To eliminate the

possibility that our results are merely an artifact of incorrectly identified mRNA targets of miRNA regulation, we repeated our analyses using targets predicted by a variety of prediction algorithms, as well as, targets experimentally validated in a series of transfection experiments conducted in an EOC cell line. Our results consistently support the conclusion that the expected IC between changes in miRNA levels and levels of their target mRNAs occurs relatively infrequently in EOC cells isolated from patient samples. Our findings underscore the complexities of miRNA-mediated regulation *in vivo* and the inadequacy of current models to accurately predict the molecular consequences of fluctuations in levels of miRNAs within the complex context of tumor cells.

Materials and Methods

Tissue samples

Ovarian tumor samples were collected at Northside Hospital (Atlanta, GA) during surgery and snap frozen in liquid nitrogen within one minute of removal from patients. All ovarian tumor samples used in this study were from patients diagnosed with serous papillary epithelial ovarian carcinoma. Brushings of normal ovarian surface epithelial cells (OSE) were preserved immediately in RNAlater (Ambion, Austin, TX). Patient consent and approval from the Institutional Review Boards of Georgia Institute of Technology and Northside Hospital were obtained. The written consent and our protocol (#H09227) were approved by the IRB. Detailed clinical information for each patient used in this study is provided in Table 2.10.

Laser capture micro-dissection (LCM)

Fresh frozen tissues from tumors were cut into seven-micron sections, applied to non-charged slides, then fixed in 75 % ethanol for 30 seconds, stained and dehydrated using the HistoGene LCM Frozen Section Staining Kit (Arcturus, Mountain View, CA). LCM was performed with an AutoPix Automated Laser Capture Micro-dissection System using the CapSure Macro Caps (Arcturus, Mountain View, CA). Approximately 10,000 cells were captured on each of five-six caps per sample. MiRNA was extracted from captured cells using the mirVana miRNA Isolation Kit (Ambion, Austin, TX). MRNA was isolated from cells from the same patients using the PicoPure RNA Isolation Kit (Arcturus, Mountain View, CA).

Table 2.10. Clinical information of patients analyzed in this study. Clinical information relevant to this study for each patient is shown. In addition, a legend is given to identify which patient was used for each microarray and qPCR experiment. Abbreviations used- Cerv: Cervix; Endo: Endometrium; Ov: Ovary; ca.: Carcinoma; hx: History.

Patient ID	Ovarian Histopathology	Stage/Grade	Age at Surgery (years)
551[a,b,c]	papillary serous carcinoma	IIIc/IV/3	59
588[a,b,c]	papillary serous carcinoma	IIIc/2-3	71
489[a,b]	papillary serous carcinoma	IV/3	48
620[c]	papillary serous carcinoma	III/IV/3	62
434[a]	within normal limits	N/A	41
440[a]	within normal limits	N/A	50
475[a]	within normal limits	N/A	63
470[a]	Ov-within normal limits; hx of endometrial ca.	Ov-N/A Endo-1b/1	44
437[a]	Ov-within normal limits; hx of cervical ca.	Ov-N/A Cerv-1b/3	54
482[b]	within normal limits	N/A	44
665[b]	within normal limits	N/A	84

Table 2.10 (continued)

Patient ID	Ovarian Histopathology	Stage/Grade	Age at Surgery (years)
783 [b,c]	within normal limits	N/A	52
838 [c]	within normal limits	N/A	51
846 [c]	within normal limits	N/A	51

a: mRNA microarray; b: microRNA microarray; c: qPCR

RNA extraction from ovarian surface epithelial (OSE) cells

For miRNA qPCR and microarray normal ovarian surface epithelial cells were spun down and resuspended in lysis buffer from the mirVana miRNA Isolation Kit, following the manufacturer's recommended protocol (Ambion, Austin, TX). cDNA for quantitative real-time PCR (qPCR) was synthesized from RNA (10ng) using the TaqMan miRNA Reverse Transcription Kit (Applied Biosystems, Foster City, CA).

For mRNA qPCR and microarray total RNA extraction from OSE was carried out using the PicoPure RNA Isolation Kit, following the manufacturer's recommended protocol (Arcturus, Mountain View, CA). Due to limited number of cells collected from surface epithelial brushings, OSE RNA was extracted from five patients with non-malignant ovaries for mRNA microarray and from two *different* sets of three patients with non-malignant ovaries for miRNA (one set for miRNA microarray, another for qPCR; see Table 2.10 for more details on patient information).

Quantitative (real-time) PCR (qPCR)

Total RNA (10ng) extracted from LCM captured ovarian tumor cells and normal OSE cells was converted to amplified cDNA for qPCR. TaqMan miRNA Assays

(Applied Biosystems, Foster City, CA) were conducted following manufacturer's protocol for hsa-miR-141, hsa-miR-429, hsa-miR-205, hsa-miR-320, hsa-miR-383 and for RNU6B endogenous control using the StepOnePlus Real-Time PCR machine (Applied Biosystems, Foster City, CA). For each sample miRNA expression values are normalized to an endogenous control (RNU6B). Statistical significance was determined using the Relative Expression Software Tool (REST; Pfaffl et al., 2002). Specificity of TaqMan miRNA assays is supported by publications from the manufacturer (Chen et al., 2007; Liang et al., 2007; Tavazoie et al., 2008) as well as subsequent literature from independent groups (Huang et al., 2011; Shibata et al., 2011; Wilson et al., 2011). RNU6B was used as endogenous control as it was recommended by the reagent manufacturer (http://www.ambion.com/techlib/tn/151/3.html) and is expressed at high levels in ovarian tissues (http://www3.appliedbiosystems.com/cms/groups/mcb_marketing/documents/generaldocuments/cms_044972.pdf).

For mRNA qPCR, total RNA (1-5µg) extracted from cells was converted to cDNA using the Superscript III First Strand synthesis system (Invitrogen). cDNA was then purified using the QIAGEN PCR purification kit (QIAGEN) following manufacturer's instructions. QPCR experiments were carried out for the EGFR, BMI and GAPDH genes using iQ SYBR Green Supermix (Bio-Rad, Hercules, CA). The sequence specific primers used for SYBR green assays are as follows: EGFR-forward: GGAGAACTGCCAGAAACTGACC, EGFR-reverse: GCCTGCAGCACACTGGTTG, GAPDH-forward: GGTCTCCTCTGACTTCAACA, GAPDH-reverse: AGCCAAATTCGTTGTCATAC, BMI1-forward: ACTTCATTGATGCCACAACC,

BMI1-reverse: CAGAAGGATGAGCTGCATAA. The EGFR primers were as designed by (Micallef et al., 2009) and GAPDH primers were as designed by (Koppelstaetter et al., 2005). BMI1 primers were obtained from the qPCR primer database RTPrimerDB (Pattyn et al., 2003). The GAPDH primer efficiencies were calculated to be ~1. Specificity of the other primers can be obtained from the relevant publications/database. All reactions were optimized with non-template controls, and -RT (minus reverse transcriptase) controls prior to experiment. All qPCR experiments were carried out with at least three technical replicates and three independent biological replicates.

Cell culture and miRNA transfections

HEY cells were provided by Gordon B. Mills, Department of Systems Biology, the University of Texas, M. D. Anderson Cancer Center. The cells were cultured in RPMI 1640 (Mediatech, Manassas, VA) supplemented with 10 % v/v heat-inactivated fetal calf serum (Invitrogen, Carlsbad, CA), 2 mM L-glutamine (Mediatech), 10 mM HEPES buffer (Mediatech), penicillin (100 U/ml), and streptomycin (100 µg/mL). Approximately 12h before transfection, these cells (1.5×10^5) were seeded on six-well plates (two-three replicates per group) in growth medium and allowed to adhere overnight at 37°C in a 5 % CO_2 atmosphere. The following day after washing the wells with PBS and replacing the growth medium with reduced serum medium Opti-MEM (Invitrogen), cells were transfected with the miRNA [hsa-miR-7 miRIDIAN mimic, miRIDIAN miRNA mimic negative control #1 (miR-NC, a *C.elegans* miRNA, cel-miR-67, with confirmed minimal sequence identity in humans), or hsa-miR-128 miRIDIAN mimic (Thermo Fisher Scientific, Lafayette, CO)] using Lipofectamine 2000 transfection agent (Invitrogen)

according to the manufacturer's instructions at a final concentration of 25nM. Cells were incubated for 4 hours, washed with PBS, and then incubated at 37°C and 5 % CO_2 for 44h (total 48h) after adding fresh growth medium (RPMI 1640) to the wells. Transfection efficiency was estimated from the relative knock-down of previously validated targets (EGFR for miR-7 and BMI-1 for miR-128 (Godlewski et al., 2008; Webster et al., 2009), Figure A.1), based on recommendations by the reagent manufacturer (Thermo Fisher Scientific). Cell culture experiments were carried out using at least two-three independent biological replicates.

Tissue whole genome microarray

Biotin labeled cRNA was synthesized, hybridized to Affymetrix HG-U133 Plus 2.0 oligonucleotide arrays and analyzed with a GeneChip Scanner 3000 (Affymetrix, Santa Clara, CA).

CEL files generated by the Affymetrix Gene Chip Operating System (GCOS) were converted to expression level values using the MAS 5.0 package implemented using the Affymetrix Expression Console software. The log base 2 transformed expression values were then normalized across samples by Z-score calculations using Spotfire DecisionSite for Microarray Analysis (DSMA). Probesets with "Absent" call in all groups were removed from further statistical analysis. Probeset intensities were filtered with DSMA using a modulation threshold of 1.0 to include only those probesets with at least a log base 2 expression value of $\geq$1.0 or fold change $\geq$2. Differentially expressed probesets were identified using the t-test function of the Profile ANOVA Tool of DSMA ($p < 0.005$). Annotations for probesets were obtained from the NetAffx website

(http://www.affymetrix.com/analysis/index.affx).

HEY cell RNA isolation and whole genome microarray

Total RNA was isolated using the RNeasy Mini RNA isolation kit (QIAGEN, Valencia, CA) according to the manufacturer's instructions. The integrity of the RNA was verified using an Agilent 2100 Bioanalyzer (1.8-2.0; Agilent Technologies, Palo Alto, CA). MRNAs were converted to double stranded (ds)-cDNA and amplified using Applause 3'-Amp System (NuGen, San Carlos, CA). This cDNA was then biotin labeled and fragmented by using Encode Biotin Module (NuGen). The labeled cDNA was hybridized to Affymetrix HG-U133 Plus 2.0 oligonucleotide arrays and analyzed with a GeneChip Scanner 3000 (Affymetrix, Santa Clara, CA). Raw data in the form of CEL files were produced by Affymetrix GeneChip Operating System (GCOS) software. Raw data from mRNA microarray were analyzed using the Expression Console software (Affymetrix) and using R (www.r-project.org). Normalization was performed using MAS 5.0, and PLIER available on the Expression Console software, while GCRMA algorithm was implemented using the "gcrma" package on R. The log base 2 transformed expression values from MAS5.0 were then analyzed for Affymetrix "Present/Absent" calls using Spotfire DecisionSite for Microarray Analysis (DSMA). Probesets with "Absent" call in all groups were removed from statistical analysis. Average probeset intensities for each group was calculated based on the log 2 transformed values from PLIER and then filtered with DSMA using a modulation threshold of 0.5 to include only those probesets with at least a fold change ≥ 1.4 [$\log_2$ difference ≥ 0.5]. The false discovery rate for each probeset was calculated from the log 2 transformed values after

GCRMA normalization using the SAM algorithm (Tusher et al., 2001). Finally, differentially expressed probesets were identified using a threshold 5 % false discovery rate correction, a fold change ≥1.4 and at least "Present/Marginal" call in 1 sample. These three different filtering approaches were used based on recommendations from recent publication by Mieczkowski et al. (2010) and the combination of all three was used to achieve the most stringent filtering.

MiRNA microarray

Samples for our miRNA profiling study were processed by Asuragen Services (Austin,TX), according to the company's standard operating procedures. A custom-manufactured Affymetrix GeneChip® from Ambion was designed to miRNA probes derived from the Sanger miRBase and published reports (Bentwich et al., 2005; Berezikov et al., 2005; Griffiths-Jones, 2004; Griffiths-Jones et al., 2006; Griffiths-Jones et al., 2008; Xie et al., 2005). Background signal was estimated from antigenomic probe sequences provided by Affymetrix and derived from a larger set of controls used on the Affymetrix human exon array. Spike-in external reference controls were based on non-miRNA control probes that lack homology to the human genome. Arrays within a specific analysis experiment were normalized according to the variance stabilization method described by Huber et al. (2002). A Wilcoxon rank-sum test was used to determine detection calls of the miRNA probe signals compared to the distribution of signals from GC-content matched anti-genomic probes.

A two-sample t-test, with assumption of equal variance, was applied for statistical hypothesis testing. This test defined which probes are considered to be significantly

differentially expressed based on a p-value of 0.01 and $\log_2$ difference ≥1. The signal intensities from these differentially expressed probes were z-score normalized prior to hierarchical clustering.

All microarray data from this study are MIAME compliant and have been submitted to GEO under the accession no. GSE23392

MiRNA target download

The miRNA targets prediction file based on miRanda was downloaded from www.microrna.org (August 2010 release; Betel et al., 2008; Enright et al., 2003; John et al., 2004). Information about the prediction algorithm, parameter settings and raw data source is available on the above link. Only predicted targets with "good" mirSVR score were used. "Good" mirSVR score refers to miRNA targets with <-0.1 score, and "non-good" mirSVR score refers to targets with >-0.1 score obtained from the support vector regression algorithm mirSVR, available with target predictions in the above link. The miRNA targets prediction file based on TargetScan (release 5.1) was downloaded from www.targetscan.org (Friedman et al., 2009; Grimson et al., 2007; Lewis et al., 2005). Targets based on PicTar (Chen and Rajewsky, 2006; Grun et al., 2005; Krek et al., 2005; Lall et al., 2006) prediction were also bulk downloaded from the UCSC database. MiRNAs for which PicTar predictions were not present in the bulk data file, were manually curated from the tables available on the PicTar web interface (www.pictar.org).

Predicted target sites analysis

Target sites for 12 differentially expressed miRNAs were selected from the

downloaded target prediction files or from the web interface (PicTar). Of those, target sites with Affymetrix "Absent" call in every sample were excluded from further analysis. Each target mRNA was classified as IC, NC or PC depending on the direction of its change in level of expression between OSE and CEPI and that of each targeting miRNA.

Predicted targets of the miRNAs miR-7 and miR-128 identified by miRanda, TargetScan, PicTar and all combinations of the three programs were used to calculated IC, NC, and PC fraction of targets in HEY cells transfected by each miRNA (miR-7 or miR-128) based on significance at a fold change threshold of 1.4 and maximum false discovery rate of 5 %. Predicted targets that were down-regulated in the transfection experiments were assumed to be experimentally validated and the expression patterns of these experimentally validated targets subsequently used in comparisons between the CEPI and OSE samples (as described above) to identify IC, PC and NC fractions based on significance at a fold change threshold of 2 and t-test p-value <0.005.

CHAPTER 3

MOLECULAR ANALYSIS OF THE INDIRECT EFFECTS OF TARGET GENE SILENCING BY MICRORNAS

Abstract

MicroRNAs (miRNAs) are a class of small non-coding RNAs that have been linked to a number of diseases including cancer. The potential application of miRNAs in cancer diagnostics and therapeutics is an area of particular current interest. A challenge to the use of miRNAs in cancer therapy is our current inability to accurately predict the indirect or off-target consequences of exogenous modulations in the levels of potentially therapeutic miRNAs. In an initial effort to systematically address this issue, we conducted miRNA transfection experiments using two miRNAs (miR-7, miR-128) predicted to down-regulate expression of the epidermal growth factor receptor oncogene (EGFR). In addition to observing the effect of miRNA transfection on the targeted oncogene, we monitored and characterized changes in levels of off-target gene expression. While ~ 20 % of the changes in expression patterns of hundreds to thousands of off-target genes could be attributed to direct miRNA-mRNA interactions, the majority of the changes are indirect, likely involving the downstream consequences of miRNA-mediated changes in regulatory gene expression. We found that changes in patterns of off-target gene expression are not random but functionally coordinated. We conclude that while the molecular consequences of miRNA transfection are complex, they are not capricious or intractable suggesting that miRNAs have significant potential as cancer therapeutic agents.

Introduction

MicroRNAs (miRNAs) are a class of small (18-24 nt) regulatory RNAs that play critical roles in many essential cellular processes including development, angiogenesis, cell cycle and cellular migration (Bushati and Cohen, 2007; Farazi et al., 2011). These small RNAs are encoded in the genomes of both unicellular (Zhao et al., 2007) and multicellular organisms and typically act to repress gene expression at the post-transcriptional level (Fabian et al., 2010). In mammals, miRNAs have been shown to repress translation and induce degradation of the target message by interacting with the 3'untranslated region (UTR) in a sequence specific manner (Guo et al., 2010; Tang et al., 2008b). In rare instances, miRNAs have also been reported to increase translation (Vasudevan et al., 2007) and/or transcription (Majid et al., 2010; Place et al., 2008) of target genes.

There is a large and growing body of evidence that many diseases, including cancer, are associated with changes in cellular levels of miRNAs (Chang and Mendell, 2007). In cancer, levels of specific miRNAs have been reported to be significantly down- or up-regulated in various cancer types indicating that these regulatory RNAs may be operationally defined as either tumor suppressor genes or oncogenes depending upon the cellular context (Chen, 2005). Based on these findings, the clinical potential of miRNAs as cancer biomarkers and/or therapeutic agents is being actively pursued (Tong and Nemunaitis, 2008; Wahid et al., 2010).

A continuing challenge to the effective use of miRNAs in cancer therapy is our limited ability to accurately predict the molecular consequences of exogenous

perturbations in cellular levels of miRNAs (Mishra and Merlino, 2009). The difficulty in anticipating the full molecular consequences of miRNA therapy may be due, in part, to the limitations of *in silico* target prediction algorithms (Saito and Saetrom, 2010) and to the fact that miRNAs can directly and/or indirectly modulate expression levels of multiple genes in addition to the intended target(s) (e.g., Baek et al., 2008; Lim et al., 2005; see also CHAPTER 2).

In an effort to better understand the range of molecular changes potentially associated with miRNA therapy, we conducted a series of controlled experiments in which single miRNAs are targeted to a specific cellular oncogene (epidermal growth factor receptor, EGFR) that is over-expressed in a well-characterized human ovarian cancer cell line (HEY; Dickerson et al., 2010). The effect of these miRNAs on target gene expression, as well as, on "off-target" global patterns of gene expression was monitored by microarray (Affymetrix, HG-U133 Plus 2.0) and quantitative (real-time) polymerase chain reaction (qPCR). MiRNAs were found to have a substantially greater impact on global patterns of gene expression than a target gene-specific siRNA. We categorize the miRNA induced changes in global patterns of gene expression with respect to possible underlying molecular mechanisms and discuss their potential biological significance.

Results

Ectopic expression of miR-7 or miR-128 significantly down-regulates EGFR in HEY cells.

EGFR is often over-expressed in ovarian and other epithelial cancers (Hynes and MacDonald, 2009; Normanno et al., 2006; Thaker et al., 2005) and is considered an attractive therapeutic target (Ciardiello and Tortora, 2008; Thaker et al., 2005; Zeineldin et al., 2010). We have previously shown that EGFR is over expressed in the well-characterized HEY ovarian cancer cell line and can be effectively down-regulated by EGFR-specific siRNAs (Dickerson et al., 2010). Earlier studies (Webster et al., 2009; Weiss et al., 2008) conducted in lung, brain, breast and prostate cancer cells have shown that the expression of EGFR may be subject to regulation by the miRNAs miR-7 and miR-128. These findings are consistent with the fact that the 3'UTR of EGFR is predicted to contain four potential binding sites for miR-7 and two potential binding sites for miR-128 (Figure 3.1A and 3.1B).

To determine if over-expression of miR-7 and miR-128 in ovarian cancer cells can induce down-regulation of EGFR, we independently transfected HEY cells with miR-7 or miR-128 and measured EGFR RNA and protein levels 48 hours after transfection relative to negative controls (miR-NC, miRIDIAN miRNA mimic negative control, Thermo Fisher Scientific). The results demonstrate that over-expression of either miR-7 or miR-128 in HEY cells results in significant down-regulation of EGFR expression (Figure 3.1C-F).

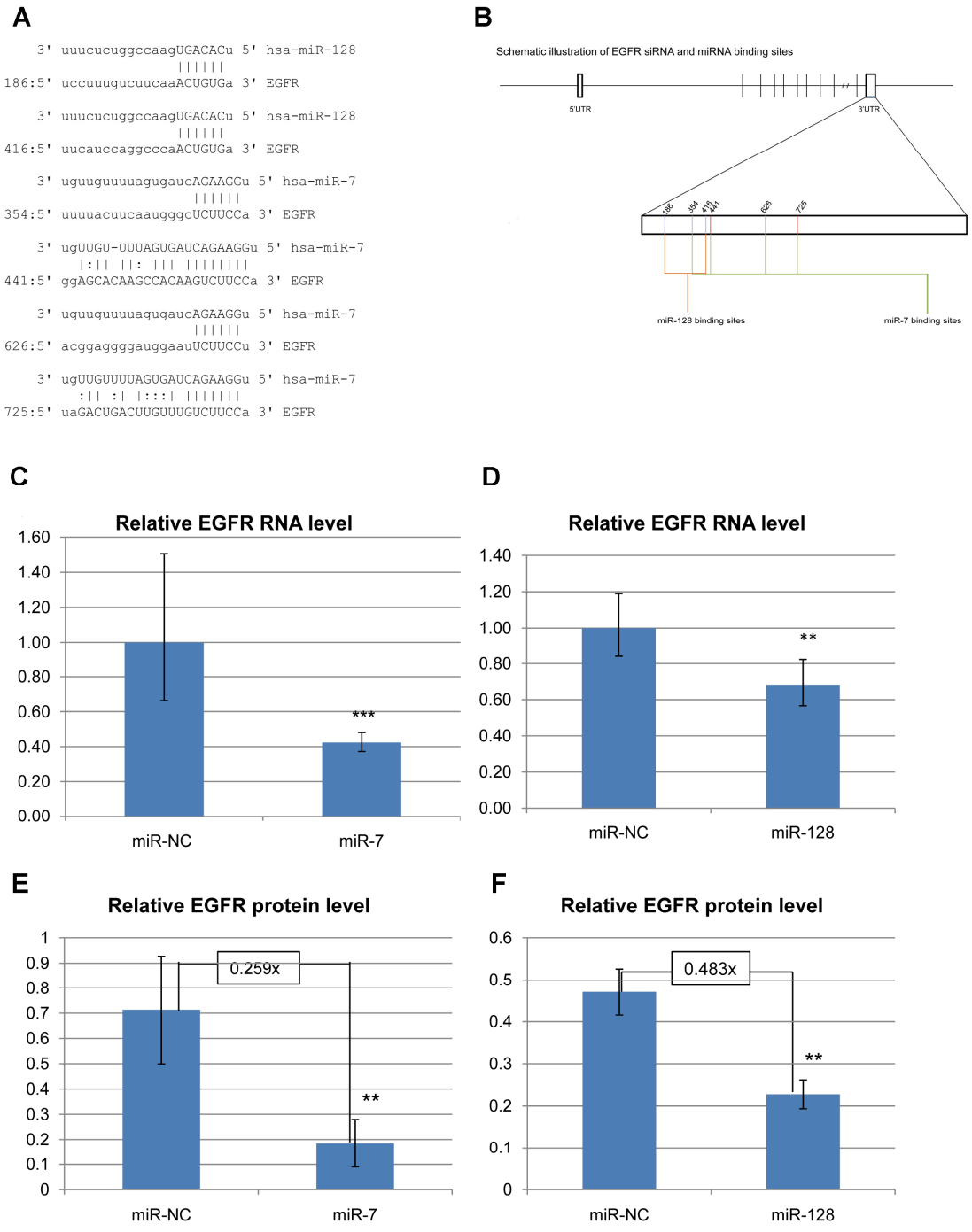

Figure 3.1. MiRNAs miR-7 and miR-128 down-regulate EGFR in HEY cells. Predicted miR-7 and miR-128 sites (miRanda) on EGFR 3'UTR are shown in (A) and (B). Complementary nucleotides and their relative positions on the UTR are depicted in (A). Vertical lines (|) denote Watson-Crick base pairing, while the colon (:) sign denotes wobble between G and U on opposite strands. The relative location of each target site on

the EGFR gene is shown schematically in (B). Red bars show the sites with "good" mirSVR score (<-0.1) and purple bars show those with "non-good" scores (see methods). (C) and (D) show relative EGFR RNA levels following transfection of (C) miR-7 or miR-NC, and (D) miR-128 or miR-NC in HEY cells using GAPDH as endogenous control. (E) and (F) show densitometric analysis of immunoblots measuring protein levels of EGFR following transfection of (E) miR-7 and (F) miR-128 relative to miR-NC. β-Actin is used as loading control for the immunoblots. The numbers in boxes are the fold change differences in EGFR protein levels between miR-NC and miR-7/miR-128 transfections. Error bars show standard deviations from the mean based on RNA/protein levels of three independent biological replicates. Statistical analysis for qPCR was done using randomization with the help of REST 2008 software with at least 1000 iterations. Statistical analysis of immunoblots was done using a 2-tailed t-test. *** $p < 0.001$, ** $p < 0.05$.

miR-7 or miR-128 transfection induces changes in expression of hundreds of off-target genes

To study the effect of over-expression of miR-7 or miR-128 on global patterns of gene expression, we isolated total RNA from cells 48 hrs after transfection and conducted microarray analysis (Affymetrix HG-U133 Plus 2.0). The results indicate that transfection of miR-7 induced significant changes in the expression of 754 genes (fold change ≥1.4, FDR ≤5 %; Table B.1) and that miR-128 transfection induced significant changes in the expression of 2338 genes (Figure 3.2A, Table B.2), both relative to controls. The fractions of transcripts up-regulated or down-regulated in each transfection were also variable. For miR-7, the majority of the differentially expressed genes (DEGs) were down-regulated (599, ~80 %), while for cells transfected with miR-128, most (1624, ~70 %) of the DEGs were up-regulated (Figure 3.2B).

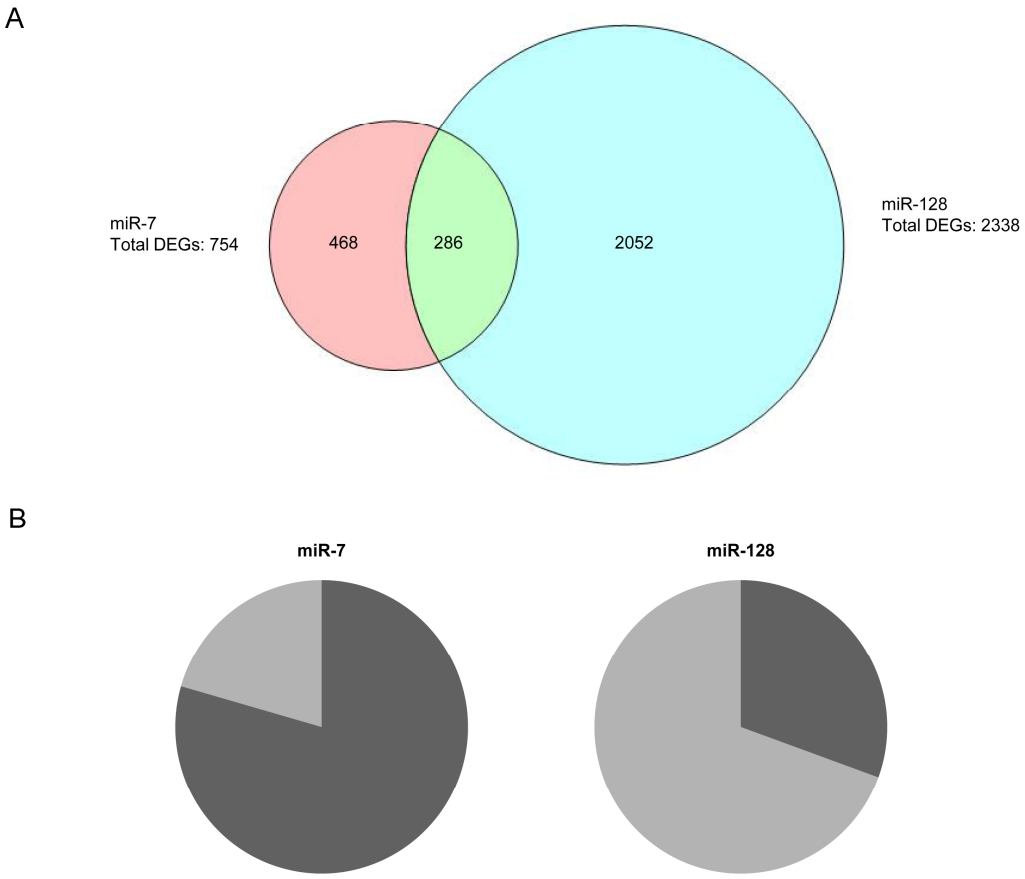

Figure 3.2. miR-7 and miR-128 alter the expression of hundreds to thousands of genes. (A) Transfection of miR-7 leads to differential expression of 754 genes and miR-128 leads to the alteration of 2338 genes (fold change ≥1.4, FDR ≤5 %) in HEY cells relative to miR-NC transfection. The number of genes differentially expressed in each experiment and in both (286) is represented by the Venn diagram. The proportions of genes up-regulated or down-regulated also vary between the transfections, as shown in (B). The pie-charts show that the majority of the altered genes are down-regulated (dark grey) after miR-7 transfection, but are up-regulated (light grey) after miR-128 transfection.

Less than 1 % of the miR-7 or miR-128 induced changes in gene expression are the consequence of down-regulation of EGFR

To determine the extent to which miRNA induced changes in "off-target" gene expression may be explained by the down-regulation of EGFR, we monitored the effect of anti-EGFR siRNA transfection on global patterns of gene expression and contrasted the results with expression patterns observed after miR-7 or miR-128 expression. After verifying knock-down of EGFR by siRNA transfection (Figure 3.3) we monitored global patterns of gene expression by microarray. Employing identical criteria to that used for the detection of differentially expressed genes after the miRNA transfections (fold change ≥1.4, FDR ≤5 %), we found that only eight genes (in addition to EGFR) were significantly differentially expressed (Table 3.1). These findings indicate that the vast majority of changes in gene expression observed after miR-7 or miR-128 transfection are not merely the consequence of knock-down in EGFR expression (Figure 3.4).

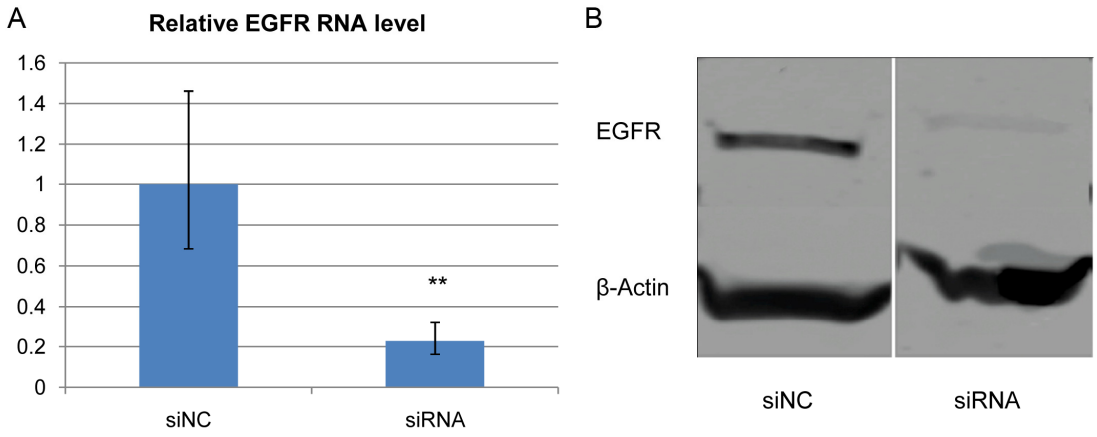

Figure 3.3. Confirmation of EGFR down-regulation by siRNA. (A) Relative EGFR RNA levels determined by qPCR following transfection of anti EGFR siRNA (siRNA) or negative control siRNA (siNC) in HEY cells using GAPDH as endogenous control. Error bars show standard deviations from the mean based on RNA levels of three independent

biological replicates. Statistical analysis was done using randomization with the help of REST 2008 software with at least 1000 iterations. ** $p < 0.05$. (B) Representative image of Western blot analysis of EGFR protein levels after transfection with anti-EGFR siRNA or negative control siRNA (siNC). β-Actin is used as loading control for the immunoblot.

Table 3.1. Differentially expressed genes in siRNA transfected HEY cells.
Significantly differentially expressed genes (fold change ≥1.4, FDR ≤5 %) following anti-EGFR siRNA transfection, compared to siNC transfection of HEY cells. 'Probeset ID' refers to Affymetrix HG-U133 Plus 2.0 probeset identifier. 'Gene Symbol' shows the official gene symbol for the corresponding Probeset ID. 'siRNA-siNC' refers to the difference between average log2 signal values of siRNA transfected cells and the siNC transfected cells. 'q-value (%)' shows the false discovery rate calculated using the SAM algorithm. All transfections were carried out in triplicates.

Probeset ID	Gene Symbol	siRNA-siNC	q-value (%)
201110_s_at	THBS1	1.15	3.43
201109_s_at	THBS1	1.06	3.43
202310_s_at	COL1A1	0.87	4.02
201108_s_at	THBS1	0.76	3.43
207950_s_at	ANK3	0.75	3.43
203139_at	DAPK1	0.57	3.43
231618_s_at	SUNC1	-0.82	0.00
229672_at	UQCC	-0.96	0.00
201983_s_at	EGFR	-1.04	0.00
208885_at	LCP1	-1.04	0.00
211607_x_at	EGFR	-1.15	0.00
210984_x_at	EGFR	-1.17	0.00
221786_at	C6orf120	-1.26	0.00

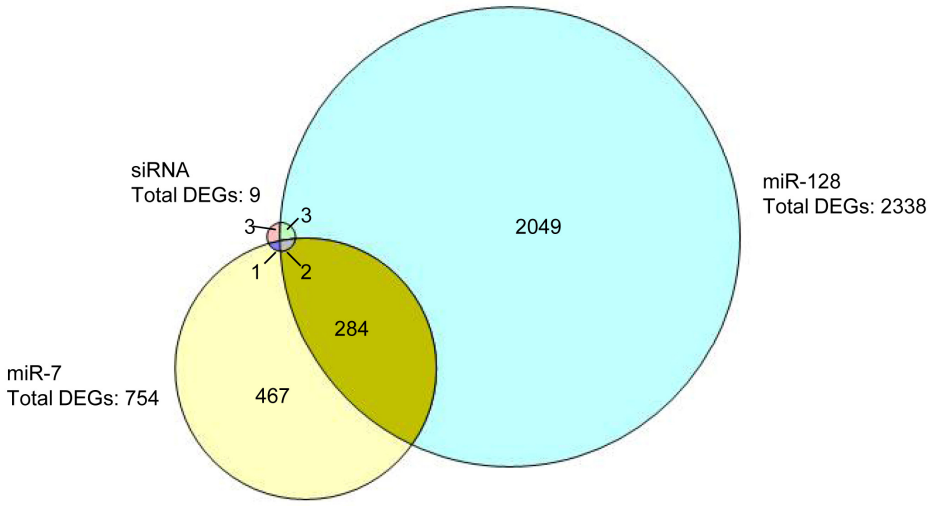

Figure 3.4. Overlap of genes differentially expressed following miR-7, miR-128 and anti-EGFR siRNA transfection. Transfection of anti-EGFR siRNA results in differential expression of only nine genes (including EGFR, fold change ≥1.4, FDR ≤5 %) in HEY cells relative to siNC transfection. Only two genes (including EGFR) are altered in all three transfections. Only three of the genes differentially expressed after siRNA transfection are also differentially expressed after miR-7 transfection, only five of the nine are also differentially expressed after miR-128 transfection, and only three were differentially expressed only in the siRNA transfection.

Less than 20 % of the genes differentially expressed after miR-7 or miR-128 transfection are predicted targets of these miRNAs

A single miRNA can potentially target hundreds of genes (Brennecke et al., 2005; Krek et al., 2005; Lewis et al., 2005). To explore the possibility that the global changes in expression patterns observed after miR-7 or miR-128 transfection were the result of direct targeting, we first computed the percentage of the down-regulated genes potentially regulated by miR-7 or miR-128 as predicted by the three major target prediction algorithms (miRanda, TargetScan, and PicTar). The results indicate that on average <20 % of the down-regulated genes differentially expressed after miR-7 or miR-128

transfection are direct regulatory targets of these miRNAs (Table 3.2, Figure 3.5). For example, of the 599 genes down-regulated after miR-7 transfection, only 194 or 32.4 % are predicted to be targets of this miRNA by miRanda. The percentages are lower using targets predicted by the PicTar (6.5 %) and TargetScan (10.2 %) algorithms.

Although increased levels of miRNAs are generally expected to down-regulate the expression of target genes, there have been isolated reports of the expression of target genes being increased after miRNA transfection (Majid et al., 2010; Place et al., 2008). If we include all genes that are either down-regulated or up-regulated after miR-7 or miR-128 expression, the percentage of predicted targets remains, on average, <20 % (Table 3.2). We conclude that less than one-fifth of the genes differentially expressed after miR-7 or miR-128 transfection are likely the result of regulatory effects directly exerted by these miRNAs.

Table 3.2. Fraction of down-regulated, up-regulated and differentially expressed genes predicted to be targets of miRNAs. Significantly down-regulated (down), up-regulated (up) or all differentially expressed genes (all) after miR-7 or miR-128 transfections in HEY cells were searched for targets of the respective miRNAs using miRanda (M), TargetScan (TS) and PicTar (PT) algorithms. The fraction (%) of targets within each group and the average (AVG) of all three algorithms are reported in this table.

	miR-7				**miR-128**			
	M	**TS**	**PT**	**AVG**	**M**	**TS**	**PT**	**AVG**
Down	32.4	10.2	6.5	16.4	36.0	14.7	9.1	19.9
Up	12.3	1.9	0.6	4.9	18.8	3.8	2.6	8.4
All	28.2	8.5	5.3	14	24.0	7.1	4.6	11.9

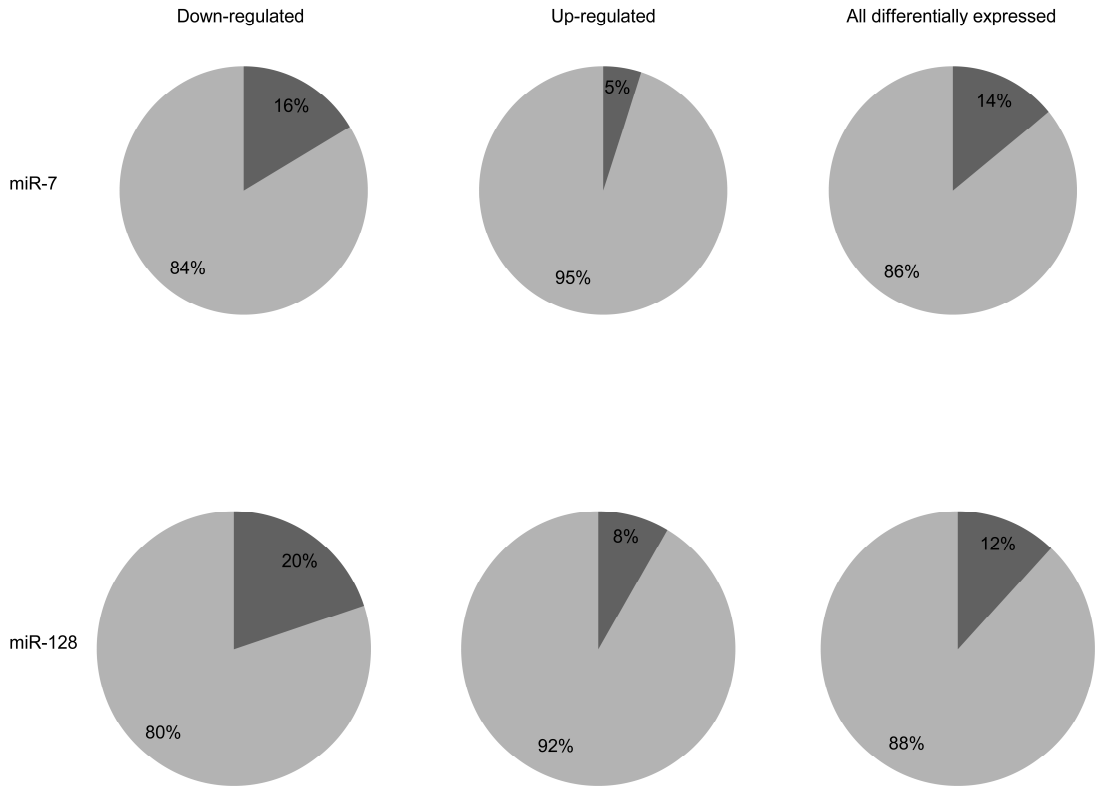

Figure 3.5. Contribution of canonical miRNA targeting on the number of differentially expressed genes. The pie-charts show the proportion of differentially expressed genes following miR-7 (top row) or miR-128 (bottom row) transfection that may be explained by direct 3'UTR targeting (dark grey), or indirect mechanisms (light grey). These proportions are calculated for only down-regulated (left), only up-regulated (middle) or all differentially expressed (right) genes. In each transfection a majority (≥80 %) of the differentially expressed genes are not predicted to be directly regulated by the miRNAs. Only the average number of predictions from miRanda, TargetScan and PicTar algorithms were used to generate this figure.

An indirect effect of miR-128 transfection may be the de-repression of endogenous miRNA targets

It has been previously proposed that transfection of exogenous miRNA molecules may interfere with endogenous miRNA targeting of mRNAs due to competition for a

limited number of RNA-Induced Silencing Complexes (RISC; Khan et al., 2009). According to this model, if endogenous miRNAs are out competed for RISC complexes by exogenous miRNAs, the targets of the endogenous miRNAs may be expected to be up-regulated. In a pre-transfected cell, endogenous miRNAs with higher expression values are predicted to have a higher likelihood of being in the RISC complex and, thus, more likely to be affected by introduction of exogenous miRNAs (Khan et al., 2009; Landthaler et al., 2008; Sood et al., 2006; Tang et al., 2008a).

As mentioned above, a majority (~70 %) of the 2338 genes displaying significant changes in expression after miR-128 transfection were up-regulated (Figure 3.2, Table B.2). To determine if the RISC competition model might help explain some of these indirect effects of miR-128 transfection, we sought to determine if the target sequences of miRNAs most highly expressed in pre-transfected HEY cells were significantly enriched in genes up-regulated after miR-128 transfection.

We employed a previously established gene set enrichment analysis algorithm (Genomica; Lubling and Segal, accessed on July 7, 2010) to identify miRNA target sites enriched in mRNAs up-regulated after miR-128 expression. The results indicate that target sites of 78 miRNAs are significantly enriched among genes (mRNAs) up-regulated after miR-128 expression (Tables 3.3 and B.3). [Note: A similar analysis of genes significantly up-regulated after miR-7 transfection (i.e., only ~20 % of differentially expressed genes-see above) indicated that targets of only two miRNAs were significantly enriched in up-regulated genes (Table B.4)].

Table 3.3. MiRNAs with targets enriched among up-regulated genes after miR-128 transfection. List of genes up-regulated after miR-128 transfection into HEY cells are

overlapped with list of miRNA targets and the targets of 78 miRNAs are found to be significantly enriched (hypergeometric probability, FDR <0.05) by Genomica gene set enrichment analysis among these genes.

miRNAs		
hsa-let-7a	hsa-miR-187	hsa-miR-29a
hsa-let-7c	hsa-miR-189#	hsa-miR-29c
hsa-let-7d	hsa-miR-18a	hsa-miR-302a*
hsa-let-7e	hsa-miR-18b	hsa-miR-30a-3p
hsa-let-7f	hsa-miR-191	hsa-miR-30b
hsa-let-7g	hsa-miR-192	hsa-miR-30c
hsa-let-7i	hsa-miR-193	hsa-miR-30d
hsa-miR-1	hsa-miR-194	hsa-miR-30e
hsa-miR-106a	hsa-miR-199	hsa-miR-324-3p
hsa-miR-122a	hsa-miR-19a	hsa-miR-329
hsa-miR-135	hsa-miR-19b	hsa-miR-33
hsa-miR-136	hsa-miR-20	hsa-miR-335
hsa-miR-137	hsa-miR-205	hsa-miR-363
hsa-miR-139	hsa-miR-206	hsa-miR-377
hsa-miR-140	hsa-miR-208	hsa-miR-378
hsa-miR-145	hsa-miR-21	hsa-miR-409-5p
hsa-miR-146a	hsa-miR-210	hsa-miR-452
hsa-miR-146b	hsa-miR-217	hsa-miR-485-3p
hsa-miR-148	hsa-miR-219	hsa-miR-485-5p
hsa-miR-150	hsa-miR-22	hsa-miR-486
hsa-miR-15a	hsa-miR-221	hsa-miR-503
hsa-miR-15b	hsa-miR-222	hsa-miR-542-3p
hsa-miR-17	hsa-miR-23b	hsa-miR-7
hsa-miR-181a	hsa-miR-26a	hsa-miR-9
hsa-miR-183	hsa-miR-26b	hsa-miR-93
hsa-miR-185	hsa-miR-299	hsa-miR-98

* miRNA* strand; # This miRNA has recently been removed from miRBase as it was found to originate from the same precursor as miR-24. We did not include this in subsequent analysis.

To test whether these 78 miRNAs were expressed at higher levels in pre-transfected HEY cells relative to all expressed miRNAs, we measured levels of human miRNAs in pre-transfected HEY cells by microarray (Affymetrix GeneChip miRNA

array; Table B.5). Out of 847 human miRNAs present on the Affymetrix chip, 281 were found to be expressed in pre-transfected HEY cells, and out of the 78 miRNAs with target sites enriched among up-regulated genes after miR-128 transfection, 45 were expressed in pre-transfected HEY cells. Figure 3.6 displays a histogram of $\log_2$ signal values for all expressed miRNAs (281) and for the subset of miRNAs (45) with target sites significantly enriched in genes/mRNAs up-regulated after miR-128 transfection. The results demonstrate that miRNAs with binding sites significantly enriched in up-regulated genes display a significantly greater fraction of signal values above $\log_2(10)$ relative to all miRNAs (Mann-Whitney p-value <0.0001) indicating a generally higher level of expression in pre-transfected HEY cells. These findings are consistent with the hypothesis that a significant fraction of the increased level of gene expression observed after miR-128 transfection may be the indirect effect of the displacement of endogenous miRNAs from the RISC.

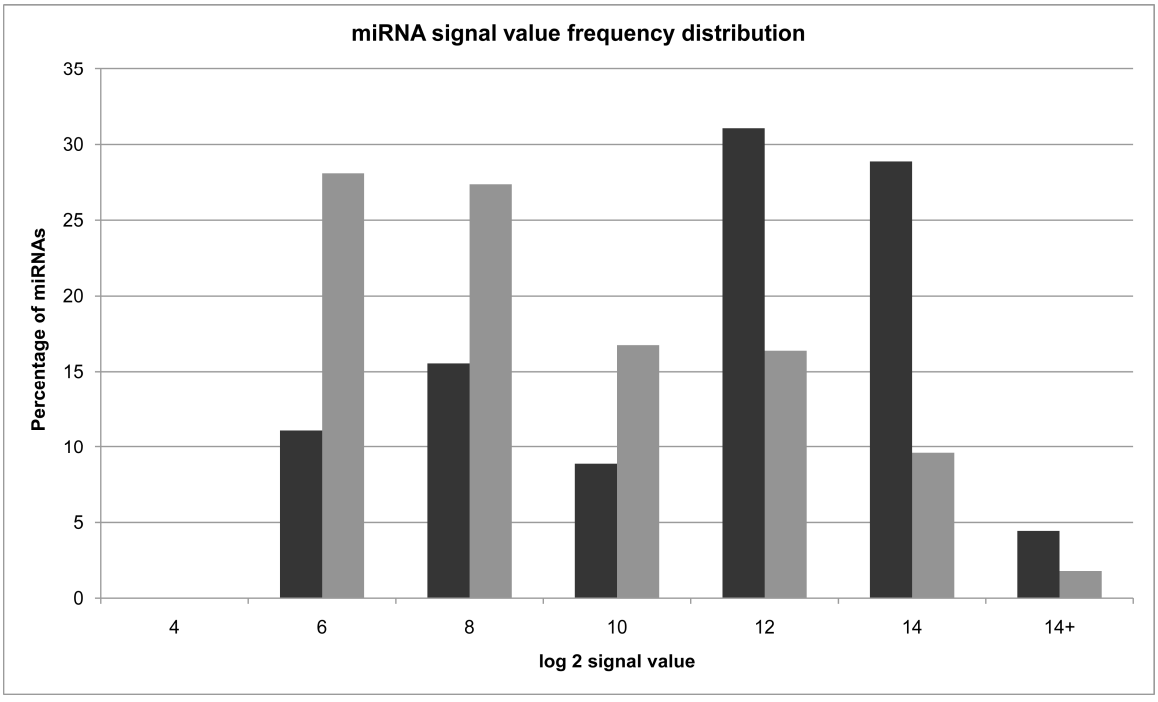

Figure 3.6. Endogenous miRNAs targeting up-regulated genes are expressed at higher levels than other miRNAs. Frequency distribution of $\log_2$ signal values for all 281 miRNAs expressed in HEY cells (grey) compared with signal value distribution for 45 miRNAs expressed among those targeting up-regulated genes after miR-128 transfection (black). The bar chart shows that the 45 miRNAs targeting up-regulated genes have a higher frequency of being expressed at $\log_2$ signal value >10, while most miRNAs frequently have $\log_2$ (signal value) ≤10 (Mann-Whitney p-value <0.0001).

miR-7 or miR-128 transfection can trigger cascades of indirect regulatory changes in gene expression

GeneGo functional network analysis was used to identify genes with the most significant number of interactions ("hub genes") among genes differentially expressed after miR-7 or miR-128 transfection. Hub genes typically encode transcription factors or other regulatory proteins (or RNAs) capable of trans-regulating down-stream genes (Seo et al., 2009; Wang et al., 2007). MiRNA induced changes in the expression level of hub genes are expected to induce subsequent changes in the expression of genes regulated by these hub-genes. If these regulated genes include other hub genes, the regulatory "ripple effect" can be significant.

Table 3.4. Hub genes identified among differentially expressed genes after miR-7 transfection. Genes connected via network interactions with the most significant number (FDR <0.05) of genes (nodes) among the list of differentially expressed genes following miR-7 transfection are listed. Genes which are predicted to be miR-7 targets by miRanda or may act as transcription factors are marked with 'x'.

Gene Symbol [Designated GeneGo Object Name]	miR-7tgts_miRanda	Transcription Factor
RELA [RelA (p65 NF-kB subunit)]	x	x
MMP14 [MMP-14]		
CASP1 [Caspase-1]	x	

Table 3.4 (continued)

Gene Symbol [Designated GeneGo Object Name]	miR-7tgts_miRanda	Transcription Factor
EHD1 [EHD1]	x	
CDKN1B [p27KIP1]		
VLDLR [VLDLR]		
EGFR [EGFR]	x	
TCF7L2 [TCF7L2 (TCF4)]		x
FMR1 [FMR1]		
PPHLN1 [PPHLN1]		

Table 3.5. Hub genes identified among differentially expressed genes after miR-128 transfection. Genes connected via network interactions with the most significant number (FDR <0.05) of genes (nodes) among the list of differentially expressed genes following miR-128 transfection are listed. Genes which are predicted to be miR-128 targets by miRanda or may act as transcription factors are marked with 'x'.

Gene Symbol [Designated GeneGo Object Name]	miR-128tgts_miRanda	Transcription Factor
CASP1 [Caspase-1]	x	
SH3KBP1 [CIN85]		
EGFR [EGFR]		
SKP1 [SKP1]	x	
PPP1CC [PP1-cat gamma]	x	
PTP4A1 [PTP4A1]		
ODC1 [DCOR]		
FKBP4 [FKBP4]		
PXN [Paxillin]		
TUBA1B [Tubulin alpha-1B]		
NFKBIA [NFKBIA]		
EGR1 [EGR1]		x
LRRFIP1 [LRRFIP1]	x	x
PLK1 [PLK1]		
FOXM1 [FOXM1]		x
PIAS3 [PIAS3]		x
CAV1 [Caveolin-1]	x	
CDK1 [CDK1 (p34)]		
SPRY2 [SPRY2]	x	
AURKA [Aurora-A]		
HEC [HEC]		
VDR [VDR]		x

Table 3.5 (continued)

Gene Symbol [Designated GeneGo Object Name]	miR-128tgts_miRanda	Transcription Factor
PLCG2 [PLC-gamma 2]		
BTRC [beta-TrCP]		
CENPA [CENP-A]		
CENPE [CENP-E]		
ITGB3BP [NRIF3]		x
XIAP [XIAP]		
SERPINH1 [HSP47]	x	
SEPHS1 [SEPHS1]		
STAT3 [STAT3]		x
TSC1 [Hamartin]		
PAK1 [PAK1]		
TAPBP [Tapasin]		
ERAP1 [ARTS-1]		
MAPK14 [p38alpha (MAPK14)]	x	x
CAMKK2 [CaMKK2]	x	x
PTBP1 [PTBP1]		
PTPN2 [PTPN2]		
CCNA2 [Cyclin A2]		x
SRC [c-Src]		
PCBP2 [PCBP-2]		
CTTN [Cortactin]		
BUB1 [BUB1]	x	
RBX1 [RING-box protein 1]	x	
SMAD3 [SMAD3]		x
CCRN4L [Nocturnin]		
HNRNPA1 [hnRNP A1]	x	
CTNNB1 [Beta-catenin]		x
FOXO3 [FOXO3A]		x
MIR21 [microRNA 21]		
PDPK1 [PDK (PDPK1)]		
VAPA [VAPA]		
TSEN15 [Sen15]		
CREB1 [CREB1]		x
SMAD2 [SMAD2]		x
RPS6KB1 [p70 S6 kinase1]	x	
SYTL4 [SYTL4]	x	
ARHGEF7 [BETA-PIX]		
MED6 [MED6]		x
HDAC2 [HDAC2]		x

Functional network analysis identified 10 hub genes among those differentially expressed after miR-7 transfection and 61 among genes differentially expressed after miR-128 transfection (FDR <0.05; Tables 3.4, 3.5, B.6 and B.7). Many of these hub genes are predicted to be direct targets of miR-7 or miR-128 regulation (Tables 3.4 and 3.5). For example, the gene encoding the RELA component of the NF-κB regulatory protein is a predicted target of miR-7 and was significantly down-regulated after miR-7 transfection (Table B.1). Consistent with the hypothesis that down-stream effects of RELA may be contributing to indirect changes in expression levels, we found that a number of the genes differentially expressed after miR-7 transfection are documented targets of NF-κB regulation. Among these is the cytokine IL-1 beta (Basak et al., 2005; Goto et al., 1999) that, in turn, is predicted to regulate genes that were also differentially expressed after miR-7 transfection (Figure 3.7, Table 3.6).

Similar changes in patterns of gene expression were observed after miR-128 transfection. For example, Caveolin-1 (CAV1) is a negative regulator of the Ras-p42/44 MAP kinase cascade (Williams and Lisanti, 2005). Levels of CAV1 were significantly reduced after miR-128 transfection and down-stream targets of CAV1 were among those genes significantly differentially expressed (Tables 3.7 and B.2). Among the CAV1 regulated genes displaying significant changes in expression after miR-128 transfection is another hub gene, the transcription factor SMAD2 (Razani et al., 2001). Genes known to be trans-regulated by SMAD2 were also differentially expressed after miR-128 transfection (Table 3.7, Figure 3.8). Collectively, our results are consistent with the hypothesis that a majority of the changes in expression induced after miR-7 or miR-128

transfection are likely the indirect or down-stream consequences of changes in hub gene expression.

Table 3.6. Differentially expressed genes that are targeted by NF-κB or IL-1 Beta. Differentially expressed genes following miR-7 transfection in HEY cells that are directly regulated by NF-κB, by IL-1 beta, or by both are listed. IL-1 beta (IL1B) is a transcriptional target of NF-κB and both are significantly down-regulated following miR-7 transfection. The genes that are only targeted by IL-1 beta may be differentially expressed because RELA/NF-κB is a target of miR-7 and in turn regulates IL-1 beta.

NF-κB only		IL1-β only	Common targets
ACO2	KCTD12	CASP1	ASS1
ADAM19	LIFR	DPP4	BID
ASPH	LITAF	IGFBP3	BMP2
ATXN3	MAT2A	IL1RAP	CXCL1
BACE1	MATR3	IL7	CXCL2
CALM1	NQO1	IRS1	DDIT3
CALM3	OGT	LAMC1	FN1
CBS	PAX6	ME1	HBEGF
CCND2	PCK2	MMP14	ICAM1
CCRL2	PDPN	NFKBIZ	IL8
CDK6	PHLDA1	NR1H3	MIR21
CDKN1B	PMEPA1	NRP1	NUPR1
CSNK1A1	PSME3	NRP2	PTX3
DDIT4	RRM2	PAPPA	RUNX2
DDX21	S100A6	PRLR	SAA1
DLG1	SH2B3	SERPINH1	SAA2
DTNA	SLC11A2	SLC38A2	SERPINE2
EHD1	SLC44A1	SLC7A2	SOD2
EIF4A1	ST6GAL1	SOCS7	SPP1
ERAP1	ST8SIA1	THBD	TGFA
GAS5	TFRC	THBS1	TGFB2
GFPT2	TGM2	TIMP3	TGFBR2
GLO1	TNIP1		VEGFA
GREM1	TXNIP		VEGFC
HSPA9	VIM		XIAP
IL1B	ZBED4		
IL7R			

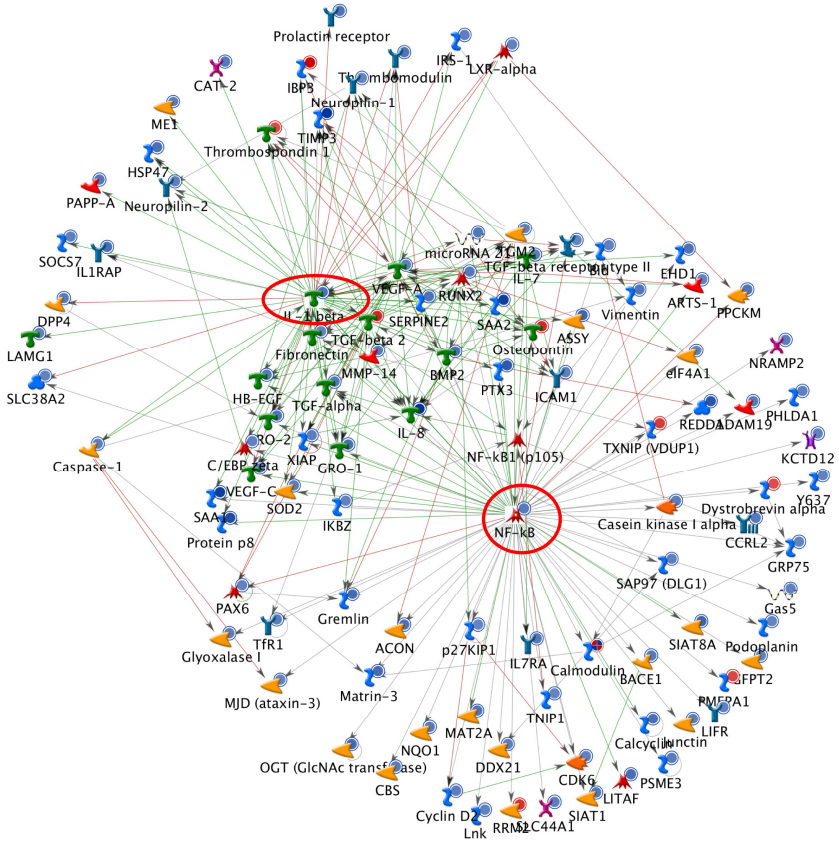

Figure 3.7. miR-7 regulation of NF-κB may cause down-regulation of IL-1 beta, which may target additional differentially expressed genes. Among genes differentially expressed after miR-7 transfection, RELA/NF-κB (circled in red) acts as a hub gene, and is found to target many of the differentially expressed genes. One of these, IL1-beta (circled in red) is significantly down-regulated and targets additional differentially expressed genes, thus, multiplying the effect of NF-κB down-regulation. Key: blue filled circle - significantly down-regulated gene; red filled circle – significantly up-regulated gene; green edges: activating interaction; red edges: inhibitory interaction; grey edges: unknown interaction.

Table 3.7. Direct downstream targets of Caveolin-1 and SMAD2. Caveolin-1 and SMAD2 are both identified as "hub genes" among the genes differentially expressed after miR-128 transfection. CAV1 is a predicted target of miR-128 but SMAD2 is not. By targeting CAV1, miR-128 indirectly regulates SMAD2 and triggers the differential expression of genes regulated by SMAD2 as well. Differentially expressed genes that are direct targets of either Caveolin-1 or SMAD2 are listed. The relative fold change of these genes following miR-128 transfection into HEY cells are also provided.

Caveolin-1 and its direct targets		SMAD2 and its direct targets	
Gene Symbol	**Fold change**	**Gene Symbol**	**Fold change**
CAV1	-2.44	BUB3	-1.65
CD40	2.25	COL1A1	2.40
CFL1	-1.70	DAB2IP	2.06
ENO2	1.78	DCAF7	-1.61
EPHB1	-2.66	DOCK9	1.57
FLNA	-2.09	ERC1	1.80
FOLR1	-1.86	FGFBP1	-1.55
GNAQ	1.53	HMGA2	-1.64
ITGA2	2.00	HMGN3	-1.49
ITPR1	2.09	ITGB5	-1.60
MAPK14	-1.83	KLF4	-1.42
NEDD8	-1.57	NEDD9	1.97
NGFRAP1	-1.79	NFIB	-1.54
NT5E	-1.73	OPA1	-2.03
PDE3B	-1.59	PKNOX1	1.58
PTEN	-2.74	PLIN3	-1.54
PTGS1	4.12	PRKAR1A	2.84
SEPT7	-1.98	SERPINE1	2.23
SLC9A7	1.71	SMAD2	-1.59
SMAD2	-1.59	ST13	-1.95
SPRY4	1.71	SURF6	1.55
STMN1	-1.72	TAF3	1.53
TNFRSF10A	1.70	TIMP3	-2.99
		TNFRSF11B	1.47
		TOB1	-1.69
		VEGFA	2.15
		WRNIP1	1.48
		WWP2	1.73
		ZFP106	2.10
		ZNHIT6	-1.63

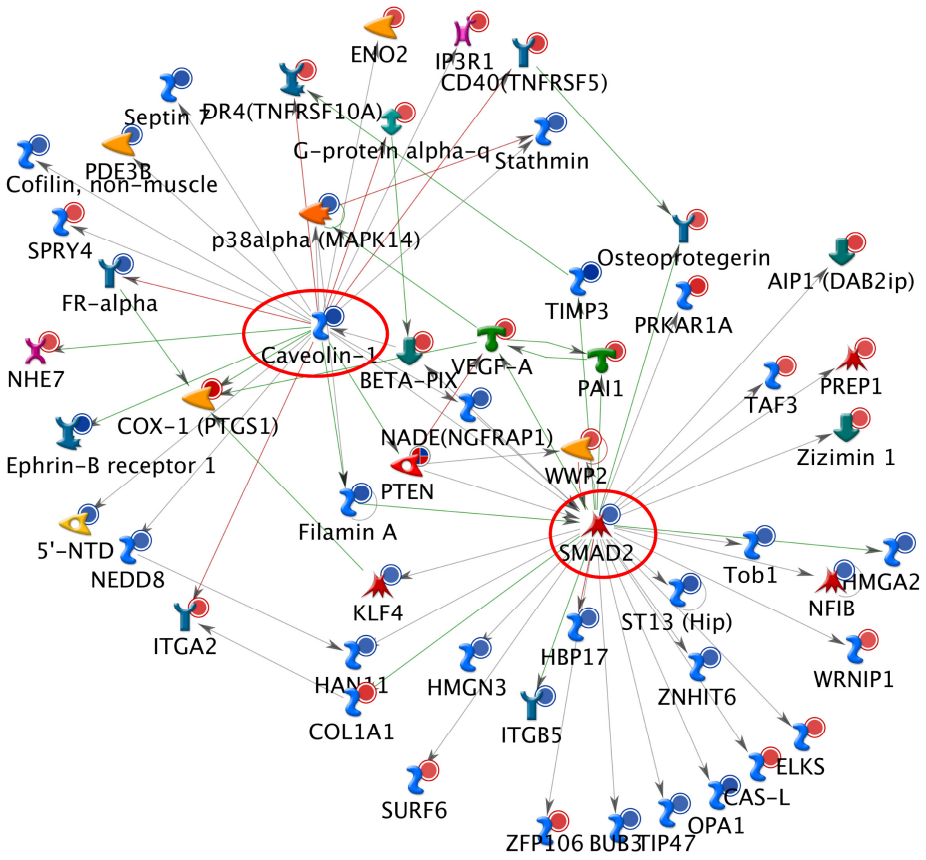

Figure 3.8. miR-128 may target the hub gene CAV1 which may regulate another hub gene SMAD2. Caveolin-1 (circled in red) is a significantly down-regulated hub gene and a predicted target of miR-128. One of its many direct downstream target genes is SMAD2 (also circled in red; regulation shown by arrow/edge pointing from Caveolin-1 to SMAD2), which itself acts as another hub gene. Several downstream targets of SMAD2 are also differentially expressed following miR-128 transfection. Thus by targeting the hub gene CAV1, miR-128 regulates the non-target hub gene SMAD2 and triggers a ripple effect on down-stream genes. Key: blue filled circle - significantly down-regulated gene; red filled circle – significantly up-regulated gene; green edges: activating interaction; red edges: inhibitory interaction; grey edges: unknown interaction.

miR-7 and miR-128 transfection modulates changes in the expression of genes involved in distinct developmental and cell cycle related pathways

While transfection of miR-7 or miR-128 were both found to significantly down-regulate EGFR expression, their direct and indirect effects on the expression of other genes were quite distinct. Of the 754 genes differentially expressed after miR-7 transfection and 2338 genes differentially expressed after miR-128 transfection, only 286 genes were in common among those differentially expressed by the two miRNAs. To evaluate the potential functional significance of the genes uniquely differentially expressed after miRNA transfection, we subjected the data to GeneGo pathway enrichment analysis.

The results of our functional pathway analysis indicate that genes differentially expressed after miR-7 transfection are significantly over-represented in 91 functional pathways (Figure 3.9A, Table B.8). The 20 most significantly over-represented pathways are listed in Table 3.8 and include several cell adhesion and developmental functions previously associated with aberrant levels of miR-7 expression in a variety of cancers (Chen et al., 2010a; Chou et al., 2010; Webster et al., 2009). We found that genes differentially expressed after miR-128 transfection are over-represented in 231 pathways (Figure 3.9B, Table B.9). The 20 most significantly over-represented pathways listed in Table 3.9 include a variety of pathways associated with cell cycle control consistent with previous studies linking miR-128 with cell proliferation functions in several cancers (Ciafre et al., 2005; Evangelisti et al., 2009; Godlewski et al., 2008; Guidi et al., 2010; Khan et al., 2010; Silber et al., 2008; Zhang et al., 2009).

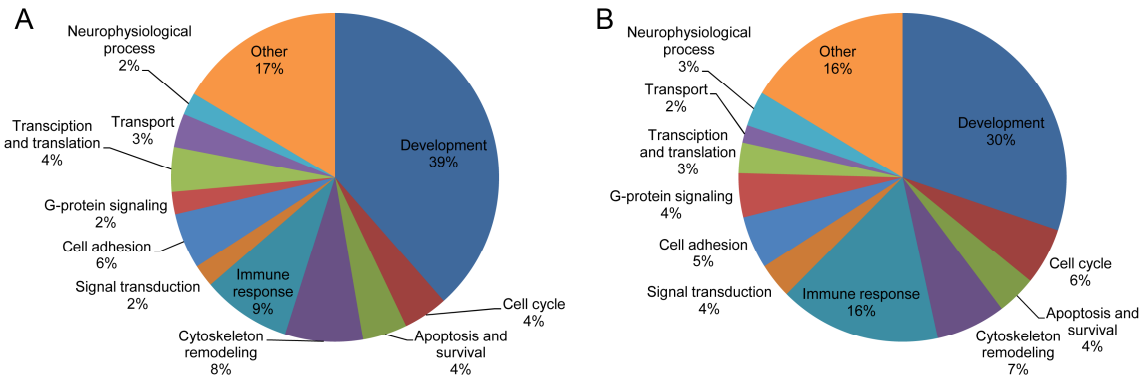

Figure 3.9. Pathways regulated by differentially expressed genes after miR-7 or miR-128 transfection. The majority of pathways enriched (FDR <0.05) among differentially expressed genes after either (A) miR-7 or (B) miR-128 transfection are related to development. However cell cycle, cytoskeleton remodeling, apoptosis and signal transduction pathways are also enriched and may signify cancer specific processes.

Table 3.8. Twenty most significantly enriched pathways among differentially expressed genes after miR-7 transfection into HEY cells. The 20 most significantly enriched (FDR <0.05) GeneGo pathway maps among the significantly differentially expressed genes after miR-7 transfection into HEY cells. The pathways that are also enriched among differentially expressed genes after miR-128 transfection are highlighted in **bold**.

Maps	p-value
Cell adhesion_Chemokines and adhesion	1.31E-07
Cell cycle_Regulation of G1/S transition (part 1)	8.68E-07
Cell adhesion_Ephrin signaling	3.96E-06
Development_EGFR signaling pathway	1.02E-05
Development_ERBB-family signaling	1.13E-05
Development_WNT signaling pathway. Part 1. Degradation of beta-catenin in the absence WNT signaling	1.42E-05
Development_VEGF-family signaling	1.68E-05
Cytoskeleton remodeling_Cytoskeleton remodeling	3.13E-05
Neurophysiological process_Receptor-mediated axon growth repulsion	3.43E-05
Proteolysis_Putative ubiquitin pathway	3.44E-05
Development_TGF-beta-dependent induction of EMT via RhoA, PI3K and ILK.	4.05E-05
Cell adhesion_Plasmin signaling	4.85E-05
Development_TGF-beta-dependent induction of EMT via SMADs	4.85E-05

Table 3.8 (continued)

Maps	p-value
Transport_RAB5A regulation pathway	5.75E-05
Cytoskeleton remodeling_TGF, WNT and cytoskeletal remodeling	7.29E-05
Cell cycle_Regulation of G1/S transition (part 2)	7.30E-05
Apoptosis and survival_HTR1A signaling	7.54E-05
Development_Regulation of epithelial-to-mesenchymal transition (EMT)	7.67E-05
Translation _Regulation of EIF2 activity	1.01E-04
Cell adhesion_ECM remodeling	1.01E-04

Table 3.9. Twenty most significantly enriched pathways among differentially expressed genes after miR-128 transfection into HEY cells. The 20 most significantly enriched (FDR <0.05) GeneGo Pathway maps among the significantly differentially expressed genes after miR-128 transfection into HEY cells. The pathways that are also enriched among differentially expressed genes after miR-7 transfection are highlighted in **bold**.

Maps	p-value
Cell cycle_The metaphase checkpoint	1.01E-11
Cytoskeleton remodeling_TGF, WNT and cytoskeletal remodeling	1.29E-09
Cell cycle_Role of Nek in cell cycle regulation	1.77E-09
Transport_Clathrin-coated vesicle cycle	4.15E-09
Cell cycle_Initiation of mitosis	4.37E-09
Immune response_Histamine H1 receptor signaling in immune response	1.78E-07
Cell cycle_Role of APC in cell cycle regulation	1.79E-07
Cell cycle_Spindle assembly and chromosome separation	2.75E-07
Cytoskeleton remodeling_Cytoskeleton remodeling	2.98E-07
Proteolysis_Role of Parkin in the Ubiquitin-Proteasomal Pathway	3.68E-07
Cytoskeleton remodeling_Neurofilaments	6.14E-07
Cell cycle_Chromosome condensation in prometaphase	8.18E-07
Immune response_Gastrin in inflammatory response	1.85E-06
Neurophysiological process_Receptor-mediated axon growth repulsion	2.69E-06
Translation_Non-genomic (rapid) action of Androgen Receptor	3.55E-06
Development_PIP3 signaling in cardiac myocytes	4.80E-06
Cytoskeleton remodeling_Role of Activin A in cytoskeleton remodeling	5.34E-06
Apoptosis and survival_Apoptotic Activin A signaling	5.76E-06
Apoptosis and survival_BAD phosphorylation	6.54E-06
Immune response_Fc epsilon RI pathway	7.40E-06

Of the 252 pathways (not additive due to overlap) significantly over-represented among genes differentially expressed after miR-7 or miR-128 transfection, only 71 pathways were found to overlap (including the EGFR pathway). Among the 20 most significantly enriched pathways only 3 were found to overlap. Among genes down-regulated following miR-7 transfection most pathways are involved in development, while among those down-regulated following miR-128 transfection most pathways are involved in cell cycle regulation (Figure 3.10, Tables B.10 and B.11) [Note a similar analysis of enriched pathways among up-regulated genes revealed only 1 pathway enriched for miR-7 and 70 pathways enriched for miR-128 (Tables B.12 and B.13)]. These results are consistent with the view that the targets of miRNA regulation are often functionally distinct (He et al., 2010).

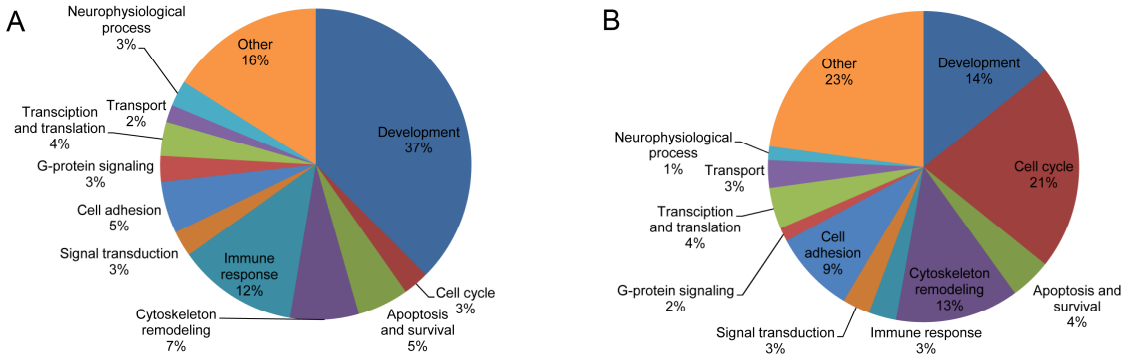

Figure 3.10. Pathways regulated by down-regulated genes after miR-7 or miR-128 transfection. Distribution of groups of pathways enriched among down-regulated genes after (A) miR-7 or (B) miR-128 transfection. While pathways involved in development made up the largest fraction of enriched pathways for miR-7, the genes down-regulated by miR-128 were enriched for more pathways involved in cell cycle regulation, revealing a distinct pathway signature for each miRNA.

Discussion and Conclusion

Although the role of miRNAs and other non-encoding RNAs in the regulation of cellular function is only beginning to be understood, the diagnostic and therapeutic potential of these regulatory RNAs is already widely recognized and accepted (Garofalo and Croce, 2011; Kota et al., 2009). Indeed, a number of pre-clinical diagnostic and therapeutic trials of miRNAs are currently in progress (Wahid et al., 2010). The initial results of these studies appear to be generally supportive of the diagnostic potential of miRNAs (Chan et al., 2011; Krutovskikh and Herceg, 2010; Metias et al., 2009), but significant questions remain with respect to their potential therapeutic value.

One of the challenges to the use of miRNAs as therapeutic agents is technical in nature and deals with the problems of the packaging and the targeted delivery of miRNAs to cancer cells. Significant progress has been made in this area in recent years and all indications are that these technical challenges are not insurmountable (Chen et al., 2010b; Esau and Monia, 2007; Liu et al., 2011). The second challenge is more scientific in nature and centers around our current inability to precisely predict the molecular consequences of modulating miRNA levels on cell function. While the exogenous administration of miRNAs (or miRNA-antagomirs) have been shown to be capable of effectively regulating targeted oncogenes and tumor suppressor genes in specific cellular contexts (Garofalo and Croce, 2011), the off-target or indirect effects of perturbing miRNA levels remain difficult to predict. Since this molecular unpredictability could translate into clinically unanticipated side-effects, it may significantly mitigate the intended therapeutic benefits (Barh et al., 2010; Mishra and Merlino, 2009; Small et al., 2010). It is generally agreed that increased therapeutic predictability of miRNAs and

other regulatory RNAs will require a better understanding of the processes underlying the molecular function of these molecules *in vivo* (Budhu et al., 2010; Mishra and Merlino, 2009; Phalon et al., 2010).

In an initial effort to systematically dissect the molecular consequences of exogenously modulating levels of miRNA in cancer cells, we transfected two distinct human miRNAs, miR-7 and miR-128, into a well-characterized ovarian cancer cell line and monitored the consequent changes on endogenous levels of gene expression. These specific miRNAs were chosen because they have both been previously implicated in ovarian cancer (Sorrentino et al., 2008; Wyman et al., 2009, see also CHAPTER 2) and because both are predicted to regulate the expression of EGFR (Webster et al., 2009; Weiss et al., 2008), the oncogene selected for targeting in our study. EGFR is known to be over-expressed in ovarian and many other cancers and is often selected for targeted chemotherapy (Thaker et al., 2005; Zeineldin et al., 2010).

We found that transfection of miR-7 and miR-128 were equally effective at knocking down EGFR expression and that both resulted in significant changes in expression of hundreds of "off-target" genes. We tested the hypothesis that these off-target effects were not simply the downstream consequences of the knock-down of EGFR by transfecting HEY cells with an siRNA specifically designed against EGFR. The siRNA transfection also resulted in effective knock-down of EGFR, but in addition, significant changes in the expression of only eight off-target genes. Thus, the observed changes in expression of hundreds of off-target genes after the miRNA transfections are not merely the down-stream consequences of reduced EGFR expression.

Consistent with the fact that miR-7 is predicted to target fewer genes than miR-128 (using miRanda, TargetScan or PicTar), we found that the number of genes differentially expressed after miR-7 transfection was substantially less (approximately one-third) than the number differentially expressed after miR-128 transfection. To determine if the large number of genes differentially expressed after the miRNA transfections were likely due to the direct regulatory action of the miRNAs, we computed the proportion of differentially expressed genes that are direct targets of miR-7 or miR-128 regulation as predicted by the three major target prediction algorithms. On average, the percentage of differentially expressed genes that are predicted to be directly regulated by either miRNA was less than one-fifth indicating that most of the off-target changes in gene expression induced by the miRNA transfections are indirect.

One recently described model to account for indirect effects of miRNA transfection postulates that transfected miRNAs may out compete endogenous miRNAs for available RISC complexes (Khan et al., 2009). Under this model mRNA targets of the displaced miRNAs are expected to experience lower levels of degradation and thus display an increase in relative abundance after miRNA transfection. Accordingly, those genes targeted by miRNAs in high abundance in pre-transfected cells are predicted to experience the greatest change in expression (Khan et al., 2009; Landthaler et al., 2008; Sood et al., 2006; Tang et al., 2008a). This model may be particularly relevant with respect to our miR-128 transfection experiment where the majority (80 %) of differentially expressed genes displayed a significant increase in gene expression.

Consistent with the predictions of the RISC-competition model, we found that mRNAs enriched for binding sites of those miRNAs most highly expressed in pre-

transfected HEY cells were significantly over-represented among mRNAs up-regulated after miR-128 transfection. These results indicate that the RISC-competition model is a plausible explanation of the high proportion of genes displaying increased expression after miR-128 transfection. The fact that we observed a much lower proportion of genes displaying increased levels of expression after miR-7 transfection suggests that the relative importance of RISC-competition may be miRNA dependent.

Perhaps the most commonly observed mechanism underlying coordinated changes in global patterns of gene expression involves the modulation of centralized or "hub" regulatory genes (Seo et al., 2009; Shalgi et al., 2007). Hub genes have the potential to exert control on suites of down-stream genes thereby inducing cascades of regulatory mediated changes in patterns of gene expression (Wang et al., 2007). Our network analyses revealed that a substantial number of genes differentially expressed after miR-7 or miR-128 transfection (and predicted to be targeted by these miRNAs) are regulatory hubs capable of controlling many of the down-stream genes that were differentially expressed after miR-7 and miR-128 transfection. These findings indicate that miRNAs can both directly and indirectly induce changes in cellular regulatory networks that may be responsible for a significant fraction of the off-target effects associated with miRNA transfection.

In general, our experiments demonstrate that exogenous expression of miRNAs induce regulatory changes far in excess of those on the intended target. From the clinical perspective, this begs the question as to whether miRNAs are appropriate agents for cancer therapy. Clearly, if the clinical intent is to precisely silence a specific gene and if the collateral off-target effects induced by miRNAs are counter-therapeutic, the answer

would be “no”. However, it is important to keep in mind that miRNAs have been evolving as essential components of the eukaryotic regulatory system for millions of years. Thus, the network of regulatory effects exerted by miRNAs is unlikely to be random and indeed may eventually provide clinicians with a strategy to treat cancer cells from a systems rather than a single gene perspective.

Our functional analysis of the pathways most significantly affected by miR-7 and miR-128 transfection demonstrate that while both miRNAs can effectively down-regulate the targeted EGFR gene, the off-target changes are significantly diverse in their predicted functional consequences. The pathways most significantly affected by miR-7 transfection are predicted to be involved with cell adhesion and other developmental networks previously associated with epithelial-to-mesenchymal transitions (EMT) and other processes linked with metastasis (Yang and Weinberg, 2008). In contrast, the pathways most significantly affected by miR-128 transfection are more focused on cell cycle control and other processes commonly linked with cellular replication (Hanahan and Weinberg, 2011). Although both sets of functions are generally characteristic of cancer cells, particular pathways may be relatively more important in particular tumors. As we learn more about the functional specialization of different families of miRNAs, we will be in a better position to interpret the significance of changes in miRNA expression in particular cancer types and to become more precise in our selection of miRNAs for possible use in targeted cancer therapy.

In summary, we have confirmed earlier studies showing that miRNAs can be effectively used to knock-down the expression of specific genes implicated in cancer. We have additionally shown that changes in the expression of off-target genes is not merely

the down-stream consequence of target gene inactivation but the result of direct and indirect regulatory effects mediated by the transfected miRNAs. We found that these off-target effects are not random but can be explained, in large measure, by molecular models derived from our current understanding of miRNA function. Clearly, additional studies will be required to further evaluate the validity of these and other explanatory models in various types of cancer cells and other families of miRNAs. Nevertheless, the results of our preliminary studies indicate that while the molecular regulatory mechanisms underlying miRNA functions *in vivo* are extremely complex, they are not intractable. Validated models that can be used today to retrospectively explain the impact of exogenously expressed miRNAs, may be used in the future to prospectively design optimal system-wide strategies for the effective treatment of cancer.

Materials and Methods

Cell culture and miRNA/siRNA transfections

HEY cells were provided by Gordon B. Mills, Department of Systems Biology, the University of Texas, M. D. Anderson Cancer Center and were cultured according to methods described in CHAPTER 2. Briefly, the cells were transfected with the miRNA hsa-miR-7 miRIDIAN mimic, miRIDIAN miRNA mimic negative control #1 (miR-NC, a *C.elegans* miRNA, cel-miR-67, with confirmed minimal sequence identity in humans), hsa-miR-128 miRIDIAN mimic (same negative control transfected cells were used to compare miR-7 and miR-128 transfected cells), ON-TARGET *plus* Anti-EGFR siRNA or ON-TARGET *plus* non-targeting siRNA (siNC) (Thermo Fisher Scientific, Lafayette, CO) using Lipofectamine 2000 transfection agent (Invitrogen) according to the

manufacturer's instructions at a final concentration of 25nM (or left untransfected for naïve cells). All transfections were carried out with two or three replicates. The cells were incubated with the reduced serum transfection medium (Opti-MEM, Invitrogen) for 4 hours, washed and then allowed to grow in growth medium (RPMI 1640, Mediatech, Manassas, VA) for 44 hours before collecting RNA or protein. Transfection efficiency was estimated from the relative knock-down of EGFR for miR-7 and the anti-EGFR siRNA, and for BMI1 for miR-128 (Figure A.1), based on recommendations by the siRNA/miRNA reagent manufacturer (Thermo Fisher Scientific).

RNA isolation and whole genome microarray

Total RNA was isolated using the RNeasy Mini RNA isolation kit (QIAGEN, Valencia, CA) according to the manufacturer's instructions. The integrity of the RNA was verified using an Agilent 2100 Bioanalyzer (1.8-2.0; Agilent Technologies, Palo Alto, CA). MRNAs were converted to double stranded (ds)-cDNA and amplified using Applause 3'-Amp System (NuGen, San Carlos, CA). This cDNA was then biotin labeled and fragmented by using Encode Biotin Module (NuGen). The labeled cDNA was hybridized to Affymetrix HG-U133 Plus 2.0 oligonucleotide arrays and analyzed with a GeneChip Scanner 3000 (Affymetrix, Santa Clara, CA).

RNA isolation and miRNA microarray

Total RNA was isolated from two independent samples of HEY cells using the mirVana miRNA isolation kit according to the manufacturer's instructions (Applied Biosystems, Foster City, CA). The quantity and size of microRNA was verified using an

Agilent 2100 Bioanalyzer (Agilent Technologies, Palo Alto, CA). MiRNAs were labeled with Genisphere FlashTag HSR Biotin RNA labeling kit (Genisphere, Hatfield, PA) followed by hybridization with GeneChip miRNA Array chips (Affymetrix, Santa Clara, CA) according to the manufacturer's instructions. The chips were washed and then scanned with a GeneChip Scanner 3000 (Affymetrix). Raw data in the form of CEL files were produced by the Affymetrix GeneChip Operating System (GCOS) software.

Quantitative (real-time) PCR (qPCR)

Total RNA (1-5 μg) extracted from cells (three biological replicates) was converted to cDNA using the Superscript III First Strand synthesis system (Invitrogen). cDNA was then purified using the QIAGEN PCR purification kit (QIAGEN) following manufacturer's instructions. QPCR experiments were carried out for the EGFR, BMI1 and GAPDH genes using iQ SYBR Green Supermix (Bio-Rad, Hercules, CA). The sequence specific primers used for SYBR green assays are as follows: EGFR-forward: GGAGAACTGCCAGAAACTGACC, EGFR-reverse: GCCTGCAGCACACTGGTTG, GAPDH-forward: GGTCTCCTCTGACTTCAACA, GAPDH-reverse: AGCCAAATTCGTTGTCATAC. The EGFR primers were as designed by (Micallef et al., 2009) and GAPDH primers were as designed by (Koppelstaetter et al., 2005). Description of BMI1 primers is provided in CHAPTER 2. The GAPDH primer efficiencies were calculated to be ~1. All reactions were optimized with non-template controls, and -RT (minus reverse transcriptase) controls prior to experiment.

All qPCR reactions were carried out using at least three technical replicates and three biological replicates on the CFX96 Real Time PCR detection system (Bio-Rad). Expression values were normalized to an endogenous control (GAPDH). Relative fold change of target RNA level between transfection groups was determined by the ΔΔCt method. Statistical significance was determined using the pair-wise fixed reallocation randomization test in the Relative Expression Software Tool (REST 2008; Pfaffl et al., 2002).

Immunoblotting

Immunoblotting for EGFR and β-Actin was performed as described previously (Blackburn et al., 2009) with the following modifications. The blots were washed three times with TBST and probed with goat antirabbit IgG (Southern Biotech, Birmingham, AL) linked to Fluorescein (FITC), or with donkey antimouse IgG (Southern Biotech) linked to Phycoerythrin (PE) secondary antibodies [primary anti-EGFR antibodies are described in (Blackburn et al., 2009)]. Bands were visualized using a Typhoon 9400 Imager (GE Healthcare, Piscataway, NJ) followed by densitometric analysis using the ImageQuant TL Software (GE Healthcare). Statistical significance of difference between average levels from at least three replicates quantified by densitometry was determined using a 2-tailed unpaired Student's t-test.

Microarray data analysis

Raw data from miRNA microarray were analyzed using miRNA QC Tool software (Affymetrix, Santa Clara, CA). Normalization was performed using the default

workflow of the miRNA QC Tool software. Briefly, probesets were tested for detection above background using a Wilcoxon Rank-Sum test ($p < 0.06$) and then normalized using quantile normalization. Probesets with 'FALSE' call in all groups were removed from statistical analysis. A constant (16) is added for variance stabilization and then values are summarized using the median polish method. The log base 2 transformed expression values were then used for calculations. Annotations for probesets were obtained from the Affymetrix website (http://www.affymetrix.com).

MRNA microarray data were normalized and processed according to the procedure described in CHAPTER 2.

Frequency distribution of miRNA signal values

Only miRNAs with at least one 'TRUE' detection call across all samples and 'hsa'- prefix in probeset names were used for plotting the distribution of signal values. A histogram of signal value distribution was plotted using the 'data analysis' package in Microsoft Excel. Percentage of values within each bin were then calculated and plotted on a chart in Excel.

Venn diagram of differentially expressed genes

A Venn diagram of the different number of DEGs was plotted using the PAST toolkit Venn Diagram Plotter downloaded from the http://omics.pnl.gov website (also www.pnl.gov)

Pathway enrichment analysis, identification of hub genes and network building

After identification of differentially expressed genes, GeneGo Pathway Maps analyses, and GeneGo Process Networks analyses were carried out using GeneGo (http://www.GeneGo.com/) gene ontology software. Hub genes were identified using the GeneGo interactome analyses with the 'Significant interactions within sets' algorithm. In all cases significance was based on a false discovery rate filter at a stringency of q-value <0.05. Networks were built using functional and binding interactions unless transcriptional regulation is specified.

MiRNA target download

The miRNA targets prediction files based on miRanda were downloaded from www.microrna.org (August 2010 release; Betel et al., 2008; Enright et al., 2003; John et al., 2004). "Good" mirSVR score refers to miRNA targets with <-0.1 score, and "non-good" mirSVR score refers to targets with >-0.1 score obtained from the support vector regression algorithm mirSVR, available with target predictions in the above link. Information about the prediction algorithm, parameter settings and raw data source is available on the above link. Target predictions based on TargetScan were downloaded from www.targetscan.org (Friedman et al., 2009; Grimson et al., 2007; Lewis et al., 2005) and predictions for PicTar were obtained from www.pictar.org (Ge and Manley, 1990; Krainer et al., 1990; Krek et al., 2005; Zhou et al., 2002).

MiRNA target enrichment analysis among up-regulated genes

Gene set enrichment analysis for predicted microRNA targets among differentially expressed genes was carried out using the web interface of Genomica, a

software for analysis and visualization of genomic data available at http://genomica.weizmann.ac.il/ (Lubling and Segal). All parameters were kept in default settings for our analyses. Differentially expressed genes were divided into up-regulated and down-regulated gene sets, uploaded onto the Genomica server for analysis, and finally enrichment was performed against the 'Human MicroRNA RNA' gene set with a FDR correction threshold of 0.05. When only a miRNA family is identified (without specifying the identity of the paralog) all members of the family were considered (e.g., hsa-miR-146a and hsa-miR-146b were both considered when Genomica identified hsa-miR-146).

CHAPTER 4

MICRORNAS CAN INDIRECTLY REGULATE OTHER MICRORNAS

Abstract

MicroRNAs (miRNAs) are a class of regulatory RNAs that control the expression of genes critical to cell function. Ectopic expression of miRNAs has been shown to result in genome-wide changes in patterns of gene expression. While the reasons for these global alterations in gene expression patterns have been attributed to the ability of miRNAs to target multiple genes, and/or to induce indirect effects downstream of target genes, the molecular basis of indirect effects of miRNA regulation remains poorly understood. In this study, we demonstrate the potential of miRNAs to regulate other miRNAs. Using miRNA microarray analysis, we show that over 70 different miRNAs are differentially expressed (fold change ≥1.4, FDR ≤5 %) in human ovarian cancer cells after transfection with a single miRNA (miR-7). We present evidence that a major component of miR-7 induced changes in levels of miRNAs is the indirect consequence of miR-7 mediated alterations in levels of protein coding genes (e.g., transcription and splicing factors) that exert trans-regulatory control on miRNAs.

Introduction

MicroRNAs (miRNAs) are a conserved class of small RNAs that can regulate gene expression by altering the translation and/or mRNA stability of target genes (Bartel, 2004; Fabian et al., 2010). Since miRNAs are differentially expressed in cancer and other

diseases (Calin and Croce, 2006a; Esquela-Kerscher and Slack, 2006; Farazi et al., 2011; Lee and Dutta, 2009; Visone and Croce, 2009; Wiemer, 2007), they may have clinical potential as diagnostic, prognostic and/or therapeutic agents (Garofalo and Croce, 2011; Wahid et al., 2010). However, the molecular causes and consequences of perturbations in levels of miRNAs in cancer cells can be varied and complex (e.g., Baek et al., 2008; Lim et al., 2005; Selbach et al., 2008; see also CHAPTER 3). Thus, the potential clinical impact that miRNAs will ultimately have in cancer medicine rests heavily upon our ability to understand the basis of this complexity. We report here that perturbations in levels of a single miRNA can not only induce significant changes in levels of mRNAs but also significantly modulate levels of other miRNAs. We discuss the potential significance of miRNA-miRNA regulation in cancer cells and present evidence for molecular mechanisms that may underlie the process.

Results

Ectopic expression of miR-7 alters the levels of endogenous microRNAs

To study the effect of changes in levels of a single microRNA on expression levels of other miRNAs in cancer cells, we transfected a well-characterized ovarian cancer cell line (HEY) with a miRNA (miR-7) previously shown to be significantly up-regulated in ovarian and other cancers (Chou et al., 2010; Jiang et al., 2010; Kefas et al., 2008; Reddy et al., 2008; Saydam et al., 2010; Veerla et al., 2009; Webster et al., 2009; Wyman et al., 2009; see also CHAPTER 2). To assess the biological effectiveness of our transfection, we monitored changes in levels of EGFR, a previously validated target of miR-7 (Kefas et al., 2008; Webster et al., 2009). Since it has previously been

demonstrated that EGFR is highly expressed in HEY cells (Dickerson et al., 2010), we expected levels of EGFR mRNA and protein to be significantly reduced after a successful miR-7 transfection. Our results confirm that levels of EGFR mRNA and protein are both significantly reduced after miR-7 transfection (Figure 4.1) relative to a negative control (miR-NC, miRIDIAN miRNA mimic negative control, Thermo Fisher Scientific).

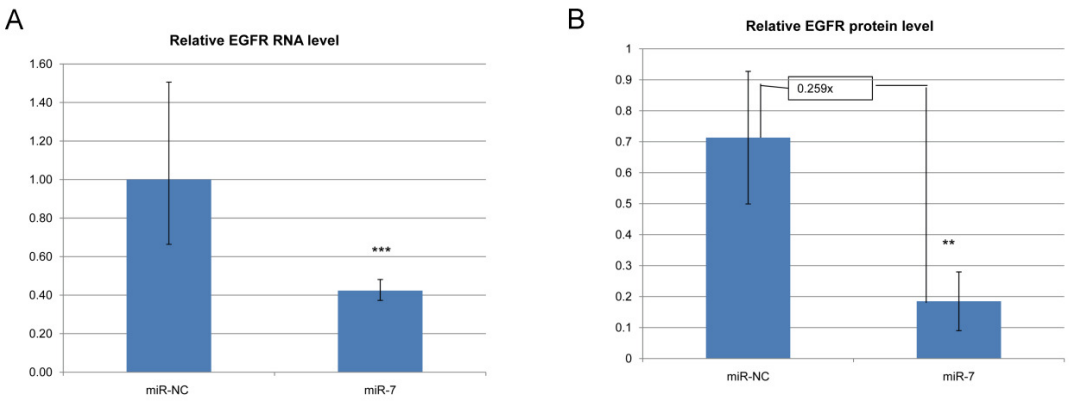

Figure 4.1. Confirmation of successful transfection of miR-7 into HEY cells. Successful transfection of miR-7 into HEY cells is confirmed by measuring the level of EGFR RNA (A) by qPCR and (B) protein by Western blot analysis. In both cases EGFR expression is down-regulated significantly (*** $p < 0.001$, ** $p < 0.05$) after miR-7 transfection compared to negative control (miR-NC) transfection. The bars in (B) reflect relative quantitation of the bands of the immunoblot using densitometry (based on three replicate samples). Relative expression values are shown on the Y-axis. EGFR expression is normalized to (A) GAPDH used as endogenous control, or (B) β-Actin used as loading control. Error bars reflect standard deviation of the means calculated from three independent replicate samples. The number in the box is the fold change difference in EGFR protein levels between miR-NC and miR-7 transfections.

A

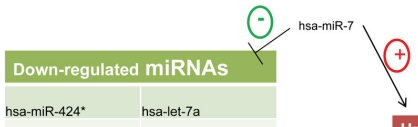

Down-regulated miRNAs	
hsa-miR-424*	hsa-let-7a
hsa-miR-503	hsa-let-7g
hsa-miR-7-1*	hsa-miR-98
hsa-miR-199a-3p	hsa-miR-137
hsa-miR-199b-3p	hsa-miR-30e*
hsa-miR-224	hsa-miR-10a
hsa-miR-29b-1*	hsa-miR-199a-5p
hsa-miR-1274a	hsa-miR-193a-3p
hsa-miR-494	hsa-miR-126
hsa-miR-30a*	hsa-let-7f
hsa-miR-218	hsa-miR-92a-1*
hsa-miR-155	hsa-miR-1224-5p
hsa-miR-221*	hsa-miR-10b
hsa-miR-584	hsa-miR-424
hsa-miR-374b	hsa-miR-15b
hsa-miR-198	hsa-miR-17
hsa-miR-223	hsa-miR-100*
hsa-miR-204	hsa-miR-30d*
hsa-mir-139-5p	hsa-miR-20b
hsa-miR-92a	hsa-let-7c

Up-regulated miRNAs	
hsa-let-7i*	hsa-miR-330-3p
hsa-mir-1180	hsa-miR-337-5p
hsa-mir-1246	hsa-miR-338-3p
hsa-miR-1303	hsa-miR-33a
hsa-miR-140-5p	hsa-miR-421
hsa-miR-142-5p	hsa-miR-425*
hsa-miR-146a	hsa-mir-542-5p
hsa-miR-149	hsa-miR-550a
hsa-miR-181a-2*	hsa-miR-551b
hsa-miR-181b	hsa-miR-590-5p
hsa-miR-181c	hsa-miR-628-3p
hsa-miR-181d	hsa-miR-652
hsa-miR-200b	hsa-miR-877
hsa-miR-210	hsa-miR-93*
hsa-miR-26b*	hsa-miR-99b*
hsa-miR-301b	

B

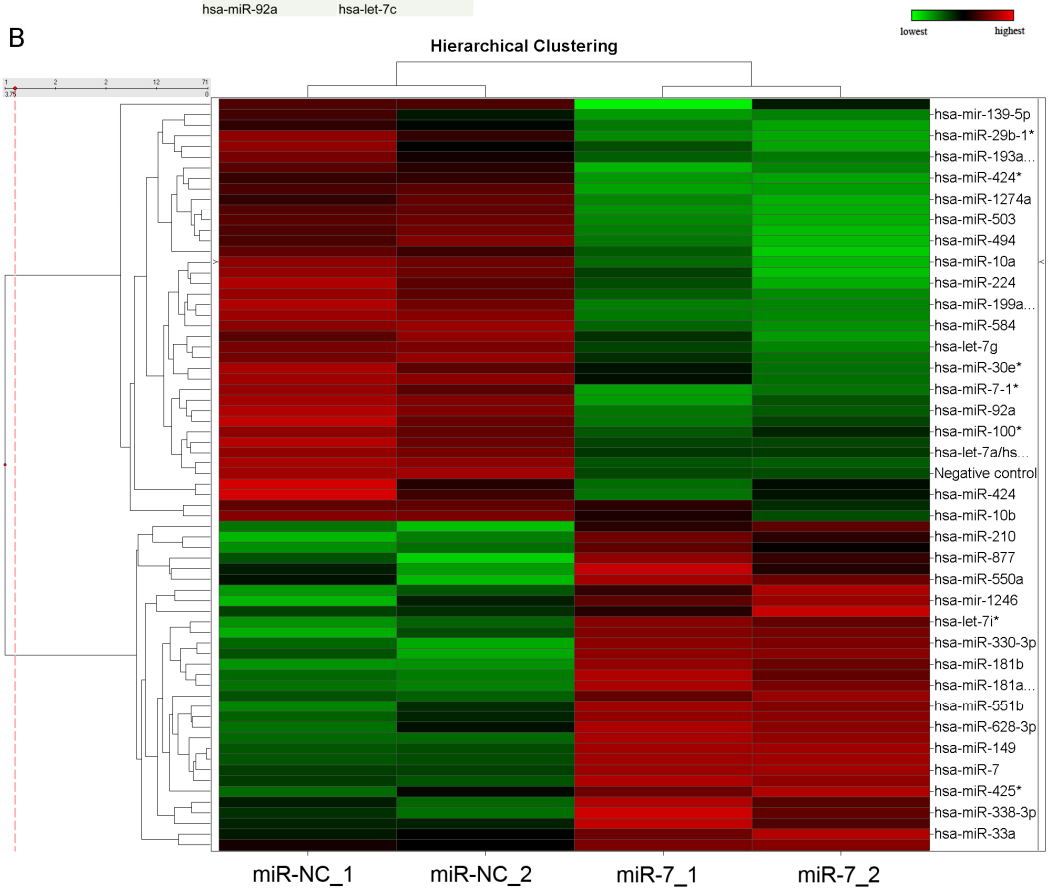

Figure 4.2. MicroRNAs differentially expressed after miR-7 transfection in HEY cells. (A) List of differentially expressed (fold change ≥1.4 and FDR ≤5 %) miRNAs following transfection of hsa-miR-7 into HEY cells compared to miR-NC transfected cells. There were 40 different human miRNAs significantly down-regulated and 31 miRNAs significantly up-regulated (excluding miR-7) after miR-7 transfection. (B) Hierarchical clustering of significantly differentially expressed miRNAs between cells transfected with either miR-7 or miR-NC. Each column of the heat map corresponds to a sample. The two negative control samples are on the left and the two miR-7 transfected samples are on the right. Selected IDs of the human miRNAs homologous to the sequences specified by the probesets are shown on the right side of the heat map. [Note some of the miRNA names have an asterisk (*) indicating miRNA star strand].

To evaluate the effect of miR-7 transfection on global miRNA expression profiles, we isolated total RNA from cells transfected with either miR-7 or a negative control miRNA (miR-NC) 48h after transfection and monitored changes in levels of miRNA expression by microarray analysis. The results demonstrate that 259 distinct miRNA probesets corresponding to 71 mature miRNAs (excluding miR-7) were significantly altered in expression (31 up-regulated; 40 down-regulated) in the miR-7 transfected cells relative to controls (Figure 4.2, Table C.1). Eight of the miRNAs displaying significant changes in expression by microarray (hsa-miR-198, hsa-miR-628-3p, hsa-miR-149, hsa-miR-10b, hsa-let-7f, hsa-miR-503, hsa-miR-218 and hsa-miR-224) were randomly selected for confirmatory qPCR analysis. The results were uniformly consistent with the microarray results (Figure 4.3).

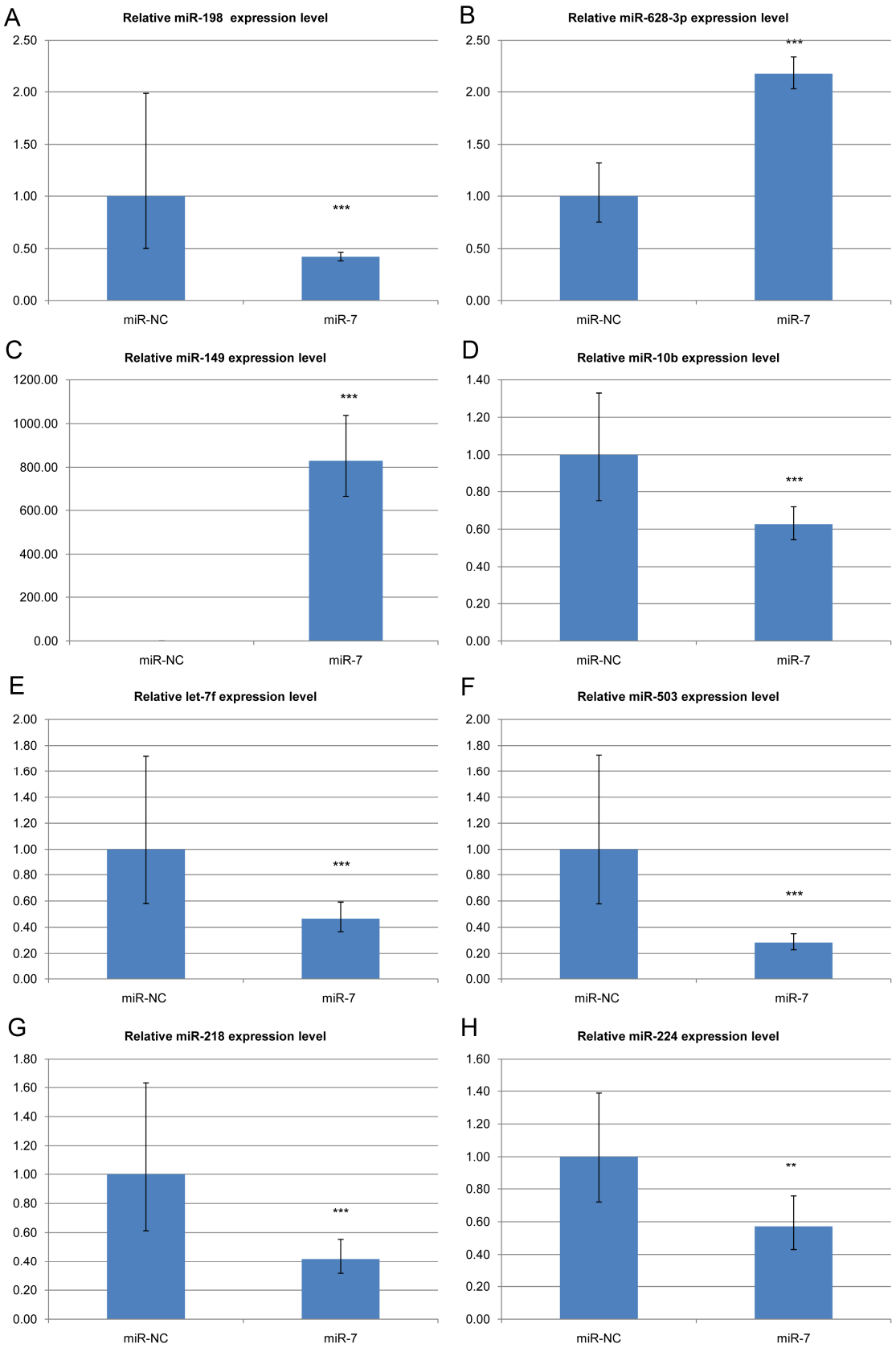
A
Relative miR-198 expression level
2.50
2.00
1.50
1.00
0.50
0.00
***
miR-NC
miR-7
B
Relative miR-628-3p expression level
2.50
2.00
1.50
1.00
0.50
0.00
***
miR-NC
miR-7
C
Relative miR-149 expression level
1200.00
1000.00
800.00
600.00
400.00
200.00
0.00
***
miR-NC
miR-7
D
Relative miR-10b expression level
1.40
1.20
1.00
0.80
0.60
0.40
0.20
0.00
***
miR-NC
miR-7
E
Relative let-7f expression level
2.00
1.80
1.60
1.40
1.20
1.00
0.80
0.60
0.40
0.20
0.00
***
miR-NC
miR-7
F
Relative miR-503 expression level
2.00
1.80
1.60
1.40
1.20
1.00
0.80
0.60
0.40
0.20
0.00
***
miR-NC
miR-7
G
Relative miR-218 expression level
1.80
1.60
1.40
1.20
1.00
0.80
0.60
0.40
0.20
0.00
***
miR-NC
miR-7
H
Relative miR-224 expression level
1.60
1.40
1.20
1.00
0.80
0.60
0.40
0.20
0.00
**
miR-NC
miR-7

Figure 4.3. Quantitative PCR confirmation of miRNAs differentially expressed after miR-7 transfection. Quantitative (real-time) PCR analysis of (A) hsa-miR-198, (B) hsa-miR-628-3p, (C) hsa-miR-149, (D) hsa-miR-10b, (E) hsa-let-7f, (F) hsa-miR-503, (G) hsa-miR-218, and (H) hsa-miR-224 in HEY ovarian cancer cells 48h after transfecting hsa-miR-7 or miR-NC. RNA expression levels were normalized to human U6 small nucleolar RNA (RNU6B) used as the endogenous control. Relative expression values are shown on the Y-axis. The relative fold change of each miRNA is also shown (in text box). Error bars reflect standard deviation of the means calculated from three independent replicate samples. *** $p < 0.001$, ** $p < 0.05$.

The majority of genes in which differentially expressed miRNAs are embedded do not display correlated changes in expression

Human miRNAs have been mapped to exons and introns of protein coding and non-protein coding genes (i.e. embedded in genes), as well as to intergenic miRNA encoding loci (Kim and Nam, 2006). Some embedded miRNAs have been shown to display changes in expression levels that positively correlate with those of their host genes. Such correlated patterns of expression are consistent with the hypothesis that embedded miRNAs and their host genes are under the same and/or coordinated regulatory controls (Baskerville and Bartel, 2005; Rodriguez et al., 2004). In other cases, changes in patterns of embedded miRNAs do not correlate with those of their host genes (Bargaje et al., 2010) indicating that at least some embedded miRNAs are under independent regulatory control (Fujita and Iba, 2008; Monteys et al., 2010; Ozsolak et al., 2008).

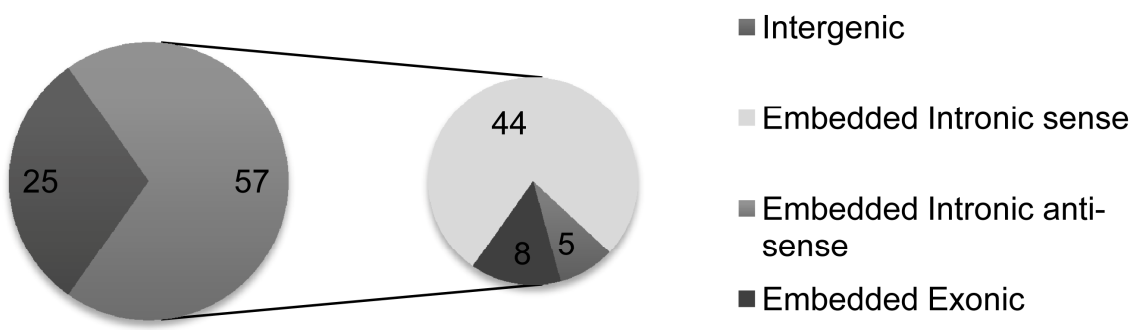

Figure 4.4. Genomic location of differentially expressed miRNAs between miR-7 transfected and negative control transfected HEY cells. The pie-chart on the left shows the proportion of differentially expressed miRNAs that are either embedded in known genes or intergenic. The pie-chart on the right shows that the embedded miRNAs can be classified further based on whether they come from intronic, exonic or anti-sense regions. MiRNAs that can be either from intron or exon are counted under both categories (scored twice). The raw numbers used for generating the pie-charts are also shown.

Table 4.1. MiRNAs embedded in protein coding and non-protein coding genes. Differentially expressed embedded miRNAs (fold change ≥1.4, FDR ≤5 %) and their respective host genes are listed. The difference between $\log_2$ average expression values of miR-7 and miR-NC transfected cells calculated from microarray analysis is shown for both the miRNAs (miRNA LR) and their host genes (Gene LR). Transcripts with Affymetrix "Absent" calls in every sample are marked absent. MiRNAs encoded from the same cluster are in cells shaded using the same color. MiRNAs with putative independent promoters are also marked with the letters a, b, or c in superscript (see references at bottom of table). The number (#) of NF-κB sites near pre-miRNAs and SFRS1 binding sites overlapping pri-miRNAs are listed. The direction of change of miRNAs following RELA knockdown (k.d.) or SF2 induction experiments are also shown with arrows pointing down (↓) for down-regulation or upwards (↑) for up-regulation. Host genes with miRanda predicted miR-7 sites are demarcated with a superscript (^{T}) next to the gene symbol.

miRNA	miRNA LR	Host Gene	Gene LR	# NF-κB sites, RELA k.d. ↑↓	# SFRS1 sites , SF2 induction ↑↓
Embedded in protein coding genes					
hsa-let-7a-3	-0.59325	RP4-695020__B.10 (EX)	Absent	2, n.c.	2, n.c.
hsa-let-7c [b, c]	-0.56115	C21orf34[T]*** (IN)	-1.195	n.s., n.c.	n.s., ↓
hsa-let-7f-2 [b, c]	-0.76342	HUWE1 (IN)	-0.177	1, n.c.	21, n.c.
hsa-miR-98 [b, c]	-0.56841	HUWE1 (IN)	-0.177	1, n.c.	21, n.c.
hsa-let-7g [b]	-0.63766	WDR82[T] (IN)	-0.28	4, n.c.	n.s., n.c.
hsa-miR-10a	-0.54619	HOXB3[T] (IN)	-0.574	8, n.c.	1, n.c.
hsa-miR-10b	-0.6476	HOXD3 (IN)	0.348	2, n.c.	1, n.c.
hsa-miR-1180	0.781506	B9D1 (IN)	0.063	1, n.c.	n.s., n.c.
hsa-miR-1224-5p [b]	-0.5179	VWA5B2 (IN)	Absent	1, n.c.	n.s., n.c.
hsa-miR-126 [b]	-0.52106	EGFL7 (IN)	0.1913	1, n.c.	n.s., n.c.
hsa-miR-1274a	-0.94684	PLCXD3 (AS)	0.212	n.s., n.c.	n.s., n.c.
hsa-miR-139-5p	-0.62283	PDE2A (IN)	-1.227	3, n.c.	n.s., n.c.
hsa-miR-140-5p	0.596344	WWP2 (IN)	0.286	1, ↓	3, ↓
hsa-miR-149 [b, c]	6.223235	GPC1 (IN)	0.042	n.s., ↑	n.s., n.c.
hsa-miR-15b [b]	-0.52393	SMC4 (IN)	-0.0699	6, n.c.	5, n.c.
hsa-miR-198	-0.6282	FSTL1[I] (EX-3'UTR)	-0.822	1, n.c.	2, n.c.
hsa-miR-199a-1 (3p)	-1.1451	DNM2[T] (AS)	-0.185	n.s, ↓	n.s., n.c.
hsa-miR-199a-1 (5p)	-0.54362	DNM2[T] (AS)	-0.185	n.s., ↓	n.s., n.c.
hsa-miR-199b-3p	-1.1451	DNM1 (AS)	0.291	n.s., n.c.	n.s., n.c.
hsa-miR-204	-0.79504	TRPM3 (IN)	0.0536	n.s., n.c.	n.s., n.c.
hsa-miR-218-1 [b]	-0.72675	SLIT2 (IN)	-0.419	n.s., n.c.	15, n.c.
hsa-miR-218-2 [b]	-0.72675	SLIT3 (IN)	Absent	n.s., n.c.	n.s., n.c.
hsa-miR-224 [b]	-0.96649	GABRE (IN/EX)	-0.868	n.s., n.c.	n.s., ↓
hsa-miR-26b*	0.533673	CTDSP1 (IN)	-0.402	5, n.c.	n.s., n.c.
hsa-miR-301b	0.690126	PPIL2 (IN)	-0.223	5, n.c.	1, n.c.
hsa-miR-30a* [a]	-0.84209	C6orf155*** (IN)	-0.709	4, ↓	1, n.c.
hsa-miR-30e* [b, c]	-0.54983	NFYC (IN)	-0.166	4, ↓	2, n.c.
hsa-miR-330-3p [c, b]	0.911218	EML2 (IN)	-0.509	7, n.c.	n.s., n.c.

Table 4.1 (continued)

miRNA	miRNA LR	Host Gene	Gene LR	# NF-κB sites, RELA k.d. ↑↓	# SFRS1 sites , SF2 induction ↑↓
hsa-miR-338-3p [b]	0.711282	AATK (IN)	Absent	n.s., n.c.	n.s., n.c.
hsa-miR-33a [b]	0.515493	SREBF2[T] (IN)	-0.706	n.s., n.c.	4, ↓
hsa-miR-424 [c]	-0.69542	MGC16121*** (EX)	-1.903	5, n.c.	n.s., n.c.
hsa-miR-424* [c]	-1.61066	MGC16121*** (EX)	-1.903	5, n.c.	n.s., n.c.
hsa-miR-503 [c]	-1.46896	MGC16121*** (IN)	-1.903	5, ↓	n.s., n.c.
hsa-miR-425*	0.589535	DALRD3 (IN)	-0.1346	7, n.c.	1, n.c.
hsa-miR-550a-1	0.518992	ZNRF2[T] (IN)	-0.206	3, n.c.	n.s., n.c.
hsa-miR-550a-2	0.518992	AVL9 (IN)	-0.684	1, n.c.	1, n.c.
hsa-miR-584	-0.65834	SH3TC2 (IN)	-1.29	n.s., n.c.	n.s., n.c.
hsa-miR-590-5p [b]	0.606382	EIF4H[T] (IN)	-0.398	n.s., n.c.	7, n.c.
hsa-miR-628-3p	0.911418	CCPG1 (IN)	0.0708	1, n.c.	n.s., n.c.
hsa-miR-652	0.638374	TMEM164 (IN)	-0.181	4, n.c.	n.s., n.c.
hsa-miR-7-1* [b]	-1.18854	HNRNPK (IN/EX)	-0.099	3, n.c.	8, n.c.
hsa-miR-877 [b]	0.582268	ABCF1 (IN)	-0.419	n.s., n.c.	6, n.c.
hsa-miR-93* [b]	0.577574	MCM7 (IN)	-0.317	3, n.c.	7, n.c.
Embedded in non-protein coding genes					
hsa-miR-137 [a]	-0.70379	RP11-490G2.1 (EX)	-0.5	3, n.c.	n.s, ↑
hsa-miR-155	-0.69576	MIR155HG (EX)	-0.842	8, n.c.	n.s, ↑
hsa-miR-17	-0.50919	MIR17HG (IN)	-1.23	5, ↓	2, n.c.
hsa-miR-92a-1 [b, c]	-0.59852	MIR17HG (IN)	-1.23	5, n.c.	2, ↓
hsa-miR-92a-1* [b, c]	-0.56639	MIR17HG (IN)	-1.23	5, n.c.	2, n.c.
hsa-miR-181a-2*	1.325246	MIR181A2HG (IN)	0.912	1, n.c.	n.s., n.c.
hsa-miR-181b-2	0.706968	MIR181A2HG (IN)	0.912	1, n.c.	n.s., n.c.
hsa-miR-181b-1 [a]	0.706968	RP11-31E23.1 (IN)	NA	n.s., n.c.	n.s., n.c.
hsa-miR-199a-2 (3p) [a]	-1.1451	RP5-1116C7.1 IN)	0.7498	1, ↓	n.s., n.c.
hsa-miR-199a-2 (5p) [a]	-0.54362	RP5-1116C7.1 IN)	0.7498	1, ↓	n.s., n.c.

Table 4.1 (continued)

miRNA	miRNA LR	Host Gene	Gene LR	# NF-κB sites, RELA k.d. ↑↓	# SFRS1 sites , SF2 induction ↑↓
hsa-miR-29b-1*	-0.94939	AC016831.7 (AS)	-0.367	4, ↓	n.s., n.c.
hsa-miR-551b [a]	0.810934	C3orf50[T] (IN)[p]	Absent	n.s., n.c.	1, ↓

(IN) intron, (EX) exon, (IN/EX) intron or exon, and (AS) antisense strand. *** hypothetical protein may exist. [a] Fujita and Iba (2008); [b] Monteys et al. (2010); [c] Ozsolak et al. (2008). n.s. = no sites; n.c. = no change. [p] This mRNA is designated as a pseudogene/non-coding RNA on the UCSC genome browser and does not have any predicted protein sequences, although microRNA.org predicts a miR-7 binding site on this transcript using miRanda.

Table 4.2. MiRNAs mapped to intergenic regions. Differentially expressed miRNAs (fold change ≥1.4, FDR ≤5 %) transcribed from intergenic regions are listed. The difference between $\log_2$ average expression values of miR-7 and miR-NC transfected cells calculated from microarray analysis is shown for the miRNAs (miRNA LR). MiRNAs encoded from the same cluster are in cells shaded using the same color. The number (#) of NF-κB sites near pre-miRNAs and SFRS1 binding sites overlapping pri-miRNAs are listed. The direction of change of miRNAs following RELA knockdown or SF2 induction experiments is also shown with arrows pointing down (↓) for down-regulation or upwards (↑) for up-regulation.

miRNA	miRNA LR	# NF-κB sites, RELA k.d. ↑↓	# of SFRS1 sites, SF2 induction ↑↓
hsa-let-7a-1	-0.59325	7, n.c.	n.s., n.c.
hsa-let-7f-1	-0.76342	7, n.c.	n.s., n.c.
hsa-let-7a-2	-0.59325	n.s., n.c.	n.s., n.c.
hsa-miR-100*	-0.50474	n.s., n.c.	n.s., n.c.
hsa-let-7i*	0.505132	3, n.c.	1, n.c.
hsa-miR-1246	1.415944	n.s., n.c.	n.s, ↑
hsa-miR-1303	0.60768	1, n.c.	n.s., n.c.
hsa-miR-142-5p	0.54093	2, n.c.	n.s., n.c.
hsa-miR-146a	0.506805	11, ↓	n.s., n.c.
hsa-miR-181c	0.546773	3, ↓	n.s, ↓
hsa-miR-181d	0.57838	3, n.c.	n.s., n.c.
hsa-miR-193a-3p	-0.53848	2, ↓	n.s., n.c.
hsa-miR-200b	2.113596	3, n.c.	n.s., n.c.
hsa-miR-20b	-0.50919	5, n.c.	n.s., n.c.

Table 4.2 (continued)

miRNA	miRNA LR	# NF-κB sites, RELA k.d. ↑↓	# of SFRS1 sites, SF2 induction ↑↓
hsa-miR-92a-2	-0.59852	5, n.c.	n.s, ↓
hsa-miR-210	0.526599	6, ↓	1, ↓
hsa-miR-221*	-0.68268	2, n.c.	n.s., n.c.
hsa-miR-223	-0.62695	8, n.c.	n.s., n.c.
hsa-miR-30d*	-0.84209	n.s., n.c.	n.s., n.c.
hsa-miR-337-5p	1.314976	n.s., n.c.	n.s., n.c.
hsa-miR-374b	-0.63622	n.s., n.c.	n.s, ↓
hsa-miR-421	0.531948	n.s., n.c.	n.s., n.c.
hsa-miR-494	-0.84363	n.s., n.c.	n.s., n.c.
hsa-miR-542-5p [cl]	0.607361	5, n.c.	n.s., n.c.
hsa-miR-99b*	0.819847	1, ↓	n.s., n.c.

[cl] This miRNA is clustered with 3 other miRNAs differentially expressed in our experiment, miR-424, miR-424* and miR-503; all 3 are expressed from a hypothetical protein coding gene MGC16121. n.s. = no sites; n.c. = no change.

Of the 71 miRNAs differentially expressed after miR-7 transfection, 50 were found to map to annotated genes (55 including paralogs) and 21 (25 including paralogs) map to intergenic miRNA genes (Figure 4.4, Tables 4.1 and 4.2). To determine if changes in miRNA levels are correlated with changes in mRNA levels of the 50 genes in which miRNAs are embedded, we compared changes in miRNA profiles with changes in the mRNA levels of host genes in miR-7 transfected HEY cells (Figure 4.5, Table C.2). We found that 9 of the 50 host genes were significantly differentially expressed (fold change ≥1.3, $p < 0.05$) in miR-7 transfected cells relative to controls (Table 4.3, Figure 4.6). Eight of these nine genes displayed changes in expression positively correlated with thirteen embedded miRNAs while one of the genes displayed a change in expression inversely correlated with a single embedded miRNA (Table 4.3). The majority of genes (41/50) hosting differentially expressed miRNAs did not display a significant change in expression in miR-7 transfected cells relative to controls (Tables 4.1 and 4.2).

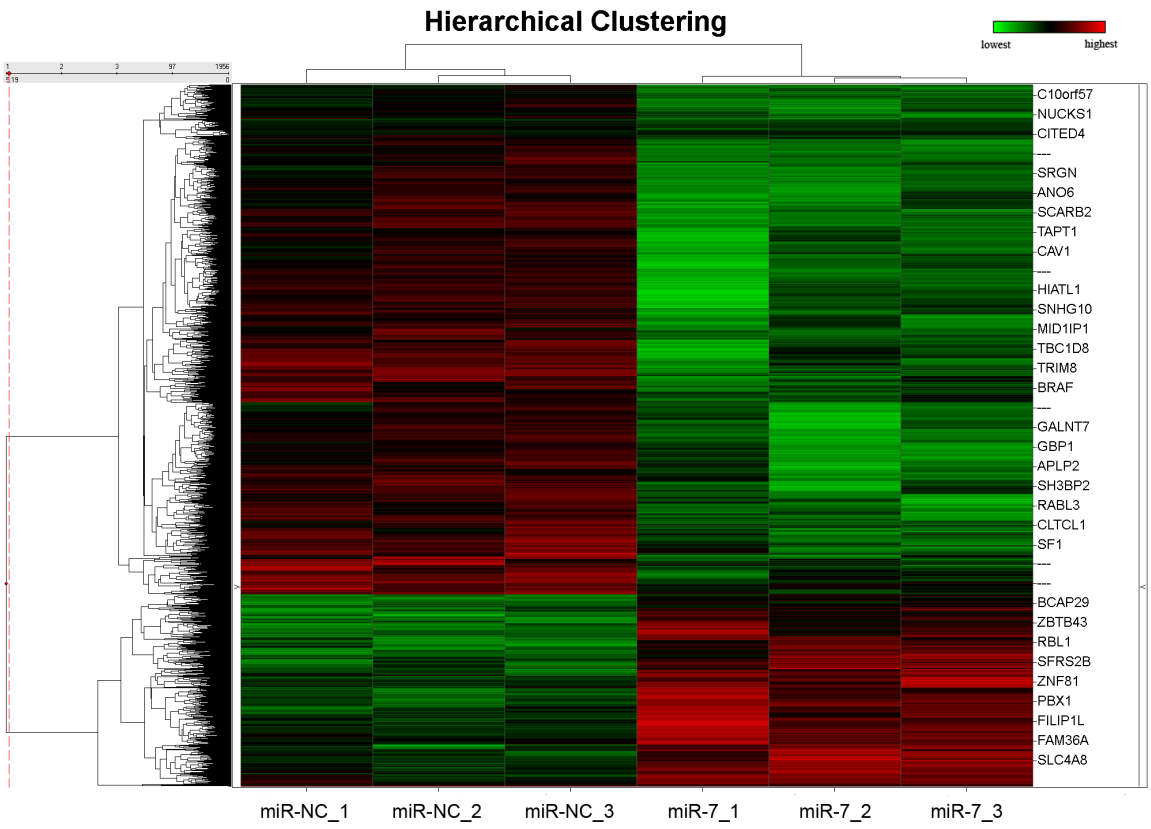

Figure 4.5. Significantly differentially expressed mRNAs following miR-7 transfection into HEY cells. Hierarchical clustering of significantly differentially expressed genes (fold change ≥1.3, $p < 0.05$) between cells transfected with either miR-7 or miR-NC. There were 403 mRNAs significantly up-regulated and 965 different mRNAs significantly down-regulated after miR-7 transfection. Each column of the heat map corresponds to a sample. Three independent samples transfected with negative control are on the left and three independent samples transfected with miR-7 are on the right. Selected gene symbols corresponding to the Affymetrix probeset ID are shown on the right side of the heat map.

Table 4.3. Significantly differentially expressed embedded miRNA-mRNA pairs. Embedded miRNAs and their host genes are listed when both the miRNA (fold change ≥1.4 and FDR ≤5 %) and the host gene (fold change ≥1.3, t-test p-value <0.05) are detected to be significantly changing in the same direction (positively correlated) or opposite direction (inversely correlated) after transfecting HEY cells with miR-7 or miR-NC. For two of these mRNAs (as well as the miRNAs) differential expression was confirmed by qPCR (Figure 4.6; Pair-wise fixed reallocation randomization test p-value <0.05).

miRNA	mRNA/ncRNA	Host gene detection method
miRNAs positively correlated in expression with host genes		
hsa-let-7c	C21orf34[T] (IN)	Microarray
hsa-miR-139-5p	PDE2A (IN)	Microarray
hsa-miR-198	FSTL1[T] (EX-3'UTR)	Microarray and qPCR
hsa-miR-30a*	C6orf155 (IN)	Microarray
hsa-miR-424	MGC16121 (EX)	Microarray and qPCR
hsa-miR-424*	MGC16121 (EX)	Microarray and qPCR
hsa-miR-503	MGC16121 (EX)	Microarray and qPCR
hsa-miR-155	MIR155HG (EX-ncRNA)	Microarray
hsa-miR-181a-2*	MIR181A2HG (IN-ncRNA)	Microarray
hsa-miR-181b-2	MIR181A2HG (IN-ncRNA)	Microarray
hsa-miR-17	MIR17HG (IN-ncRNA)	Microarray
hsa-miR-92a-1	MIR17HG (IN-ncRNA)	Microarray
hsa-miR-92a-1*	MIR17HG (IN-ncRNA)	Microarray
miRNAs inversely correlated in expression with host genes		
hsa-miR-550a-2	AVL9 (IN)	Microarray

IN: intron, EX: exon. [T] Predicted targets of miR-7. ncRNA: Non-protein coding transcripts.

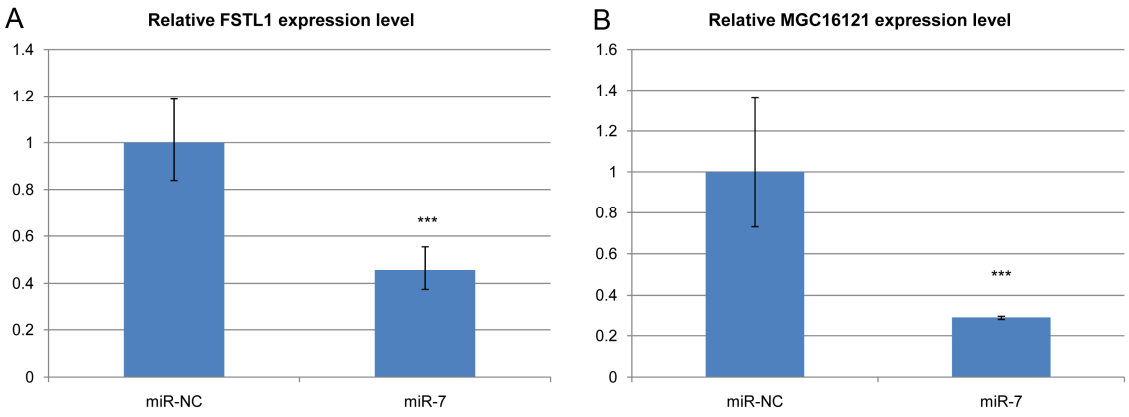

Figure 4.6. Quantitative PCR confirmation of host mRNAs differentially expressed after miR-7 transfection. Quantitative (real-time) PCR analysis of (A) FSTL1, and (B) MGC16121 expression in HEY ovarian cancer cells 48h after transfection with either hsa-miR-7 or miR-NC. RNA expression levels were normalized to human GAPDH used as the endogenous control. Relative expression values are shown on the Y-axis. Error bars reflect standard deviation of the means calculated from three replicate samples. *** $p < 0.001$.

miR-7 regulates expression of some miRNAs by altering the level of the transcription factor RELA/NF-κB

We found that transfection of miR-7 into HEY cells results in significant changes in the expression levels of 1368 genes including genes known to encode transcription factors previously linked with cancer onset and progression (Figure 4.5, Table C.2; Karin and Greten, 2005). Since miRNAs are under transcriptional regulatory control (Krol et al., 2010), transcription factor genes regulated by miR-7 may exert indirect regulatory effects on other miRNAs. To explore this possibility, we selected RELA, one of the transcription factor coding genes that were significantly differentially expressed after miR-7 transfection in HEY cells (Table 4.4) and in A549 lung cancer cells (Webster et al., 2009; see also Table C.3). Moreover, RELA is a component of the well-studied transcription factor NF-κB that is a well-documented regulator of miRNA expression (Mott et al., 2010; Pacifico et al., 2010; Zhou et al., 2009). Significant down-regulation of RELA in miR-7 transfected HEY cells was confirmed by quantitative real-time PCR (Figure 4.7A).

We found that 17 (68 %) of the 25 intergenic miRNAs and 38 (69 %) of our 55 embedded miRNAs (Tables 4.1, 4.2, Figure 4.8; Table C.4) map to within 10 kb of experimentally validated (ChIP-seq) RELA/NF-κB binding sites (Birney et al., 2007). In addition, nearly half (33 out of 71) of the miRNAs that were differentially expressed in our miR-7 transfection experiment have previously been reported to be altered when NF-κB is induced or inhibited in other cellular contexts (Gao et al., 2010; Kluiver et al., 2007; Mott et al., 2010; Pacifico et al., 2010; Wang et al., 2009; Wang et al., 2010; Zhou

et al., 2009). Collectively, these findings suggest that at least some of the changes in miRNA levels observed after miR-7 transfection into HEY cells may be mediated by RELA/NF-κB transcription factor.

Table 4.4. Differentially expressed transcription factors following miR-7 transfection. These 22 transcription factors were identified as being significantly differentially expressed (1.3 fold change, $p < 0.05$) in miR-7 transfected HEY cells and A549 lung cancer cells (Webster et al., 2009). The difference between the $\log_2$ signal values for each gene in HEY cells transfected with either miR-7 or miR-NC is given in the 'miR7-miR-NC'. Out of the 22, only 8 have miRanda predicted miR-7 binding sites (marked with 'x') and only 2, RELA and SP1 have ChIP-seq data showing genome-wide binding sites (marked with 'E').

Gene Symbol	miR7-miR-NC	miR7 tgts_miRanda	ENCODE ChIP-seq Data
BACH1	-0.45255		
CNOT6	-0.60309	x	
CNOT8	-1.26668	x	
CREBL2	0.433388		
IFT57	0.664064		
IRF2BP2	-0.43606		
KLF3	-0.60824		
KLF4	-1.06432	x	
LITAF	-1.52641		
NOTCH2	-0.7116	x	
PBX1	1.134572	x	
PPM1A	-0.52971		
RELA	-1.08425	x	E
SETD8	-1.07335	x	
SP1	-0.42641	x	E
TAF4B	-0.54876		
TLE4	-0.61978		
UBTF	0.614296		
VGLL4	-0.72098		
ZBTB20	0.399861		
ZNF512	-0.49876		
ZNF580	0.457916		

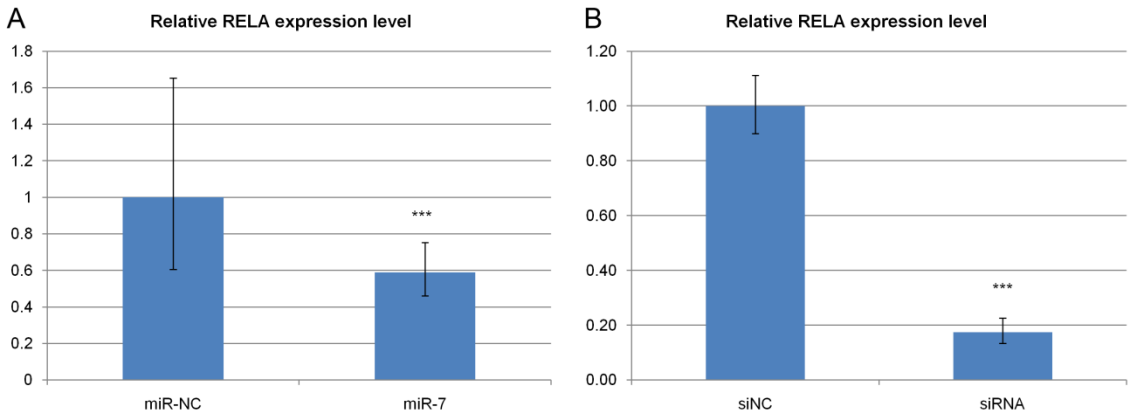

Figure 4.7. Confirmation of RELA down-regulation following miR-7 or anti-RELA siRNA transfection. QPCR confirms successful down-regulation of RELA expression 48 hours after transfection of HEY cells with A. miR-7 or miR-NC, and B. anti-RELA siRNA or siNC. Relative expression of RELA was measured using GAPDH as endogenous control. Error bars reflect standard deviation of the means calculated from three independent replicate samples. *** $p < 0.001$.

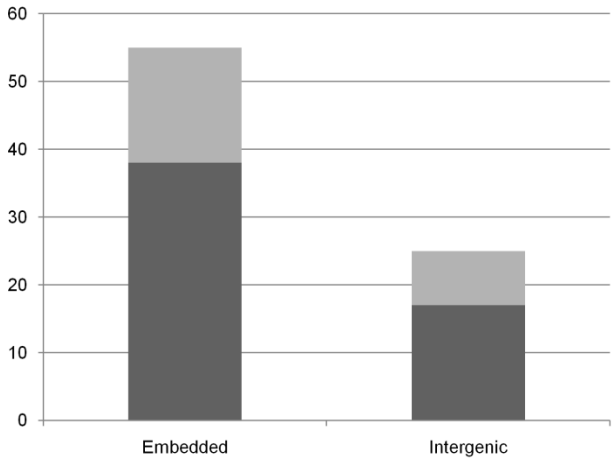

Figure 4.8. Distribution of NF-κB binding sites near embedded and intergenic miRNAs. Number of embedded and intergenic differentially expressed miRNAs with (dark grey) or without (light grey) NF-κB binding sites within ±10 kb. The number of differentially expressed miRNAs (fold change ≥1.4, FDR ≤5 %) following miR-7

transfection that are either embedded in coding/non-coding genes or intergenic is represented by the height of the bars.

To further investigate this hypothesis, we transfected HEY cells with RELA siRNA or a negative control siRNA and collected total RNA (48 hrs post-transfection) for microarray analysis (Affymetrix GeneChip miRNA array). Knock down of RELA expression was confirmed by qPCR (Figure 4.7B). The results of the microarray analysis demonstrated that 235 miRNA probesets corresponding to 51 known human miRNAs (Figure 4.9; Table C.5) were significantly differentially expressed (fold change ≥1.4, FDR ≤5 %) after RELA-siRNA transfection relative to controls. Seven of the miRNAs displaying changes in expression after miR-7 transfection displayed similar changes in expression after transfection with RELA-siRNA (Table 4.5). Twenty additional miRNAs that displayed significant changes in expression after RELA siRNA transfection either originate from the same pre-miRNA transcript or are clustered within the same locus (<10 kb) with 19 miRNAs displaying significant changes in expression after miR-7 transfection (Table 4.5). Our findings are consistent with the hypothesis that at least some of the changes in miRNA levels observed after miR-7 transfection into HEY cells are mediated by RELA.

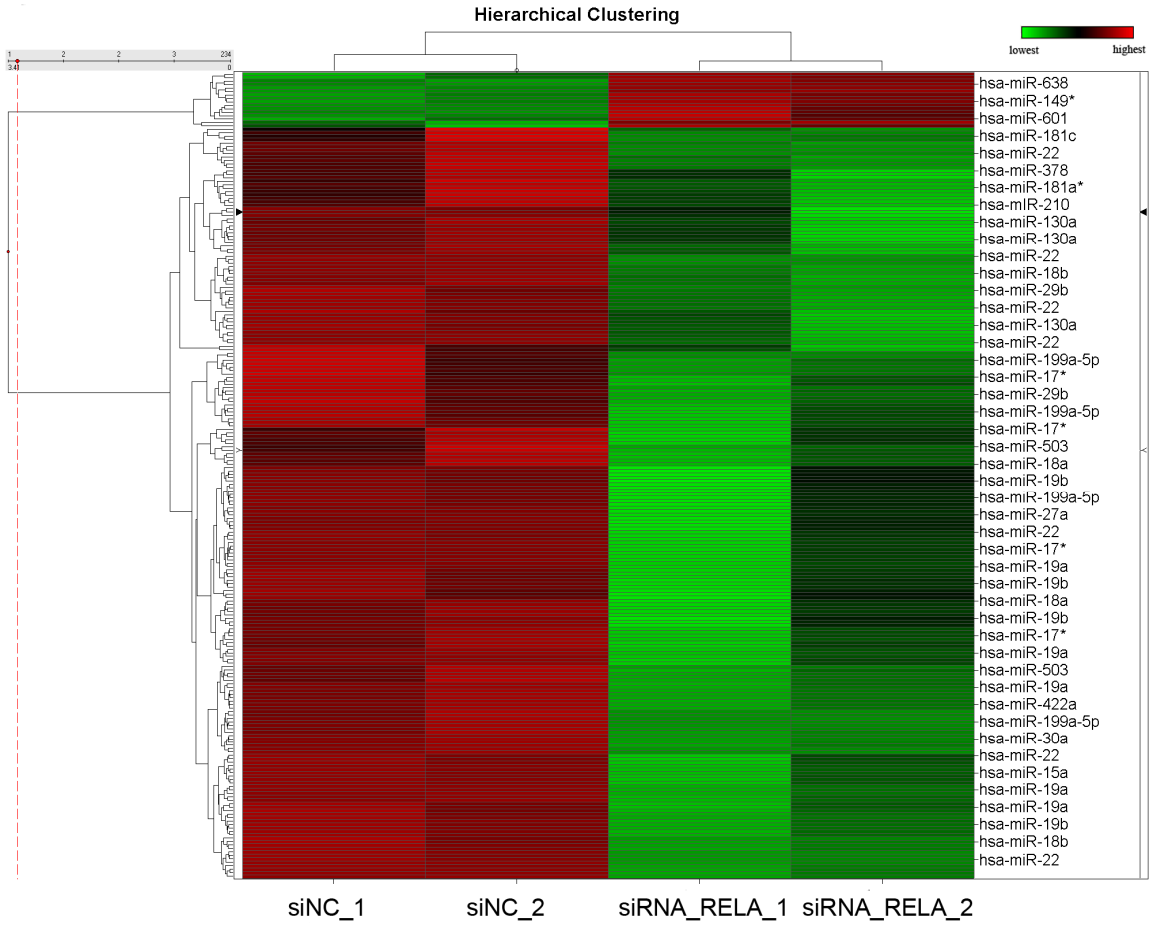

Figure 4.9. Differentially expressed miRNAs in HEY cells following anti-RELA siRNA transfection. Significantly differentially expressed (fold change ≥1.4 and FDR ≤5 %) miRNAs in HEY cells following transfection with anti-RELA siRNA or siNC were used for hierarchical clustering of samples. Each column of the heat map corresponds to a sample. Two samples transfected with siNC are on the left and the two anti-RELA siRNA transfected samples are on the right. Some of the IDs of the human miRNAs homologous to the sequences specified by the probesets are shown on the right side of the heat map.

Table 4.5. Significantly differentially expressed miRNAs altered by both miR-7 transfection and RELA knock-down. The lists of miRNAs that were significantly differentially expressed (fold change ≥1.4, FDR ≤5 %) after either miR-7 or RELA-siRNA transfection were compared and the miRNAs that were altered in both, had the

Table 4.5 (continued)

same pre-miRNA, or that originated in the same cluster are listed. MiRNA names followed by parenthesis containing a number refers to a corresponding paralogous miRNA (for e.g., hsa-miR-19b(-2) refers to hsa-miR-19b originating from hsa-miR-19-2).

Mature miRNAs altered in both		
hsa-miR-210		
hsa-miR-503		
hsa-miR-99b*		
hsa-miR-181c		
hsa-miR-146a		
hsa-miR-193a-3p		
hsa-miR-199a-5p		
miRNAs transcribed from the same pre-miRNA		
RELA knock down	**miR-7 transfection**	
hsa-miR-29b(-1)	hsa-miR-29b-1*	
hsa-miR-140-3p	hsa-miR-140-5p	
hsa-miR-149*	hsa-miR-149	
hsa-miR-17*	hsa-miR-17	
hsa-miR-199a-5p	hsa-miR-199a-3p, hsa-miR-199a-5p	
hsa-miR-30a	hsa-miR-30a*	
hsa-miR-30e	hsa-miR-30e*	
miRNAs transcribed from the same cluster		
Cluster	**RELA knock down**	**miR-7 transfection**
miR-17~92	hsa-miR-17*	hsa-miR-17
miR-17~92	hsa-miR-18a*	hsa-miR-92a(-1)
miR-17~92	hsa-miR-18a	hsa-miR-92a-1*
miR-17~92	hsa-miR-19a	
miR-17~92	hsa-miR-19b(-1)	
miR-18~106	hsa-miR-18b	hsa-miR-20b
miR-18~106	hsa-miR-19b(-2)	hsa-miR-92a(-2)
miR-15-16	hsa-miR-16(-2)	hsa-miR-15b
let-7c, miR-99a	hsa-miR-99a	hsa-let-7c
miR-181a-1, miR-181b-1	hsa-miR-181a*	hsa-miR-181b(-1)
miR-130b, miR-301b	hsa-miR-130b	hsa-miR-301b
miR-424~542	hsa-miR-503	hsa-miR-424, hsa-miR-424*, hsa-miR-503
miR-181c, miR-181d	hsa-miR-181c	hsa-miR-181c, hsa-miR-181d

miR-7 may regulate expression of miRNAs by altering levels of the splicing factor SF2/ASF

Wu et al. (2010) have recently reported that SF2, a gene involved in the splicing of pre-mRNAs (Ge and Manley, 1990; Krainer et al., 1990; Zhou et al., 2002), can form a negative feedback circuit with miR-7. Over-expression of SF2 in HeLa cells was shown to result in significant alterations in levels of several (40) miRNAs including a significant elevation in levels of miR-7. Wu et al. (2010) go on to show that elevation in levels of miR-7 results in the down-regulation of SF2 (a predicted target of miR-7) indicating a negative feed-back loop.

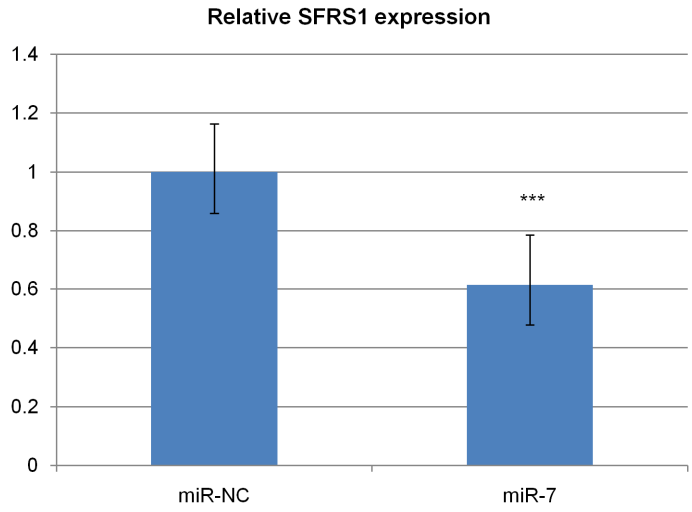

Figure 4.10. Quantitative PCR confirmation of SFRS1 down-regulation in miR-7 transfected HEY cells. Quantitative (real-time) PCR of SFRS1 expression in HEY cells 48h after transfection with miR-7 or miR-NC. Relative expression of SFRS1 was normalized to human GAPDH expression used as endogenous control. Error bars reflect standard deviation of the means calculated from three replicate samples. *** $p < 0.001$.

Since our microarray results (confirmed by qPCR, Figure 4.10) indicate that expression levels of the gene (SFRS1) encoding SF2 is significantly down-regulated in miR-7 transfected cells, it is possible that at least some of the miR-7 induced changes in levels of miRNAs in these cells may have been mediated by SF2. Consistent with this hypothesis, we found that 12 of the 40 miRNAs reported by Wu et al. (2010) to display significant changes in levels of expression in HeLa cells after SF2 over-expression also display significant changes in expression after miR-7 transfection in HEY cells (Table 4.6). In addition, we found that nine additional miRNAs differentially expressed after miR-7 transfection map to primary transcripts containing eight of the differentially expressed miRNAs detected in the Wu et al. (2010) study (Table 4.6; also Tables 4.1 and 4.2).

To further explore the possibility that some of the miR-7 induced changes in miRNA levels in transfected HEY cells may have been mediated by SF2, we overlaid the positions of experimentally validated (CLIP-seq or cross-linked immunoprecipitation and sequencing) SF2 binding sites (Sanford et al., 2009) with the genomic locations of miRNAs displaying significant changes in levels of expression after miR-7 transfection. The results indicate that SF2 binding sites are located within the pri-miRNAs of 25 miRNAs (23 embedded, 2 intergenic) displaying significant changes in expression after miR-7 transfection (Tables 4.1, 4.2, C.6 and C.7). Collectively, our findings are consistent with the hypothesis that some of the miR-7 induced changes in miRNA levels in transfected HEY cells are mediated by miR-7 induced changes in levels of SF2.

Table 4.6. Significantly differentially expressed miRNAs altered by both miR-7 transfection and SF2 induction. The miRNAs that were significantly differentially expressed in either HEY cells after miR-7 transfection (fold change ≥1.4, FDR ≤5 %) or in HeLa cells following SF2 induction (fold change ≥1.5, FDR ≤1 %, criterion used in the Wu et al. (2010) study) were compared and the miRNAs that were altered in both or had the same putative pri-miRNA are listed. Mature miRNAs differentially expressed after both miR-7 transfection and SF2 induction are written in **bold** letters.

miRNAs altered in SF2 induction	miRNAs altered in miR-7 transfection
hsa-let-7c	**hsa-let-7c**
hsa-miR-1246	**hsa-miR-1246**
hsa-miR-137	**hsa-miR-137**
hsa-miR-140-5p	**hsa-miR-140-5p**
hsa-miR-155	**hsa-miR-155**
hsa-miR-210	**hsa-miR-210**
hsa-miR-224	**hsa-miR-224**
hsa-miR-33a	**hsa-miR-33a**
hsa-miR-551b	**hsa-miR-551b**
hsa-miR-181c	**hsa-miR-181c**, hsa-miR-181d
hsa-miR-374b	**hsa-miR-374b**, hsa-miR-421
hsa-miR-92a	**hsa-miR-92a**, hsa-miR-92a-1*, hsa-miR-17
hsa-miR-221	hsa-miR-221*
hsa-miR-29b	hsa-miR-29b-1*
hsa-miR-7	hsa-miR-7-1*
hsa-miR-191	hsa-miR-425*
hsa-miR-125a-5p	hsa-miR-99b*

Discussion and Conclusion

Previously it has been shown that a single miRNA can alter the expression of hundreds of genes (Baek et al., 2008; Lim et al., 2005; Selbach et al., 2008). While some of these changes can be attributed to canonical 3' UTR miRNA targeting, the vast majority (~70 %) of genes altered by a miRNA may be indirectly regulated (Chen et al., 2011; see also CHAPTER 3). In this study, we explore the possibility that one

mechanism that may be contributing to these "off-target" effects is miRNA-miRNA regulation.

Our experimental approach was to transfect a well-characterized ovarian cancer cell line (HEY) with a single miRNA and to monitor the effect on the expression levels of other miRNAs and mRNAs by microarray analysis. We selected miR-7 for use in our transfection experiments because levels of this miRNA previously have been shown to be significantly changed in ovarian (Wyman et al., 2009; see also CHAPTER 2) and other cancers (Chou et al., 2010; Foekens et al., 2008; Jiang et al., 2010; Kefas et al., 2008; Reddy et al., 2008; Veerla et al., 2009; Webster et al., 2009) relative to normal tissue. Gene expression profiling by microarray revealed that transfection of miR-7 into HEY cells resulted in significant changes in expression levels of 71 miRNAs and 1370 mRNAs.

In principle, miRNAs may regulate expression of other miRNAs either directly or indirectly. For example, it has been proposed that if miRNAs share significant sequence complementarity with other miRNAs, the resulting nucleotide pairing could serve as the basis of direct miRNA-miRNA regulation (Lai et al., 2004). We found that among 71 miRNAs differentially expressed in our study, only 3 displayed even partial (38-62 %, Figure 4.11) Watson-Crick complementarity to miR-7 indicating that miRNA-miRNA pairing is unlikely to be a significant mechanism used by miR-7 to regulate other miRNAs in our study.

Figure 4.11. Alignment of three differentially expressed miRNAs with partial complementarity to miR-7. Sequences of three miRNAs (hsa-miR-7-1*, hsa-miR-224 and hsa-miR-92a) are aligned with miR-7 based on BLAST alignment. Vertical straight lines (|) represents Watson-Crick complementarity and the colon (:) symbol represents GU wobble.

The primary mechanism by which miRNAs regulate expression of mRNA-encoding genes is through translational inhibition and associated mRNA degradation (Djuranovic et al., 2011; Fabian et al., 2010). While this mechanism is presumably not applicable to miRNAs and other untranslated RNAs, there have been reports of miRNAs directly serving as activators (Majid et al., 2010; Place et al., 2008) and repressors (Kim et al., 2008) of transcriptional initiation. It is certainly possible that miRNAs may directly influence the expression of other miRNAs by regulating or co-regulating promoters of miRNA genes and/or protein coding genes in which miRNAs are embedded. However,

current evidence suggests that a direct role of miRNAs in promotional control occurs relatively infrequently (Tang et al., 2008b; Tang and Zen, 2011). Thus, we believe it is more likely that miRNAs may modulate the expression of other miRNAs indirectly by regulating transcription factors or other regulatory proteins that, in turn, exert direct regulatory control on miRNA expression.

We observed significant changes in expression of 188 transcription factor coding genes after miR-7 transfection. Forty-nine of these, including RELA/NF-κB, are predicted targets of miR-7 regulation (Table C.8). We selected RELA/NF-κB for further investigation because this transcription factor has been previously implicated in miRNA regulation (Mott et al., 2010; Pacifico et al., 2010; Zhou et al., 2009) and was also down-regulated in a lung cancer cell line following miR-7 transfection (Webster et al., 2009). We found that siRNA knockdown of RELA resulted in a significant change in expression of 51 miRNAs, many of which were also significantly differentially expressed after miR-7 transfection. These results coupled with our finding that ~70 % of the miRNAs differentially expressed after miR-7 transfection map to within 10 kb of RELA/NF-κB binding sites suggest that this transcription factor plays a significant indirect role in miR-7 induced changes in miRNA expression.

Further support for the hypothesis that miR-7 induced changes in the expression levels of protein coding regulatory genes may play a significant role in affecting changes in levels of miRNAs comes from our analysis of another direct target of miR-7 regulation, the splicing factor SF2. We found that SF2 binding sites are located within the pri-miRNAs of 25 miRNAs that displayed significant changes in expression after miR-7 transfection into HEY cells. This result coupled with previous findings implicating SF2

in the regulation of miR-7 in HeLa cells (Wu et al., 2010a) suggests that SF2 may also be playing a role in miR-7 induced changes in the expression of miRNAs in HEY cells.

Once considered "junk" DNA, a large component of the non-protein coding human genome is now known to encode untranslated RNAs that play important, albeit diverse, roles in gene regulation (Eddy, 2001; Mattick, 2007). Among the most intensively studied of these regulatory molecules are short (~22 nucleotides) regulatory RNAs, called miRNAs. This class of small regulatory RNAs inhibits the translation and/or facilitates the degradation of their targeted messenger RNAs (Fabian et al., 2010). The fact that miRNAs are aberrantly expressed in many cancers has made them attractive candidates for potential use in cancer therapy (Garofalo and Croce, 2011). However, the clinical utility of miRNAs in cancer therapy rests heavily upon our ability to understand and accurately predict the consequences of fluctuations in levels of miRNAs within the context of complex tumor cells. While the regulatory effects of miRNAs in tumor cells is known to be complex (Farazi et al., 2011; Lee and Dutta, 2009) the molecular basis of this complexity is only beginning to be explored (Chang et al., 2007; Farazi et al., 2011; Hatley et al., 2010; He et al., 2007b; He et al., 2005; Huang et al., 2009). In this paper, we present evidence that a significant component of this complexity may involve the ability of miRNAs to regulate other miRNAs indirectly through the action of trans-regulatory proteins. Our findings underscore the complexity of miRNA-mediated regulation in cancer cells and the necessity of better understanding the basis of this complexity if we are to fully realize the therapeutic potential of this versatile class of regulatory RNAs.

Materials and Methods

Cell culture and miRNA/siRNA transfections

Cell culture conditions and miRNA/siRNA transfection procedures were done as described previously (CHAPTER 2 and CHAPTER 3). Briefly, the cells were transfected with the miRNA hsa-miR-7 miRIDIAN mimic, miRIDIAN miRNA mimic negative control #1 (miR-NC, a *C.elegans* miRNA, cel-miR-67, with confirmed minimal sequence identity in humans), ON-TARGET *plus* Anti-EGFR siRNA, ON-TARGET *plus* Anti-RELA siRNA or ON-TARGET *plus* non-targeting siRNA (siNC; Thermo Fisher Scientific, Lafayette, CO) using Lipofectamine 2000 transfection agent (Invitrogen, Carlsbad, CA) according to the manufacturer's instructions at a final concentration of 25nM. All transfections were carried out with at least two to three independent replicates. The cells were incubated with the reduced serum transfection medium (Opti-MEM, Invitrogen) for 4 hours, washed and then allowed to grow in growth medium (RPMI 1640, Mediatech, Manassas, VA) for 44 hours before collecting RNA or protein. Transfection efficiency was estimated from the relative knock-down of EGFR/RELA, based on recommendations by the reagent manufacturer (Thermo Fisher Scientific).

Quantitative (real-time) PCR

For miRNA qPCR, total RNA was extracted from HEY cells using the mirVana miRNA isolation kit according to the manufacturer's instructions (Applied Biosystems, Foster City, CA). The RNA (10 ng) was then converted to amplified cDNA for qPCR by using the TaqMan miRNA Reverse Transcription Kit and miRNA specific primers (Applied Biosystems, Foster City, CA) following manufacturer’s protocols. TaqMan

miRNA assays (Applied Biosystems) were conducted following manufacturer's protocol for hsa-miR-198, hsa-miR-628-3p, hsa-miR-149, hsa-miR-10b, hsa-let-7f, hsa-miR-503, hsa-miR-218, hsa-miR-224, and for RNU6B. Specificity of TaqMan miRNA assays is supported by publications from the manufacturer (Chen et al., 2007; Liang et al., 2007; Tavazoie et al., 2008) as well as subsequent literature from independent groups (Huang et al., 2011; Shibata et al., 2011; Wilson et al., 2011).

For mRNA qPCR, total RNA (1-5µg) extracted from cells was converted to cDNA using the Superscript III First Strand synthesis system (Invitrogen). cDNA was then purified using the QIAGEN PCR purification kit (QIAGEN) following manufacturer's instructions. TaqMan gene expression assays were conducted following manufacturer's protocol for MGC16121, FSTL1, GAPDH, RELA, and SFRS1. QPCR experiments were also carried out for the EGFR and GAPDH genes as described in CHAPTER 3. All reactions were optimized with non-template controls, and -RT (minus reverse transcriptase) controls prior to experiment. Specificity of TaqMan gene expression assays is supported by thousands of independent citations (e.g., Bergmann et al., 2011; Colazzo et al., 2011; Hevir et al., 2011; Lossos et al., 2004)

All qPCR experiments were carried out using at least three technical replicates and two-three independent biological replicates on the CFX96 Real Time PCR detection system (Bio-Rad). For each target expression values were normalized to an endogenous control (RNU6B/GAPDH). Relative fold change of target RNA level between transfection groups was determined by the ΔΔCt method. Statistical significance was determined using the pair-wise fixed reallocation randomization test in the Relative Expression Software Tool (REST 2008; Pfaffl et al., 2002).

Immunoblotting

Immunoblotting for EGFR and β-Actin was performed as described previously in CHAPTER 3.

RNA isolation for miRNA microarray

Total RNA was isolated from HEY cells (two replicates per group) using the mirVana miRNA isolation kit according to the manufacturer's instructions (Applied Biosystems, Foster City, CA). The quantity and size of miRNA was verified using an Agilent 2100 Bioanalyzer (Agilent Technologies, Palo Alto, CA). MiRNAs were labeled with Genisphere FlashTag HSR Biotin RNA labeling kit (Genisphere, Hatfield, PA) followed by hybridization with GeneChip miRNA Array chips (Affymetrix, Santa Clara, CA) according to the manufacturer's instructions. The chips were washed and then scanned with a GeneChip Scanner 3000 (Affymetrix). Raw data in the form of CEL files were produced by the Affymetrix GeneChip Operating System (GCOS) software.

RNA isolation for whole genome microarray

Total RNA isolation for whole genome microarray was performed as described in CHAPTER 2 using the RNeasy Mini RNA isolation kit (QIAGEN, Valencia, CA) according to the manufacturer’s instructions. The integrity of the RNA was verified using an Agilent 2100 Bioanalyzer (1.8-2.0; Agilent Technologies, Palo Alto, CA). Subsequently cDNA synthesis, amplification and hybridization on Affymetrix HG-U133 Plus 2.0 arrays were carried out as described in CHAPTER 2.

Microarray data analysis

Raw data from miRNA microarray were analyzed using miRNA QC Tool software (Affymetrix, Santa Clara, CA). Normalization was performed using the default workflow of the miRNA QC Tool software. The log base 2 transformed expression values were then normalized across samples by Z-score calculations using Spotfire DecisionSite for Microarray Analysis (DSMA). Probesets with 'FALSE' call in all groups were removed from statistical analysis. Probeset intensities were filtered with DSMA using a modulation threshold of 0.5 to include only those probesets with at least a fold change ≥1.4. Differentially expressed probesets were identified using the SAM algorithm at a threshold 5 % false discovery rate correction. Sequence of each differentially expressed miRNA probeset was then used to find the corresponding human miRNA using BLASTN algorithm available on the miRBase webpage with the default E-value cut-off of 10. In each case, only the human miRNA with the highest score and lowest E-value was considered. If two miRNAs had the same high score, then both were included. Sequences with 1<E-value<10 were included in the table but were excluded from further analysis because of their "poor homology". Sequences with E-value >10 for human miRNAs are ignored and marked with "N/A" under the 'homolog' columns of Tables C.1 and C.5. Genomic locations of miRNA paralogs were obtained from the miRBase registry as well. In the miR-7 transfection experiment these probesets correspond to seventy-one unique mature human miRNAs (excluding miR-7), three sequences with very poor (BLASTN E-value >1) homology to human miRNAs, two snoRNAs, one vault RNA (a type of small RNA), one tRNA, an mRNA (KIAA1407)

fragment, and some sequences that we could not map to the human genome (E-value >10).

Raw data from mRNA microarray were analyzed using the Expression Console software (Affymetrix) and using R (www.r-project.org) as described previously in CHAPTER 2 with the following modifications. Average probeset intensities for each group were calculated based on the log 2 transformed values from PLIER and then filtered with DSMA using a modulation threshold of 0.379 to include only those probesets with a fold change ≥1.3. The Student's t-test p-value for each probeset was calculated by using the log 2 transformed values after GCRMA normalization. Raw data from a previous miR-7 transfection paper (Webster et al., 2009) were downloaded from GEO and processed in a similar fashion.

Identification of transcription factors

Transcription factors were identified by searching for the Gene Ontology (GO) biological process annotation "regulation of transcription" for every probeset differentially expressed after miR-7 transfection.

MiRNA target download

The miRNA target prediction file based on miRanda-mirSVR was downloaded from www.microrna.org (August 2010 release; Betel et al., 2008; Enright et al., 2003; John et al., 2004). Information about the prediction algorithm, parameter settings and raw data source is available on the above link.

Identification of putative NF-κB regulated miRNAs

The coordinates of the putative NF-κB binding sites identified by ChIP-seq in the ENCODE project (Birney et al., 2007) were downloaded from the UCSC table browser (http://genome.ucsc.edu) based on the NCBI36/hg18 assembly of the human genome for each miRNA using a window of ±10 kb around the locus of each pre-miRNA corresponding to the differentially expressed miRNAs following miR-7 transfection.

Identification of putative SFRS1 regulated miRNAs

SFRS1 binding sites identified by (Sanford et al., 2009) using genome-wide cross-linked immunoprecipitation and sequencing (CLIP-seq) were downloaded from the authors website (with authors permission; http://sanfordlab.mcdb.ucsc.edu/Sanford_Lab/Datasets.html). For miRNAs embedded in known transcriptional units the SFRS1 sites were searched within the genomic coordinates of the host transcript. For intergenic miRNAs, length of the pri-miRNA was assumed to be ~4 kb on average with the transcription start site located ~2 kb upstream and the poly(A) signal located ~2 kb downstream of the pre-miRNA, and thus the SFRS1 sites were searched within ±2 kb around each pre-miRNA, based on the average lengths of pri-miRNAs described by (Saini et al., 2007). Coordinates of coding transcriptional units and pre-miRNAs were obtained from the UCSC genome browser (http://genome.ucsc.edu) based on the NCBI36/hg18 assembly of the human genome.

BLAST alignment of miRNAs

Sequences of miRNA probesets obtained from the Affymetrix annotation file corresponding to the differentially miRNAs following miR-7 transfection were searched for significant complementarity to miR-7 using NCBI nucleotide BLAST algorithm (http://blast.ncbi.nlm.nih.gov) with the following parameter settings. Under program selection optimize for "more dissimilar sequences" was selected, and under algorithm parameters "automatically adjust parameters for short input sequences" was selected.

CHAPTER 5

CONCLUSIONS

Because miRNAs can affect the expression of hundreds of genes, we sought to identify the molecular consequences of miRNA expression pattern changes in an ovarian cancer model and the mechanisms responsible for these consequences. The reductionist view of single-miRNA/single-target interaction may be inadequate for analyzing regulatory networks inside the cell (Shalgi et al., 2009). Hence we took a systems approach to identify and characterize the miRNA-mRNA interactions in the preceding chapters. In the first study (CHAPTER 2), the global miRNA and mRNA expression patterns in ovarian cancer cells were profiled to reveal the underlying complexity of miRNA regulation *in vivo*. Building upon our results, miRNA regulation was examined in more detail (CHAPTER 3) uncovering both direct and indirect mechanisms used by miRNAs to alter the levels of their target mRNAs. In the final chapter (CHAPTER 4), we present the novel finding that miRNA mediated gene regulation has the ability to affect the levels of other miRNAs.

Until recently, regulators of gene expression were thought to be proteins, such as transcription factors, activators and repressors (Mattick, 2007). However this paradigm was challenged with the discovery of RNA silencing (Napoli et al., 1990). The genomic regions encoding non-coding RNAs (ncRNA), once considered "junk" DNA (Doolittle and Sapienza, 1980; Orgel and Crick, 1980), have now been demonstrated to be capable of regulating the expression of their protein coding counterparts (Friedman and Jones, 2009). MiRNAs have emerged as an important class of ncRNAs regulating gene expression and affecting pathways important in mammalian development and disease (Friedman and Jones, 2009). Because the basic principles of miRNA-target interaction are still only partially understood (Brodersen and Voinnet, 2009) and because the indirect

effects induced by miRNAs can sometimes mask the predicted direct effects of miRNAs, the molecular consequences of altered miRNA levels can be hard to predict and interpret. Nevertheless, such knowledge is essential in order to translate the discovery of miRNAs and their targets from the bench to life saving drugs at the bedside.

The study of these miRNA-target mRNA interactions and subsequent downstream effects become even more complex when examined *in vivo*. This is especially true in the context of cancer where genetic mutations, epigenetic modifications, altered protein and metabolic networks further add to the regulatory complexity (Volinia et al., 2010; Wang et al., 2007). With the advent of high throughput transcriptome analysis in the form of microarray and new generation sequencing technologies, changes in the cancer cell have been found to occur not only in protein coding genes, but also in the non-coding parts of the genome. Understanding the effects of such large-scale changes using a reductionist approach is challenging and even impractical (McDonald, in press). However, the argument for this 'bottom-up' approach is that it allows us to understand the mechanisms of regulation with a significant degree of detail. Here, molecular biology and systems level analysis were used in combination to analyze the global changes in miRNA and mRNA expression in ovarian cancer. The finding described in CHAPTER 2 that only 11 % of changes in miRNA targets can be attributed to the existing model of miRNA regulation is consistent with the ever expanding complexity found in cancer, and it suggests the involvement of additional regulatory modalities in the control of transcript levels. In light of this finding, the naïve expectation that miRNA up-regulation or down-regulation in cancer would result in inversely correlated changes in its target genes is inadequate. Our results therefore necessitate a more detailed analysis of miRNA regulatory networks in the cancer cell.

In CHAPTER 3, just such an undertaking is accomplished by using microarray analysis to assay changes in global mRNA output caused by single miRNA transfections. The results of our analyses suggest that the direct effects of miRNA targeting on the

transcriptome are magnified by 3-4 fold because of mRNA changes that occur downstream of the initial target(s). While changes in such a large number of transcripts potentially could disrupt a large number of pathways, enrichment analysis of pathways and network analysis of differentially expressed genes suggest miRNAs are likely to affect specific pathways by regulating key genes. In combination with the recent findings that miRNAs tend to regulate functionally related genes (He et al., 2010), our results suggest that these molecules could be used in a therapeutic setting to target specific disease related processes when the genome-wide effects of miRNAs are not counter-therapeutic and modulate pathways implicated in diseases.

The reasons for the large numbers of downstream effects described and presented in CHAPTER 3 led us to conclude that there are modes of regulation by miRNAs that were previously uncharacterized. In CHAPTER 4, we designed studies to test the hypothesis that miRNAs may affect the levels of other mature miRNAs and the data presented are consistent with this hypothesis. As each miRNA is predicted to target hundreds of genes (Trang et al., 2011), this novel finding may help explain the altered expression of thousands of transcripts by a single miRNA. We propose that by having the capability to trigger such large scale changes, miRNAs ensure that they maintain cellular homeostasis, especially in the face of potential insults from the environment, as well as metabolic and inflammatory pathways (Bates et al., 2009). This model is consistent with recent reports suggesting several miRNAs may act in a coordinated manner to ensure the regulation of target genes and corresponding cellular processes (Volinia et al., 2010; Xu et al., 2011).

These studies provide new insights on the mechanisms used by miRNAs to regulate gene expression and their consequences on the transcriptome and other cellular processes. While the discovery of these small regulatory RNAs holds great promise for fighting cancer and other diseases, therapeutic success will come only from a systems level understanding of the consequences of altering the miRNA levels within the cell.

The results presented here suggest that despite the large numbers of off-target transcripts altered by miRNAs, they may regulate specific functions within the cell. Recent genomic studies of cancer suggest that it is not a disease with random disruptions in genes, but rather involves multiple genes within specific regulatory pathways (Jones et al., 2008; Parsons et al., 2008). Thus, using miRNAs therapeutically may be a useful strategy as they have evolved over millions of years to regulate multiple genes in pathways important for eukaryotic development. Future studies need to address the cell and tissue specific effects of these molecules *in vivo*. Additionally, novel delivery tools must be able to specifically direct miRNAs to the target sites to avoid the potential harmful effects of disrupting miRNA levels in the surrounding cells. Questions related to dosage, kinetics, and targeting efficacy also need to be addressed in detail before these miRNAs can be used with confidence in the clinic. In combination with existing chemotherapy regimens, miRNA based therapy may emerge as an effective strategy for treating cancer and other diseases associated with processes regulated by miRNAs.

APPENDIX A

SUPPLEMENTARY INFORMATION FOR CHAPTER 2

Table A.1. Differentially expressed miRNA probesets detected by microarray. Forty-two differentially expressed miRNA probesets in three CEPI and three OSE samples as analyzed by microarray (Ambion miRChip V1). These probesets were selected based on a p-value <0.01, $\log_2$ difference ≥1, and Affymetrix "Present/Marginal" call in at least 1 sample. The mature miRNA names and the sequences corresponding to each probeset, the average log expression values from the OSE and CEPI samples, as well as, the log2 difference and t-test p-value calculated from these are given. Probesets that do not refer to miRNAs currently annotated in Sanger miRBase are given as "exploratory". Sequences of these exploratory miRNAs are based on computational predictions from previous studies.

Probe_ID	Mature miRNA name	miRNA sequence	t-test/Anova	Avg log exp (normals)	Avg log exp (cancers)	Log difference (ca-norm)
hsa-miR-383_st1	hsa-miR-383	AGAUCAGAAGGUGAUUGUGGCU	0.008072629	4.571	2.204	-2.367
hsa-asg-8878_st2	hsa-miR-193a-5p	UGGGUCUUUGCGGGCGAGAUGA	0.003964239	10.408	8.268	-2.141
hsa-asg-14245_st1	hsa-miR-768 (REMOVED**)	NA (has been removed from database due to changes in annotation)	0.007681288	12.425	10.358	-2.068
hsa-miR-320_st1	hsa-miR-320a	AAAAGCUGGGUUGAGAGGGCGAA	0.002455114	10.227	8.363	-1.864
hsa-asg-5208_st1	Exploratory	UUCUAGUGGGGGGUAGAUGUCA	0.001721781	6.827	4.985	-1.842
hsa-asg-4118_st1	Exploratory	UUGGAAAGGGGGUUUGGGACUC	0.001094825	7.325	5.825	-1.500

Table A.1 (continued)

Probe_ID	Mature miRNA name	miRNA sequence	t-test/Anova	Avg log exp (normals)	Avg log exp (cancers)	Log difference (ca-norm)
hsa-asg-11500_st1	Exploratory	AGGAGCAGGCUGUGUGGGCCUC	0.00650681	6.053	4.677	-1.375
hsa-asg-3670_st1	Exploratory	GGAGGUGGAGGGGAGCAGGAUU	9.07E-05	9.369	8.184	-1.185
hsa-asg-6021_st2	Exploratory	UGGGGGAGGAGGUCAGUGAGGC	0.0055479	8.550	7.412	-1.138
hsa-asg-11373_st1	Exploratory	UUGUGAGAGGGGAGACUUGGCA	0.001975077	7.042	8.174	1.132
hsa-asg-13500_st1	Exploratory	GGUGGCCAGGUGCAUAUCUUGG	0.004985624	7.302	9.039	1.737
hsa-asg-3101_st2	Exploratory	AAAUGGGGAGAAGGCAGG	0.008239333	5.341	7.195	1.854
hsa-asg-8336_st2	Exploratory	UGUUGAAUCUGAGGGCCAGGCU	0.003692066	6.330	8.236	1.905
hsa-asg-5405_st2	Exploratory	UAGGCUGAGCUCAGGGUUCAGG	0.005112173	3.859	5.838	1.980
hsa-asg-11695_st2	Exploratory	CCUGGCAAGGCUUGAUUGCUUU	0.001549414	2.365	4.521	2.156
hsa-asg-6895_st1	Exploratory	AGUAUUCAGCUGGAGGAGCUGA	0.003869916	2.365	4.556	2.190
cel-miR-38_st1	cel-miR-38	UCACCGGGAGAAAAACUGGAGU	0.009709809	4.452	6.911	2.459
hsa-cand493_st1	Exploratory	UAAAAUAUGCCUGUGGGGAGC	0.006326216	6.025	8.552	2.527

Table A.1 (continued)

Probe_ID	Mature miRNA name	miRNA sequence	t-test/Anova	Avg log exp (normals)	Avg log exp (cancers)	Log difference (ca-norm)
hsa-asg-12049_st2	Exploratory	UAAUCACUAGAGCGGGGACUCA	0.006562359	6.340	8.929	2.589
hsa-asg-9752_st2	Exploratory	UAGAGCAAUGUGUAGGAGAGGC	0.006853174	3.575	6.488	2.913
hsa-asg-6879_st1	Exploratory	CCAAACUAUGGAUGGACGAAGA	9.79E-05	4.339	7.468	3.129
hsa-asg-1514_st1	Exploratory	GCCUAGUCCCAGGGAGACAGCC	0.006838428	3.014	6.266	3.252
hsa-asg-6932_st1	Exploratory	CAGGGAGCCUGAGUAACUGGAA	0.002984173	5.404	8.947	3.543
hsa-asg-5640_st1	Exploratory	UCCCAGCGGUGCCUCCA	0.003286316	11.494	15.040	3.547
hsa-asg-11988_st1	Exploratory	GGUGCUGUUUAUGGGAGCAGGG	0.005693259	3.996	7.630	3.635
hsa-cand794_st2	Exploratory	CUCCAGCGGGGAGUUUGCCAG	0.005342086	3.267	7.249	3.981
hsa-asg-8711_st1	Exploratory	CAAGGCCAGAGGGCAUUCAAGU	0.001001302	2.150	6.281	4.131
hsa-asg-2267_st2	Exploratory	UGUCAUUUGGGCUGGGCU	0.008303415	2.825	7.124	4.299
hsa-miR-128a_st2	hsa-miR-128	UCACAGUGAACCGGUCUCUUUU	0.009837739	2.968	7.907	4.938
hsa-miR-18b_st1	hsa-miR-18b	UAAGGUGCAUCUAGUGCAGUUA	0.00085144	1.732	6.893	5.162
hsa-miR-7_st1	hsa-miR-7	UGGAAGACUAGUGAUUUUGUUG	0.000683997	1.824	7.210	5.386

Table A.1 (continued)

Probe_ID	Mature miRNA name	miRNA sequence	t-test/Anova	Avg log exp (normals)	Avg log exp (cancers)	Log difference (ca-norm)
hsa-asg-7839_st2	Exploratory	CCUGGGACUCUGAAUCCAGCUG	0.003526797	1.924	7.334	5.410
hsa-cand497_st1	hsa-miR-126	UCGUACCGUGAGUAAUAAUGC	0.008383114	3.526	8.970	5.444
hsa-miR-429_st1	hsa-miR-429	UAAUACUGUCUGGUAAAACCGU	0.004302851	2.322	7.773	5.451
hsa-asg-2025_st2	hsa-miR-93*	ACUGCUGAGCUAGCACUUCCCG	0.005915096	0.164	5.811	5.647
ppy-miR-141_st1	ppy-miR-141	AACACUGUCUGGUAAAGAUGG	0.002244399	3.149	8.835	5.686
hsa-miR-18a_st1	hsa-miR-18a	UAAGGUGCAUCUAGUGCAGAUA	0.00182884	1.569	7.354	5.785
hsa-asg-14002_st1	Exploratory	CCUCUCAGUUUAGGAGGGCCGU	0.002658157	3.071	8.922	5.851
hsa-asg-10048_st1	Exploratory	AUCACCCAGGUGACAGCGAGCA	0.005840041	0.423	6.538	6.115
hsa-miR-141_st1	hsa-miR-141	UAACACUGUCUGGUAAAGAUGG	0.000944845	2.852	9.210	6.358
hsa-miR-205_st1	hsa-miR-205	UCCUUCAUUCCACCGGAGUCUG	0.004225528	1.901	8.409	6.507
hsa-miR-126_st2	hsa-miR-126	UCGUACCGUGAGUAAUAAUGC	0.000925874	1.922	9.057	7.135

** miR-768 overlaps an annotated snoRNA, HBII-239. Phylogenetic analysis in all vertebrates supports the snoRNA annotation, with poor conservation of the reported mature miRNA sequence (Weber M, pers comm). It is therefore removed from miRBase.

Table A.2. Differentially expressed mRNA probes in CEPI compared to OSE. Differentially expressed mRNA probesets between three CEPI samples and OSE from five normal samples as analyzed by microarray (Affymetrix HG-U133 Plus 2.0). These probesets were selected based on a p-value <0.005, fold change ≥2, and Affymetrix "Present/Marginal" call in at least 1 sample. The gene symbols corresponding to each probeset ID, the average log expression values from the OSE and CEPI samples as well as the log2 difference and t-test p-value calculated from these are given.

Please see table on our website:

http://www.mcdonaldlab.biology.gatech.edu/shubin_shahab.htm

Table A.3. IC, PC and NC targets of miRNAs in tissue samples. Target predictions from miRanda (M), TargetScan (TS) and PicTar (PT) programs were downloaded (see methods for details) for each of the 12 annotated miRNAs. MiRNA targets that were differentially expressed between CEPI and OSE based on t-test p <0.005 and fold change of at least 2 were classified as being IC or PC with their regulating miRNAs (while target genes that do not meet the above criteria are classified as NC). The IC targets are shown in green, PC targets are shown in red, and blue represents NC targets. Targets with "Absent" calls in all samples have been removed. For miR-93*, TargetScan custom (TScustom; http://www.targetscan.org/vert_50/seedmatch.html) was used to generate TargetScan predictions. For hsa-miR-429 and hsa-miR-93* there were no PicTar predictions and thus targets of these miRNAs were excluded for analysis when calculating intersections.

Please see table on our website:

http://www.mcdonaldlab.biology.gatech.edu/shubin_shahab.htm

Table A.4. Differentially expressed genes between miR-7 transfected and negative control transfected HEY cells. Differentially expressed genes (fold change ≥1.4, FDR ≤5%) in three samples of miR-7 transfected cells compared to three samples of miR-NC transfected cells. 'Probeset ID' refers to Affymetrix HG-U133 Plus 2.0 probeset identifier. 'Gene Symbol' shows the official gene symbol for the corresponding Probeset ID. 'Log difference (miR7-miR-NC)' refers to the difference between average log2 signal values of miR-7 transfected group and the miR-NC transfected group. 'q-value (%)' shows the false discovery rate calculated using the SAM algorithm. Targets of miR-7 predicted by miRanda (M), TargetScan (TS), and PicTar (PT) programs are also shown.

Please see table on our website:

http://www.mcdonaldlab.biology.gatech.edu/shubin_shahab.htm

Table A.5. Differentially expressed genes between miR-128 transfected and negative control transfected HEY cells. Differentially expressed genes (fold change ≥1.4, FDR ≤5 %) between two samples of miR-128 transfected cells compared to three samples of miR-NC transfected cells. 'Probeset ID' refers to Affymetrix HG-U133 Plus 2.0 probeset identifier. 'Gene Symbol' shows the official gene symbol for the corresponding Probeset ID. 'Log difference (miR128-miR-NC)' refers to the difference between average log2 signal values of miR-128 transfected group and the miR-NC transfected group. 'q-value (%)' shows the false discovery rate calculated using the SAM algorithm. Predicted targets from miRanda (M), TargetScan (TS), and PicTar (PT) are also shown.

Please see table on our website:

http://www.mcdonaldlab.biology.gatech.edu/shubin_shahab.htm

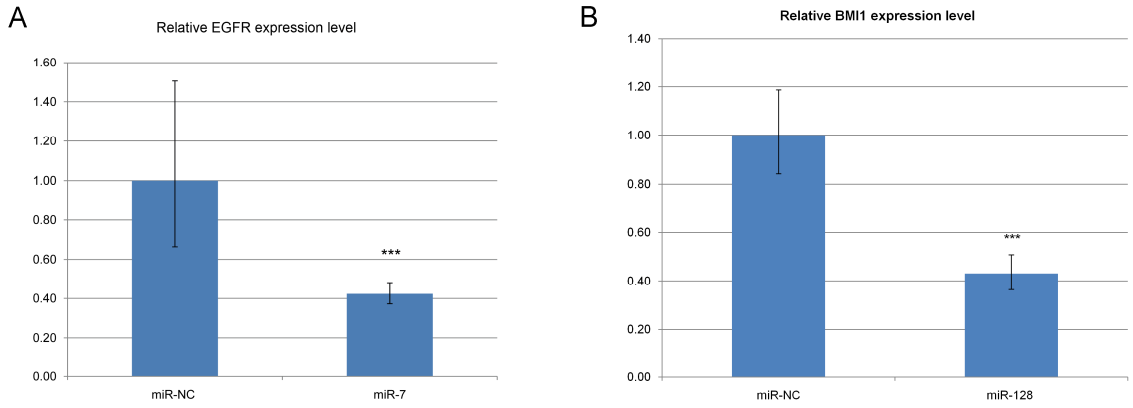

Figure A.1. Confirmation of successful miR-7 and miR-128 transfection into HEY cells. Successful transfection of miR-7 and miR-128 was confirmed by assaying the relative down-regulation of their respective validated targets EGFR and BMI1. Here we confirmed successful transfection of the miRNAs into HEY cells by measuring EGFR and BMI1 RNA levels using qPCR following transfection of either miR-NC or

miR7/miR-128 into HEY cells. Transfection of miR-7 or miR-128 down-regulated EGFR or BMI1 by ~60 % relative to miR-NC. *** $p < 0.005$.

APPENDIX B

SUPPLEMENTARY INFORMATION FOR CHAPTER 3

Table B.1. Differentially expressed genes in miR-7 transfected HEY cells. Genes differentially expressed (fold change ≥1.4, FDR ≤5 %) in three samples of HEY ovarian cancer cells transfected with miR-7 compared to three samples of HEY cells transfected with negative control miRNA (miR-NC). 'Probeset ID' refers to Affymetrix HG-U133 Plus 2.0 probeset identifier. 'Gene Symbol' shows the official gene symbol for the corresponding Probeset ID. 'miR7-miR-NC' refers to the difference between average log2 signal values (i.e. the $\log_2$ of the ratio of signal values) of miR-7 transfected group and the miR-NC transfected group. 'q-value (%)' shows the false discovery rate calculated using the SAM algorithm. miRanda predicted targets of miR-7 are listed in the column titled 'miR7tgts_M', TargetScan predicted targets of miR-7 are listed under the heading miR-7tgts_TS, and predicted PicTar targets of miR-7 are listed under the heading miR-7tgts_PT.

Please see our table on our website:
http://www.mcdonaldlab.biology.gatech.edu/shubin_shahab.htm

Table B.2. Differentially expressed genes in miR-128 transfected HEY cells. Differentially expressed genes (fold change ≥1.4, FDR ≤5 %) between two samples of miR-128 transfected cells, compared to three samples of miR-NC transfected cells. 'Probeset ID' refers to Affymetrix HG-U133 Plus 2.0 probeset identifier. 'Gene Symbol' shows the official gene symbol for the corresponding Probeset ID. 'miR128-miR-NC' refers to the difference between average $\log_2$ signal values of miR-128 transfected group and the miR-NC transfected group. 'q-value (%)' shows the false discovery rate calculated using the SAM algorithm. miRanda predicted targets of miR-128 are listed in the column titled 'miR-128tgts_M', TargetScan predicted targets of miR-128 are listed under the heading miR-128tgts_TS, and PicTar predicted targets of miR-128 are listed under the heading miR-128tgts_PT.

Please see table on our website:
http://www.mcdonaldlab.biology.gatech.edu/shubin_shahab.htm

Table B.3. MiRNA target enrichment analysis among up-regulated genes following miR-128 transfection. Genomica enrichment (FDR <0.05) of miRNA targets among significantly up-regulated genes following miR-128 transfection into HEY cells. Regulating miRNAs are predicted based on prediction programs miRanda (those with the prefix John04 or SloanKettering), TargetScan or PicTar. The sets are classified into either

Table B.3 (continued)

targeting "down" genes, i.e. down-regulated in the transfection, or "up" genes. The other columns show the p-value of enrichment, the number of genes that are in each set in our dataset, compared to the number of genes in each set in the background Affymetrix chip. The percentages calculated from raw numbers of genes that belong in each set are also shown.

Set	Enriched Set	Enriched Value	P-value	Set Hits	Set Size	Set Hits (%)	Total Hits	Total Size	Total Hits (%)
Up	John04_hsa-miR-191	1	1.32E-08	36	2148	1.68	253	43407	0.59
Up	John04_hsa-miR-363	1	2.62E-04	36	2148	1.68	389	43407	0.9
Up	Targetscan_hsa-miR-409-5p	1	3.07E-03	28	2148	1.31	323	43407	0.75
Up	SloanKettering_hsa-miR-20	1	1.93E-07	44	2148	2.05	381	43407	0.88
Up	SloanKettering_hsa-miR-17_5p	1	1.27E-05	34	2148	1.59	309	43407	0.72
Up	John04_hsa-miR-106a	1	2.06E-03	43	2148	2.01	547	43407	1.27
Up	John04_hsa-miR-148	1	3.83E-03	67	2148	3.12	968	43407	2.24
Up	John04_hsa-miR-18	1	7.64E-09	87	2148	4.06	921	43407	2.13
Up	John04_hsa-miR-183	1	2.48E-03	60	2148	2.8	832	43407	1.92
Up	John04_hsa-miR-93	1	6.30E-05	56	2148	2.61	657	43407	1.52
Up	John04_mmu-miR-148a	1	3.83E-03	67	2148	3.12	968	43407	2.24
Up	John04_mmu-miR-291_3p	1	7.17E-04	66	2148	3.08	887	43407	2.05
Up	John04_mmu-miR-300	1	2.84E-03	61	2148	2.84	854	43407	1.97
Up	Pictar_hsa-miR-183	1	1.20E-03	64	2148	2.98	872	43407	2.01
Up	Pictar_hsa-miR-33	1	7.07E-03	57	2148	2.66	823	43407	1.9
Up	Pictar_hsa-miR-145	1	2.21E-05	71	2148	3.31	862	43407	1.99
Up	Targetscan_hsa-miR-183	1	4.05E-04	66	2148	3.08	868	43407	2

Table B.3 (continued)

Set	Enriched Set	Enriched Value	P-value	Set Hits	Set Size	Set Hits (%)	Total Hits	Total Size	Total Hits (%)
Up	Targetscan_hsa-miR-199	1	2.16E-04	64	2148	2.98	816	43407	1.88
Up	Targetscan_hsa-miR-324-3p	1	4.00E-04	42	2148	1.96	488	43407	1.13
Up	Targetscan_hsa-miR-33	1	1.88E-03	55	2148	2.57	739	43407	1.71
Up	John04_hsa-miR-145	1	1.84E-04	58	2148	2.71	716	43407	1.65
Up	John04_hsa-miR-30d	1	5.69E-04	68	2148	3.17	912	43407	2.11
Up	Pictar_hsa-miR-122a	1	8.67E-04	32	2148	1.49	355	43407	0.82
Up	Targetscan_hsa-miR-122a	1	1.29E-03	34	2148	1.59	394	43407	0.91
Up	Targetscan_hsa-miR-299	1	1.87E-04	56	2148	2.61	685	43407	1.58
Up	Targetscan_hsa-miR-378	1	1.97E-04	71	2148	3.31	926	43407	2.14
Up	John04_hsa-let-7a	1	1.71E-04	63	2148	2.94	793	43407	1.83
Up	John04_hsa-let-7c	1	5.12E-03	53	2148	2.47	742	43407	1.71
Up	John04_hsa-let-7d	1	1.31E-04	65	2148	3.03	817	43407	1.89
Up	John04_hsa-let-7e	1	6.60E-03	52	2148	2.43	735	43407	1.7
Up	John04_hsa-let-7f	1	8.98E-08	73	2148	3.4	767	43407	1.77
Up	John04_hsa-let-7g	1	1.50E-04	67	2148	3.12	853	43407	1.97
Up	John04_hsa-let-7i	1	4.47E-04	61	2148	2.84	790	43407	1.82
Up	John04_hsa-miR-221	1	3.72E-04	38	2148	1.77	426	43407	0.99
Up	John04_hsa-miR-98	1	6.58E-06	66	2148	3.08	755	43407	1.74
Up	John04_rno-miR-327	1	5.94E-04	45	2148	2.1	544	43407	1.26
Up	John04_hsa-miR-29c	1	4.14E-03	62	2148	2.89	886	43407	2.05
Up	John04_mmu-miR-291_5p	1	6.92E-04	57	2148	2.66	739	43407	1.71

Table B.3 (continued)

Set	Enriched Set	Enriched Value	P-value	Set Hits	Set Size	Set Hits (%)	Total Hits	Total Size	Total Hits (%)
Up	Targetscan_hsa-miR-219	1	6.13E-03	54	2148	2.52	766	43407	1.77
Up	John04_hsa-miR-30c	1	8.29E-03	59	2148	2.75	864	43407	2
Up	John04_hsa-miR-30e	1	6.78E-03	66	2148	3.08	976	43407	2.25
Up	Pictar_hsa-miR-205	1	2.92E-04	62	2148	2.89	793	43407	1.83
Up	Targetscan_hsa-miR-18	1	1.30E-03	42	2148	1.96	518	43407	1.2
Up	Targetscan_hsa-miR-205	1	4.48E-07	72	2148	3.36	785	43407	1.81
Up	Targetscan_hsa-miR-486	1	1.32E-04	31	2148	1.45	305	43407	0.71
Up	John04_hsa-miR-30b	1	7.86E-03	51	2148	2.38	725	43407	1.68
Up	Targetscan_hsa-miR-485-5p	1	1.40E-04	45	2148	2.1	509	43407	1.18
Up	Targetscan_hsa-miR-140	1	8.18E-03	38	2148	1.77	509	43407	1.18
Up	John04_hsa-miR-208	1	4.23E-03	26	2148	1.22	300	43407	0.7
Up	Targetscan_hsa-miR-329	1	3.03E-03	52	2148	2.43	706	43407	1.63
Up	SloanKettering_hsa-miR-135	1	3.07E-03	15	2148	0.7	136	43407	0.32
Up	John04_rno-miR-345	1	3.10E-03	19	2148	0.89	191	43407	0.45
Up	Pictar_hsa-miR-150	1	1.35E-04	53	2148	2.47	630	43407	1.46
Up	Pictar_hsa-miR-185	1	1.42E-03	62	2148	2.89	845	43407	1.95
Up	Targetscan_hsa-miR-136	1	5.89E-03	31	2148	1.45	386	43407	0.89
Up	Targetscan_hsa-miR-210	1	7.84E-04	8	2148	0.38	41	43407	0.1
Up	SloanKettering_hsa-miR-181a	1	5.31E-03	16	2148	0.75	158	43407	0.37
Up	Pictar_hsa-miR-21	1	4.97E-06	50	2148	2.33	514	43407	1.19
Up	Targetscan_hsa-miR-21	1	9.77E-05	49	2148	2.29	561	43407	1.3

Table B.3 (continued)

Set	Enriched Set	Enriched Value	P-value	Set Hits	Set Size	Set Hits (%)	Total Hits	Total Size	Total Hits (%)
Up	Targetscan_hsa-miR-503	1	9.91E-08	80	2148	3.73	871	43407	2.01
Up	Pictar_hsa-miR-30a-3p	1	7.84E-03	54	2148	2.52	776	43407	1.79
Up	Pictar_hsa-miR-30e-3p	1	6.77E-03	54	2148	2.52	770	43407	1.78
Up	Targetscan_hsa-miR-30-3p	1	5.30E-04	71	2148	3.31	959	43407	2.21
Up	Pictar_hsa-miR-146b	1	1.06E-07	44	2148	2.05	373	43407	0.86
Up	Pictar_hsa-miR-146a	1	5.50E-08	46	2148	2.15	390	43407	0.9
Up	Targetscan_hsa-miR-146	1	2.61E-09	49	2148	2.29	390	43407	0.9
Up	Targetscan_hsa-miR-377	1	1.29E-03	63	2148	2.94	858	43407	1.98
Up	John04_hsa-miR-137	1	5.65E-03	41	2148	1.91	546	43407	1.26
Up	Pictar_hsa-miR-335	1	5.03E-04	40	2148	1.87	463	43407	1.07
Up	Targetscan_hsa-miR-335	1	2.45E-05	46	2148	2.15	487	43407	1.13
Up	Targetscan_hsa-miR-193	1	3.30E-03	36	2148	1.68	449	43407	1.04
Up	SloanKettering_hsa-miR-145	1	7.50E-07	15	2148	0.7	67	43407	0.16
Up	Pictar_hsa-miR-18a	1	8.24E-04	42	2148	1.96	506	43407	1.17
Up	Pictar_hsa-miR-18b	1	2.06E-03	41	2148	1.91	515	43407	1.19
Up	Targetscan_hsa-miR-139	1	1.03E-03	54	2148	2.52	703	43407	1.62
Up	SloanKettering_hsa-miR-19a	1	2.96E-03	26	2148	1.22	292	43407	0.68
Up	SloanKettering_hsa-miR-1	1	7.19E-03	15	2148	0.7	149	43407	0.35
Up	SloanKettering_hsa-miR-19b	1	1.11E-05	30	2148	1.4	255	43407	0.59
Up	SloanKettering_hsa-miR-206	1	2.30E-03	15	2148	0.7	132	43407	0.31
Up	John04_hsa-miR-194	1	8.34E-05	56	2148	2.61	664	43407	1.53

Table B.3 (continued)

Set	Enriched Set	Enriched Value	P-value	Set Hits	Set Size	Set Hits (%)	Total Hits	Total Size	Total Hits (%)
Up	John04_hsa-miR-205	1	1.35E-03	42	2148	1.96	519	43407	1.2
Up	John04_mmu-miR-290	1	1.80E-03	44	2148	2.05	559	43407	1.29
Up	Pictar_hsa-miR-221	1	6.66E-04	58	2148	2.71	754	43407	1.74
Up	Pictar_hsa-miR-222	1	1.64E-03	54	2148	2.52	718	43407	1.66
Up	Pictar_hsa-miR-187	1	2.74E-03	7	2148	0.33	39	43407	0.09
Up	Targetscan_hsa-miR-191	1	1.58E-03	13	2148	0.61	102	43407	0.24
Up	SloanKettering_hsa-miR-26a	1	3.30E-04	21	2148	0.98	184	43407	0.43
Up	John04_hsa-miR-150	1	6.16E-03	32	2148	1.49	403	43407	0.93
Up	John04_hsa-miR-26a	1	1.48E-06	83	2148	3.87	978	43407	2.26
Up	John04_hsa-miR-26b	1	2.57E-06	83	2148	3.87	992	43407	2.29
Up	Targetscan_hsa-miR-485-3p	1	6.37E-03	41	2148	1.91	550	43407	1.27
Up	Targetscan_hsa-miR-192	1	5.19E-07	39	2148	1.82	330	43407	0.77
Up	Pictar_hsa-miR-22	1	1.50E-03	65	2148	3.03	897	43407	2.07
Up	Targetscan_hsa-miR-542-3p	1	8.50E-05	51	2148	2.38	588	43407	1.36
Up	Targetscan_hsa-miR-452	1	1.78E-03	41	2148	1.91	511	43407	1.18
Up	Targetscan_hsa-miR-221	1	9.92E-04	55	2148	2.57	718	43407	1.66
Up	SloanKettering_hsa-miR-9	1	6.76E-03	21	2148	0.98	235	43407	0.55
Up	SloanKettering_hsa-miR-150	1	6.06E-03	8	2148	0.38	56	43407	0.13
Up	SloanKettering_hsa-miR-15a	1	3.07E-03	20	2148	0.94	205	43407	0.48
Up	SloanKettering_hsa-miR-15b	1	1.72E-03	21	2148	0.98	209	43407	0.49
Up	John04_hsa-miR-23b	1	3.16E-03	66	2148	3.08	943	43407	2.18

Table B.3 (continued)

Set	Enriched Set	Enriched Value	P-value	Set Hits	Set Size	Set Hits (%)	Total Hits	Total Size	Total Hits (%)
Up	SloanKettering_hsa-miR-29c	1	3.48E-03	19	2148	0.89	193	43407	0.45
Up	SloanKettering_hsa-let-7f	1	1.62E-05	19	2148	0.89	127	43407	0.3
Up	SloanKettering_hsa-miR-29a	1	1.08E-03	14	2148	0.66	110	43407	0.26
Up	Pictar_hsa-miR-217	1	7.97E-04	49	2148	2.29	615	43407	1.42
Up	SloanKettering_hsa-let-7e	1	2.68E-03	14	2148	0.66	121	43407	0.28
Up	SloanKettering_hsa-let-7g	1	5.02E-05	18	2148	0.84	126	43407	0.3
Up	Targetscan_hsa-miR-189	1	2.31E-04	27	2148	1.26	259	43407	0.6
Up	SloanKettering_hsa-let-7a	1	9.30E-04	17	2148	0.8	146	43407	0.34
Up	Pictar_hsa-miR-302a-star	1	9.57E-04	15	2148	0.7	121	43407	0.28
Up	John04_mmu-miR-292_3p	1	9.28E-04	21	2148	0.98	199	43407	0.46
Up	SloanKettering_hsa-miR-7	1	1.20E-03	13	2148	0.61	99	43407	0.23
Up	SloanKettering_hsa-miR-363	1	9.07E-04	6	2148	0.28	24	43407	0.06
Up	SloanKettering_rno-miR-352	1	5.10E-03	6	2148	0.28	33	43407	0.08
Up	SloanKettering_hsa-miR-221	1	1.85E-05	12	2148	0.56	57	43407	0.14

Table B.4. MiRNA target enrichment analysis among up-regulated genes following miR-7 transfection. Genomica enrichment (FDR <0.05) of miRNA targets among significantly up-regulated genes following miR-7 transfection into HEY cells. Regulating miRNAs are predicted based on prediction programs miRanda (those with the prefix John04 or SloanKettering), TargetScan or PicTar. The sets are classified into either targeting "down" genes, i.e. down-regulated in the transfection, or "up" genes. The other columns show the p-value of enrichment, the number of genes that are in each set in our dataset, compared to the number of genes in each set in the background. The percentages calculated from raw numbers of genes that belong in each set are also shown.

Set	Enriched Set	Enriched Value	P-value	Set Hits	Set Size	Set Hits (%)	Total Hits	Total Size	Total Hits (%)
Up	Pictar_hsa-miR-199b	1	4.12E-05	11	174	6.33	613	43407	1.42
Up	Pictar_hsa-miR-199a	1	3.60E-06	11	174	6.33	471	43407	1.09

Table B.5. Microarray expression levels of untransfected HEY cell miRNAs. Signal values from Affymetrix microarray analysis of miRNA expression from two independent samples of untransfected HEY cells. 'Probeset name' refers to the unique Affymetrix identifier for sequences on the chip. The $\log_2$ transformed signal values for each cell sample and the p-value of detection is also shown. Signal values with Wilcoxon $p < 0.06$ of detection are called "TRUE". The 'mean signal' column shows the average of the $\log_2$ signal values from the two HEY cell signal columns.

Please see table on our website:
http://www.mcdonaldlab.biology.gatech.edu/shubin_shahab.htm

Table B.6. Hub genes and their targets affected by miR-7 in HEY cells. GeneGo was used to analyze the most significant interactions within the set of differentially expressed genes following miR-7 transfection. The analysis gives a list of "hub" genes interacting with other differentially expressed genes (i.e. nodes) which suggests that miRNA are regulating the node genes indirectly through regulating the hubs. 'IDs in active dataset' refer to the Probeset IDs in the dataset that passed the GeneGo FDR threshold of 5 % and are acting as hubs. Corresponding GeneGo gene identifiers are given in 'Object name' column. 'IDs of corresponding network object from GeneGo network' refer to probeset IDs of objects in the dataset that the hubs are interacting with in GeneGo networks. The names of these nodes are given in the last column. If a hub gene is found to regulate another gene which may also act as a hub then the row is shaded.

IDs in active data set	Object name	IDs of corresponding network object from GeneGo network	Corresponding network object name
201783_s_at; 230202_at	RelA (p65 NF-kB subunit)	1555938_x_at	Vimentin
201783_s_at; 230202_at	RelA (p65 NF-kB subunit)	1564907_s_at; 242260_at	Matrin-3

Table B.6 (continued)

IDs in active data set	Object name	IDs of corresponding network object from GeneGo network	Corresponding network object name
201783_s_at; 230202_at	RelA (p65 NF-kB subunit)	1568574_x_at; 209875_s_at	Osteopontin
201783_s_at; 230202_at	RelA (p65 NF-kB subunit)	1569788_at	SIAT8A
201783_s_at; 230202_at	RelA (p65 NF-kB subunit)	200690_at	GRP75
201783_s_at; 230202_at	RelA (p65 NF-kB subunit)	201042_at	TGM2
201783_s_at; 230202_at	RelA (p65 NF-kB subunit)	201244_s_at	c-Raf-1
201783_s_at; 230202_at	RelA (p65 NF-kB subunit)	202443_x_at; 212377_s_at	NOTCH2 (2ICD)
201783_s_at; 230202_at	RelA (p65 NF-kB subunit)	202847_at	PPCKM
201783_s_at; 230202_at	RelA (p65 NF-kB subunit)	202859_x_at; 211506_s_at	IL-8
201783_s_at; 230202_at	RelA (p65 NF-kB subunit)	202886_s_at	PPP2R1B
201783_s_at; 230202_at	RelA (p65 NF-kB subunit)	203220_s_at; 203222_s_at	TLE1
201783_s_at; 230202_at	RelA (p65 NF-kB subunit)	204296_at	DCTN1(p150Glued)
201783_s_at; 230202_at	RelA (p65 NF-kB subunit)	204470_at	GRO-1
201783_s_at; 230202_at	RelA (p65 NF-kB subunit)	204799_at	Y637
201783_s_at; 230202_at	RelA (p65 NF-kB subunit)	205067_at; 39402_at	IL-1 beta

Table B.6 (continued)

IDs in active data set	Object name	IDs of corresponding network object from GeneGo network	Corresponding network object name
201783_s_at; 230202_at	RelA (p65 NF-kB subunit)	205289_at	BMP2
201783_s_at; 230202_at	RelA (p65 NF-kB subunit)	205416_s_at	MJD (ataxin-3)
201783_s_at; 230202_at	RelA (p65 NF-kB subunit)	205798_at	IL7RA
201783_s_at; 230202_at	RelA (p65 NF-kB subunit)	207196_s_at	TNIP1
201783_s_at; 230202_at	RelA (p65 NF-kB subunit)	207563_s_at; 207564_x_at; 209240_at; 212307_s_at; 220594_at; 229787_s_at	OGT (GlcNAc transferase)
201783_s_at; 230202_at	RelA (p65 NF-kB subunit)	209383_at	C/EBP zeta
201783_s_at; 230202_at	RelA (p65 NF-kB subunit)	209774_x_at	GRO-2
201783_s_at; 230202_at	RelA (p65 NF-kB subunit)	209946_at	VEGF-C
201783_s_at; 230202_at	RelA (p65 NF-kB subunit)	210385_s_at; 212580_at	ARTS-1
201783_s_at; 230202_at	RelA (p65 NF-kB subunit)	211434_s_at	CCRL2
201783_s_at; 230202_at	RelA (p65 NF-kB subunit)	212188_at	KCTD12
201783_s_at; 230202_at	RelA (p65 NF-kB subunit)	214528_s_at	PAX8
201783_s_at; 230202_at	RelA (p65 NF-kB subunit)	215485_s_at	ICAM1
201783_s_at; 230202_at	RelA (p65 NF-kB subunit)	217996_at	PHLDA1

Table B.6 (continued)

IDs in active data set	Object name	IDs of corresponding network object from GeneGo network	Corresponding network object name
201783_s_at; 230202_at	RelA (p65 NF-kB subunit)	220266_s_at; 221841_s_at	KLF4
201783_s_at; 230202_at	RelA (p65 NF-kB subunit)	221477_s_at	SOD2
201783_s_at; 230202_at	RelA (p65 NF-kB subunit)	223217_s_at	IKBZ
201783_s_at; 230202_at	RelA (p65 NF-kB subunit)	224654_at	DDX21
201783_s_at; 230202_at	RelA (p65 NF-kB subunit)	224917_at	microRNA 21
201783_s_at; 230202_at	RelA (p65 NF-kB subunit)	227143_s_at	Bid
201783_s_at; 230202_at	RelA (p65 NF-kB subunit)	228363_at; 235222_x_at	XIAP
201783_s_at; 230202_at	RelA (p65 NF-kB subunit)	235020_at	TAF4B
201783_s_at; 230202_at	RelA (p65 NF-kB subunit)	235795_at	PAX6
201783_s_at; 230202_at	RelA (p65 NF-kB subunit)	240221_at	Casein kinase I alpha
202827_s_at	MMP-14	201010_s_at	TXNIP (VDUP1)
202827_s_at	MMP-14	201042_at	TGM2
202827_s_at	MMP-14	201147_s_at; 201149_s_at; 201150_s_at	TIMP3
202827_s_at	MMP-14	201646_at; 201647_s_at; 224983_at	CD36L2
202827_s_at	MMP-14	201920_at; 230494_at	GLVR1

Table B.6 (continued)

IDs in active data set	Object name	IDs of corresponding network object from GeneGo network	Corresponding network object name
202827_s_at	MMP-14	202007_at	Nidogen
202827_s_at	MMP-14	202267_at	LAMC2
202827_s_at	MMP-14	202443_x_at; 212377_s_at	NOTCH2
202827_s_at	MMP-14	202620_s_at	PLOD2
202827_s_at	MMP-14	202859_x_at; 211506_s_at	IL-8
202827_s_at	MMP-14	203821_at; 38037_at	HB-EGF
202827_s_at	MMP-14	203888_at	Thrombomodulin
202827_s_at	MMP-14	205227_at	IL1RAP
202827_s_at	MMP-14	207332_s_at; 208691_at	TfR1
202827_s_at	MMP-14	209281_s_at	PMCA1
202827_s_at	MMP-14	210495_x_at; 211719_x_at; 212464_s_at; 216442_x_at	Fibronectin
202827_s_at	MMP-14	211607_x_at	EGFR
202827_s_at	MMP-14	212097_at	Caveolin-1
202827_s_at	MMP-14	212761_at	TCF7L2 (TCF4)
202827_s_at	MMP-14	224953_at	YIPF5
202827_s_at	MMP-14	226217_at	ZnT7
202827_s_at	MMP-14	226545_at; 229900_at	CD109
202827_s_at	MMP-14	232231_at	RUNX2
202827_s_at	MMP-14	239627_at	TMED9
202827_s_at	MMP-14	34478_at	Rab-11B

Table B.6 (continued)

IDs in active data set	Object name	IDs of corresponding network object from GeneGo network	Corresponding network object name
206011_at	Caspase-1	1554479_a_at; 204950_at	CARD8
206011_at	Caspase-1	1555938_x_at	Vimentin
206011_at	Caspase-1	1556607_at; 209536_s_at; 233660_at	EHD4
206011_at	Caspase-1	1564907_s_at; 242260_at	Matrin-3
206011_at	Caspase-1	200681_at	Glyoxalase I
206011_at	Caspase-1	200755_s_at; 200756_x_at; 200757_s_at; 214845_s_at	Calumenin
206011_at	Caspase-1	203555_at	PTPN18
206011_at	Caspase-1	205067_at; 39402_at	IL-1 beta
206011_at	Caspase-1	205416_s_at	MJD (ataxin-3)
206011_at	Caspase-1	208374_s_at	CAPZA1
206011_at	Caspase-1	209615_s_at; 226507_at	PAK1
206011_at	Caspase-1	209822_s_at	VLDLR
206011_at	Caspase-1	214291_at	RPL17
206011_at	Caspase-1	218850_s_at	LIMD1
206011_at	Caspase-1	222519_s_at	HIPPI
209037_s_at	EHD1	1556607_at; 209536_s_at; 233660_at	EHD4
209037_s_at	EHD1	201783_s_at; 230202_at	RelA (p65 NF-kB subunit)
209037_s_at	EHD1	222597_at	SNAP-29
209037_s_at	EHD1	226581_at	Rabenosyn-5

Table B.6 (continued)

IDs in active data set	Object name	IDs of corresponding network object from GeneGo network	Corresponding network object name
209037_s_at	EHD1	227428_at	GABP alpha
209112_at	p27KIP1	200952_s_at	Cyclin D2
209112_at	p27KIP1	201549_x_at; 211202_s_at	PLU-1
209112_at	p27KIP1	201783_s_at; 230202_at	RelA (p65 NF-kB subunit)
209112_at	p27KIP1	203358_s_at	EZH2
209112_at	p27KIP1	204254_s_at	VDR
209112_at	p27KIP1	204872_at	TLE4
209112_at	p27KIP1	205899_at	Cyclin A1
209112_at	p27KIP1	210743_s_at	CDC14a
209112_at	p27KIP1	211716_x_at	RhoGDI alpha
209112_at	p27KIP1	212265_at; 212636_at; 214541_s_at	QKI
209112_at	p27KIP1	220266_s_at; 221841_s_at	KLF4
209112_at	p27KIP1	224851_at	CDK6
209112_at	p27KIP1	225984_at	AMPK alpha 1 subunit
209112_at	p27KIP1	232466_at	Cullin 4A
209822_s_at	VLDLR	201042_at	TGM2
209822_s_at	VLDLR	201109_s_at	Thrombospondin 1
209822_s_at	VLDLR	209676_at; 213258_at	TFPI
209822_s_at	VLDLR	223130_s_at	MIR (Idol)
211607_x_at	EGFR	1564907_s_at; 242260_at	Matrin-3

Table B.6 (continued)

IDs in active data set	Object name	IDs of corresponding network object from GeneGo network	Corresponding network object name
211607_x_at	EGFR	200690_at	GRP75
211607_x_at	EGFR	200998_s_at; 200999_s_at	CLIMP-63
211607_x_at	EGFR	201096_s_at	ARF4
211607_x_at	EGFR	201244_s_at	c-Raf-1
211607_x_at	EGFR	202267_at	LAMC2
211607_x_at	EGFR	203821_at; 38037_at	HB-EGF
211607_x_at	EGFR	204011_at	SPRY2
211607_x_at	EGFR	204254_s_at	VDR
211607_x_at	EGFR	204686_at	IRS-1
211607_x_at	EGFR	205016_at; 211258_s_at	TGF-alpha
211607_x_at	EGFR	205447_s_at	ZPK(MAP3K12)
211607_x_at	EGFR	206011_at	Caspase-1
211607_x_at	EGFR	208958_at	ERp44
211607_x_at	EGFR	209409_at	GRB10
211607_x_at	EGFR	209615_s_at; 226507_at	PAK1
211607_x_at	EGFR	210495_x_at; 211719_x_at; 212464_s_at; 216442_x_at	Fibronectin
211607_x_at	EGFR	210517_s_at	AKAP12
211607_x_at	EGFR	211063_s_at	NCK1
211607_x_at	EGFR	212097_at	Caveolin-1
211607_x_at	EGFR	212761_at	TCF7L2 (TCF4)

Table B.6 (continued)

IDs in active data set	Object name	IDs of corresponding network object from GeneGo network	Corresponding network object name
211607_x_at	EGFR	212870_at	SOS2
211607_x_at	EGFR	213070_at	PI3K class II (CII-alpha)
211607_x_at	EGFR	215485_s_at	ICAM1
211607_x_at	EGFR	216971_s_at	Plectin 1
211607_x_at	EGFR	218310_at	RABGEF1
211607_x_at	EGFR	224657_at	MIG6
211607_x_at	EGFR	224844_at	SLAIN2
211607_x_at	EGFR	224938_at	NUFIP2
211607_x_at	EGFR	225231_at; 243475_at	c-Cbl
211607_x_at	EGFR	226572_at	SOCS7
211607_x_at	EGFR	226934_at	CPSF6
211607_x_at	EGFR	234932_s_at	CDCP1
211607_x_at	EGFR	235057_at	Itch
211607_x_at	EGFR	238855_at	AHNAK
211607_x_at	EGFR	241755_at	UQCRC2
212761_at	TCF7L2 (TCF4)	1552721_a_at; 205117_at; 208240_s_at	FGF1
212761_at	TCF7L2 (TCF4)	1555938_x_at	Vimentin
212761_at	TCF7L2 (TCF4)	1568574_x_at; 209875_s_at	Osteopontin
212761_at	TCF7L2 (TCF4)	200794_x_at	DAZAP2
212761_at	TCF7L2 (TCF4)	200952_s_at	Cyclin D2

Table B.6 (continued)

IDs in active data set	Object name	IDs of corresponding network object from GeneGo network	Corresponding network object name
212761_at	TCF7L2 (TCF4)	202859_x_at; 211506_s_at	IL-8
212761_at	TCF7L2 (TCF4)	204254_s_at	VDR
212761_at	TCF7L2 (TCF4)	205168_at; 225442_at; 227561_at	DDR2
212761_at	TCF7L2 (TCF4)	209383_at	C/EBP zeta
212761_at	TCF7L2 (TCF4)	210172_at	ZNF162
212761_at	TCF7L2 (TCF4)	210255_at	RAD51B
212761_at	TCF7L2 (TCF4)	211527_x_at	VEGF-A
212761_at	TCF7L2 (TCF4)	220266_s_at; 221841_s_at	KLF4
212761_at	TCF7L2 (TCF4)	222449_at	PMEPA1
212761_at	TCF7L2 (TCF4)	224851_at	CDK6
212761_at	TCF7L2 (TCF4)	224994_at; 225019_at	CaMK II delta
212761_at	TCF7L2 (TCF4)	228938_at	Myelin basic protein
212761_at	TCF7L2 (TCF4)	232231_at	RUNX2
212761_at	TCF7L2 (TCF4)	235795_at	PAX6
215245_x_at	FMR1	1567213_at; 1567214_a_at; 212037_at	Pinin
215245_x_at	FMR1	202920_at; 202921_s_at	Ankyrin-B
215245_x_at	FMR1	209615_s_at; 226507_at	PAK1
215245_x_at	FMR1	220099_s_at	LUC7L2
215245_x_at	FMR1	220563_s_at	SHANK1
215245_x_at	FMR1	222576_s_at	eIF2C1 (Argonaute-1)

Table B.6 (continued)

IDs in active data set	Object name	IDs of corresponding network object from GeneGo network	Corresponding network object name
215245_x_at	FMR1	222956_at	Fidgetin
215245_x_at	FMR1	224662_at	KIF5B
215245_x_at	FMR1	224938_at	NUFIP2
215245_x_at	FMR1	225984_at	AMPK alpha 1 subunit
215245_x_at	FMR1	228938_at	Myelin basic protein
215245_x_at	FMR1	235057_at	Itch
227025_at	PPHLN1	1555938_x_at	Vimentin
227025_at	PPHLN1	201042_at	TGM2
227025_at	PPHLN1	206011_at	Caspase-1
227025_at	PPHLN1	237833_s_at	Synphilin 1

Table B.7. Hub genes and their targets affected by miR-128 in HEY cells. GeneGo was used to analyze the most significant interactions within the set of differentially expressed genes following miR-128 transfection. The analysis gives a list of "hub" genes interacting with other differentially expressed genes (i.e. nodes) which suggests that miRNA are regulating the node genes indirectly through regulating the hubs. 'IDs in active dataset' refer to the probeset IDs in the dataset that passed the GeneGo FDR threshold of 5 % and are acting as hubs. Corresponding GeneGo gene identifiers are given in 'object name' column. 'IDs of corresponding network object from GeneGo network' refer to probeset IDs of objects in the dataset that the hubs are interacting with in GeneGo networks. The names of these nodes are given in the last column. If a hub gene is found to regulate another gene which may also act as a hub then the row is shaded.

Please see table on our website:
http://www.mcdonaldlab.biology.gatech.edu/shubin_shahab.htm

Table B.8. Significantly enriched GeneGo pathway maps among the differentially expressed genes following miR-7 transfection into HEY cells. GeneGo pathway maps significantly enriched (FDR <0.05) among the differentially expressed genes after miR-7 transfection into HEY cells are listed. Also shown are the hypergeometric distribution p-values of enrichments from GeneGo and the ratio of number of genes actually present in the dataset to the number of genes in the Affymetrix array that are in each pathway. Pathways are sorted based on p-values.

Maps	p-value	ratio
Cell adhesion_Chemokines and adhesion	1.31E-07	15/100
Cell cycle_Regulation of G1/S transition (part 1)	8.68E-07	9/38
Cell adhesion_Ephrin signaling	3.96E-06	9/45
Development_EGFR signaling pathway	1.02E-05	10/63
Development_ERBB-family signaling	1.13E-05	8/39
Development_WNT signaling pathway. Part 1. Degradation of beta-catenin in the absence WNT signaling	1.42E-05	6/20
Development_VEGF-family signaling	1.68E-05	8/41
Cytoskeleton remodeling_Cytoskeleton remodeling	3.13E-05	12/102
Neurophysiological process_Receptor-mediated axon growth repulsion	3.43E-05	8/45
Proteolysis_Putative ubiquitin pathway	3.44E-05	6/23
Development_TGF-beta-dependent induction of EMT via RhoA, PI3K and ILK.	4.05E-05	8/46
Cell adhesion_Plasmin signaling	4.85E-05	7/35
Development_TGF-beta-dependent induction of EMT via SMADs	4.85E-05	7/35
Transport_RAB5A regulation pathway	5.75E-05	6/25
Cytoskeleton remodeling_TGF, WNT and cytoskeletal remodeling	7.29E-05	12/111
Cell cycle_Regulation of G1/S transition (part 2)	7.30E-05	6/26
Apoptosis and survival_HTR1A signaling	7.54E-05	8/50
Development_Regulation of epithelial-to-mesenchymal transition (EMT)	7.67E-05	9/64
Translation _Regulation of EIF2 activity	1.01E-04	7/39
Cell adhesion_ECM remodeling	1.01E-04	8/52
Translation _Regulation of EIF4F activity	1.16E-04	8/53
Translation_Non-genomic (rapid) action of Androgen Receptor	1.19E-04	7/40
Apoptosis and survival_NO synthesis and signaling	1.51E-04	8/55
Immune response_Neurotensin-induced activation of IL-8 in colonocytes	1.64E-04	7/42
Apoptosis and survival_TNFR1 signaling pathway	1.91E-04	7/43

Table B.8 (continued)

Maps	p-value	ratio
Role of alpha-6/beta-4 integrins in carcinoma progression	2.57E-04	7/45
Development_EPO-induced MAPK pathway	2.57E-04	7/45
dCTP/dUTP metabolism	2.66E-04	9/75
Development_GDNF family signaling	2.95E-04	7/46
Signal transduction_PTEN pathway	2.95E-04	7/46
Cytoskeleton remodeling_CDC42 in cellular processes	3.24E-04	5/22
Development_TGF-beta-dependent induction of EMT via MAPK	3.39E-04	7/47
Development_Gastrin in cell growth and proliferation	3.54E-04	8/62
Proteolysis_Role of Parkin in the Ubiquitin-Proteasomal Pathway	4.99E-04	5/24
Development_Dopamine D2 receptor transactivation of EGFR	4.99E-04	5/24
Development_TGF-beta receptor signaling	5.00E-04	7/50
Transport_RAB3 regulation pathway	5.20E-04	4/14
Development_IGF-1 receptor signaling	5.66E-04	7/51
Membrane-bound ESR1: interaction with G-proteins signaling	5.66E-04	7/51
Immune response_Role of integrins in NK cells cytotoxicity	6.57E-04	6/38
Development_WNT signaling pathway. Part 2	7.18E-04	7/53
Neurophysiological process_Dopamine D2 receptor transactivation of PDGFR in CNS	7.36E-04	5/26
Immune response_Gastrin in inflammatory response	7.37E-04	8/69
Transcription_Receptor-mediated HIF regulation	7.58E-04	6/39
Regulation of degradation of deltaF508 CFTR in CF	8.83E-04	5/27
PGE2 pathways in cancer	9.00E-04	7/55
Regulation of lipid metabolism_Stimulation of Arachidonic acid production by ACM receptors	9.80E-04	8/72
Development_Mu-type opioid receptor regulation of proliferation	1.05E-03	5/28
Cytoskeleton remodeling_FAK signaling	1.12E-03	7/57
Apoptosis and survival_BAD phosphorylation	1.14E-03	6/42
Development_Role of IL-8 in angiogenesis	1.24E-03	7/58
Development_VEGF signaling and activation	1.29E-03	6/43
Regulation of degradation of wt-CFTR	1.45E-03	4/18
Immune response_IL-4 - antiapoptotic action	1.45E-03	5/30
dATP/dITP metabolism	1.64E-03	9/96
Cytoskeleton remodeling_Fibronectin-binding integrins in cell motility	1.69E-03	5/31
Cytoskeleton remodeling_Reverse signaling by ephrin B	1.69E-03	5/31
Development_Alpha-2 adrenergic receptor activation of ERK	1.84E-03	7/62
Development_Endothelin-1/EDNRA transactivation of EGFR	1.84E-03	6/46
Development_PDGF signaling via STATs and NF-kB	1.96E-03	5/32
Development_EGFR signaling via small GTPases	1.96E-03	5/32
Transport_Macropinocytosis regulation by growth factors	2.02E-03	7/63
Development_FGF2-dependent induction of EMT	2.20E-03	4/20

Table B.8 (continued)

Maps	p-value	ratio
Immune response_CD40 signaling	2.22E-03	7/64
Development_Angiotensin activation of ERK	2.26E-03	5/33
Development_A3 receptor signaling	2.56E-03	6/49
Development_PEDF signaling	2.56E-03	6/49
G-protein signaling_G-Protein beta/gamma signaling cascades	2.59E-03	5/34
Cell cycle_Cell cycle (generic schema)	2.66E-03	4/21
Development_EPO-induced Jak-STAT pathway	2.95E-03	5/35
Development_EGFR signaling via PIP3	3.76E-03	4/23
Development_Beta-adrenergic receptors transactivation of EGFR	3.78E-03	5/37
Development_FGFR signaling pathway	3.82E-03	6/53
Cell cycle_Influence of Ras and Rho proteins on G1/S Transition	3.82E-03	6/53
Regulation of lipid metabolism_Regulation of lipid metabolism via LXR, NF-Y and SREBP	4.25E-03	5/38
Regulation of lipid metabolism_Insulin regulation of glycogen metabolism	4.61E-03	6/55
Cell adhesion_PLAU signaling	4.77E-03	5/39
G-protein signaling_K-RAS regulation pathway	5.13E-03	4/25
Cytoskeleton remodeling_Neurofilaments	5.13E-03	4/25
Development_Prolactin receptor signaling	5.99E-03	6/58
Regulation of CFTR activity (norm and CF)	5.99E-03	6/58
Translation_Insulin regulation of translation	6.57E-03	5/42
Immune response_Signaling pathway mediated by IL-6 and IL-1	6.81E-03	4/27
Immune response_IL-17 signaling pathways	7.07E-03	6/60
Development_ACM2 and ACM4 activation of ERK	7.27E-03	5/43
Signal transduction_AKT signaling	7.27E-03	5/43
Immune response_IL-4 signaling pathway	8.01E-03	5/44
Development_Flt3 signaling	8.01E-03	5/44
Development_Activation of Erk by ACM1, ACM3 and ACM5	8.01E-03	5/44
Development_Ligand-independent activation of ESR1 and ESR2	8.01E-03	5/44
Transcription_CREB pathway	8.01E-03	5/44

Table B.9. Significantly enriched GeneGo pathway maps among the differentially expressed genes following miR-128 transfection into HEY cells. GeneGo pathway maps significantly enriched (FDR <0.05) among the differentially expressed genes after miR-128 transfection into HEY cells are listed. Also shown are the hypergeometric distribution p-values of enrichments from GeneGo and the ratio of number of genes actually present in the dataset to the number of genes in the Affymetrix array that are in each pathway. Pathways are sorted based on p-values.

Table B.9 (continued)

Maps	p-value	Ratio
Cell cycle_The metaphase checkpoint	1.01E-11	18/36
Cytoskeleton remodeling_TGF, WNT and cytoskeletal remodeling	1.29E-09	29/111
Cell cycle_Role of Nek in cell cycle regulation	1.77E-09	15/32
Transport_Clathrin-coated vesicle cycle	4.15E-09	22/71
Cell cycle_Initiation of mitosis	4.37E-09	13/25
Immune response_Histamine H1 receptor signaling in immune response	1.78E-07	16/48
Cell cycle_Role of APC in cell cycle regulation	1.79E-07	13/32
Cell cycle_Spindle assembly and chromosome separation	2.75E-07	13/33
Cytoskeleton remodeling_Cytoskeleton remodeling	2.98E-07	24/102
Proteolysis_Role of Parkin in the Ubiquitin-Proteasomal Pathway	3.68E-07	11/24
Cytoskeleton remodeling_Neurofilaments	6.14E-07	11/25
Cell cycle_Chromosome condensation in prometaphase	8.18E-07	10/21
Immune response_Gastrin in inflammatory response	1.85E-06	18/69
Neurophysiological process_Receptor-mediated axon growth repulsion	2.69E-06	14/45
Translation_Non-genomic (rapid) action of Androgen Receptor	3.55E-06	13/40
Development_PIP3 signaling in cardiac myocytes	4.80E-06	14/47
Cytoskeleton remodeling_Role of Activin A in cytoskeleton remodeling	5.34E-06	9/20
Apoptosis and survival_Apoptotic Activin A signaling	5.76E-06	10/25
Apoptosis and survival_BAD phosphorylation	6.54E-06	13/42
Immune response_Fc epsilon RI pathway	7.40E-06	15/55
Cytoskeleton remodeling_Reverse signaling by ephrin B	7.70E-06	11/31
Development_Gastrin in cell growth and proliferation	8.04E-06	16/62
Immune response_Function of MEF2 in T lymphocytes	1.07E-05	14/50
Development_Activation of Erk by ACM1, ACM3 and ACM5	1.16E-05	13/44
Immune response_CD40 signaling	1.25E-05	16/64
Cell cycle_Role of 14-3-3 proteins in cell cycle regulation	1.38E-05	9/22
Cell adhesion_Histamine H1 receptor signaling in the interruption of cell barrier integrity	1.52E-05	13/45
Signal transduction_Calcium signaling	1.52E-05	13/45
Development_TGF-beta-dependent induction of EMT via RhoA, PI3K and ILK.	1.98E-05	13/46
Proteolysis_Putative ubiquitin pathway	2.12E-05	9/23
Cell cycle_Influence of Ras and Rho proteins on G1/S Transition	2.22E-05	14/53
Cell cycle_Role of SCF complex in cell cycle regulation	2.69E-05	10/29
Development_Role of HDAC and calcium/calmodulin-dependent kinase (CaMK) in control of skeletal myogenesis	2.79E-05	14/54
Development_Angiopoietin - Tie2 signaling	2.88E-05	11/35
Neurophysiological process_EphB receptors in dendritic spine morphogenesis and synaptogenesis	2.88E-05	11/35

Table B.9 (continued)

Maps	p-value	Ratio
Development_Slit-Robo signaling	3.76E-05	10/30
Cell adhesion_Chemokines and adhesion	3.83E-05	20/100
Signal transduction_AKT signaling	4.73E-05	12/43
Development_A2A receptor signaling	4.73E-05	12/43
Development_Regulation of epithelial-to-mesenchymal transition (EMT)	5.28E-05	15/64
Cytoskeleton remodeling_FAK signaling	5.37E-05	14/57
Cell adhesion_Cadherin-mediated cell adhesion	6.61E-05	9/26
Development_Role of IL-8 in angiogenesis	6.61E-05	14/58
Role of alpha-6/beta-4 integrins in carcinoma progression	7.72E-05	12/45
Development_Endothelin-1/EDNRA transactivation of EGFR	9.75E-05	12/46
Cytoskeleton remodeling_CDC42 in cellular processes	1.14E-04	8/22
Development_Leptin signaling via PI3K-dependent pathway	1.22E-04	12/47
Immune response_CD28 signaling	1.23E-04	13/54
Cell adhesion_Alpha-4 integrins in cell migration and adhesion	1.25E-04	10/34
G-protein signaling_G-Protein alpha-q signaling cascades	1.25E-04	10/34
Development_Role of CDK5 in neuronal development	1.25E-04	10/34
Immune response_IL-15 signaling via JAK-STAT cascade	1.63E-04	8/23
Cytoskeleton remodeling_Regulation of actin cytoskeleton by Rho GTPases	1.63E-04	8/23
Delta508-CFTR traffic / ER-to-Golgi in CF	1.82E-04	6/13
Normal wtCFTR traffic / ER-to-Golgi	1.82E-04	6/13
Immune response_Neurotensin-induced activation of IL-8 in colonocytes	1.83E-04	11/42
Immune response_TREM1 signaling pathway	1.83E-04	13/56
Immune response_IL-2 activation and signaling pathway	1.88E-04	12/49
Signal transduction_IP3 signaling	1.88E-04	12/49
Immune response_IL-15 signaling	2.05E-04	14/64
Immune response_IL-7 signaling in B lymphocytes	2.29E-04	11/43
Apoptosis and survival_Anti-apoptotic action of Gastrin	2.29E-04	11/43
Development_A2B receptor: action via G-protein alpha s	2.31E-04	12/50
Immune response_CCR5 signaling in macrophages and T lymphocytes	2.66E-04	13/58
wtCFTR and delta508 traffic / Clathrin coated vesicles formation (norm and CF)	2.82E-04	7/19
Development_IGF-1 receptor signaling	2.82E-04	12/51
Mucin expression in CF via TLRs, EGFR signaling pathways	2.82E-04	12/51
Development_Flt3 signaling	2.86E-04	11/44
Transcription_CREB pathway	2.86E-04	11/44
Cytoskeleton remodeling_Fibronectin-binding integrins in cell motility	3.04E-04	9/31

Table B.9 (continued)

Maps	p-value	Ratio
Development_Leptin signaling via JAK/STAT and MAPK cascades	3.15E-04	8/25
Signal transduction_Activation of PKC via G-Protein coupled receptor	3.42E-04	12/52
Immune response_Human NKG2D signaling	3.43E-04	10/38
Regulation of lipid metabolism_Regulation of lipid metabolism via LXR, NF-Y and SREBP	3.43E-04	10/38
Cell cycle_Regulation of G1/S transition (part 1)	3.43E-04	10/38
Development_Angiotensin signaling via STATs	3.96E-04	9/32
Development_FGFR signaling pathway	4.13E-04	12/53
Development_A1 receptor signaling	4.13E-04	12/53
Development_Cross-talk between VEGF and Angiopoietin 1 signaling pathways	4.26E-04	8/26
Immune response_IL-10 signaling pathway	4.26E-04	8/26
Development_GDNF family signaling	4.33E-04	11/46
Immune response_MIF - the neuroendocrine-macrophage connector	4.33E-04	11/46
Signal transduction_PTEN pathway	4.33E-04	11/46
Immune response _IFN gamma signaling pathway	4.96E-04	12/54
Immune response_BCR pathway	4.96E-04	12/54
Signal transduction_Activin A signaling regulation	5.08E-04	9/33
Neurophysiological process_Circadian rhythm	5.28E-04	11/47
Cytoskeleton remodeling_Role of PKA in cytoskeleton reorganization	5.37E-04	10/40
Reproduction_Progesterone-mediated oocyte maturation	5.37E-04	10/40
Apoptosis and survival_Anti-apoptotic TNFs/NF-kB/IAP pathway	5.66E-04	8/27
PGE2 pathways in cancer	5.92E-04	12/55
Apoptosis and survival_NO synthesis and signaling	5.92E-04	12/55
Development_EGFR signaling pathway	6.26E-04	13/63
Transport_Macropinocytosis regulation by growth factors	6.26E-04	13/63
Cell adhesion_Integrin-mediated cell adhesion and migration	6.40E-04	11/48
Development_NOTCH1-mediated pathway for NF-KB activity modulation	6.46E-04	9/34
Transport_ACM3 in salivary glands	6.64E-04	10/41
Muscle contraction_ACM regulation of smooth muscle contraction	7.03E-04	12/56
Development_A3 receptor signaling	7.71E-04	11/49
Cell cycle_Sister chromatid cohesion	7.83E-04	7/22
Transcription_Role of heterochromatin protein 1 (HP1) family in transcriptional silencing	7.83E-04	7/22
Development_EPO-induced Jak-STAT pathway	8.14E-04	9/35
Immune response_PIP3 signaling in B lymphocytes	8.14E-04	10/42
Development_TGF-beta receptor signaling	9.23E-04	11/50

Table B.9 (continued)

Maps	p-value	Ratio
Regulation of CFTR activity (norm and CF)	9.79E-04	12/58
Development_VEGF signaling and activation	9.92E-04	10/43
Cytoskeleton remodeling_Keratin filaments	1.01E-03	9/36
Development_EGFR signaling via PIP3	1.05E-03	7/23
Muscle contraction_ GPCRs in the regulation of smooth muscle tone	1.07E-03	15/83
Immune response_NFAT in immune response	1.10E-03	11/51
Transport_Macropinocytosis	1.15E-03	5/12
Immune response_IL-1 signaling pathway	1.20E-03	10/44
Muscle contraction_EDG5-mediated smooth muscle contraction	1.22E-03	8/30
Cell adhesion_Gap junctions	1.22E-03	8/30
G-protein signaling_G-Protein alpha-12 signaling pathway	1.25E-03	9/37
Cell adhesion_Role of tetraspanins in the integrin-mediated cell adhesion	1.25E-03	9/37
Development_Hedgehog and PTH signaling pathways in bone and cartilage development	1.25E-03	9/37
Development_Glucocorticoid receptor signaling	1.39E-03	7/24
Immune response_Inhibitory action of Lipoxins on pro-inflammatory TNF-alpha signaling	1.44E-03	10/45
Development_VEGF signaling via VEGFR2 - generic cascades	1.44E-03	10/45
Immune response _CCR3 signaling in eosinophils	1.46E-03	14/77
Development_WNT signaling pathway. Part 2	1.54E-03	11/53
Development_Gastrin in differentiation of the gastric mucosa	1.54E-03	9/38
Development_Angiotensin activation of Akt	1.72E-03	10/46
Immune response_ICOS pathway in T-helper cell	1.72E-03	10/46
Development_WNT5A signaling	1.72E-03	10/46
Transcription_Transcription regulation of aminoacid metabolism	1.81E-03	7/25
Translation _Regulation of EIF2 activity	1.87E-03	9/39
G-protein signaling_Regulation of p38 and JNK signaling mediated by G-proteins	1.87E-03	9/39
Development_TGF-beta-dependent induction of EMT via MAPK	2.04E-03	10/47
Neurophysiological process_NMDA-dependent postsynaptic long-term potentiation in CA1 hippocampal neurons	2.14E-03	14/80
Development_Role of Activin A in cell differentiation and proliferation	2.25E-03	9/40
Immune response_MIF in innate immunity response	2.25E-03	9/40
Regulation of lipid metabolism_Stimulation of Arachidonic acid production by ACM receptors	2.28E-03	13/72
DNA damage_ATM / ATR regulation of G2 / M checkpoint	2.32E-03	7/26
Development_EDG5 and EDG3 in cell proliferation and differentiation	2.32E-03	7/26

Table B.9 (continued)

Maps	p-value	Ratio
Normal and pathological TGF-beta-mediated regulation of cell proliferation	2.38E-03	8/33
Development_Keratinocyte differentiation	2.45E-03	11/56
Development_WNT signaling pathway. Part 1. Degradation of beta-catenin in the absence WNT signaling	2.62E-03	6/20
Development_FGF2-dependent induction of EMT	2.62E-03	6/20
Neurophysiological process_Netrin-1 in regulation of axon guidance	2.70E-03	9/41
Development_Melanocyte development and pigmentation	2.83E-03	10/49
Development_PEDF signaling	2.83E-03	10/49
Signal transduction_Erk Interactions: Inhibition of Erk	2.91E-03	8/34
G-protein signaling_RhoA regulation pathway	2.91E-03	8/34
Neurophysiological process_GABA-A receptor life cycle	2.94E-03	7/27
Regulation of degradation of deltaF508 CFTR in CF	2.94E-03	7/27
Development_Prolactin receptor signaling	3.27E-03	11/58
Development_EDNRB signaling	3.31E-03	10/50
Apoptosis and survival_HTR1A signaling	3.31E-03	10/50
Immune response_Histamine signaling in dendritic cells	3.31E-03	10/50
Development_GM-CSF signaling	3.31E-03	10/50
Blood coagulation_GPIb-IX-V-dependent platelet activation	3.32E-03	13/75
Cell cycle_Cell cycle (generic schema)	3.45E-03	6/21
Atherosclerosis_Role of ZNF202 in regulation of expression of genes involved in Atherosclerosis	3.45E-03	6/21
Apoptosis and survival_Anti-apoptotic action of membrane-bound ESR1	3.53E-03	8/35
Development_Regulation of telomere length and cellular immortalization	3.53E-03	8/35
Development_Growth hormone signaling via STATs and PLC/IP3	3.53E-03	8/35
Development_EDG3 signaling pathway	3.80E-03	9/43
Immune response_HTR2A-induced activation of cPLA2	3.80E-03	9/43
Signal transduction_PKA signaling	3.85E-03	10/51
Membrane-bound ESR1: interaction with G-proteins signaling	3.85E-03	10/51
Chemotaxis_Inhibitory action of lipoxins on IL-8- and Leukotriene B4-induced neutrophil migration	3.85E-03	10/51
Some pathways of EMT in cancer cells	3.85E-03	10/51
Immune response_IL-17 signaling pathways	4.29E-03	11/60
Apoptosis and survival_nAChR in apoptosis inhibition and cell cycle progression	4.53E-03	7/29
NGF activation of NF-kB	4.53E-03	7/29
Immune response_CD137 signaling in immune cell	4.53E-03	7/29
Cytoskeleton remodeling_ACM3 and ACM4 in keratinocyte migration	5.08E-03	8/37

Table B.9 (continued)

Maps	p-value	Ratio
Development_Delta-type opioid receptor mediated cardioprotection	5.08E-03	8/37
Development_Beta-adrenergic receptors transactivation of EGFR	5.08E-03	8/37
Development_Endothelin-1/EDNRA signaling	5.14E-03	10/53
Neurophysiological process_Glutamate regulation of Dopamine D1A receptor signaling	5.23E-03	9/45
Transcription_Androgen Receptor nuclear signaling	5.23E-03	9/45
Cell adhesion_Ephrin signaling	5.23E-03	9/45
Development_Thrombopoietin-regulated cell processes	5.23E-03	9/45
Cytoskeleton remodeling_RalA regulation pathway	5.54E-03	7/30
Immune response_Role of DAP12 receptors in NK cells	5.90E-03	10/54
Immune response_Role of integrins in NK cells cytotoxicity	6.02E-03	8/38
Immune response_IL-7 signaling in T lymphocytes	6.02E-03	8/38
Development_Mu-type opioid receptor signaling	6.02E-03	8/38
Chemotaxis_Lipoxin inhibitory action on fMLP-induced neutrophil chemotaxis	6.09E-03	9/46
Neurophysiological process_ACM regulation of nerve impulse	6.09E-03	9/46
Reproduction_GnRH signaling	6.49E-03	12/72
Transcription_Transcription factor Tubby signaling pathways	6.59E-03	5/17
Development_HGF signaling pathway	7.04E-03	9/47
Development_Dopamine D2 receptor transactivation of EGFR	7.06E-03	6/24
Apoptosis and survival_NO signaling in survival	7.06E-03	6/24
HIV-1 signaling via CCR5 in macrophages and T lymphocytes	7.09E-03	8/39
Development_ERBB-family signaling	7.09E-03	8/39
Cell adhesion_PLAU signaling	7.09E-03	8/39
Muscle contraction_Regulation of eNOS activity in endothelial cells	7.11E-03	11/64
Cell adhesion_Integrin inside-out signaling	7.67E-03	10/56
Development_PDGF signaling via STATs and NF-kB	8.05E-03	7/32
Development_Neurotrophin family signaling	8.30E-03	8/40
Inhibitory action of Lipoxins on neutrophil migration	8.70E-03	10/57
Immune response_IL-23 signaling pathway	8.71E-03	6/25
Development_Angiotensin signaling via beta-Arrestin	8.71E-03	6/25
Cytoskeleton remodeling_Integrin outside-in signaling	9.30E-03	9/49
Immune response_Bacterial infections in normal airways	9.30E-03	9/49
Development_Angiotensin activation of ERK	9.57E-03	7/33
Development_Activation of astroglial cells proliferation by ACM3	9.57E-03	7/33
Development_Signaling of Beta-adrenergic receptors via Beta-arrestins	1.06E-02	6/26
Cytoskeleton remodeling_Alpha-1A adrenergic receptor-dependent inhibition of PI3K	1.09E-02	5/19

Table B.9 (continued)

Maps	p-value	Ratio
G-protein signaling_G-Protein beta/gamma signaling cascades	1.13E-02	7/34
wtCFTR and deltaF508 traffic / Membrane expression (norm and CF)	1.13E-02	7/34
Muscle contraction_Oxytocin signaling in uterus and mammary gland	1.24E-02	10/60
Immune response_CD16 signaling in NK cells	1.24E-02	11/69
G-protein signaling_G-Protein alpha-i signaling cascades	1.28E-02	6/27
Development_ACM2 and ACM4 activation of ERK	1.29E-02	8/43
Development_Angiotensin signaling via PYK2	1.29E-02	8/43
Cell adhesion_Plasmin signaling	1.32E-02	7/35
Development_TGF-beta-dependent induction of EMT via SMADs	1.32E-02	7/35
G-protein signaling_EDG5 signaling	1.32E-02	7/35
ENaC regulation in airways (normal and CF)	1.37E-02	9/52
Immune response_T cell receptor signaling pathway	1.37E-02	9/52
G-protein signaling_Proinsulin C-peptide signaling	1.37E-02	9/52
Cytoskeleton remodeling_ESR1 action on cytoskeleton remodeling and cell migration	1.37E-02	5/20
Translation_IL-2 regulation of translation	1.37E-02	5/20
Regulation of lipid metabolism_Alpha-1 adrenergic receptors signaling via arachidonic acid	1.38E-02	11/70
Development_Ligand-independent activation of ESR1 and ESR2	1.47E-02	8/44
Immune response_IL-5 signalling	1.47E-02	8/44
Blood coagulation_GPCRs in platelet aggregation	1.53E-02	11/71
Development_Delta-type opioid receptor signaling via G-protein alpha-14	1.53E-02	6/28
Translation _Regulation of EIF4F activity	1.54E-02	9/53
Immune response_IL-9 signaling pathway	1.54E-02	7/36
Cell adhesion_Tight junctions	1.54E-02	7/36
G-protein signaling_Regulation of RAC1 activity	1.54E-02	7/36
G-protein signaling_RAC1 in cellular process	1.54E-02	7/36
Development_Alpha-2 adrenergic receptor activation of ERK	1.55E-02	10/62
Cell cycle_Nucleocytoplasmic transport of CDK/Cyclins	1.67E-02	4/14
Immune response_Delta-type opioid receptor signaling in T-cells	1.81E-02	6/29

Table B.10. Significantly enriched GeneGo pathway maps among the down-regulated genes following miR-7 transfection into HEY cells. Significantly enriched (FDR <0.05) GeneGo pathway maps among the down-regulated genes after miR-7 transfection into HEY cells are listed. Also shown are the hypergeometric distribution p-values of enrichments from GeneGo and the ratio of number of genes actually present in

the dataset to the number of genes in the Affymetrix array that are in each pathway. Pathways are sorted based on enrichment p-values.

Maps	p-value	Ratio
Cell adhesion_Chemokines and adhesion	6.99E-08	14/100
Cell adhesion_Ephrin signaling	7.47E-07	9/45
Development_EGFR signaling pathway	1.70E-06	10/63
Development_ERBB-family signaling	2.57E-06	8/39
Development_VEGF-family signaling	3.83E-06	8/41
Cytoskeleton remodeling_Cytoskeleton remodeling	4.10E-06	12/102
Development_WNT signaling pathway. Part 1. Degradation of beta-catenin in the absence WNT signaling	4.47E-06	6/20
Neurophysiological process_Receptor-mediated axon growth repulsion	7.97E-06	8/45
Cytoskeleton remodeling_TGF, WNT and cytoskeletal remodeling	9.97E-06	12/111
Apoptosis and survival_HTR1A signaling	1.80E-05	8/50
Transport_RAB5A regulation pathway	1.85E-05	6/25
Cell cycle_Regulation of G1/S transition (part 1)	2.35E-05	7/38
Cell adhesion_ECM remodeling	2.42E-05	8/52
Translation _Regulation of EIF4F activity	2.79E-05	8/53
Translation _Regulation of EIF2 activity	2.81E-05	7/39
Translation_Non-genomic (rapid) action of Androgen Receptor	3.33E-05	7/40
Apoptosis and survival_NO synthesis and signaling	3.69E-05	8/55
Immune response_Neurotensin-induced activation of IL-8 in colonocytes	4.64E-05	7/42
Apoptosis and survival_TNFR1 signaling pathway	5.43E-05	7/43
Role of alpha-6/beta-4 integrins in carcinoma progression	7.35E-05	7/45
Development_GDNF family signaling	8.50E-05	7/46
Signal transduction_PTEN pathway	8.50E-05	7/46
Development_Gastrin in cell growth and proliferation	8.90E-05	8/62
Development_Regulation of epithelial-to-mesenchymal transition (EMT)	1.12E-04	8/64
Cell adhesion_Plasmin signaling	1.40E-04	6/35
Development_TGF-beta receptor signaling	1.47E-04	7/50
Proteolysis_Putative ubiquitin pathway	1.59E-04	5/23
Membrane-bound ESR1: interaction with G-proteins signaling	1.67E-04	7/51
Immune response_Gastrin in inflammatory response	1.91E-04	8/69
Development_Dopamine D2 receptor transactivation of EGFR	1.97E-04	5/24
Development_WNT signaling pathway. Part 2	2.13E-04	7/53
Immune response_Role of integrins in NK cells cytotoxicity	2.24E-04	6/38
Regulation of lipid metabolism_Stimulation of Arachidonic acid production by ACM receptors	2.58E-04	8/72

Table B.10 (continued)

Maps	p-value	Ratio
PGE2 pathways in cancer	2.70E-04	7/55
Neurophysiological process_Dopamine D2 receptor transactivation of PDGFR in CNS	2.93E-04	5/26
Cell cycle_Regulation of G1/S transition (part 2)	2.93E-04	5/26
Cytoskeleton remodeling_FAK signaling	3.38E-04	7/57
Regulation of degradation of deltaF508 CFTR in CF	3.53E-04	5/27
Development_Role of IL-8 in angiogenesis	3.77E-04	7/58
Apoptosis and survival_BAD phosphorylation	3.94E-04	6/42
Development_Mu-type opioid receptor regulation of proliferation	4.22E-04	5/28
Development_VEGF signaling and activation	4.50E-04	6/43
Development_Alpha-2 adrenergic receptor activation of ERK	5.70E-04	7/62
Development_EPO-induced MAPK pathway	5.78E-04	6/45
Immune response_IL-4 - antiapoptotic action	5.89E-04	5/30
Transport_Macropinocytosis regulation by growth factors	6.28E-04	7/63
Development_TGF-beta-dependent induction of EMT via RhoA, PI3K and ILK.	6.52E-04	6/46
Development_Endothelin-1/EDNRA transactivation of EGFR	6.52E-04	6/46
Regulation of degradation of wt-CFTR	6.87E-04	4/18
Cytoskeleton remodeling_Fibronectin-binding integrins in cell motility	6.89E-04	5/31
Cytoskeleton remodeling_Reverse signaling by ephrin B	6.89E-04	5/31
Immune response_CD40 signaling	6.92E-04	7/64
Development_EGFR signaling via small GTPases	8.01E-04	5/32
Development_PDGF signaling via STATs and NF-kB	8.01E-04	5/32
Development_PEDF signaling	9.18E-04	6/49
Development_Angiotensin activation of ERK	9.27E-04	5/33
Development_FGF2-dependent induction of EMT	1.05E-03	4/20
G-protein signaling_G-Protein beta/gamma signaling cascades	1.07E-03	5/34
Development_IGF-1 receptor signaling	1.14E-03	6/51
Development_EPO-induced Jak-STAT pathway	1.22E-03	5/35
Development_FGFR signaling pathway	1.40E-03	6/53
Cell cycle_Influence of Ras and Rho proteins on G1/S Transition	1.40E-03	6/53
Cytoskeleton remodeling_CDC42 in cellular processes	1.53E-03	4/22
Development_Beta-adrenergic receptors transactivation of EGFR	1.58E-03	5/37
Regulation of lipid metabolism_Insulin regulation of glycogen metabolism	1.70E-03	6/55
Regulation of lipid metabolism_Regulation of lipid metabolism via LXR, NF-Y and SREBP	1.78E-03	5/38
Development_EGFR signaling via PIP3	1.81E-03	4/23
Transcription_Receptor-mediated HIF regulation	2.01E-03	5/39
Cell adhesion_PLAU signaling	2.01E-03	5/39

Table B.10 (continued)

Maps	p-value	Ratio
Proteolysis_Role of Parkin in the Ubiquitin-Proteasomal Pathway	2.14E-03	4/24
Regulation of CFTR activity (norm and CF)	2.23E-03	6/58
Development_Prolactin receptor signaling	2.23E-03	6/58
Cytoskeleton remodeling_Neurofilaments	2.50E-03	4/25
Immune response_IL-17 signaling pathways	2.66E-03	6/60
Translation_Insulin regulation of translation	2.80E-03	5/42
Development_ACM2 and ACM4 activation of ERK	3.11E-03	5/43
Signal transduction_AKT signaling	3.11E-03	5/43
Immune response_Signaling pathway mediated by IL-6 and IL-1	3.34E-03	4/27
Immune response_IL-4 signaling pathway	3.45E-03	5/44
Transcription_CREB pathway	3.45E-03	5/44
Development_Flt3 signaling	3.45E-03	5/44
Development_Activation of Erk by ACM1, ACM3 and ACM5	3.45E-03	5/44
Development_Ligand-independent activation of ESR1 and ESR2	3.45E-03	5/44
Development_Thrombopoietin-regulated cell processes	3.80E-03	5/45
Development_PIP3 signaling in cardiac myocytes	4.60E-03	5/47
Development_TGF-beta-dependent induction of EMT via MAPK	4.60E-03	5/47
Immune response_Histamine H1 receptor signaling in immune response	5.04E-03	5/48
Muscle contraction_Relaxin signaling pathway	5.04E-03	5/48
Development_A3 receptor signaling	5.51E-03	5/49
Signal transduction_IP3 signaling	5.51E-03	5/49
Cytoskeleton remodeling_Integrin outside-in signaling	5.51E-03	5/49
Apoptosis and survival_Role of IAP-proteins in apoptosis	5.57E-03	4/31
Immune response_Histamine signaling in dendritic cells	6.00E-03	5/50
Immune response_IL-13 signaling via PI3K-ERK	6.00E-03	5/50
Chemotaxis_Inhibitory action of lipoxins on IL-8- and Leukotriene B4-induced neutrophil migration	6.53E-03	5/51
Mucin expression in CF via TLRs, EGFR signaling pathways	6.53E-03	5/51
Apoptosis and survival_Caspase cascade	6.99E-03	4/33
G-protein signaling_Proinsulin C-peptide signaling	7.09E-03	5/52
Development_Endothelin-1/EDNRA signaling	7.69E-03	5/53
Cell adhesion_Alpha-4 integrins in cell migration and adhesion	7.77E-03	4/34
Development_CNTF receptor signaling	7.77E-03	4/34
G-protein signaling_G-Protein alpha-q signaling cascades	7.77E-03	4/34
Development_Angiopoietin - Tie2 signaling	8.62E-03	4/35
Development_TGF-beta-dependent induction of EMT via SMADs	8.62E-03	4/35
Development_FGF-family signaling	8.62E-03	4/35
Neurophysiological process_EphB receptors in dendritic spine morphogenesis and synaptogenesis	8.62E-03	4/35
Immune response_Fc epsilon RI pathway	8.98E-03	5/55

Table B.10 (continued)

Maps	p-value	Ratio
Immune response_IL-9 signaling pathway	9.52E-03	4/36
Muscle contraction_ACM regulation of smooth muscle contraction	9.67E-03	5/56
Immune response_TREM1 signaling pathway	9.67E-03	5/56
Inhibitory action of Lipoxins on neutrophil migration	1.04E-02	5/57
Development_Delta-type opioid receptor mediated cardioprotection	1.05E-02	4/37

Table B.11. Significantly enriched GeneGo pathway maps among the down-regulated genes following miR-128 transfection into HEY cells. Significantly enriched (FDR <0.05) GeneGo pathway maps among the down-regulated genes after miR-128 transfection into HEY cells are listed. Also shown are the hypergeometric distribution p-values of enrichments from GeneGo and the ratio of number of genes actually present in the dataset to the number of genes in the Affymetrix array that belong to each pathway. Pathways are sorted based on the enrichment p-values.

Maps	p-value	Ratio
Cell cycle_The metaphase checkpoint	2.30E-19	18/36
Cell cycle_Role of Nek in cell cycle regulation	8.80E-16	15/32
Cell cycle_Role of APC in cell cycle regulation	1.88E-11	12/32
Cell cycle_Spindle assembly and chromosome separation	2.88E-11	12/33
Cell cycle_Chromosome condensation in prometaphase	5.33E-11	10/21
Cell cycle_Initiation of mitosis	4.49E-10	10/25
Cytoskeleton remodeling_Neurofilaments	2.04E-07	8/25
Cytoskeleton remodeling_Regulation of actin cytoskeleton by Rho GTPases	1.79E-06	7/23
Proteolysis_Putative ubiquitin pathway	1.79E-06	7/23
Cytoskeleton remodeling_Cytoskeleton remodeling	3.78E-06	13/102
Cytoskeleton remodeling_Keratin filaments	4.40E-06	8/36
Cytoskeleton remodeling_TGF, WNT and cytoskeletal remodeling	9.76E-06	13/111
Cell cycle_Role of SCF complex in cell cycle regulation	9.89E-06	7/29
Cell cycle_Role of 14-3-3 proteins in cell cycle regulation	2.05E-05	6/22
Development_Role of IL-8 in angiogenesis	2.47E-05	9/58
Role of alpha-6/beta-4 integrins in carcinoma progression	2.53E-05	8/45
Development_PIP3 signaling in cardiac myocytes	3.52E-05	8/47
Proteolysis_Role of Parkin in the Ubiquitin-Proteasomal Pathway	3.53E-05	6/24
DNA damage_ATM / ATR regulation of G2 / M checkpoint	5.77E-05	6/26
Cell cycle_Influence of Ras and Rho proteins on G1/S Transition	8.61E-05	8/53
Apoptosis and survival_BAD phosphorylation	1.26E-04	7/42
Development_Slit-Robo signaling	1.36E-04	6/30

Table B.11 (continued)

Maps	p-value	Ratio
Cytoskeleton remodeling_RalA regulation pathway	1.36E-04	6/30
Cell adhesion_Gap junctions	1.36E-04	6/30
Signal transduction_AKT signaling	1.47E-04	7/43
Neurophysiological process_Receptor-mediated axon growth repulsion	1.98E-04	7/45
Cell cycle_Cell cycle (generic schema)	2.10E-04	5/21
Transport_Macropinocytosis	2.29E-04	4/12
Immune response _CCR3 signaling in eosinophils	2.38E-04	9/77
Cell cycle_Sister chromatid cohesion	2.66E-04	5/22
Cell adhesion_Integrin-mediated cell adhesion and migration	2.99E-04	7/48
Development_EGFR signaling via PIP3	3.33E-04	5/23
Cell adhesion_Chemokines and adhesion	3.93E-04	10/100
Muscle contraction_ GPCRs in the regulation of smooth muscle tone	4.20E-04	9/83
Development_Beta-adrenergic receptors transactivation of EGFR	4.53E-04	6/37
Regulation of lipid metabolism_Regulation of lipid metabolism via LXR, NF-Y and SREBP	5.25E-04	6/38
Development_Role of HDAC and calcium/calmodulin-dependent kinase (CaMK) in control of skeletal myogenesis	6.27E-04	7/54
Immune response_BCR pathway	6.27E-04	7/54
Transport_Clathrin-coated vesicle cycle	6.77E-04	8/71
Reproduction_Progesterone-mediated oocyte maturation	6.98E-04	6/40
Cytoskeleton remodeling_Role of PKA in cytoskeleton reorganization	6.98E-04	6/40
Regulation of degradation of deltaF508 CFTR in CF	7.30E-04	5/27
Cell cycle_Transition and termination of DNA replication	8.69E-04	5/28
Transcription_CREB pathway	1.17E-03	6/44
Muscle contraction_EDG5-mediated smooth muscle contraction	1.20E-03	5/30
Apoptosis and survival_Granzyme A signaling	1.20E-03	5/30
Cell adhesion_Histamine H1 receptor signaling in the interruption of cell barrier integrity	1.32E-03	6/45
Cytoskeleton remodeling_Fibronectin-binding integrins in cell motility	1.40E-03	5/31
Cytoskeleton remodeling_Reverse signaling by ephrin B	1.40E-03	5/31
Chemotaxis_Lipoxin inhibitory action on fMLP-induced neutrophil chemotaxis	1.49E-03	6/46
Signal transduction_PTEN pathway	1.49E-03	6/46
wtCFTR and delta508 traffic / Clathrin coated vesicles formation (norm and CF)	1.54E-03	4/19
Cell cycle_Start of DNA replication in early S phase	1.63E-03	5/32
Cell adhesion_Alpha-4 integrins in cell migration and adhesion	2.15E-03	5/34

Table B.11 (continued)

Maps	p-value	Ratio
Chemotaxis_Inhibitory action of lipoxins on IL-8- and Leukotriene B4-induced neutrophil migration	2.55E-03	6/51
Transcription_Role of heterochromatin protein 1 (HP1) family in transcriptional silencing	2.73E-03	4/22
G-protein signaling_G-Protein alpha-12 signaling pathway	3.15E-03	5/37
Cell adhesion_Role of tetraspanins in the integrin-mediated cell adhesion	3.15E-03	5/37
Development_MAG-dependent inhibition of neurite outgrowth	3.15E-03	5/37
Cell cycle_Regulation of G1/S transition (part 1)	3.55E-03	5/38
Translation _Regulation of EIF2 activity	3.98E-03	5/39
Muscle contraction_ACM regulation of smooth muscle contraction	4.10E-03	6/56
Apoptosis and survival_Apoptotic Activin A signaling	4.42E-03	4/25
Translation_Non-genomic (rapid) action of Androgen Receptor	4.45E-03	5/40
Inhibitory action of Lipoxins on neutrophil migration	4.48E-03	6/57
Immune response_IL-10 signaling pathway	5.11E-03	4/26
Development_EDG5 and EDG3 in cell proliferation and differentiation	5.11E-03	4/26
Cell cycle_Nucleocytoplasmic transport of CDK/Cyclins	5.91E-03	3/14
Development_Flt3 signaling	6.73E-03	5/44
Development_Gastrin in cell growth and proliferation	6.78E-03	6/62

Table B.12. Significantly enriched GeneGo pathway maps among the up-regulated genes following miR-7 transfection into HEY cells. Significantly enriched (FDR <0.05) GeneGo pathway map(s) among the up-regulated genes after miR-7 transfection into HEY cells are listed. Also shown are the hypergeometric distribution p-value(s) of enrichments from GeneGo and the ratio of number of genes actually present in the dataset to the number of genes in the Affymetrix array that are in each pathway. In this case only one pathway was found to be significant.

Maps	p-value	Ratio
Transport_RAB3 regulation pathway	8.01E-07	4/14

Table B.13. Significantly enriched GeneGo pathway maps among the up-regulated genes following miR-128 transfection into HEY cells. Significantly enriched (FDR <0.05) GeneGo pathway maps among the up-regulated genes after miR-128 transfection into HEY cells are listed. Also shown are the hypergeometric distribution p-values of enrichments from GeneGo and the ratio of number of genes actually present in the dataset

to the number of genes in the Affymetrix array that belong to each pathway. Pathways are sorted based on the enrichment p-values.

Maps	p-value	Ratio
Immune response_Histamine H1 receptor signaling in immune response	2.89E-07	13/48
Transport_Clathrin-coated vesicle cycle	1.18E-06	15/71
Immune response_Fc epsilon RI pathway	1.59E-06	13/55
Development_Activation of Erk by ACM1, ACM3 and ACM5	5.67E-06	11/44
Development_Regulation of epithelial-to-mesenchymal transition (EMT)	9.65E-06	13/64
Neurophysiological process_Circadian rhythm	1.13E-05	11/47
Cytoskeleton remodeling_FAK signaling	1.45E-05	12/57
Development_Angiotensin signaling via STATs	1.45E-05	9/32
Development_Leptin signaling via JAK/STAT and MAPK cascades	1.53E-05	8/25
Development_Cross-talk between VEGF and Angiopoietin 1 signaling pathways	2.12E-05	8/26
Cell adhesion_Cadherin-mediated cell adhesion	2.12E-05	8/26
Immune response_Gastrin in inflammatory response	2.27E-05	13/69
Cytoskeleton remodeling_TGF, WNT and cytoskeletal remodeling	2.32E-05	17/111
Immune response_Neurotensin-induced activation of IL-8 in colonocytes	2.42E-05	10/42
Cytoskeleton remodeling_Role of Activin A in cytoskeleton remodeling	2.74E-05	7/20
Neurophysiological process_EphB receptors in dendritic spine morphogenesis and synaptogenesis	3.20E-05	9/35
Development_Hedgehog and PTH signaling pathways in bone and cartilage development	5.17E-05	9/37
Development_TGF-beta-dependent induction of EMT via RhoA, PI3K and ILK.	5.62E-05	10/46
Immune response_Human NKG2D signaling	6.48E-05	9/38
Immune response_IL-15 signaling via JAK-STAT cascade	7.64E-05	7/23
Development_A3 receptor signaling	9.94E-05	10/49
Signal transduction_IP3 signaling	9.94E-05	10/49
Translation_Non-genomic (rapid) action of Androgen Receptor	9.97E-05	9/40
Development_Glucocorticoid receptor signaling	1.03E-04	7/24
Immune response_Function of MEF2 in T lymphocytes	1.19E-04	10/50
Mucin expression in CF via TLRs, EGFR signaling pathways	1.42E-04	10/51
Development_A2A receptor signaling	1.81E-04	9/43
Development_A1 receptor signaling	1.98E-04	10/53
Development_Angiopoietin - Tie2 signaling	2.17E-04	8/35
Immune response_CD40 signaling	2.28E-04	11/64

Table B.13 (continued)

Maps	p-value	Ratio
Apoptosis and survival_Anti-apoptotic TNFs/NF-kB/IAP pathway	2.34E-04	7/27
Signal transduction_Calcium signaling	2.60E-04	9/45
Apoptosis and survival_NO synthesis and signaling	2.73E-04	10/55
Development_GDNF family signaling	3.10E-04	9/46
Development_Gastrin in differentiation of the gastric mucosa	3.96E-04	8/38
Immune response_CCR5 signaling in macrophages and T lymphocytes	4.27E-04	10/58
Development_Role of Activin A in cell differentiation and proliferation	5.72E-04	8/40
Cytoskeleton remodeling_Reverse signaling by ephrin B	5.84E-04	7/31
Development_EDNRB signaling	5.93E-04	9/50
Apoptosis and survival_HTR1A signaling	5.93E-04	9/50
Development_A2B receptor: action via G-protein alpha s	5.93E-04	9/50
Reproduction_GnRH signaling	6.54E-04	11/72
Transport_ACM3 in salivary glands	6.81E-04	8/41
Neurophysiological process_Netrin-1 in regulation of axon guidance	6.81E-04	8/41
Development_Gastrin in cell growth and proliferation	7.39E-04	10/62
Signal transduction_Activation of PKC via G-Protein coupled receptor	7.99E-04	9/52
Proteolysis_Role of Parkin in the Ubiquitin-Proteasomal Pathway	8.15E-04	6/24
Immune response_IL-7 signaling in B lymphocytes	9.49E-04	8/43
Development_Angiotensin signaling via PYK2	9.49E-04	8/43
Apoptosis and survival_Apoptotic Activin A signaling	1.03E-03	6/25
Development_NOTCH1-mediated pathway for NF-KB activity modulation	1.05E-03	7/34
G-protein signaling_G-Protein alpha-q signaling cascades	1.05E-03	7/34
Immune response _IFN gamma signaling pathway	1.06E-03	9/54
Immune response_CD28 signaling	1.06E-03	9/54
PGE2 pathways in cancer	1.21E-03	9/55
Development_EPO-induced Jak-STAT pathway	1.26E-03	7/35
Cytoskeleton remodeling_Cytoskeleton remodeling	1.28E-03	13/102
Neurophysiological process_Receptor-mediated axon growth repulsion	1.30E-03	8/45
Neurophysiological process_Glutamate regulation of Dopamine D1A receptor signaling	1.30E-03	8/45
Cell adhesion_Histamine H1 receptor signaling in the interruption of cell barrier integrity	1.30E-03	8/45
Transcription_Androgen Receptor nuclear signaling	1.30E-03	8/45
Development_Keratinocyte differentiation	1.39E-03	9/56
Immune response_TREM1 signaling pathway	1.39E-03	9/56
Development_Endothelin-1/EDNRA transactivation of EGFR	1.50E-03	8/46

Table B.13 (continued)

Maps	p-value	Ratio
Immune response_MIF - the neuroendocrine-macrophage connector	1.50E-03	8/46
Development_WNT5A signaling	1.50E-03	8/46
Development_TGF-beta-dependent induction of EMT via MAPK	1.74E-03	8/47
Development_Leptin signaling via PI3K-dependent pathway	1.74E-03	8/47
Cytoskeleton remodeling_ACM3 and ACM4 in keratinocyte migration	1.78E-03	7/37
Development_Prolactin receptor signaling	1.79E-03	9/58
Development_Delta-type opioid receptor signaling via G-protein alpha-14	1.93E-03	6/28
Immune response_IL-7 signaling in T lymphocytes	2.09E-03	7/38
Cell cycle_Regulation of G1/S transition (part 1)	2.09E-03	7/38
Development_WNT signaling pathway. Part 1. Degradation of beta-catenin in the absence WNT signaling	2.25E-03	5/20
Development_Melanocyte development and pigmentation	2.29E-03	8/49
Immune response_IL-2 activation and signaling pathway	2.29E-03	8/49
Immune response_Bacterial infections in normal airways	2.29E-03	8/49
Development_PACAP signaling in neural cells	2.44E-03	7/39
Transcription_NF-kB signaling pathway	2.44E-03	7/39
G-protein signaling_Regulation of p38 and JNK signaling mediated by G-proteins	2.44E-03	7/39
Development_Thyroliberin signaling	2.56E-03	9/61
Immune response_Histamine signaling in dendritic cells	2.61E-03	8/50
Development_GM-CSF signaling	2.61E-03	8/50
Delta508-CFTR traffic / ER-to-Golgi in CF	2.78E-03	4/13
Normal wtCFTR traffic / ER-to-Golgi	2.78E-03	4/13
Development_IGF-1 receptor signaling	2.97E-03	8/51
Membrane-bound ESR1: interaction with G-proteins signaling	2.97E-03	8/51
Immune response_NFAT in immune response	2.97E-03	8/51
Some pathways of EMT in cancer cells	2.97E-03	8/51
Development_EGFR signaling pathway	3.21E-03	9/63
Cell adhesion_Chemokines and adhesion	3.24E-03	12/100
Blood coagulation_GPIb-IX-V-dependent platelet activation	3.25E-03	10/75
Immune response_PGE2 common pathways	3.36E-03	8/52
Immune response_Antiviral actions of Interferons	3.36E-03	8/52
Cytoskeleton remodeling_CDC42 in cellular processes	3.53E-03	5/22
Muscle contraction_Regulation of eNOS activity in endothelial cells	3.58E-03	9/64
Immune response_PIP3 signaling in B lymphocytes	3.78E-03	7/42
Development_FGFR signaling pathway	3.79E-03	8/53
Development_Endothelin-1/EDNRA signaling	3.79E-03	8/53

Table B.13 (continued)

Maps	p-value	Ratio
Development_WNT signaling pathway. Part 2	3.79E-03	8/53
Development_PDGF signaling via STATs and NF-kB	3.95E-03	6/32
Immune response_Role of DAP12 receptors in NK cells	4.27E-03	8/54
Development_Role of HDAC and calcium/calmodulin-dependent kinase (CaMK) in control of skeletal myogenesis	4.27E-03	8/54
Development_ACM2 and ACM4 activation of ERK	4.33E-03	7/43
Development_VEGF signaling and activation	4.33E-03	7/43
Apoptosis and survival_Anti-apoptotic action of Gastrin	4.33E-03	7/43
Immune response_HTR2A-induced activation of cPLA2	4.33E-03	7/43
Development_Angiotensin activation of ERK	4.63E-03	6/33
Normal and pathological TGF-beta-mediated regulation of cell proliferation	4.63E-03	6/33
Transcription_CREB pathway	4.94E-03	7/44
Neurophysiological process_NMDA-dependent postsynaptic long-term potentiation in CA1 hippocampal neurons	5.20E-03	10/80
Signal transduction_Erk Interactions: Inhibition of Erk	5.40E-03	6/34
Development_Role of CDK5 in neuronal development	5.40E-03	6/34
Development_VEGF signaling via VEGFR2 - generic cascades	5.61E-03	7/45
Development_Growth hormone signaling via STATs and PLC/IP3	6.25E-03	6/35
IL-1 beta-dependent CFTR expression	6.31E-03	4/16
Transcription_Transcription regulation of aminoacid metabolism	6.31E-03	5/25
Development_G-Proteins mediated regulation MARK-ERK signaling	6.34E-03	7/46
Neurophysiological process_ACM regulation of nerve impulse	6.34E-03	7/46
Development_Hedgehog signaling	6.34E-03	7/46
Immune response_ICOS pathway in T-helper cell	6.34E-03	7/46
Bacterial infections in CF airways	6.64E-03	8/58
Regulation of CFTR activity (norm and CF)	6.64E-03	8/58
Development_PIP3 signaling in cardiac myocytes	7.15E-03	7/47
Cell adhesion_Tight junctions	7.20E-03	6/36
G-protein signaling_RAC1 in cellular process	7.20E-03	6/36
Regulation of lipid metabolism_Stimulation of Arachidonic acid production by ACM receptors	7.86E-03	9/72
Transcription_Transcription factor Tubby signaling pathways	7.94E-03	4/17
Muscle contraction_Relaxin signaling pathway	8.03E-03	7/48
G-protein signaling_G-Protein alpha-i signaling cascades	8.85E-03	5/27
Muscle contraction_nNOS Signaling in Skeletal Muscle	8.85E-03	5/27
Neurophysiological process_Long-term depression in cerebellum	8.99E-03	7/49
Development_Mu-type opioid receptor signaling	9.41E-03	6/38
Immune response_Oncostatin M signaling via JAK-Stat in mouse cells	9.82E-03	4/18

Table B.13 (continued)

Maps	p-value	Ratio
Development_TGF-beta receptor signaling	1.00E-02	7/50
HIV-1 signaling via CCR5 in macrophages and T lymphocytes	1.07E-02	6/39
Development_ERBB-family signaling	1.07E-02	6/39
Transport_Macropinocytosis regulation by growth factors	1.09E-02	8/63
Signal transduction_PKA signaling	1.12E-02	7/51
Immune response_IL-15 signaling	1.19E-02	8/64
wtCFTR and delta508 traffic / Clathrin coated vesicles formation (norm and CF)	1.20E-02	4/19
Immune response_Delta-type opioid receptor signaling in T-cells	1.20E-02	5/29
Immune response_CD137 signaling in immune cell	1.20E-02	5/29
Immune response_MIF in innate immunity response	1.21E-02	6/40
Immune response_T cell receptor signaling pathway	1.24E-02	7/52

APPENDIX C

SUPPLEMENTARY INFORMATION FOR CHAPTER 4

Table C.1. Differentially expressed miRNAs between HEY cells transfected with either miR-7 or negative control miRNA. List of differentially expressed miRNA probesets detected by microarray following miR-7 or miR-NC transfection into HEY cells (two independent samples per group). Probe sequence names are given with the corresponding sequence, the transcript ID provided by Affymetrix annotation file, the difference between averaged $\log_2$ signal values for transfection and control groups (miR7-miR-NC), the false discovery rate [q value (%)], the nearest human homolog found using miRBase, and the genomic location (also from miRBase) are given. Probesets with 'FALSE' calls in all groups were removed from analysis. Only probesets having a fold change ≥1.4 in average signal value and FDR ≤5 % were called differentially expressed. These probesets correspond to seventy-one unique mature human miRNAs (excluding miR-7), three sequences with very poor (BLASTN E-value >1) homology to human miRNAs, two snoRNAs, one vault RNA, one tRNA, one mRNA (KIAA1407) fragment, and some sequences that we could not map to the human genome (E-value >10).

Probeset Name	Sequence	Transcript ID (Array Design)	miR7-miR-NC	q value (%)	homolog**	Genomic location
cfa-miR-1839_st	AAGGUAGAUAG AACAGGUCUUG	cfa-mir-1839	-0.898123	0.488495	ACA45	N/A

Table C.1 (continued)

Probeset Name	Sequence	Transcript ID (Array Design)	miR7-miR-NC	q value (%)	homolog**	Genomic location
ACA52_st	TGGTCCATCCT AATCCCTGCCG GTCCATCTGTG GCCTGCCAGGT TTCGCTTGTGG ACCAGAGCACC CTAGAAGCCTC ACCCGAGGAGT GAGCAGGGCTC CAGTGGGCTCA CGTCATGGGCA CTTCTAGACAC TC	ACA52	-0.536932	1.376021	ACA52	N/A
csa-let-7a_st	UGAGGUAGUAG GUUAUAUCAGU	csa-let-7a	-0.5611535	0.488495	hsa-let-7a/hsa-let-7c	let-7a-3: Exon 5 of RP4-695020__B; let-7a-1: Intergenic; let-7a-2 Intergenic; let-7c: intron 1/3/5/6/7 of C21orf34
tni-let-7g_st	UGAGGUAGUAG UUUGUAUAGUU	tni-let-7g	-0.5932545	0.488495	hsa-let-7a/hsa-let-7g/hsa-let-7f	let-7a-3: Exon 5 of RP4-695020__B; let-7a-1: Intergenic; let-7a-2 Intergenic
dre-let-7g_st	UGAGGUAGUAG UUUGUAUAGUU	dre-let-7g-1 // dre-let-7g-2	-0.5344905	0.488495	hsa-let-7a/hsa-let-7g/hsa-let-7f	let-7a-3: Exon 5 of RP4-695020__B; let-7a-1: Intergenic; let-7a-2 Intergenic

Table C.1 (continued)

Probeset Name	Sequence	Transcript ID (Array Design)	miR7-miR-NC	q value (%)	homolog**	Genomic location
gga-let-7k_st	UGAGGUAGUAGAUUGAAUAGUU	gga-let-7k	-0.7634225	0.488495	hsa-let-7f	hsa-let-7f-1: Intergenic; hsa-let-7f-2: Intron 34/59/60 of HUWE1
rno-let-7f_st	UGAGGUAGUAGAUUGUAUAGUU	rno-let-7f-1 // rno-let-7f-2	-0.585445	0.488495	hsa-let-7f	hsa-let-7f-1: Intergenic; hsa-let-7f-2: Intron 34/59/60 of HUWE1
bta-let-7f_st	UGAGGUAGUAGAUUGUAUAGUU	bta-let-7f-1 // bta-let-7f-2	-0.570095	0.488495	hsa-let-7f	hsa-let-7f-1: Intergenic; hsa-let-7f-2: Intron 34/59/60 of HUWE1
xtr-let-7f_st	UGAGGUAGUAGAUUGUAUAGUU	xtr-let-7f	-0.558275	0.488495	hsa-let-7f	hsa-let-7f-1: Intergenic; hsa-let-7f-2: Intron 34/59/60 of HUWE1
mml-let-7f_st	UGAGGUAGUAGAUUGUAUAGUU	mml-let-7f-1 // mml-let-7f-2	-0.544205	0.488495	hsa-let-7f	hsa-let-7f-1: Intergenic; hsa-let-7f-2: Intron 34/59/60 of HUWE1
mdo-let-7f_st	UGAGGUAGUAGAUUGUAUAGUU	mdo-let-7f-1 // mdo-let-7f-2	-0.543245	0.488495	hsa-let-7f	hsa-let-7f-1: Intergenic; hsa-let-7f-2: Intron 34/59/60 of HUWE1
mmu-let-7f_st	UGAGGUAGUAGAUUGUAUAGUU	mmu-let-7f-1 // mmu-let-7f-2	-0.534605	0.713954	hsa-let-7f	hsa-let-7f-1: Intergenic; hsa-let-7f-2: Intron 34/59/60 of HUWE1

Table C.1 (continued)

Probeset Name	Sequence	Transcript ID (Array Design)	miR7-miR-NC	q value (%)	homolog**	Genomic location
gga-let-7f_st	UGAGGUAGUAG AUUGUAUAGUU	gga-let-7f	-0.53172	0.488495	hsa-let-7f	hsa-let-7f-1: Intergenic; hsa-let-7f-2: Intron 34/59/60 of HUWE1
ssc-let-7f_st	UGAGGUAGUAG AUUGUAUAGUU	ssc-let-7f	-0.529395	0.488495	hsa-let-7f	hsa-let-7f-1: Intergenic; hsa-let-7f-2: Intron 34/59/60 of HUWE1
dre-let-7f_st	UGAGGUAGUAG AUUGUAUAGUU	dre-let-7f	-0.521045	0.713954	hsa-let-7f	hsa-let-7f-1: Intergenic; hsa-let-7f-2: Intron 34/59/60 of HUWE1
hsa-let-7f_st	UGAGGUAGUAG AUUGUAUAGUU	hsa-let-7f-1 // hsa-let-7f-2	-0.52087	0.713954	hsa-let-7f	hsa-let-7f-1: Intergenic; hsa-let-7f-2: Intron 34/59/60 of HUWE1
cfa-let-7f_st	UGAGGUAGUAG AUUGUAUAGUU	cfa-let-7f	-0.5177	0.713954	hsa-let-7f	hsa-let-7f-1: Intergenic; hsa-let-7f-2: Intron 34/59/60 of HUWE1
mmu-let-7g_st	UGAGGUAGUAG UUUGUACAGUU	mmu-let-7g	-0.637655	0.488495	hsa-let-7g	Intron 2/3 of WDR82
bta-let-7g_st	UGAGGUAGUAG UUUGUACAGUU	bta-let-7g	-0.627905	0.488495	hsa-let-7g	Intron 2/3 of WDR82
mml-let-7g_st	UGAGGUAGUAG UUUGUACAGUU	mml-let-7g	-0.60723	0.488495	hsa-let-7g	Intron 2/3 of WDR82
cfa-let-7g_st	UGAGGUAGUAG UUUGUACAGUU	cfa-let-7g	-0.598865	0.488495	hsa-let-7g	Intron 2/3 of WDR82

Table C.1 (continued)

Probeset Name	Sequence	Transcript ID (Array Design)	miR7-miR-NC	q value (%)	homolog**	Genomic location
hsa-let-7g_st	UGAGGUAGUAGUUUGUACAGUU	hsa-let-7g	-0.584965	0.488495	hsa-let-7g	Intron 2/3 of WDR82
rno-let-7i-star_st	CUGCGCAAGCUACUGCCUUGCU	rno-let-7i	0.5051315	0.488495	hsa-let-7i*	Intergenic
hsa-miR-100-star_st	CAAGCUUGUAUCUAUAGGUAUG	hsa-mir-100	-0.5047395	0.713954	hsa-miR-100*	Intergenic, neighboring let-7a-2
mml-miR-10a_st	UACCCUGUAGAUCCGAAUUUGUG	mml-mir-10a	-0.5461905	0.713954	hsa-miR-10a	Intron 1 of HOXB3
cfa-miR-10_st	UACCCUGUAGAUCCGAAUUUGU	cfa-mir-10	-0.538179	1.376021	hsa-miR-10a	Intron 1 of HOXB3
bmo-miR-10_st	ACCCUGUAGAUCCGAAUUUGU	bmo-mir-10	-0.5269015	0.713954	hsa-miR-10a	Intron 1 of HOXB3
ppa-miR-10a_st	UACCCUGUAGAUCCGAAUUUGUG	ppa-mir-10a	-0.515554	0.713954	hsa-miR-10a	Intron 1 of HOXB3
mne-miR-10b_st	UACCCUGUAGAACCGAAUUUGU	mne-mir-10b	-0.647604	0.713954	hsa-miR-10b	Intron 1 of HOXD3
xtr-miR-10b_st	UACCCUGUAGAACCGAAUUUGU	xtr-mir-10b	-0.542885	0.713954	hsa-miR-10b	Intron 1 of HOXD3
mml-miR-10b_st	UACCCUGUAGAACCGAAUUUGUG	mml-mir-10b	-0.5331445	0.488495	hsa-miR-10b	Intron 1 of HOXD3
bta-miR-10b_st	UACCCUGUAGAACCGAAUUUGUG	bta-mir-10b	-0.522565	0.488495	hsa-miR-10b	Intron 1 of HOXD3
ppa-miR-10b_st	UACCCUGUAGAACCGAAUUUGU	ppa-mir-10b	-0.5173075	1.376021	hsa-miR-10b	Intron 1 of HOXD3

Table C.1 (continued)

Probeset Name	Sequence	Transcript ID (Array Design)	miR7-miR-NC	q value (%)	homolog**	Genomic location
hsa-miR-1180_st	UUUCCGGCUCGCGUGGGUGUGU	hsa-mir-1180	0.781506	0	hsa-miR-1180	Intron 5 of B9D1
mml-miR-1224_st	GUGAGGACUCGGGAGGUGG	mml-mir-1224	-0.5178975	2.815705	hsa-miR-1224-5p	Intron 13/16/18 of VWA5B2, intron 15 of EIF2B5
hsa-miR-1246_st	AAUGGAUUUUUGGAGCAGG	hsa-mir-1246	1.4159435	0	hsa-miR-1246	Intergenic
tni-miR-126_st	UCGUACCGUGAGUAAUAAUGC	tni-mir-126	-0.5210625	0.713954	hsa-miR-126	Intron 5/6/7 of EGFL7
hsa-miR-1274a_st	GUCCCUGUUCAGGCGCCA	hsa-mir-1274a	-0.9468385	0.488495	hsa-miR-1274a	Antisense to Intron 1 of PLCXD3
hsa-miR-1303_st	UUUAGAGACGGGGUCUUGCUCU	hsa-mir-1303	0.60768	4.102276	hsa-miR-1303	Intergenic
mml-miR-137_st	UUAUUGCUUAAGAAUACGCGUAG	mml-mir-137	-0.703785	0.713954	hsa-miR-137	Exon 3 of RP11-490G2.1
hsa-miR-137_st	UUAUUGCUUAAGAAUACGCGUAG	hsa-mir-137	-0.56398	1.376021	hsa-miR-137	Exon 3 of RP11-490G2.1
mmu-miR-139-5p_st	UCUACAGUGCACGUGUCUCCAG	mmu-mir-139	-0.622833	0.488495	hsa-miR-139-5p	Intron 1/2/3/6 of PDE2A
hsa-miR-139-5p_st	UCUACAGUGCACGUGUCUCCAG	hsa-mir-139	-0.601006	0.713954	hsa-miR-139-5p	Intron 1/2/3/6 of PDE2A
mml-miR-139-5p_st	UCUACAGUGCACGUGUCUCCAG	mml-mir-139	-0.562391	0.488495	hsa-miR-139-5p	Intron 1/2/3/6 of PDE2A
bta-miR-139_st	UCUACAGUGCACGUGUCUCCAGU	bta-mir-139	-0.5498285	0.488495	hsa-miR-139-5p	Intron 1/2/3/6 of PDE2A

Table C.1 (continued)

Probeset Name	Sequence	Transcript ID (Array Design)	miR7-miR-NC	q value (%)	homolog**	Genomic location
rno-miR-139-5p_st	UCUACAGUGCACGUGUCUCCAG	rno-mir-139	-0.5198765	1.376021	hsa-miR-139-5p	Intron 1/2/3/6 of PDE2A
dre-miR-140_st	CAGUGGUUUUACCCUAUGGUAG	dre-mir-140	0.568629	0.488495	hsa-miR-140-5p	Intron 15/16 of WWP2
mml-miR-140-5p_st	CAGUGGUUUUACCCUAUGGUAG	mml-mir-140	0.5963435	0.488495	hsa-miR-140-5p	Intron 15/16 of WWP2
mmu-miR-142-5p_st	CAUAAAGUAGAAAGCACUACU	mmu-mir-142	0.54093	0.488495	hsa-miR-142-5p	Intergenic
rno-miR-146a_st	UGAGAACUGAAUUCCAUGGGUU	rno-mir-146a	0.506805	0.488495	hsa-miR-146a	Intergenic
cfa-miR-146a_st	UGAGAACUGAAUUCCAUGGGUU	cfa-mir-146a	0.537795	0.312856	hsa-miR-146a	Intergenic
mmu-miR-149_st	UCUGGCUCCGUGUCUUCACUCCC	mmu-mir-149	6.0962705	0	hsa-miR-149	Intron 1 of GPC1
mml-miR-149_st	UCUGGCUCCGUGUCUUCACUCCC	mml-mir-149	6.1961005	0	hsa-miR-149	Intron 1 of GPC1
hsa-miR-149_st	UCUGGCUCCGUGUCUUCACUCCC	hsa-mir-149	6.223235	0	hsa-miR-149	Intron 1 of GPC1
mmu-miR-155_st	UUAAUGCUAAUUGUGAUAGGGGU	mmu-mir-155	-0.6957595	0.488495	hsa-miR-155	Exon 4 of MIR155HG
xtr-miR-155_st	UUAAUGCUAAUCGUGAUAGGGG	xtr-mir-155	-0.53156	0.713954	hsa-miR-155	Exon 4 of MIR155HG
ssc-miR-15b_st	CCGCAGCACAUCAUGGUUUACA	ssc-mir-15b	-0.52393	1.376021	hsa-miR-15b	Intron 1/2/3/4/5 of SMC4

Table C.1 (continued)

Probeset Name	Sequence	Transcript ID (Array Design)	miR7-miR-NC	q value (%)	homolog**	Genomic location
mmu-miR-15b_st	UAGCAGCACAUCAUGGUUUACA	mmu-mir-15b	-0.515075	1.376021	hsa-miR-15b	Intron 1/2/3/4/5 of SMC4
bta-miR-20b_st	CAAAGUGCUCACAGUGCAGGUA	bta-mir-20b	-0.509185	0.713954	hsa-miR-17/hsa-miR-20b	hsa-miR-17: Intron 3 of MIR17HG; hsa-miR-20b: intergenic
hsa-miR-181a-2-star_st	ACCACUGACCGUUGACUGUACC	hsa-mir-181a-1 // hsa-mir-181a-2	1.325246	0	hsa-miR-181a-2*	Intron 1 of MIR181A2HG
rno-miR-181b_st	AACAUUCAUUGCUGUCGGUGGGU	rno-mir-181b-1 // rno-mir-181b-2	0.564765	0.312856	hsa-miR-181b	hsa-miR-181b-1: Intron 2 of RP11-31E23.1; hsa-miR-181b-2: Intron 1 MIR181A2HG
bta-miR-181b_st	AACAUUCAUUGCUGUCGGUGGGUUU	bta-mir-181b	0.56671	0.488495	hsa-miR-181b	hsa-miR-181b-1: Intron 2 of RP11-31E23.1; hsa-miR-181b-2: Intron 1 MIR181A2HG
ptr-miR-181b_st	AACAUUCAUUGCUGUCGGUGGGUU	ptr-mir-181b	0.567385	0.312856	hsa-miR-181b	hsa-miR-181b-1: Intron 2 of RP11-31E23.1; hsa-miR-181b-2: Intron 1 MIR181A2HG
hsa-miR-181b_st	AACAUUCAUUGCUGUCGGUGGGU	hsa-mir-181b-1 // hsa-mir-181b-2	0.57814	0	hsa-miR-181b	hsa-miR-181b-1: Intron 2 of RP11-31E23.1; hsa-miR-181b-2: Intron 1 MIR181A2HG

Table C.1 (continued)

Probeset Name	Sequence	Transcript ID (Array Design)	miR7-miR-NC	q value (%)	homolog**	Genomic location
ssc-miR-181b_st	AACAUUCAUUGCUGUCGGUGGGUU	ssc-mir-181b	0.602485	0	hsa-miR-181b	hsa-miR-181b-1: Intron 2 of RP11-31E23.1; hsa-miR-181b-2: Intron 1 MIR181A2HG
tni-miR-181b_st	AACAUUCAUUGCUGUCGGUGGG	tni-mir-181b-1 // tni-mir-181b-2	0.60343	0	hsa-miR-181b	hsa-miR-181b-1: Intron 2 of RP11-31E23.1; hsa-miR-181b-2: Intron 1 MIR181A2HG
lla-miR-181b_st	AACAUUCAUUGCUGUCGGUGGGUU	lla-mir-181b	0.606425	0.312856	hsa-miR-181b	hsa-miR-181b-1: Intron 2 of RP11-31E23.1; hsa-miR-181b-2: Intron 1 MIR181A2HG
ppa-miR-181b_st	AACAUUCAUUGCUGUCGGUGGGUU	ppa-mir-181b	0.60706	0	hsa-miR-181b	hsa-miR-181b-1: Intron 2 of RP11-31E23.1; hsa-miR-181b-2: Intron 1 MIR181A2HG
ggo-miR-181b_st	AACAUUCAUUGCUGUCGGUGGGUU	ggo-mir-181b	0.609995	0.312856	hsa-miR-181b	hsa-miR-181b-1: Intron 2 of RP11-31E23.1; hsa-miR-181b-2: Intron 1 MIR181A2HG

Table C.1 (continued)

Probeset Name	Sequence	Transcript ID (Array Design)	miR7-miR-NC	q value (%)	homolog**	Genomic location
dre-miR-181c_st	CACAUUCAUUGCUGUCGGUGGG	dre-mir-181c	0.620615	0	hsa-miR-181b	hsa-miR-181b-1: Intron 2 of RP11-31E23.1; hsa-miR-181b-2: Intron 1 MIR181A2HG
gga-miR-181b_st	AACAUUCAUUGCUGUCGGUGGG	gga-mir-181b-2 // gga-mir-181b-1	0.62653	0	hsa-miR-181b	hsa-miR-181b-1: Intron 2 of RP11-31E23.1; hsa-miR-181b-2: Intron 1 MIR181A2HG
mml-miR-181b_st	AACAUUCAUUGCUGUCGGUGGGUU	mml-mir-181b-2 // mml-mir-181b-1	0.627875	0.312856	hsa-miR-181b	hsa-miR-181b-1: Intron 2 of RP11-31E23.1; hsa-miR-181b-2: Intron 1 MIR181A2HG
mne-miR-181b_st	AACAUUCAUUGCUGUCGGUGGGUU	mne-mir-181b	0.631765	0	hsa-miR-181b	hsa-miR-181b-1: Intron 2 of RP11-31E23.1; hsa-miR-181b-2: Intron 1 MIR181A2HG
mmu-miR-181b_st	AACAUUCAUUGCUGUCGGUGGGU	mmu-mir-181b-1 // mmu-mir-181b-2	0.632975	0	hsa-miR-181b	hsa-miR-181b-1: Intron 2 of RP11-31E23.1; hsa-miR-181b-2: Intron 1 MIR181A2HG

Table C.1 (continued)

Probeset Name	Sequence	Transcript ID (Array Design)	miR7-miR-NC	q value (%)	homolog**	Genomic location
fru-miR-181b_st	AACAUUCAUUGCUGUCGGUGGG	fru-mir-181b-2 // fru-mir-181b-1	0.64212	0	hsa-miR-181b	hsa-miR-181b-1: Intron 2 of RP11-31E23.1; hsa-miR-181b-2: Intron 1 MIR181A2HG
mdo-miR-181b_st	AACAUUCAUUGCUGUCGGUGGG	mdo-mir-181b	0.662585	0	hsa-miR-181b	hsa-miR-181b-1: Intron 2 of RP11-31E23.1; hsa-miR-181b-2: Intron 1 MIR181A2HG
xtr-miR-181b_st	AACAUUCAUUGCUGUCGGUGGG	xtr-mir-181b-1 // xtr-mir-181b-2	0.671735	0	hsa-miR-181b	hsa-miR-181b-1: Intron 2 of RP11-31E23.1; hsa-miR-181b-2: Intron 1 MIR181A2HG
dre-miR-181b_st	AACAUUCAUUGCUGUCGGUGGG	dre-mir-181b-1 // dre-mir-181b-2	0.673785	0	hsa-miR-181b	hsa-miR-181b-1: Intron 2 of RP11-31E23.1; hsa-miR-181b-2: Intron 1 MIR181A2HG
ppy-miR-181b_st	AACAUUCAUUGCUGUCGGUGGGUU	ppy-mir-181b	0.681285	0	hsa-miR-181b	hsa-miR-181b-1: Intron 2 of RP11-31E23.1; hsa-miR-181b-2: Intron 1 MIR181A2HG

Table C.1 (continued)

Probeset Name	Sequence	Transcript ID (Array Design)	miR7-miR-NC	q value (%)	homolog**	Genomic location
rno-miR-181d_st	AACAUUCAUUGUUGUCGGUGGGU	rno-mir-181d	0.706968	0	hsa-miR-181b	hsa-miR-181b-1: Intron 2 of RP11-31E23.1; hsa-miR-181b-2: Intron 1 MIR181A2HG
ssc-miR-181c_st	AACAUUCAACCUGUCGGUGAGU	ssc-mir-181c	0.5467725	0.713954	hsa-miR-181c	Intergenic
cfa-miR-181c_st	AACAUUCAACCUGUCGGUGAGUU	cfa-mir-181c	0.5765945	0.713954	hsa-miR-181c	Intergenic
cfa-miR-181d_st	AACAUUCAUUGUUGUCGGUGGGU	cfa-mir-181d	0.5783795	0.312856	hsa-miR-181d	Intergenic
hsa-miR-181d_st	AACAUUCAUUGUUGUCGGUGGGU	hsa-mir-181d	0.6058705	0	hsa-miR-181d	Intergenic
mml-miR-181d_st	AACAUUCAUUGUUGUCGGUGGGU	mml-mir-181d	0.6169345	0.488495	hsa-miR-181d	Intergenic
mmu-miR-181d_st	AACAUUCAUUGUUGUCGGUGGGU	mmu-mir-181d	0.6487065	0	hsa-miR-181d	Intergenic
bta-miR-193a_st	AACUGGCCUACAAAGUCCCAGU	bta-mir-193a	-0.5384805	1.376021	hsa-miR-193a-3p	Intergenic
ggo-miR-198_st	GGUCCAGAGGGGAGAUAGG	ggo-mir-198	-0.6281995	0.488495	hsa-miR-198	Exon 11 of FSTL1

Table C.1 (continued)

Probeset Name	Sequence	Transcript ID (Array Design)	miR7-miR-NC	q value (%)	homolog**	Genomic location
dre-miR-199-star_st	UACAGUAGUCUGCACAUUGGUU	dre-mir-199-1 // dre-mir-199-3 // dre-mir-199-2	-1.1451045	0.488495	hsa-miR-199a-3p/hsa-miR-199b-3p	hsa-miR-199a-1: intergenic; hsa-miR-199a-2: Intron 1 of RP5-1116C7.1; hsa-miR-199b: intergenic
cfa-miR-199_st	ACAGUAGUCUGCACAUUGGUU	cfa-mir-199-1 // cfa-mir-199-2 // cfa-mir-199-3	-1.1248445	0.488495	hsa-miR-199a-3p/hsa-miR-199b-3p	hsa-miR-199a-1: intergenic; hsa-miR-199a-2: Intron 1 of RP5-1116C7.1; hsa-miR-199b: intergenic
bta-miR-199a-3p_st	ACAGUAGUCUGCACAUUGGUUA	bta-mir-199a	-1.0836625	0.488495	hsa-miR-199a-3p/hsa-miR-199b-3p	hsa-miR-199a-1: Antisense to DNM2; hsa-miR-199a-2: Intron 1 of RP5-1116C7.1; hsa-miR-199b: intergenic
mml-miR-199a-3p_st	ACAGUAGUCUGCACAUUGGUUA	mml-mir-199a-2 // mml-mir-199a-1	-1.081488	0.488495	hsa-miR-199a-3p/hsa-miR-199b-3p	hsa-miR-199a-1: Antisense to DNM2; hsa-miR-199a-2: Intron 1 of RP5-1116C7.1; hsa-miR-199b: intergenic
hsa-miR-199a-3p_st	ACAGUAGUCUGCACAUUGGUUA	hsa-mir-199a-1 // hsa-mir-199a-2	-1.064386	0.488495	hsa-miR-199a-3p/hsa-miR-199b-3p	hsa-miR-199a-1: Antisense to DNM2; hsa-miR-199a-2: Intron 1 of RP5-1116C7.1; hsa-miR-199b: intergenic

Table C.1 (continued)

Probeset Name	Sequence	Transcript ID (Array Design)	miR7-miR-NC	q value (%)	homolog**	Genomic location
mmu-miR-199a-3p_st	ACAGUAGUCUGCACAUUGGUUA	mmu-mir-199a-2 // mmu-mir-199a-1	-1.026266	0.488495	hsa-miR-199a-3p/hsa-miR-199b-3p	hsa-miR-199a-1: Antisense to DNM2; hsa-miR-199a-2: Intron 1 of RP5-1116C7.1; hsa-miR-199b: intergenic
xtr-miR-199a-star_st	UACAGUAGUCUGCACAUUGGUU	xtr-mir-199a	-0.996835	0.488495	hsa-miR-199a-3p/hsa-miR-199b-3p	hsa-miR-199a-1: Antisense to DNM2; hsa-miR-199a-2: Intron 1 of RP5-1116C7.1; hsa-miR-199b: intergenic
mmu-miR-199b_st	ACAGUAGUCUGCACAUUGGUUA	mmu-mir-199b	-0.995966	0.488495	hsa-miR-199a-3p/hsa-miR-199b-3p	hsa-miR-199a-1: Antisense to DNM2; hsa-miR-199a-2: Intron 1 of RP5-1116C7.1; hsa-miR-199b: intergenic
hsa-miR-199b-3p_st	ACAGUAGUCUGCACAUUGGUUA	hsa-mir-199b	-0.9902205	0.488495	hsa-miR-199a-3p/hsa-miR-199b-3p	hsa-miR-199a-1: Antisense to DNM2; hsa-miR-199a-2: Intron 1 of RP5-1116C7.1; hsa-miR-199b: intergenic

Table C.1 (continued)

Probeset Name	Sequence	Transcript ID (Array Design)	miR7-miR-NC	q value (%)	homolog**	Genomic location
rno-miR-199a-3p_st	ACAGUAGUCUGCACAUUGGUUA	rno-mir-199a	-0.987082	0.488495	hsa-miR-199a-3p/hsa-miR-199b-3p	hsa-miR-199a-1: Antisense to DNM2; hsa-miR-199a-2: Intron 1 of RP5-1116C7.1; hsa-miR-199b: intergenic
gga-miR-199-star_st	UACAGUAGUCUGCACAUUGG	gga-mir-199-1 // gga-mir-199-2	-0.906778	0.488495	hsa-miR-199a-3p/hsa-miR-199b-3p	hsa-miR-199a-1: Antisense to DNM2; hsa-miR-199a-2: Intron 1 of RP5-1116C7.1; hsa-miR-199b: intergenic
xtr-miR-199a_st	CCCAGUGUUCAGACUACCUGUUC	xtr-mir-199a	-0.543621	0.488495	hsa-miR-199a-5p	hsa-miR-199a-1: Antisense to DNM2; hsa-miR-199a-2: Intron 1 of RP5-1116C7.1
rno-miR-200b_st	UAAUACUGCCUGGUAAUGAUGAC	rno-mir-200b	0.6259935	1.376021	hsa-miR-200b	Intergenic
xtr-miR-200b_st	UAAUACUGCCUGGUAAUGAUGAU	xtr-mir-200b	1.716313	0	hsa-miR-200b	Intergenic
gga-miR-200b_st	UAAUACUGCCUGGUAAUGAUGAU	gga-mir-200b	1.733742	0	hsa-miR-200b	Intergenic
dre-miR-200c_st	UAAUACUGCCUGGUAAUGAUGC	dre-mir-200c	1.8636275	0	hsa-miR-200b	Intergenic

Table C.1 (continued)

Probeset Name	Sequence	Transcript ID (Array Design)	miR7-miR-NC	q value (%)	homolog**	Genomic location
mmu-miR-200b_st	UAAUACUGCCUGGUAAUGAUGA	mmu-mir-200b	1.929068	0	hsa-miR-200b	Intergenic
bta-miR-200b_st	UAAUACUGCCUGGUAAUGAUG	bta-mir-200b	1.93374	0	hsa-miR-200b	Intergenic
fru-miR-200b_st	UAAUACUGCCUGGUAAUGAUGA	fru-mir-200b	2.00013	0	hsa-miR-200b	Intergenic
dre-miR-200b_st	UAAUACUGCCUGGUAAUGAUGA	dre-mir-200b	2.0644885	0	hsa-miR-200b	Intergenic
mdo-miR-200b_st	UAAUACUGCCUGGUAAUGAUGA	mdo-mir-200b	2.090665	0	hsa-miR-200b	Intergenic
tni-miR-200b_st	UAAUACUGCCUGGUAAUGAUGA	tni-mir-200b	2.0908695	0	hsa-miR-200b	Intergenic
hsa-miR-200b_st	UAAUACUGCCUGGUAAUGAUGA	hsa-mir-200b	2.113596	0	hsa-miR-200b	Intergenic
csa-miR-200_st	UAAUACUGCCUGGUAAUGAUGA	csa-mir-200	2.2164865	0	hsa-miR-200b	Intergenic
xtr-miR-204_st	UUCCCUUUGUCAUCCUAUGCCU	xtr-mir-204-1 // xtr-mir-204-2	-0.7950435	0.488495	hsa-miR-204	Intron 3/4/5/6/7 of TRPM3
sla-miR-204_st	UUCCCUUUGUCAUCCUAUGCCU	sla-mir-204	-0.7922195	1.376021	hsa-miR-204	Intron 3/4/5/6/7 of TRPM3
tni-miR-204a_st	UUCCCUUUGUCAUCCUAUGCCU	tni-mir-204a	-0.725559	0.488495	hsa-miR-204	Intron 3/4/5/6/7 of TRPM3
rno-miR-204_st	UUCCCUUUGUCAUCCUAUGCCU	rno-mir-204	-0.720936	0.488495	hsa-miR-204	Intron 3/4/5/6/7 of TRPM3
fru-miR-204_st	UUCCCUUUGUCAUCCUAUGCCU	fru-mir-204	-0.6663135	0.713954	hsa-miR-204	Intron 3/4/5/6/7 of TRPM3
mdo-miR-204_st	UUCCCUUUGUCAUCCUAUGCCU	mdo-mir-204	-0.64758	0.488495	hsa-miR-204	Intron 3/4/5/6/7 of TRPM3

Table C.1 (continued)

Probeset Name	Sequence	Transcript ID (Array Design)	miR7-miR-NC	q value (%)	homolog**	Genomic location
mmu-miR-204_st	UUCCCUUUGUCAUCCUAUGCCU	mmu-mir-204	-0.616617	0.488495	hsa-miR-204	Intron 3/4/5/6/7 of TRPM3
ppy-miR-204_st	UUCCCUUUGUCAUCCUAUGCCU	ppy-mir-204	-0.6079145	0.713954	hsa-miR-204	Intron 3/4/5/6/7 of TRPM3
ssc-miR-204_st	UUCCCUUUGUCAUCCUAUGCCU	ssc-mir-204	-0.5880915	0.713954	hsa-miR-204	Intron 3/4/5/6/7 of TRPM3
dre-miR-204_st	UUCCCUUUGUCAUCCUAUGCCU	dre-mir-204-1 // dre-mir-204-2	-0.5807335	2.815705	hsa-miR-204	Intron 3/4/5/6/7 of TRPM3
mml-miR-204_st	UUCCCUUUGUCAUCCUAUGCCU	mml-mir-204	-0.561063	0.488495	hsa-miR-204	Intron 3/4/5/6/7 of TRPM3
cfa-miR-204_st	UUCCCUUUGUCAUCCUAUGCCU	cfa-mir-204	-0.511261	1.376021	hsa-miR-204	Intron 3/4/5/6/7 of TRPM3
dre-miR-210_st	CUGUGCGUGUGACAGCGGCUAA	dre-mir-210	0.526599	0.488495	hsa-miR-210	Intergenic
fru-miR-210_st	CUGUGCGUGUGACAGCGGCUAA	fru-mir-210	0.5649155	0.488495	hsa-miR-210	Intergenic
tni-miR-210_st	CUGUGCGUGUGACAGCGGCUAA	tni-mir-210	0.616175	2.815705	hsa-miR-210	Intergenic
mml-miR-210_st	CUGUGCGUGUGACAGCGGCUGA	mml-mir-210	0.617453	0.312856	hsa-miR-210	Intergenic
xtr-miR-210_st	CUGUGCGUGUGACAGCGGCUAA	xtr-mir-210	0.660193	0	hsa-miR-210	Intergenic
hsa-miR-210_st	CUGUGCGUGUGACAGCGGCUGA	hsa-mir-210	0.523612	1.376021	hsa-miR-210	N/A
dre-miR-218a_st	UUGUGCUUGAUCUAACCAUGUG	dre-mir-218a-1 // dre-mir-218a-2	-0.7267525	0.488495	hsa-miR-218	hsa-miR-218-1: Intron 14/15/15 of SLIT2; hsa-miR-218-2: Intron 10/14 of SLIT3

Table C.1 (continued)

Probeset Name	Sequence	Transcript ID (Array Design)	miR7-miR-NC	q value (%)	homolog**	Genomic location
fru-miR-218a_st	UUGUGCUUGAUCUAACCAUGUG	fru-mir-218a-2 // fru-mir-218a-1	-0.591393	0.713954	hsa-miR-218	hsa-miR-218-1: Intron 14/15/15 of SLIT2; hsa-miR-218-2: Intron 10/14 of SLIT3
hsa-miR-221-star_st	ACCUGGCAUACAAUGUAGAUUU	hsa-mir-221	-0.6826845	0.713954	hsa-miR-221*	Intergenic
ggo-miR-223_st	UGUCAGUUUGUCAAAUACCCC	ggo-mir-223	-0.626947	0.713954	hsa-miR-223	Intergenic
hsa-miR-224_st	CAAGUCACUAGUGGUUCCGUU	hsa-mir-224	-0.9664915	0.488495	hsa-miR-224	Exon 1/3 or Intron 4/6/7 of GABRE
rno-miR-224_st	CAAGUCACUAGUGGUUCCGUUUA	rno-mir-224	-0.950823	0.488495	hsa-miR-224	Exon 1/3 or Intron 4/6/7 of GABRE
ptr-miR-224_st	CAAGUCACUAGUGGUUCCGUUUA	ptr-mir-224	-0.832212	0.488495	hsa-miR-224	Exon 1/3 or Intron 4/6/7 of GABRE
ggo-miR-224_st	CAAGUCACUAGUGGUUCCGUUUA	ggo-mir-224	-0.820565	0.488495	hsa-miR-224	Exon 1/3 or Intron 4/6/7 of GABRE
ppy-miR-224_st	CAAGUCACUAGUGGUUCCGUUUA	ppy-mir-224	-0.7884285	0.713954	hsa-miR-224	Exon 1/3 or Intron 4/6/7 of GABRE
ppa-miR-224_st	CAAGUCACUAGUGGUUCCGUUUA	ppa-mir-224	-0.7669285	0.488495	hsa-miR-224	Exon 1/3 or Intron 4/6/7 of GABRE
ssc-miR-224_st	CAAGUCACUAGUGGUUCCGUUUA	ssc-mir-224	-0.7626635	0.713954	hsa-miR-224	Exon 1/3 or Intron 4/6/7 of GABRE

Table C.1 (continued)

Probeset Name	Sequence	Transcript ID (Array Design)	miR7-miR-NC	q value (%)	homolog**	Genomic location
cfa-miR-224_st	CAAGUCACUAGUGGUUCCGUUU	cfa-mir-224	-0.727016	0.488495	hsa-miR-224	Exon 1/3 or Intron 4/6/7 of GABRE
mne-miR-224_st	CAAGUCACUAGUGGUUCCGUUUA	mne-mir-224	-0.639669	0.713954	hsa-miR-224	Exon 1/3 or Intron 4/6/7 of GABRE
mmu-miR-224_st	UAAGUCACUAGUGGUUCCGUU	mmu-mir-224	-0.617886	0.713954	hsa-miR-224	Exon 1/3 or Intron 4/6/7 of GABRE
mml-miR-224_st	CAAGUCACUAGUGGUUCCGUUUA	mml-mir-224	-0.580054	0.713954	hsa-miR-224	Exon 1/3 or Intron 4/6/7 of GABRE
hsa-miR-26b-star_st	CCUGUUCUCCAUUACUUGGCUC	hsa-mir-26b	0.533673	4.102276	hsa-miR-26b*	Intron 3/4/5 of CTDSP1
hsa-miR-29b-1-star_st	GCUGGUUUCAUAUGGUGGUUUAGA	hsa-mir-29b-2 // hsa-mir-29b-1	-0.949386	0.488495	hsa-miR-29b-1*	Antisense to Intron 2 of AC016831.7
mmu-miR-29b-star_st	GCUGGUUUCAUAUGGUGGUUUA	mmu-mir-29b-2 // mmu-mir-29b-1	-0.841947	0.488495	hsa-miR-29b-1*	Antisense to Intron 2 of AC016831.7
hsa-miR-301b_st	CAGUGCAAUGAUAUUGUCAAAGC	hsa-mir-301b	0.50897	2.815705	hsa-miR-301b	Intron 1 of PPIL2
mml-miR-301b_st	CAGUGCAAUGAUAUUGUCAAAGC	mml-mir-301b	0.690126	0.312856	hsa-miR-301b	Intron 1 of PPIL2
ggo-miR-30a-3p_st	CUUUCAGUCGGAUGUUUGCAGC	ggo-mir-30a	-0.5554675	0.488495	hsa-miR-30a*	Intron 3 of C6orf155
ppa-miR-30a-3p_st	CUUUCAGUCGGAUGUUUGCAGC	ppa-mir-30a	-0.5472125	0.713954	hsa-miR-30a*	Intron 3 of C6orf155

Table C.1 (continued)

Probeset Name	Sequence	Transcript ID (Array Design)	miR7-miR-NC	q value (%)	homolog**	Genomic location
mmu-miR-30a-star_st	CUUUCAGUCGGAUGUUUGCAGC	mmu-mir-30a	-0.535228	0.488495	hsa-miR-30a*	Intron 3 of C6orf155
hsa-miR-30a-star_st	CUUUCAGUCGGAUGUUUGCAGC	hsa-mir-30a	-0.533506	0.488495	hsa-miR-30a*	Intron 3 of C6orf155
rno-miR-30a-star_st	CUUUCAGUCGGAUGUUUGCAGC	rno-mir-30a	-0.5308425	0.713954	hsa-miR-30a*	Intron 3 of C6orf155
xtr-miR-30a-3p_st	CUUUCAGUCAGAUGUUUGCAGC	xtr-mir-30a	-0.842091	0.488495	hsa-miR-30a*/hsa-miR-30d*	hsa-miR-30a*: Intron 3 of C6orf155; hsa-miR-30d*: Intergenic
rno-miR-30e-star_st	CUUUCAGUCGGAUGUUUACAGC	rno-mir-30e	-0.549827	1.376021	hsa-miR-30e*	Intron 1/2/4/5/6/10 of NFYC
rno-miR-330-star_st	GCAAAGCACAGGGCCUGCAGAGA	rno-mir-330	0.881907	0	hsa-miR-330-3p	Intron 1 of EML2
mmu-miR-330-star_st	GCAAAGCACAGGGCCUGCAGAGA	mmu-mir-330	0.9112175	0	hsa-miR-330-3p	Intron 1 of EML2
mmu-miR-337-5p_st	GAACGGCGUCAUGCAGGAGUU	mmu-mir-337	1.3149755	0	hsa-miR-337-5p	Intergenic
dre-miR-338_st	UCCAGCAUCAGUGAUUUUGUUG	dre-mir-338-3 // dre-mir-338-1 // dre-mir-338-2	0.711282	0.488495	hsa-miR-338-3p	Intron 6/7 AATK
rno-miR-33_st	GUGCAUUGUAGUUGCAUUGCA	rno-mir-33	0.5154925	0.713954	hsa-miR-33a	Intron 1/2/10/16/17/19 of SREBF2
ppt-miR896_st	GUCAAUUUGGCCGAGUGGUUAAGGC	ppt-mir896	-1.0255465	0.488495	hsa-miR-34c-3p (poor homology)	N/A

Table C.1 (continued)

Probeset Name	Sequence	Transcript ID (Array Design)	miR7-miR-NC	q value (%)	homolog**	Genomic location
mml-miR-374b_st	AUAUAAUACAACCUGCUAAGUG	mml-mir-374b	-0.6362215	2.815705	hsa-miR-374b	Intergenic
mmu-miR-421_st	AUCAACAGACAUUAAUUGGGCGC	mmu-mir-421	0.531948	1.376021	hsa-miR-421	Intergenic
mml-miR-421_st	AUCAACAGACAUUAAUUGGGCGC	mml-mir-421	0.6122765	1.376021	hsa-miR-421	Intergenic
mmu-miR-322_st	CAGCAGCAAUUCAUGUUUUGGA	mmu-mir-322	-0.7171465	0.488495	hsa-miR-424	Exon 1 of MGC16121
mml-miR-424_st	CAGCAGCAAUUCAUGUUUUGAA	mml-mir-424	-0.695418	0.488495	hsa-miR-424	Exon 1 of MGC16121
hsa-miR-424_st	CAGCAGCAAUUCAUGUUUUGAA	hsa-mir-424	-0.5167965	2.815705	hsa-miR-424	Exon 1 of MGC16121
cfa-miR-424_st	CAAAACGUGAGGCGCUGCUAU	cfa-mir-424	-1.610662	0.488495	hsa-miR-424*	Exon 1 of MGC16121
hsa-miR-424-star_st	CAAAACGUGAGGCGCUGCUAU	hsa-mir-424	-1.5890045	0.488495	hsa-miR-424*	Exon 1 of MGC16121
mmu-miR-425-star_st	AUCGGGAAUGUCGUGUCCGCC	mmu-mir-425	0.525007	1.376021	hsa-miR-425*	Intron 1 of DALRD3
mdo-miR-425_st	AUCGGGAAUAUCGUGUCCGUCC	mdo-mir-425	0.5895345	0.488495	hsa-miR-425*	Intron 1 of DALRD3
mml-miR-494_st	UGAAACAUACACGGGAAACCUC	mml-mir-494	-0.843633	0.488495	hsa-miR-494	Intergenic
mmu-miR-503_st	UAGCAGCGGGAACAGUACUGCAG	mmu-mir-503	-1.46896	0.488495	hsa-miR-503	Intron 1 of MGC16121

Table C.1 (continued)

Probeset Name	Sequence	Transcript ID (Array Design)	miR7-miR-NC	q value (%)	homolog**	Genomic location
rno-miR-503_st	UAGCAGCGGGAACAGUACUGCAG	rno-mir-503	-1.44376	0.488495	hsa-miR-503	Intron 1 of MGC16121
hsa-miR-503_st	UAGCAGCGGGAACAGUUCUGCAG	hsa-mir-503	-1.260273	0.488495	hsa-miR-503	Intron 1 of MGC16121
mml-miR-503_st	UAGCAGCGGGAACAGUUCUGCAG	mml-mir-503	-1.2349995	0.488495	hsa-miR-503	Intron 1 of MGC16121
cfa-miR-503_st	UAGCAGCGGGAACAGUACUG	cfa-mir-503	-0.8010865	0.713954	hsa-miR-503	Intron 1 of MGC16121
mmu-miR-743a_st	GAAAGACACCAAGCUGAGUAGA	mmu-mir-743a	0.962082	0	hsa-miR-506 (poor homology)	Intergenic
hsa-miR-542-5p_st	UCGGGGAUCAUCAUGUCACGAGA	hsa-mir-542	0.607361	0.488495	hsa-miR-542-5p	Intergenic
mml-miR-542-5p_st	UCGGGGAUCAUCAUGUCACGAGA	mml-mir-542	0.660238	0	hsa-miR-542-5p	Intergenic
hsa-miR-550_st	AGUGCCUGAGGGAGUAAGAGCCC	hsa-mir-550-1 // hsa-mir-550-2	0.518992	2.815705	hsa-miR-550a	hsa-miR-550a-1: Intron 1/2 of ZNRF2; hsa-miR-550a-2: Intron 10 of AVL9
rno-miR-551b_st	GGCGACCCAUACUUGGUUUCAGU	rno-mir-551b	0.59941	0.713954	hsa-miR-551b	Intron 4 C3orf50

Table C.1 (continued)

Probeset Name	Sequence	Transcript ID (Array Design)	miR7-miR-NC	q value (%)	homolog**	Genomic location
mmu-miR-551b_st	GCGACCCAUAC UUGGUUUCAG	mmu-mir-551b	0.774779	0	hsa-miR-551b	Intron 4 C3orf50
mml-miR-551b_st	GCGACCCAUAC UUGGUUUCAG	mml-mir-551b	0.8109335	0	hsa-miR-551b	Intron 4 C3orf50
hsa-miR-584_st	UUAUGGUUUGC CUGGGACUGAG	hsa-mir-584	-0.658341	0.488495	hsa-miR-584	Intron 1 of SH3TC2
mml-miR-584_st	UUAUGGUUUGC CUGGGACUGAG	mml-mir-584	-0.641268	0.488495	hsa-miR-584	Intron 1 of SH3TC2
mml-miR-590-5p_st	GAGCUUAUUCA UAAAAGUGCAG	mml-mir-590	0.5116375	0.713954	hsa-miR-590-5p	Intron 4/5 of EIF4H
mmu-miR-590-5p_st	GAGCUUAUUCA UAAAAGUGCAG	mmu-mir-590	0.606382	0.312856	hsa-miR-590-5p	Intron 4/5 of EIF4H
mml-miR-628-3p_st	UCUAGUAAGAG UGGCAGUCGA	mml-mir-628	0.620748	2.815705	hsa-miR-628-3p	Intron 5 of CCPG1
hsa-miR-628-3p_st	UCUAGUAAGAG UGGCAGUCGA	hsa-mir-628	0.9114175	0	hsa-miR-628-3p	Intron 5 of CCPG1
cbr-miR-231_st	UAAGCUCGUGA ACAACAGGCAG GA	cbr-mir-231	1.0279965	0.312856	hsa-miR-649 (poor homology)	Intron 5 of TOP3B
cfa-miR-652_st	AAUGGCGCCAC UAGGGUUGUGC	cfa-mir-652	0.5623525	0.312856	hsa-miR-652	Intron 2 of TMEM164
mml-miR-652_st	AAUGGCGCCAC UAGGGUUGUG	mml-mir-652	0.5905725	0	hsa-miR-652	Intron 2 of TMEM164
hsa-miR-652_st	AAUGGCGCCAC UAGGGUUGUG	hsa-mir-652	0.611339	0.312856	hsa-miR-652	Intron 2 of TMEM164
rno-miR-652_st	AAUGGCGCCAC UAGGGUUGUG	rno-mir-652	0.6205725	0	hsa-miR-652	Intron 2 of TMEM164

Table C.1 (continued)

Probeset Name	Sequence	Transcript ID (Array Design)	miR7-miR-NC	q value (%)	homolog**	Genomic location
mmu-miR-652_st	AAUGGCGCCACUAGGGUUGUG	mmu-mir-652	0.638374	0	hsa-miR-652	Intron 2 of TMEM164
sme-miR-7b_st	UGGAAGACUGUCGAUUUCGUUGU	sme-mir-7b	0.9692675	0	hsa-miR-7	N/A
sme-miR-7a_st	UGGAAGACUAUUGAUUUAGUUGA	sme-mir-7a	0.9845245	0	hsa-miR-7	N/A
dre-miR-7b_st	UGGAAGACUUGUGAUUUUGUU	dre-mir-7b	1.7692205	0	hsa-miR-7	N/A
mmu-miR-7b_st	UGGAAGACUUGUGAUUUUGUUGU	mmu-mir-7b	4.0017615	0	hsa-miR-7	N/A
rno-miR-7b_st	UGGAAGACUUGUGAUUUUGUUGU	rno-mir-7b	4.1161385	0	hsa-miR-7	N/A
bta-miR-7_st	UGGAAGACUAGUGAUUUUGUUGUU	bta-mir-7	5.5653945	0	hsa-miR-7	N/A
mml-miR-7_st	UGGAAGACUAGUGAUUUUGUUGU	mml-mir-7-1 // mml-mir-7-3 // mml-mir-7-2	6.89175	0	hsa-miR-7	N/A
dme-miR-7_st	UGGAAGACUAGUGAUUUUGUUGU	dme-mir-7	6.9147465	0	hsa-miR-7	N/A
aga-miR-7_st	UGGAAGACUAGUGAUUUUGUUGU	aga-mir-7	6.953598	0	hsa-miR-7	N/A

Table C.1 (continued)

Probeset Name	Sequence	Transcript ID (Array Design)	miR7-miR-NC	q value (%)	homolog**	Genomic location
hsa-miR-7_st	UGGAAGACUAGUGAUUUUGUUGU	hsa-mir-7-2 // hsa-mir-7-3 // hsa-mir-7-1	7.001215	0	hsa-miR-7	N/A
dps-miR-7_st	UGGAAGACUAGUGAUUUUGUUGU	dps-mir-7	7.0054765	0	hsa-miR-7	N/A
csa-miR-7_st	UGGAAGACUAGUGAUUUUGUUGU	csa-mir-7	7.071394	0	hsa-miR-7	N/A
bmo-miR-7_st	UGGAAGACUAGUGAUUUUGUUGU	bmo-mir-7	7.117815	0	hsa-miR-7	N/A
tni-miR-7_st	UGGAAGACUAGUGAUUUUGUUGU	tni-mir-7	7.12679	0	hsa-miR-7	N/A
mmu-miR-7a_st	UGGAAGACUAGUGAUUUUGUUGU	mmu-mir-7a-1 // mmu-mir-7a-2	7.1681425	0	hsa-miR-7	N/A
ame-miR-7_st	UGGAAGACUAGUGAUUUUGUUGU	ame-mir-7	7.189271	0	hsa-miR-7	N/A
cfa-miR-7_st	UGGAAGACUAGUGAUUUUGUUGU	cfa-mir-7-1 // cfa-mir-7-2	7.283968	0	hsa-miR-7	N/A
dre-miR-7a_st	UGGAAGACUAGUGAUUUUGUUGU	dre-mir-7a-2 // dre-mir-7a-1 // dre-mir-7a-3	7.4055625	0	hsa-miR-7	N/A

Table C.1 (continued)

Probeset Name	Sequence	Transcript ID (Array Design)	miR7-miR-NC	q value (%)	homolog**	Genomic location
rno-miR-7a_st	UGGAAGACUAGUGAUUUUGUUGU	rno-mir-7a-1 // rno-mir-7a-2	7.450933	0	hsa-miR-7	N/A
gga-miR-7b_st	UGGAAGACUAGUGAUUUUGUU	gga-mir-7b	7.5516795	0	hsa-miR-7	N/A
mdo-miR-7_st	UGGAAGACUAGUGAUUUUGUUG	mdo-mir-7	7.6199755	0	hsa-miR-7	N/A
cin-miR-7_st	UGGAAGACUAGUGAUUUUGUUG	cin-mir-7	7.675455	0	hsa-miR-7	N/A
fru-miR-7_st	UGGAAGACUAGUGAUUUUGUU	fru-mir-7	7.690636	0	hsa-miR-7	N/A
sla-miR-7_st	UGGAAGACUAGUGAUUUUGUU	sla-mir-7	7.881972	0	hsa-miR-7	N/A
mne-miR-7_st	UGGAAGACUAGUGAUUUUGUU	mne-mir-7	7.8886565	0	hsa-miR-7	N/A
ptr-miR-7_st	UGGAAGACUAGUGAUUUUGUU	ptr-mir-7	7.9328275	0	hsa-miR-7	N/A
ppy-miR-7_st	UGGAAGACUAGUGAUUUUGUU	ppy-mir-7	7.9417035	0	hsa-miR-7	N/A
lla-miR-7_st	UGGAAGACUAGUGAUUUUGUU	lla-mir-7	8.055049	0	hsa-miR-7	N/A
ppa-miR-7_st	UGGAAGACUAGUGAUUUUGUU	ppa-mir-7	8.066156	0	hsa-miR-7	N/A
xtr-miR-7_st	UGGAAGACUAGUGAUUUUGUUG	xtr-mir-7-1 // xtr-mir-7-2 // xtr-mir-7-3	8.108839	0	hsa-miR-7	N/A
ssc-miR-7_st	UGGAAGACUAGUGAUUUUGUU	ssc-mir-7	8.1703415	0	hsa-miR-7	N/A

Table C.1 (continued)

Probeset Name	Sequence	Transcript ID (Array Design)	miR7-miR-NC	q value (%)	homolog**	Genomic location
gga-miR-7_st	UGGAAGACUAG UGAUUUUGUUG	gga-mir-7-2 // gga-mir-7-3 // gga-mir-7-1	8.172161	0	hsa-miR-7	N/A
ggo-miR-7_st	UGGAAGACUAG UGAUUUUGUU	ggo-mir-7	8.1995385	0	hsa-miR-7	N/A
odi-miR-7_st	UGGAAGACUAG UGAUUUUGUUG	odi-mir-7	8.271398	0	hsa-miR-7	N/A
hsa-miR-7-1-star_st	CAACAAAUCAC AGUCUGCCAUA	hsa-mir-7-2 // hsa-mir-7-3 // hsa-mir-7-1	-1.1885415	0.488495	hsa-miR-7-1*	Intron 1/3/15/16 or Exon 2 of HNRNPK
rno-miR-7a-star_st	ACAACAAAUCA CAGUCUGCCAU	rno-mir-7a-1 // rno-mir-7a-2	-1.091384	0.488495	hsa-miR-7-1*	Intron 1/3/15/16 or Exon 2 of HNRNPK
mmu-miR-7a-star_st	CAACAAAUCAC AGUCUGCCAUA	mmu-mir-7a-1 // mmu-mir-7a-2	-0.5598705	1.376021	hsa-miR-7-1*	Intron 1/3/15/16 or Exon 2 of HNRNPK
rno-miR-877_st	GUAGAGGAGAU GGCGCAGGG	rno-mir-877	0.582268	1.376021	hsa-miR-877	Intron 4/5/12/13/14 of ABCF1
dme-miR-92b_st	AAUUGCACUAG UCCCGGCCUGC	dme-mir-92b	-0.598515	0.488495	hsa-miR-92a	Intron 3 of MIR17HG
dps-miR-92b_st	AAUUGCACUAG UCCCGGCCUGC	dps-mir-92b	-0.575535	0.488495	hsa-miR-92a	Intron 3 of MIR17HG
csa-miR-92b_st	UAUUGCACUUG UCCCGGUCUU	csa-mir-92b	-0.566391	1.376021	hsa-miR-92a	hsa-miR-92a-1: Intron 3 of MIR17HG; hsa-miR-92a-2: intergenic
hsa-miR-92a-1-star_st	AGGUUGGGAUC GGUUGCAAUGC U	hsa-mir-92a-1 // hsa-mir-92a-2	-0.5179315	0.713954	hsa-miR-92a-1*	Intron 3 of MIR17HG
hsa-miR-93-star_st	ACUGCUGAGCU AGCACUUCCCG	hsa-mir-93	0.5775735	0.312856	hsa-miR-93*	Intron 2/4/8/12/13 of MCM7

Table C.1 (continued)

Probeset Name	Sequence	Transcript ID (Array Design)	miR7-miR-NC	q value (%)	homolog**	Genomic location
fru-let-7h_st	UGAGGUAGUAAGUUGUGUUGUU	fru-let-7h	-0.5684115	1.376021	hsa-miR-98	Intron 34/59/60 of HUWE1
bta-miR-98_st	UGAGGUAGUAAGUUGUAUUGUU	bta-mir-98	-0.5280765	0.713954	hsa-miR-98	Intron 34/59/60 of HUWE1
mmu-miR-99b-star_st	CAAGCUCGUGUCUGUGGGUCCG	mmu-mir-99b	0.8198465	0	hsa-miR-99b*	Intergenic
mmu-miR-705_st	GGUGGGAGGUGGGGUGGGCA	mmu-mir-705	-0.6009835	1.376021	KIAA1407 fragment	N/A
ppt-miR894_st	CGUUUCACGUCGGGUUCACC	ppt-mir894	-0.7261025	0.488495	N/A	N/A
dre-miR-739_st	AGGCCGAAGUGGAGAAGGGUU	dre-mir-739	-0.697482	1.376021	N/A	N/A
ppt-miR901_st	GGUAAAGUGGCGGCUAGGUUA	ppt-mir901	-0.5882015	1.376021	N/A	0
cfa-miR-1844_st	AGGACUACGGACGGGCUGAG	cfa-mir-1844	-0.508027	1.376021	N/A	N/A
cel-miR-798_st	UAAGCCUUACAUAUUGACUGA	cel-mir-798	0.703262	0.488495	N/A	N/A
mdv1-miR-M9-star_st	AAACUCCGAGGGCAGGAAAAAG	mdv1-mir-m9	0.70825	2.815705	N/A	N/A
cre-miR908.2_st	UGACGCGUUUGAUAGCAGGAUC	cre-MIR908	0.9808045	1.376021	N/A	N/A
dme-miR-252_st	CUAAGUACUAGUGCCGCAGGAG	dme-mir-252	0.549602	4.102276	N/A	N/A
cbr-miR-67_st	UCACAACCUCCUAGAAAGAGUAGA	cbr-mir-67	-8.39065	0	Negative control	N/A

Table C.1 (continued)

Probeset Name	Sequence	Transcript ID (Array Design)	miR7-miR-NC	q value (%)	homolog**	Genomic location
cel-miR-67_st	UCACAACCUCCUAGAAAGAGUAGA	cel-mir-67	-8.751703	0	Negative control	N/A
hsa-miR-1308_st	GCAUGGGUGGUUCAGUGG	hsa-mir-1308	-0.93929	0.488495	tRNA fragment (sequence removed from miRBase)	N/A
hsa-miR-886-3p_st	CGCGGGUGCUUACUGACCCUU	hsa-mir-886	-0.687022	0.713954	VTRNA2	N/A
mml-miR-886-3p_st	CGCGGGUGCUUACUGACCCUU	mml-mir-886	-0.6336085	0.713954	VTRNA2	N/A
mml-miR-886-5p_st	CGGGUCGGAGUUAGCUCAAGCGG	mml-mir-886	-0.52657	0.713954	VTRNA2	N/A

** Homology search was done using BLASTN at E-value cut-off of 10. Sequences with higher E-values are marked N/A.

Table C.2. Differentially expressed genes in miR-7 transfected HEY cells compared to negative control miRNA transfected cells. Significantly differentially expressed (fold change ≥1.3, $p < 0.05$) mRNA probeset IDs after miR-7 or miR-NC transfection into HEY cells are listed (three independent samples per group). For each probeset ID the gene title, the gene symbol, the average $\log_2$ signal value for transfected [Avg (miR-7)] and control [Avg (miR-NC)] group, difference between $\log_2$ signal values (miR7-miR-NC), and the t-test p-values are shown. Probesets with Affymetrix "Absent" calls in all samples were removed from analysis.

Please see table on our website:
http://www.mcdonaldlab.biology.gatech.edu/shubin_shahab.htm

Table C.3. Differentially expressed mRNA probeset IDs in miR-7 transfected A549 cells compared to negative control miRNA transfected cells. Result of reanalyzed data based on miR-7 transfection reported by (Webster et al., 2009) is presented. Only significantly differentially expressed genes (fold change ≤1.3, $p < 0.05$) in A549 cells transfected with miR-7 compared to cells transfected with miR-NC are listed. For each probeset ID the gene title, the gene symbol, the GO biological process ontology, the average log2 signal value for transfected [Avg (miR-7)] and control [Avg (miR-NC)] group, ratio of log2 signal values (miR7-miR-NC), and the t-test p-values are shown.

Please see table on our website:
http://www.mcdonaldlab.biology.gatech.edu/shubin_shahab.htm

Table C.4. NF-κB binding sites within 10 kb of each of the differentially expressed miRNAs after miR-7 transfection in HEY cells. NF-κB binding sites were identified by genome-wide ChIP-seq as part of the ENCODE project. This table was downloaded from the UCSC genome browser (http://genome.UCSC.edu) that is a co-host (DCC) of ENCODE data. Only sites near (± 10 kb) of miRNAs differentially expressed following miR-7 transfection into HEY cells are shown.

Please see table on our website:
http://www.mcdonaldlab.biology.gatech.edu/shubin_shahab.htm

Table C.5. Differentially expressed miRNAs in HEY cells transfected with anti-RELA siRNA compared to cells transfected with negative control siRNA. This table lists the miRNA probesets found to be significantly differentially expressed (fold change ≥1.4, FDR ≤5 %) between HEY cells transfected with either two samples of anti-RELA

siRNA or with two samples of siNC for 48 hours. Probe sequence names are given with the corresponding sequence, the alignment identified by Affymetrix software, the difference between $\log_2$ average signal values (siRNA-siNC), the false discovery rate [q value (%)], the nearest human homolog we found using miRBase are given. Probesets with 'FALSE' calls in all groups were removed from analysis.

Probeset Name	**Sequence**	**Alignments**	**siRNA-siNC**	**q-value(%)**	**homolog**
ggo-miR-17-3p_st	ACUGCAGUGAAGGCACUUGU	ggo-mir-17	-1.262586	2.683416	hsa-miR-17*
bta-miR-29b_st	UAGCACCAUUUGAAAUCAGUGUUU	bta-mir-29b	-1.2231185	1.078628	hsa-miR-29b
mmu-miR-19a_st	UGUGCAAAUCUAUGCAAAACUGA	mmu-mir-19a	-1.221328	1.333576	hsa-miR-19a
dre-miR-19a_st	UGUGCAAAUCUAUGCAAAACUGA	dre-mir-19a	-1.22031	1.078628	hsa-miR-19a
gga-miR-16_st	UAGCAGCACGUAAAUAUUGGUG	gga-mir-16-1 // gga-mir-16-2	-1.1544825	2.541717	hsa-miR-16
ppa-miR-19a_st	UGUGCAAAUCUAUGCAAAACUGA	ppa-mir-19a	-1.1526905	1.078628	hsa-miR-19a
cfa-miR-17_st	ACUGCAGUGAAGGCACUUGUAG	cfa-mir-17	-1.1415285	1.078628	hsa-miR-17*
sla-miR-19a_st	UGUGCAAAUCUAUGCAAAACUGA	sla-mir-19a	-1.1374175	1.333576	hsa-miR-19a
mml-miR-29b_st	UAGCACCAUUUGAAAUCAGUGUU	mml-mir-29b-2 // mml-mir-29b-1	-1.1353065	1.333576	hsa-miR-29b
hsa-miR-21-star_st	CAACACCAGUCGAUGGGCUGU	hsa-mir-21	-1.1211725	1.078628	hsa-miR-21*
mmu-miR-29b_st	UAGCACCAUUUGAAAUCAGUGUU	mmu-mir-29b-2 // mmu-mir-29b-1	-1.096964	2.683416	hsa-miR-29b
dre-miR-210_st	CUGUGCGUGUGACAGCGGCUAA	dre-mir-210	-1.0944205	1.993117	hsa-miR-210

Table C.5 (continued)

Probeset Name	Sequence	Alignments	siRNA-siNC	q-value(%)	homolog
mne-miR-19a_st	UGUGCAAAUCUAUGCAAAACUGA	mne-mir-19a	-1.0818635	2.683416	hsa-miR-19a
rno-miR-19a_st	UGUGCAAAUCUAUGCAAAACUGA	rno-mir-19a	-1.0618785	1.333576	hsa-miR-19a
rno-miR-17-3p_st	ACUGCAGUGAAGGCACUUGUGG	rno-mir-17-1 // rno-mir-17-2	-1.042415	1.833667	hsa-miR-17*
hsa-miR-29b_st	UAGCACCAUUUGAAAUCAGUGUU	hsa-mir-29b-2 // hsa-mir-29b-1	-1.035958	1.078628	hsa-miR-29b
gga-miR-29b_st	UAGCACCAUUUGAAAUCAGUGUU	gga-mir-29b-1 // gga-mir-29b-2	-1.028805	1.078628	hsa-miR-29b
hsa-miR-17-star_st	ACUGCAGUGAAGGCACUUGUAG	hsa-mir-17	-1.023562	1.078628	hsa-miR-17*
gga-miR-199_st	CCCAGUGUUCAGACUACCUGUUC	gga-mir-199-1 // gga-mir-199-2	-1.0156125	1.333576	hsa-miR-199a-5p
ptr-miR-19a_st	UGUGCAAAUCUAUGCAAAACUGA	ptr-mir-19a	-1.0107575	1.078628	hsa-miR-19a
dre-miR-199_st	CCCAGUGUUCAGACUACCUGUUC	dre-mir-199-1 // dre-mir-199-3 // dre-mir-199-2	-0.994966	1.333576	hsa-miR-199a-5p
xtr-miR-29b_st	UAGCACCAUUUGAAAUCAGUGUU	xtr-mir-29b	-0.9855555	1.078628	hsa-miR-29b
mdo-miR-17-3p_st	ACUGCAGUGAAGGCACUUGUA	mdo-mir-17	-0.9794485	1.078628	hsa-miR-17*
cfa-miR-29b_st	UAGCACCAUUUGAAAUCAGUGUU	cfa-mir-29b-1 // cfa-mir-29b-2	-0.9786425	1.078628	hsa-miR-29b
mdo-miR-15a_st	UAGCAGCACAUAAUGGUUUGUU	mdo-mir-15a	-0.9600185	1.078628	hsa-miR-15a
lca-miR-19a_st	UGUGCAAAUCUAUGCAAAACUGA	lca-mir-19a	-0.956088	1.078628	hsa-miR-19a

Table C.5 (continued)

Probeset Name	Sequence	Alignments	siRNA-siNC	q-value(%)	homolog
age-miR-19a_st	UGUGCAAAUCUAUGCAAAACUGA	age-mir-19a	-0.9420945	1.993117	hsa-miR-19a
ppy-miR-17-3p_st	ACUGCAGUGAAGGCACUUGU	ppy-mir-17	-0.9361395	1.447632	hsa-miR-17*
tni-miR-193_st	AACUGGCCUACAAAGUCCCAGU	tni-mir-193 // tni-mir-193	-0.9266915	1.993117	hsa-miR-193a-3p
gga-miR-17-3p_st	ACUGCAGUGAAGGCACUUGU	gga-mir-17	-0.920961	2.541717	hsa-miR-17*
mml-miR-199a_st	CCCAGUGUUCAGACUACCUGUUC	mml-mir-199a-2 // mml-mir-199a-1	-0.916911	3.39568	hsa-miR-199a-5p
age-miR-17-3p_st	ACUGCAGUGAAGGCACUUGU	age-mir-17	-0.9161615	2.541717	hsa-miR-17*
ssc-miR-19a_st	UGUGCAAAUCUAUGCAAAACUGA	ssc-mir-19a	-0.913102	2.683416	hsa-miR-19a
tni-miR-199_st	CCCAGUGUUCAGACUACCUGUUC	tni-mir-199-1 // tni-mir-199-3 // tni-mir-199-2	-0.909319	1.333576	hsa-miR-199a-5p
mmu-miR-199a-5p_st	CCCAGUGUUCAGACUACCUGUUC	mmu-mir-199a-2 // mmu-mir-199a-1	-0.907159	1.078628	hsa-miR-199a-5p
bta-miR-19a_st	UGUGCAAAUCUAUGCAAAACUGA	bta-mir-19a	-0.8969075	2.683416	hsa-miR-19a
ppa-miR-199a_st	CCCAGUGUUCAGACUACCUGUUC	ppa-mir-199a	-0.895175	1.078628	hsa-miR-199a-5p
lla-miR-19a_st	UGUGCAAAUCUAUGCAAAACUGA	lla-mir-19a	-0.887866	2.683416	hsa-miR-19a
mml-miR-193a-3p_st	AACUGGCCUACAAAGUCCCAGU	mml-mir-193a	-0.886558	1.078628	hsa-miR-193a-3p
dre-miR-19c_st	UGUGCAAAUCCAUGCAAAACUCG	dre-mir-19c	-0.8799195	1.833667	hsa-miR-19b
lla-miR-17-3p_st	ACUGCAGUGAAGGCACUUGU	lla-mir-17	-0.8790615	2.541717	hsa-miR-17*

Table C.5 (continued)

Probeset Name	Sequence	Alignments	siRNA-siNC	q-value(%)	homolog
fru-miR-19b_st	UGUGCAAAUCCAUGCAAAACUGA	fru-mir-19b	-0.8651875	4.400802	hsa-miR-19b
mmu-miR-30a_st	UGUAAACAUCCUCGACUGGAAG	mmu-mir-30a	-0.864517	1.078628	hsa-miR-30a
xtr-miR-30a-5p_st	UGUAAACAUCCUCGACUGGAAG	xtr-mir-30a	-0.863787	1.078628	hsa-miR-30a
ppy-miR-30a-5p_st	UGUAAACAUCCUCGACUGGAAG	ppy-mir-30a	-0.8617085	1.078628	hsa-miR-30a
mmu-miR-15a_st	UAGCAGCACAUAAUGGUUUGUG	mmu-mir-15a	-0.8571055	3.39568	hsa-miR-15a
gga-miR-30a-5p_st	UGUAAACAUCCUCGACUGGAAG	gga-mir-30a	-0.851093	1.078628	hsa-miR-30a
mdo-miR-30a_st	UGUAAACAUCCUCGACUGGAAG	mdo-mir-30a	-0.846671	1.078628	hsa-miR-30a
mmu-miR-21_st	UAGCUUAUCAGACUGAUGUUGA	mmu-mir-21	-0.8453195	3.778466	hsa-miR-21
bta-miR-17-3p_st	ACUGCAGUGAAGGCACUUGU	bta-mir-17	-0.8438085	1.333576	hsa-miR-17*
lca-miR-27a_st	UUCACAGUGGCUAAGUUCCGCC	lca-mir-27a	-0.8438025	3.39568	hsa-miR-27a
sla-miR-27a_st	UUCACAGUGGCUAAGUUCCGCC	sla-mir-27a	-0.8409755	4.697825	hsa-miR-27a
hsa-miR-18b_st	UAAGGUGCAUCUAGUGCAGUUAG	hsa-mir-18b	-0.836077	2.541717	hsa-miR-18b
ssc-miR-181c_st	AACAUUCAACCUGUCGGUGAGU	ssc-mir-181c	-0.832483	1.078628	hsa-miR-181c
mdo-miR-19a_st	UGUGCAAAUCUAUGCAAAACUGA	mdo-mir-19a	-0.8317935	1.833667	hsa-miR-19a
ggo-miR-30a-5p_st	UGUAAACAUCCUCGACUGGAAG	ggo-mir-30a	-0.8305745	1.333576	hsa-miR-30a
mml-miR-146a_st	UGAGAACUGAAUUCCAUGGGUU	mml-mir-146a	-0.827217	1.078628	hsa-miR-146a
sla-miR-17-3p_st	ACUGCAGUGAAGGCACUUGU	sla-mir-17	-0.822778	4.400802	hsa-miR-17*
bta-miR-18b_st	UAAGGUGCAUCUAGUGCAGUUA	bta-mir-18b	-0.820027	1.078628	hsa-miR-18b
mml-miR-19b_st	UGUGCAAAUCCAUGCAAAACUGA	mml-mir-19b-2	-0.818273	4.008016	hsa-miR-19b

Table C.5 (continued)

Probeset Name	Sequence	Alignments	siRNA-siNC	q-value(%)	homolog
mml-miR-30a-5p_st	UGUAAACAUCCUCGACUGGAAG	mml-mir-30a	-0.8140075	1.078628	hsa-miR-30a
mne-miR-17-3p_st	ACUGCAGUGAAGGCACUUGU	mne-mir-17	-0.812653	2.683416	hsa-miR-17*
ggo-miR-19a_st	UGUGCAAAUCUAUGCAAAACUGA	ggo-mir-19a	-0.806594	2.683416	hsa-miR-19a
xtr-miR-17-3p_st	ACUGCAGUGAAGGCACUUGU	xtr-mir-17	-0.8047205	2.541717	hsa-miR-17*
hsa-miR-30a_st	UGUAAACAUCCUCGACUGGAAG	hsa-mir-30a	-0.8023685	1.333576	hsa-miR-30a
mml-miR-130a_st	CAGUGCAAUGUUAAAAGGGC	mml-mir-130a	-0.80108	1.333576	hsa-miR-130a
dre-miR-19d_st	UGUGCAAACCCAUGCAAAACUGA	dre-mir-19d	-0.799694	1.333576	hsa-miR-19b
xla-miR-18_st	UAAGGUGCAUCUAGUGCAGUUAG	xla-mir-18	-0.7978315	1.447632	hsa-miR-18b
rno-miR-19b_st	UGUGCAAAUCCAUGCAAAACUGA	rno-mir-19b-1 // rno-mir-19b-2	-0.7949155	4.967704	hsa-miR-19b
hsa-miR-19a_st	UGUGCAAAUCUAUGCAAAACUGA	hsa-mir-19a	-0.794088	4.008016	hsa-miR-19a
mmu-miR-181c_st	AACAUUCAACCUGUCGGUGAGU	mmu-mir-181c	-0.791627	4.008016	hsa-miR-181c
gga-miR-140-star_st	CCACAGGGUAGAACCACGGAC	gga-mir-140	-0.7912	4.400802	hsa-miR-140-3p
mml-miR-19a_st	UGUGCAAAUCUAUGCAAAACUGA	mml-mir-19a	-0.789861	2.683416	hsa-miR-19a
hsa-miR-19b_st	UGUGCAAAUCCAUGCAAAACUGA	hsa-mir-19b-1 // hsa-mir-19b-2	-0.7897805	4.008016	hsa-miR-19b
fru-miR-19a_st	UGUGCAAAUCUAUGCAAAACUGA	fru-mir-19a	-0.789561	2.683416	hsa-miR-19a
ppa-miR-17-3p_st	ACUGCAGUGAAGGCACUUGU	ppa-mir-17	-0.7872445	2.683416	hsa-miR-17*
hsa-miR-491-5p_st	AGUGGGGAACCCUUCCAUGAGG	hsa-mir-491	-0.787157	4.967704	hsa-miR-491-5p

Table C.5 (continued)

Probeset Name	Sequence	Alignments	siRNA-siNC	q-value(%)	homolog
hsa-miR-193a-3p_st	AACUGGCCUACAAAGUCCCAGU	hsa-mir-193a	-0.786993	1.078628	hsa-miR-193a-3p
xtr-miR-19a_st	UGUGCAAAUCUAUGCAAAACUGA	xtr-mir-19a	-0.7853985	2.541717	hsa-miR-19a
lla-miR-199a_st	CCCAGUGUUCAGACUACCUGUUC	lla-mir-199a	-0.782082	1.333576	hsa-miR-199a-5p
xla-miR-19b_st	UGUGCAAAUCCAUGCAAAACUGA	xla-mir-19b	-0.779644	4.697825	hsa-miR-19b
rno-miR-503_st	UAGCAGCGGGAACAGUACUGCAG	rno-mir-503	-0.7750375	1.833667	hsa-miR-503
mml-miR-15a_st	UAGCAGCACAUAAUGGUUUGUG	mml-mir-15a	-0.7725485	2.683416	hsa-miR-15a
lla-miR-15a_st	UAGCAGCACAUAAUGGUUUGUG	lla-mir-15a	-0.771286	1.333576	hsa-miR-15a
cfa-miR-19a_st	UGUGCAAAUCUAUGCAAAACUGA	cfa-mir-19a	-0.7712315	4.967704	hsa-miR-19a
dre-miR-16b_st	UAGCAGCACGUAAAUAUUGGAG	dre-mir-16b	-0.7656065	4.400802	hsa-miR-16
sla-miR-199a_st	CCCAGUGUUCAGACUACCUGUUC	sla-mir-199a	-0.763136	2.683416	hsa-miR-199a-5p
age-miR-15a_st	UAGCAGCACAUAAUGGUUUGUG	age-mir-15a	-0.7591455	4.400802	hsa-miR-15a
lca-miR-17-3p_st	ACUGCAGUGAAGGCACUUGU	lca-mir-17	-0.7587385	3.39568	hsa-miR-17*
ppa-miR-30a-5p_st	UGUAAACAUCCUCGACUGGAAG	ppa-mir-30a	-0.7506865	1.078628	hsa-miR-30a
ppy-miR-19b_st	UGUGCAAAUCCAUGCAAAACUGA	ppy-mir-19b	-0.749318	4.967704	hsa-miR-19b
dre-miR-181a-star_st	ACCAUCGACCGUUGAUUGUACC	dre-mir-181a-1 // dre-mir-181a-2	-0.7449505	4.400802	hsa-miR-181a*

Table C.5 (continued)

Probeset Name	Sequence	Alignments	siRNA-siNC	q-value(%)	homolog
xtr-miR-199a_st	CCCAGUGUUCAGACUACCUGUUC	xtr-mir-199a	-0.743761	1.078628	hsa-miR-199a-5p
xtr-miR-15c_st	UAGCAGCACAUCAUGGUUUGUA	xtr-mir-15c	-0.7435435	4.008016	hsa-miR-15a
ggo-miR-27a_st	UUCACAGUGGCUAAGUUCCGCC	ggo-mir-27a	-0.7418565	4.400802	hsa-miR-27a
ptr-miR-181c_st	AACAUUCAACCUGUCGGUGAGU	ptr-mir-181c	-0.7403955	3.778466	hsa-miR-181c
rno-miR-301a_st	CAGUGCAAUAGUAUUGUCAAAGC	rno-mir-301a	-0.739947	4.967704	hsa-miR-301a
rno-miR-181a-star_st	ACCAUCGACCGUUGAUUGUACC	rno-mir-181a-1 // rno-mir-181a-2	-0.737395	3.39568	hsa-miR-181a*
sla-miR-19b_st	UGUGCAAAUCCAUGCAAAACUGA	sla-mir-19b	-0.7373535	4.400802	hsa-miR-19b
gga-miR-19a_st	UGUGCAAAUCUAUGCAAAACUGA	gga-mir-19a	-0.73689	3.39568	hsa-miR-19a
cfa-miR-532_st	CAUGCCUUGAGUGUAGGACCGU	cfa-mir-532	-0.732619	1.333576	hsa-miR-532-5p
sla-miR-15a_st	UAGCAGCACAUAAUGGUUUGUG	sla-mir-15a	-0.725882	2.541717	hsa-miR-15a
hsa-miR-501-3p_st	AAUGCACCCGGGCAAGGAUUCU	hsa-mir-501	-0.725765	2.683416	hsa-miR-501-3p
hsa-miR-324-5p_st	CGCAUCCCCUAGGGCAUUGGUGU	hsa-mir-324	-0.7255945	1.333576	hsa-miR-324-5p
mml-miR-27a_st	UUCACAGUGGCUAAGUUCCGCC	mml-mir-27a	-0.724656	4.400802	hsa-miR-27a
xtr-miR-210_st	CUGUGCGUGUGACAGCGGCUAA	xtr-mir-210	-0.7216065	4.008016	hsa-miR-210
age-miR-19b_st	UGUGCAAAUCCAUGCAAAACUGA	age-mir-19b	-0.7196035	4.697825	hsa-miR-19b
rno-miR-378_st	ACUGGACUUGGAGUCAGAAGG	rno-mir-378	-0.7181515	4.697825	hsa-miR-378
rno-miR-30a_st	UGUAAACAUCCUCGACUGGAAG	rno-mir-30a	-0.71561	1.078628	hsa-miR-30a

Table C.5 (continued)

Probeset Name	Sequence	Alignments	siRNA-siNC	q-value(%)	homolog
ppy-miR-199a_st	CCCAGUGUUCAGACUACCUGUUC	ppy-mir-199a	-0.714837	2.541717	hsa-miR-199a-5p
rno-miR-29b_st	UAGCACCAUUUGAAAUCAGUGUU	rno-mir-29b-2 // rno-mir-29b-1	-0.7107615	2.541717	hsa-miR-29b
dre-miR-16a_st	UAGCAGCACGUAAAUAUUGGUG	dre-mir-16a	-0.710154	2.541717	hsa-miR-16
ggo-miR-199a_st	CCCAGUGUUCAGACUACCUGUUC	ggo-mir-199a	-0.709859	1.333576	hsa-miR-199a-5p
mmu-miR-24-2-star_st	GUGCCUACUGAGCUGAAACAGU	mmu-mir-24-1 // mmu-mir-24-2	-0.70969	1.993117	hsa-miR-24-2*
xtr-miR-18a-star_st	ACUGCCCUAAGUGCUCCUUCU	xtr-mir-18a	-0.709239	2.683416	hsa-miR-18a*
tni-miR-19a_st	UGUGCAAAUCUAUGCAAAACUGA	tni-mir-19a	-0.709121	4.400802	hsa-miR-19a
ptr-miR-17-3p_st	ACUGCAGUGAAGGCACUUGU	ptr-mir-17	-0.708877	4.967704	hsa-miR-17*
ptr-miR-27a_st	UUCACAGUGGCUAAGUUCCGCC	ptr-mir-27a	-0.708858	4.008016	hsa-miR-27a
ggo-miR-15a_st	UAGCAGCACAUAAUGGUUUGUG	ggo-mir-15a	-0.7081235	1.833667	hsa-miR-15a
xtr-miR-16a_st	UAGCAGCACGUAAAUAUUGGUG	xtr-mir-16a	-0.706396	4.008016	hsa-miR-16
cfa-miR-130a_st	CAGUGCAAUGUUAAAAGGGCAU	cfa-mir-130a	-0.705965	2.541717	hsa-miR-130a
mml-miR-210_st	CUGUGCGUGUGACAGCGGCUGA	mml-mir-210	-0.704756	4.008016	hsa-miR-210
mmu-miR-378_st	ACUGGACUUGGAGUCAGAAGG	mmu-mir-378	-0.7039415	4.400802	hsa-miR-378
rno-miR-199a-5p_st	CCCAGUGUUCAGACUACCUGUUC	rno-mir-199a	-0.7035395	2.683416	hsa-miR-199a-5p
cfa-miR-130b_st	CAGUGCAAUGAUGAAAGGGCAU	cfa-mir-130b	-0.700307	4.400802	hsa-miR-130b
hsa-miR-130a_st	CAGUGCAAUGUUAAAAGGGCAU	hsa-mir-130a	-0.699144	1.078628	hsa-miR-130a

Table C.5 (continued)

Probeset Name	Sequence	Alignments	siRNA-siNC	q-value(%)	homolog
mml-miR-181a-star_st	ACCAUCGACCGUUGAUUGUACC	mml-mir-181a-2 // mml-mir-181a-1	-0.6973865	4.400802	hsa-miR-181a*
gga-miR-101_st	UACAGUACUGUGAUAACUGAAG	gga-mir-101	-0.696782	1.078628	hsa-miR-101
xtr-miR-15a_st	UAGCAGCACAUAAUGGUUUGUG	xtr-mir-15a	-0.6945635	3.39568	hsa-miR-15a
mml-miR-18b_st	UAAGGUGCAUCUAGUGCAGUUAG	mml-mir-18b	-0.694513	1.993117	hsa-miR-18b
lla-miR-19b_st	UGUGCAAAUCCAUGCAAAACUGA	lla-mir-19b	-0.690634	4.008016	hsa-miR-19b
mmu-miR-130a_st	CAGUGCAAUGUUAAAAGGGCAU	mmu-mir-130a	-0.6889635	4.008016	hsa-miR-130a
age-miR-27a_st	UUCACAGUGGCUAAGUUCCGCC	age-mir-27a	-0.6842055	4.008016	hsa-miR-27a
ptr-miR-30a-5p_st	UGUAAACAUCCUCGACUGGAAG	ptr-mir-30a	-0.681256	1.333576	hsa-miR-30a
lca-miR-19b_st	UGUGCAAAUCCAUGCAAAACUGA	lca-mir-19b	-0.678873	4.967704	hsa-miR-19b
bta-miR-30e-5p_st	UGUAAACAUCCUUGACUGGAAGCU	bta-mir-30e	-0.6783315	1.333576	hsa-miR-30e
gga-miR-18b_st	UAAGGUGCAUCUAGUGCAGUUA	gga-mir-18b	-0.675714	1.333576	hsa-miR-18b
hsa-miR-199a-5p_st	CCCAGUGUUCAGACUACCUGUUC	hsa-mir-199a-1 // hsa-mir-199a-2	-0.6704065	1.333576	hsa-miR-199a-5p
xtr-miR-18b_st	UAAGGUGCAUCUAGUGCAGUUAG	xtr-mir-18b	-0.666521	3.39568	hsa-miR-18b
lca-miR-15a_st	UAGCAGCACAUAAUGGUUUGUG	lca-mir-15a	-0.6646535	4.008016	hsa-miR-15a
tni-miR-130_st	CAGUGCAAUAUUAAAAGGGCAU	tni-mir-130	-0.66371	1.993117	hsa-miR-130a

Table C.5 (continued)

Probeset Name	Sequence	Alignments	siRNA-siNC	q-value(%)	homolog
lca-miR-16_st	UAGCAGCACGUAAAUAUUGGUG	lca-mir-16	-0.6631095	2.683416	hsa-miR-16
mmu-miR-210_st	CUGUGCGUGUGACAGCGGCUGA	mmu-mir-210	-0.662001	4.008016	hsa-miR-210
rno-miR-130a_st	CAGUGCAAUGUUAAAAGGGCAU	rno-mir-130a	-0.659378	2.541717	hsa-miR-130a
cfa-miR-22_st	AAGCUGCCAGUUGAAGAACUGU	cfa-mir-22	-0.6587605	1.078628	hsa-miR-22
bta-miR-181c_st	AACAUUCAACCUGUCGGUGAGUUU	bta-mir-181c	-0.6566785	2.541717	hsa-miR-181c
hsa-miR-22_st	AAGCUGCCAGUUGAAGAACUGU	hsa-mir-22	-0.654478	1.078628	hsa-miR-22
mml-miR-503_st	UAGCAGCGGGAACAGUUCUGCAG	mml-mir-503	-0.652644	4.008016	hsa-miR-503
sla-miR-22_st	AAGCUGCCAGUUGAAGAACUGU	sla-mir-22	-0.647989	1.078628	hsa-miR-22
cfa-miR-146a_st	UGAGAACUGAAUUCCAUGGGUU	cfa-mir-146a	-0.6462865	3.39568	hsa-miR-146a
bta-miR-140_st	UACCACAGGGUAGAACCACGGA	bta-mir-140	-0.6432505	4.697825	hsa-miR-140-3p
dre-miR-15b_st	UAGCAGCACAUCAUGGUUUGUA	dre-mir-15b	-0.642895	4.967704	hsa-miR-15a
hsa-miR-181c_st	AACAUUCAACCUGUCGGUGAGU	hsa-mir-181c	-0.6425805	4.008016	hsa-miR-181c
dre-miR-130a_st	CAGUGCAAUGUUAAAAGGGCAU	dre-mir-130a-1	-0.6424425	3.39568	hsa-miR-130a
mne-miR-199a_st	CCCAGUGUUCAGACUACCUGUUC	mne-mir-199a	-0.6414315	4.008016	hsa-miR-199a-5p
mml-miR-199a-5p_st	CCCAGUGUUCAGACUACCUGUUC	mml-mir-199a-2 // mml-mir-199a-1	-0.638774	2.683416	hsa-miR-199a-5p
ptr-miR-15a_st	UAGCAGCACAUAAUGGUUUGUG	ptr-mir-15a	-0.6383225	1.078628	hsa-miR-15a
ppa-miR-27a_st	UUCACAGUGGCUAAGUUCCGCC	ppa-mir-27a	-0.635425	4.400802	hsa-miR-27a
ppa-miR-130a_st	CAGUGCAAUGUUAAAAGGGC	ppa-mir-130a	-0.6326855	1.333576	hsa-miR-130a

Table C.5 (continued)

Probeset Name	Sequence	Alignments	siRNA-siNC	q-value(%)	homolog
mmu-miR-193_st	AACUGGCCUACAAAGUCCCAGU	mmu-mir-193	-0.628851	2.683416	hsa-miR-193a-3p
hsa-miR-502-3p_st	AAUGCACCUGGGCAAGGAUUCA	hsa-mir-502	-0.626362	2.683416	hsa-miR-502-3p
dre-miR-19b_st	UGUGCAAAUCCAUGCAAAACUGA	dre-mir-19b	-0.6245595	4.967704	hsa-miR-19b
age-miR-22_st	AAGCUGCCAGUUGAAGAACUGU	age-mir-22	-0.623613	1.333576	hsa-miR-22
dme-miR-210_st	UUGUGCGUGUGACAGCGGCUA	dme-mir-210	-0.6235365	4.400802	hsa-miR-210
mmu-miR-455_st	GCAGUCCACGGGCAUAUACAC	mmu-mir-455	-0.622226	1.993117	hsa-miR-455-3p
mml-miR-378_st	ACUGGACUUGGAGUCAGAAGG	mml-mir-378	-0.618172	4.967704	hsa-miR-378
dre-miR-29b_st	UAGCACCAUUUGAAAUCAGUGU	dre-mir-29b-2 // dre-mir-29b-3 // dre-mir-29b-1	-0.6175	4.008016	hsa-miR-29b
xtr-miR-130a_st	CAGUGCAAUGUUAAAAGGGCAU	xtr-mir-130a	-0.610537	2.541717	hsa-miR-130a
rno-miR-22_st	AAGCUGCCAGUUGAAGAACUGU	rno-mir-22	-0.6097645	1.333576	hsa-miR-22
mml-miR-455-5p_st	UAUGUGCCUUUGGACUACAUCG	mml-mir-455	-0.6059485	4.008016	hsa-miR-455-5p
cfa-miR-455_st	UAUGUGCCUUUGGACUACAUCG	cfa-mir-455	-0.605465	4.008016	hsa-miR-455-5p
cfa-miR-138b_st	AGCUGGUGUUGUGAAUCAUGCCGA	cfa-mir-138b	-0.6020385	1.833667	hsa-miR-138
fru-miR-29b_st	UAGCACCAUUUGAAAUCAGUGU	fru-mir-29b-2 // fru-mir-29b-1	-0.6009375	3.778466	hsa-miR-29b
ppa-miR-15a_st	UAGCAGCACAUAAUGGUUUGUG	ppa-mir-15a	-0.600246	2.683416	hsa-miR-15a
mne-miR-22_st	AAGCUGCCAGUUGAAGAACUGU	mne-mir-22	-0.598656	1.833667	hsa-miR-22
ptr-miR-22_st	AAGCUGCCAGUUGAAGAACUGU	ptr-mir-22	-0.5961745	3.39568	hsa-miR-22
ppa-miR-18_st	UAAGGUGCAUCUAGUGCAGAUA	ppa-mir-18	-0.590599	3.39568	hsa-miR-18a

Table C.5 (continued)

Probeset Name	Sequence	Alignments	siRNA-siNC	q-value(%)	homolog
hsa-miR-345_st	GCUGACUCCUAGUCCAGGGCUC	hsa-mir-345	-0.590467	2.683416	hsa-miR-345
lca-miR-22_st	AAGCUGCCAGUUGAAGAACUGU	lca-mir-22	-0.588223	1.447632	hsa-miR-22
ggo-miR-130a_st	CAGUGCAAUGUUAAAAGGGC	ggo-mir-130a	-0.5876705	3.39568	hsa-miR-130a
fru-miR-22b_st	AAGCUGCCAGUUGAAGAGCUGU	fru-mir-22b	-0.583878	4.400802	hsa-miR-22
mmu-miR-503_st	UAGCAGCGGGAACAGUACUGCAG	mmu-mir-503	-0.580712	4.008016	hsa-miR-503
mdo-miR-22_st	AAGCUGCCAGUUGAAGAACUGC	mdo-mir-22	-0.5759915	1.333576	hsa-miR-22
hsa-miR-15a_st	UAGCAGCACAUAAUGGUUUGUG	hsa-mir-15a	-0.5755365	4.967704	hsa-miR-15a
mmu-miR-22_st	AAGCUGCCAGUUGAAGAACUGU	mmu-mir-22	-0.574175	2.541717	hsa-miR-22
ppa-miR-22_st	AAGCUGCCAGUUGAAGAACUGU	ppa-mir-22	-0.573726	2.683416	hsa-miR-22
rno-miR-324-5p_st	CGCAUCCCCUAGGGCAUUGGUGU	rno-mir-324	-0.5734	2.541717	hsa-miR-324-5p
fru-miR-16_st	UAGCAGCACGUAAAUAUUGGAG	fru-mir-16	-0.5730095	4.697825	hsa-miR-16
mne-miR-130a_st	CAGUGCAAUGUUAAAAGGGC	mne-mir-130a	-0.5725325	3.39568	hsa-miR-130a
tni-miR-29b_st	UAGCACCAUUUGAAAUCAGUGU	tni-mir-29b-2 // tni-mir-29b-1	-0.5686735	2.541717	hsa-miR-29b
hsa-miR-210_st	CUGUGCGUGUGACAGCGGCUGA	hsa-mir-210	-0.565969	4.400802	hsa-mIR-210
hsa-miR-769-5p_st	UGAGACCUCUGGGUUCUGAGCU	hsa-mir-769	-0.5623355	3.39568	hsa-miR-769-5p
ptr-miR-18_st	UAAGGUGCAUCUAGUGCAGAUA	ptr-mir-18	-0.5594525	4.967704	hsa-miR-18a
mmu-miR-17-star_st	ACUGCAGUGAGGGCACUUGUAG	mmu-mir-17	-0.5586755	3.39568	hsa-miR-17*
mmu-miR-146a_st	UGAGAACUGAAUUCCAUGGGUU	mmu-mir-146a	-0.5573275	4.400802	hsa-miR-146a

Table C.5 (continued)

Probeset Name	Sequence	Alignments	siRNA-siNC	q-value(%)	homolog
mml-miR-339-5p_st	UCCCUGUCCUCCAGGAGCUCACG	mml-mir-339	-0.5571575	4.008016	hsa-miR-339-5p
mml-miR-301a_st	CAGUGCAAUAGUAUUGUCAAAGC	mml-mir-301a	-0.556257	4.008016	hsa-miR-301a
ptr-miR-199a_st	CCCAGUGUUCAGACUACCUGUUC	ptr-mir-199a	-0.5548855	4.008016	hsa-miR-199a-5p
mml-miR-22_st	AAGCUGCCAGUUGAAGAACUGU	mml-mir-22	-0.5546045	2.541717	hsa-miR-22
ggo-miR-181a-star_st	ACCAUCGACCGUUGAUUGUACC	ggo-mir-181a	-0.548833	2.683416	hsa-miR-181a*
ppy-miR-22_st	AAGCUGCCAGUUGAAGAACUGU	ppy-mir-22	-0.548169	1.833667	hsa-miR-22
hsa-miR-18a-star_st	ACUGCCCUAAGUGCUCCUUCUGG	hsa-mir-18a	-0.5450985	4.400802	hsa-miR-18a*
mml-miR-422a_st	ACUGGACUCAGGGUCAGAAGGC	mml-mir-422a	-0.5424935	2.541717	hsa-miR-422a
rno-miR-196b_st	UAGGUAGUUUCCUGUUGUUGGG	rno-mir-196b	-0.539302	1.333576	hsa-miR-196b
xtr-miR-22_st	AAGCUGCCAGUUGAAGAACUGU	xtr-mir-22	-0.539023	1.833667	hsa-miR-22
dre-miR-193a_st	AACUGGCCUACAAAGUCCCAGU	dre-mir-193a-1 // dre-mir-193a-2	-0.5370605	4.400802	hsa-miR-193a-3p
age-miR-18_st	UAAGGUGCAUCUAGUGCAGAUA	age-mir-18	-0.5328385	4.400802	hsa-miR-18a
gga-miR-18a_st	UAAGGUGCAUCUAGUGCAGAUA	gga-mir-18a	-0.532633	4.967704	hsa-miR-18a
lca-miR-18_st	UAAGGUGCAUCUAGUGCAGAUA	lca-mir-18	-0.5324345	4.008016	hsa-miR-18a
ppy-miR-18_st	UAAGGUGCAUCUAGUGCAGAUA	ppy-mir-18	-0.53219	3.39568	hsa-miR-18a
bta-miR-455-star_st	GCAGUCCAUGGGCAUAUACACU	bta-mir-455	-0.527941	4.008016	hsa-miR-455-3p
hsa-miR-99b-star_st	CAAGCUCGUGUCUGUGGGUCCG	hsa-mir-99b	-0.5267655	4.008016	hsa-miR-99b*
mmu-miR-324-3p_st	CCACUGCCCCAGGUGCUGCU	mmu-mir-324	-0.5220695	2.541717	hsa-miR-324-3p
xtr-miR-99_st	AACCCGUAGAUCCGAUCUUGUG	xtr-mir-99	-0.5195125	4.008016	hsa-miR-99a

Table C.5 (continued)

Probeset Name	Sequence	Alignments	siRNA-siNC	q-value(%)	homolog
bta-miR-193a_st	AACUGGCCUACAAAGUCCCAGU	bta-mir-193a	-0.517692	4.008016	hsa-miR-193a-3p
ppa-miR-99a_st	AACCCGUAGAUCCGAUCUUGUG	ppa-mir-99a	-0.5130605	2.683416	hsa-miR-99a
fru-miR-199_st	CCCAGUGUUCAGACUACCUGUUC	fru-mir-199-3 // fru-mir-199-1 // fru-mir-199-2	-0.5101145	4.967704	hsa-miR-199a-5p
lla-miR-22_st	AAGCUGCCAGUUGAAGAACUGU	lla-mir-22	-0.503347	1.333576	hsa-miR-22
mml-miR-145_st	GUCCAGUUUUCCCAGGAAUCCCUU	mml-mir-145	0.6767645	4.697825	hsa-miR-145
bta-miR-145_st	GUCCAGUUUUCCCAGGAAUCCCU	bta-mir-145	0.750314	2.481655	hsa-miR-145
cre-miR1144b_st	UGGGUAGUGUGGCGGCAGGCAG	cre-mir1144b	0.8070805	3.778466	N/A
hsa-miR-663_st	AGGCGGGGCGCCGCGGGACCGC	hsa-mir-663	0.915513	2.481655	hsa-miR-663
hsa-miR-149-star_st	AGGGAGGGACGGGGGCUGUGC	hsa-mir-149	0.9199155	1.078628	hsa-miR-149*
mml-miR-663_st	AGGCGGGGCGCUGCGGGACCGC	mml-mir-663 // mml-mir-663 // mml-mir-663 // mml-mir-663 // mml-mir-663 // mml-mir-663 // mml-mir-663 // mml-mir-663 // mml-mir-663	1.0466335	1.078628	hsa-miR-663
hsa-miR-1228-star_st	GUGGGCGGGGGCAGGUGUGUG	hsa-mir-1228	1.1134535	0	hsa-miR-1228*
ppt-miR903_st	GCUACUUCGGCGGGACAAGAGC	ppt-mir903	1.1308365	1.078628	hsa-miR-492 (poor homology)

Table C.5 (continued)

Probeset Name	Sequence	Alignments	siRNA-siNC	q-value(%)	homolog
rrv-miR-rR1-4_st	UGGGGAGGGCGGUCAGCGCGCG	rrv-mir-rr1-4	1.205251	0	hsa-miR-1234(poor homology)
cre-miR1150.3_st	UGCAGCGGCGACUGGGGCCGA	cre-MIR1150	1.227743	4.400802	hsa-miR-3130-3p/5p(poor homology); partial alignment with hypothetical protein LOC23247 on Chr16
mml-miR-638_st	AGGGAUCGCGGGCGGGCGGCGGCCU	mml-mir-638	1.242675	0	hsa-miR-638
hsa-miR-638_st	AGGGAUCGCGGGCGGGUGGCGGCCU	hsa-mir-638	1.298727	0	hsa-miR-638
hsa-miR-601_st	UGGUCUAGGAUUGUUGGAGGAG	hsa-mir-601	1.323491	1.993117	hsa-miR-601
osa-miR815b_st	AAGGGGAUUGAGGAGAUUGGG	osa-MIR815b	3.2401015	0	N/A
osa-miR815c_st	AAGGGGAUUGAGGAGAUUGGG	osa-MIR815c	3.2408825	0	N/A
osa-miR815a_st	AAGGGGAUUGAGGAGAUUGGG	osa-MIR815a	3.3593625	0	N/A

Table C.6. List of SFRS1 binding sites within the pri-miRNAs of differentially expressed embedded miRNAs. Pri-miRNAs of embedded miRNAs were searched for SFRS1 (SF2/ASF) binding sites previously identified by (Sanford et al., 2009) using genome-wide CLIP-seq technique. The pri-miRNA coordinates were assumed to be identical to the host transcriptional unit. Gene symbols of the host genes corresponding to

the pri-miRNAs are listed. The genomic coordinates of these pri-miRNAs are given along with coordinates of overlapping SFRS1 binding sites.

miRNA	Gene Symbol	Genomic coordinates of pri-miRNA	Strand	SFRS1 site identified by CLIP-seq
hsa-let-7a-3	RP4-695020__B.10	chr22:44860547-44888472	+	chr22:44875008-44875087;chr22:44879884-44879941
hsa-let-7f-2/hsa-miR-98	HUWE1	chrX:53575788-53730398	-	chrX:53580294-53580344;chrX:53583383-53583422;chrX:53583443-53583478;chrX:53586181-53586216;chrX:53595110-53595161;chrX:53598419-53598459;chrX:53602358-53602389;chrX:53602414-53602467;chrX:53605568-53605612;chrX:53605796-53605811;chrX:53608372-53608408;chrX:53608752-53608761;chrX:53627543-53627585;chrX:53627969-53628027;chrX:53633434-53633503;chrX:53634088-53634121;chrX:53636108-53636192;chrX:53637163-53637199;chrX:53659470-53659521;chrX:53660655-53660682;chrX:53727606-53727651
hsa-let-7g	HOXB3	chr17:43981231-44006809	-	chr17:43984088-43984122
hsa-miR-10b	HOXD3	chr2:176709931-176742629	+	chr2:176723253-176723287
hsa-miR-140-5p	WWP2	chr16:68353775-68533144	+	chr16:68500817-68500851;chr16:68529036-68529056;chr16:68530430-68530448
hsa-miR-15b	SMC4	chr3:161600124-161635435	+	chr3:161602540-161602570;chr3:161612818-161612864;chr3:161613992-161614066;chr3:161616798-161616849;chr3:161618222-161618269

Table C.6 (continued)

miRNA	Gene Symbol	Genomic coordinates of pri-miRNA	Strand	SFRS1 site identified by CLIP-seq
hsa-miR-198	FSTL1	chr3:121595751-121652608	-	chr3:121617501-121617549;chr3:121652441-121652487
hsa-miR-218-1	SLIT2	chr4:19864333-20229886	+	chr4:19864304-19864362;chr4:19868610-19868661;chr4:19868745-19868787;chr4:19879557-19879587;chr4:19887556-19887595;chr4:19914547-19914605;chr4:19933498-19933548;chr4:20054964-20054999;chr4:20078495-20078533;chr4:20140867-20140901;chr4:20226410-20226471;chr4:20227632-20227663;chr4:20227853-20227895;chr4:20228208-20228262;chr4:20229664-20229706
hsa-miR-301b	PPIL2	chr22:20350273-20382202	+	chr22:20378468-20378502
hsa-miR-30a*	C6orf155	chr6:72180870-72187169	-	chr6:72182831-72182869
hsa-miR-30e*	NFYC	chr1:40929829-41009862	+	chr1:40930072-40930122;chr1:40995467-40995529
hsa-miR-33a	SREBF2	chr22:40559052-40632321	+	chr22:40559888-40559934;chr22:40599844-40599878;chr22:40604028-40604070;chr22:40620852-40620883
hsa-miR-425*	DALRD3	chr3:49027439-49033471	-	chr3:49030956-49030992
hsa-miR-550a-2	AVL9	chr7:32501701-32590304	+	chr7:32549292-32549325
hsa-miR-590-5p	EIF4H	chr7:73226642-73249365	+	chr7:73226688-73226708;chr7:73239876-73239928;chr7:73242117-73242184;chr7:73242512-73242520;chr7:73242535-73242565;chr7:73247089-73247119;chr7:73247525-73247572

Table C.6 (continued)

miRNA	Gene Symbol	Genomic coordinates of pri-miRNA	Strand	SFRS1 site identified by CLIP-seq
hsa-miR-7-1*	HNRNPK	chr9:85772818-85785389	-	chr9:85773982-85774020;chr9:85776820-85776863;chr9:85781756-85781788;chr9:85782432-85782465;chr9:85782475-85782530;chr9:85782929-85782948;chr9:85783170-85783187;chr9:85785237-85785265
hsa-miR-877	ABCF1	chr6:30647149-30667288	+	chr6:30653590-30653646;chr6:30653864-30653906;chr6:30654259-30654310;chr6:30660004-30660043;chr6:30661694-30661735;chr6:30661934-30661991
hsa-miR-93*	MCM7	chr7:99528340-99537363	-	chr7:99533199-99533229;chr7:99533292-99533304;chr7:99534222-99534256;chr7:99534881-99534918;chr7:99534934-99534962;chr7:99535147-99535159;chr7:99535213-99535278
hsa-miR-17/hsa-miR-92a-1/hsa-miR-92a-1*	MIR17HG	chr13:90798075-90804830	+	chr13:90800566-90800608;chr13:90804210-90804241
hsa-miR-551b	C3orf50	chr3:169450004-170031068	+	chr3:169607916-169607970

Table C.7. List of SFRS1 binding sites within the pri-miRNAs of differentially expressed intergenic miRNAs. Pri-miRNAs of intergenic miRNAs were searched for SFRS1 (SF2/ASF) binding sites previously identified by (Sanford et al., 2009) using genome-wide CLIP-seq technique. The pri-miRNA coordinates were assumed to be within ±2 kb of each pre-miRNA. The genomic coordinates ('miR Start/End') of these pre-miRNAs are given along with the coordinates of SFRS1 binding sites within ±2kb.

miRNA	Chr	Strand	miR Start	miR End	SFRS1 Start	SFRS1 End
hsa-miR-210	chr11	-	558089	558198	557533	557577
hsa-let-7i*	chr12	+	61283733	61283816	61282744	61282800

Table C.8. Differentially expressed transcription factors between miR-7 and negative control transfected HEY cells. Significantly differentially expressed (fold change ≥1.3, $p < 0.05$) mRNA probeset IDs with the GO biological process "regulation of transcription" between HEY cells transfected with either miR-7 or miR-NC. For each probeset ID the gene symbol, the GO biological process annotation, difference between $\log_2$ signal values (miR7-miR-NC), the t-test p-value, and whether it is a miR-7 target based on miRanda is shown. Probesets with Affymetrix "Absent" calls in all samples were removed from analysis.

Please see table on our website:
http://www.mcdonaldlab.biology.gatech.edu/shubin_shahab.htm

REFERENCES

Aguda, B.D., Kim, Y., Piper-Hunter, M.G., Friedman, A., and Marsh, C.B. (2008). MicroRNA regulation of a cancer network: consequences of the feedback loops involving miR-17-92, E2F, and Myc. Proc Natl Acad Sci U S A *105*, 19678-19683.

Auersperg, N. (2011). The origin of ovarian carcinomas: a unifying hypothesis. Int J Gynecol Pathol *30*, 12-21.

Auersperg, N., Wong, A.S., Choi, K.C., Kang, S.K., and Leung, P.C. (2001). Ovarian surface epithelium: biology, endocrinology, and pathology. Endocr Rev *22*, 255-288.

Baek, D., Villen, J., Shin, C., Camargo, F.D., Gygi, S.P., and Bartel, D.P. (2008). The impact of microRNAs on protein output. Nature *455*, 64-71.

Bail, S., Swerdel, M., Liu, H., Jiao, X., Goff, L.A., Hart, R.P., and Kiledjian, M. (2010). Differential regulation of microRNA stability. RNA *16*, 1032-1039.

Bargaje, R., Hariharan, M., Scaria, V., and Pillai, B. (2010). Consensus miRNA expression profiles derived from interplatform normalization of microarray data. RNA *16*, 16-25.

Barh, D., Malhotra, R., Ravi, B., and Sindhurani, P. (2010). Microrna let-7: an emerging next-generation cancer therapeutic. Curr Oncol *17*, 70-80.

Bartel, D.P. (2004). MicroRNAs: genomics, biogenesis, mechanism, and function. Cell *116*, 281-297.

Bartel, D.P. (2009). MicroRNAs: target recognition and regulatory functions. Cell *136*, 215-233.

Bartels, C.L., and Tsongalis, G.J. (2009). MicroRNAs: novel biomarkers for human cancer. Clin Chem *55*, 623-631.

Basak, C., Pathak, S.K., Bhattacharyya, A., Mandal, D., Pathak, S., and Kundu, M. (2005). NF-kappaB- and C/EBPbeta-driven interleukin-1beta gene expression and PAK1-mediated caspase-1 activation play essential roles in interleukin-1beta release from Helicobacter pylori lipopolysaccharide-stimulated macrophages. J Biol Chem *280*, 4279-4288.

Baskerville, S., and Bartel, D.P. (2005). Microarray profiling of microRNAs reveals frequent coexpression with neighboring miRNAs and host genes. RNA *11*, 241-247.

Bates, D.J., Liang, R., Li, N., and Wang, E. (2009). The impact of noncoding RNA on the biochemical and molecular mechanisms of aging. Biochim Biophys Acta *1790*, 970-979.

Behm-Ansmant, I., Rehwinkel, J., Doerks, T., Stark, A., Bork, P., and Izaurralde, E. (2006). mRNA degradation by miRNAs and GW182 requires both CCR4:NOT deadenylase and DCP1:DCP2 decapping complexes. Genes Dev *20*, 1885-1898.

Bentwich, I., Avniel, A., Karov, Y., Aharonov, R., Gilad, S., Barad, O., Barzilai, A., Einat, P., Einav, U., Meiri, E*., et al.* (2005). Identification of hundreds of conserved and nonconserved human microRNAs. Nat Genet *37*, 766-770.

Berezikov, E., Chung, W.J., Willis, J., Cuppen, E., and Lai, E.C. (2007). Mammalian mirtron genes. Mol Cell *28*, 328-336.

Berezikov, E., Guryev, V., van de Belt, J., Wienholds, E., Plasterk, R.H., and Cuppen, E. (2005). Phylogenetic shadowing and computational identification of human microRNA genes. Cell *120*, 21-24.

Bergmann, O., Zdunek, S., Alkass, K., Druid, H., Bernard, S., and Frisen, J. (2011). Identification of cardiomyocyte nuclei and assessment of ploidy for the analysis of cell turnover. Exp Cell Res *317*, 188-194.

Bernstein, E., Caudy, A.A., Hammond, S.M., and Hannon, G.J. (2001). Role for a bidentate ribonuclease in the initiation step of RNA interference. Nature *409*, 363-366.

Betel, D., Koppal, A., Agius, P., Sander, C., and Leslie, C. (2010). Comprehensive modeling of microRNA targets predicts functional non-conserved and non-canonical sites. Genome Biol *11*, R90.

Betel, D., Wilson, M., Gabow, A., Marks, D.S., and Sander, C. (2008). The microRNA.org resource: targets and expression. Nucleic Acids Res *36*, D149-153.

Bhattacharyya, S.N., Habermacher, R., Martine, U., Closs, E.I., and Filipowicz, W. (2006). Relief of microRNA-mediated translational repression in human cells subjected to stress. Cell *125*, 1111-1124.

Birney, E., Stamatoyannopoulos, J.A., Dutta, A., Guigo, R., Gingeras, T.R., Margulies, E.H., Weng, Z., Snyder, M., Dermitzakis, E.T., Thurman, R.E.*, et al.* (2007). Identification and analysis of functional elements in 1% of the human genome by the ENCODE pilot project. Nature *447*, 799-816.

Blackburn, W.H., Dickerson, E.B., Smith, M.H., McDonald, J.F., and Lyon, L.A. (2009). Peptide-functionalized nanogels for targeted siRNA delivery. Bioconjug Chem *20*, 960-968.

Blower, P.E., Verducci, J.S., Lin, S., Zhou, J., Chung, J.H., Dai, Z., Liu, C.G., Reinhold, W., Lorenzi, P.L., Kaldjian, E.P.*, et al.* (2007). MicroRNA expression profiles for the NCI-60 cancer cell panel. Mol Cancer Ther *6*, 1483-1491.

Borchert, G.M., Lanier, W., and Davidson, B.L. (2006). RNA polymerase III transcribes human microRNAs. Nat Struct Mol Biol *13*, 1097-1101.

Borgdorff, V., Lleonart, M.E., Bishop, C.L., Fessart, D., Bergin, A.H., Overhoff, M.G., and Beach, D.H. (2010). Multiple microRNAs rescue from Ras-induced senescence by inhibiting p21(Waf1/Cip1). Oncogene *29*, 2262-2271.

Bracht, J., Hunter, S., Eachus, R., Weeks, P., and Pasquinelli, A.E. (2004). Trans-splicing and polyadenylation of let-7 microRNA primary transcripts. RNA *10*, 1586-1594.

Brase, J.C., Johannes, M., Schlomm, T., Falth, M., Haese, A., Steuber, T., Beissbarth, T., Kuner, R., and Sultmann, H. (2011). Circulating miRNAs are correlated with tumor progression in prostate cancer. Int J Cancer *128*, 608-616.

Brennecke, J., Stark, A., Russell, R.B., and Cohen, S.M. (2005). Principles of microRNA-target recognition. PLoS Biol *3*, e85.

Brodersen, P., and Voinnet, O. (2009). Revisiting the principles of microRNA target recognition and mode of action. Nat Rev Mol Cell Biol *10*, 141-148.

Budhu, A., Ji, J., and Wang, X.W. (2010). The clinical potential of microRNAs. J Hematol Oncol *3*, 37.

Buick, R.N., Pullano, R., and Trent, J.M. (1985). Comparative properties of five human ovarian adenocarcinoma cell lines. Cancer Res *45*, 3668-3676.

Bushati, N., and Cohen, S.M. (2007). microRNA functions. Annu Rev Cell Dev Biol *23*, 175-205.
Cai, X., Hagedorn, C.H., and Cullen, B.R. (2004). Human microRNAs are processed from capped, polyadenylated transcripts that can also function as mRNAs. RNA *10*, 1957-1966.
Calin, G.A., and Croce, C.M. (2006a). MicroRNA signatures in human cancers. Nat Rev Cancer *6*, 857-866.
Calin, G.A., and Croce, C.M. (2006b). MicroRNAs and chromosomal abnormalities in cancer cells. Oncogene *25*, 6202-6210.
Calin, G.A., Dumitru, C.D., Shimizu, M., Bichi, R., Zupo, S., Noch, E., Aldler, H., Rattan, S., Keating, M., Rai, K.*, et al.* (2002). Frequent deletions and down-regulation of micro- RNA genes miR15 and miR16 at 13q14 in chronic lymphocytic leukemia. Proc Natl Acad Sci U S A *99*, 15524-15529.
Calin, G.A., Sevignani, C., Dumitru, C.D., Hyslop, T., Noch, E., Yendamuri, S., Shimizu, M., Rattan, S., Bullrich, F., Negrini, M.*, et al.* (2004). Human microRNA genes are frequently located at fragile sites and genomic regions involved in cancers. Proc Natl Acad Sci U S A *101*, 2999-3004.
Catto, J.W., Miah, S., Owen, H.C., Bryant, H., Myers, K., Dudziec, E., Larre, S., Milo, M., Rehman, I., Rosario, D.J.*, et al.* (2009). Distinct microRNA alterations characterize high- and low-grade bladder cancer. Cancer Res *69*, 8472-8481.
Chan, E., Prado, D.E., and Weidhaas, J.B. (2011). Cancer microRNAs: From subtype profiling to predictors of response to therapy. Trends Mol Med.
Chang, T.C., and Mendell, J.T. (2007). microRNAs in vertebrate physiology and human disease. Annu Rev Genomics Hum Genet *8*, 215-239.
Chang, T.C., Wentzel, E.A., Kent, O.A., Ramachandran, K., Mullendore, M., Lee, K.H., Feldmann, G., Yamakuchi, M., Ferlito, M., Lowenstein, C.J.*, et al.* (2007). Transactivation of miR-34a by p53 broadly influences gene expression and promotes apoptosis. Mol Cell *26*, 745-752.
Chang, T.C., Yu, D., Lee, Y.S., Wentzel, E.A., Arking, D.E., West, K.M., Dang, C.V., Thomas-Tikhonenko, A., and Mendell, J.T. (2008). Widespread microRNA repression by Myc contributes to tumorigenesis. Nat Genet *40*, 43-50.
Chen, C., Ridzon, D., Lee, C.T., Blake, J., Sun, Y., and Strauss, W.M. (2007). Defining embryonic stem cell identity using differentiation-related microRNAs and their potential targets. Mamm Genome *18*, 316-327.
Chen, C.Z. (2005). MicroRNAs as oncogenes and tumor suppressors. N Engl J Med *353*, 1768-1771.
Chen, H., Shalom-Feuerstein, R., Riley, J., Zhang, S.D., Tucci, P., Agostini, M., Aberdam, D., Knight, R.A., Genchi, G., Nicotera, P.*, et al.* (2010a). miR-7 and miR-214 are specifically expressed during neuroblastoma differentiation, cortical development and embryonic stem cells differentiation, and control neurite outgrowth in vitro. Biochem Biophys Res Commun *394*, 921-927.
Chen, J., Wang, L., Matyunina, L.V., Hill, C.G., and McDonald, J.F. (2011). Overexpression of miR-429 induces mesenchymal-to-epithelial transition (MET) in metastatic ovarian cancer cells. Gynecol Oncol *121*, 200-205.
Chen, K., and Rajewsky, N. (2006). Natural selection on human microRNA binding sites inferred from SNP data. Nat Genet *38*, 1452-1456.

Chen, Y., Zhu, X., Zhang, X., Liu, B., and Huang, L. (2010b). Nanoparticles modified with tumor-targeting scFv deliver siRNA and miRNA for cancer therapy. Mol Ther *18*, 1650-1656.
Chendrimada, T.P., Finn, K.J., Ji, X., Baillat, D., Gregory, R.I., Liebhaber, S.A., Pasquinelli, A.E., and Shiekhattar, R. (2007). MicroRNA silencing through RISC recruitment of eIF6. Nature *447*, 823-828.
Choi, W.Y., Giraldez, A.J., and Schier, A.F. (2007). Target protectors reveal dampening and balancing of Nodal agonist and antagonist by miR-430. Science *318*, 271-274.
Chou, Y.T., Lin, H.H., Lien, Y.C., Wang, Y.H., Hong, C.F., Kao, Y.R., Lin, S.C., Chang, Y.C., Lin, S.Y., Chen, S.J.*, et al.* (2010). EGFR promotes lung tumorigenesis by activating miR-7 through a Ras/ERK/Myc pathway that targets the Ets2 transcriptional repressor ERF. Cancer Res *70*, 8822-8831.
Ciafre, S.A., Galardi, S., Mangiola, A., Ferracin, M., Liu, C.G., Sabatino, G., Negrini, M., Maira, G., Croce, C.M., and Farace, M.G. (2005). Extensive modulation of a set of microRNAs in primary glioblastoma. Biochem Biophys Res Commun *334*, 1351-1358.
Ciardiello, F., and Tortora, G. (2008). EGFR antagonists in cancer treatment. N Engl J Med *358*, 1160-1174.
Colazzo, F., Sarathchandra, P., Smolenski, R.T., Chester, A.H., Tseng, Y.T., Czernuszka, J.T., Yacoub, M.H., and Taylor, P.M. (2011). Extracellular matrix production by adipose-derived stem cells: implications for heart valve tissue engineering. Biomaterials *32*, 119-127.
Couzin, J. (2008). MicroRNAs make big impression in disease after disease. Science *319*, 1782-1784.
Cullen, B.R. (2004). Transcription and processing of human microRNA precursors. Mol Cell *16*, 861-865.
da Costa, L.F. (2001). Return of de-differentiation: why cancer is a developmental disease. Curr Opin Oncol *13*, 58-62.
Dahiya, N., Sherman-Baust, C.A., Wang, T.L., Davidson, B., Shih Ie, M., Zhang, Y., Wood, W., 3rd, Becker, K.G., and Morin, P.J. (2008). MicroRNA expression and identification of putative miRNA targets in ovarian cancer. PLoS ONE *3*, e2436.
Davis-Dusenbery, B.N., and Hata, A. (2010). Mechanisms of control of microRNA biogenesis. J Biochem *148*, 381-392.
Davis, B.N., Hilyard, A.C., Lagna, G., and Hata, A. (2008). SMAD proteins control DROSHA-mediated microRNA maturation. Nature *454*, 56-61.
Denli, A.M., Tops, B.B., Plasterk, R.H., Ketting, R.F., and Hannon, G.J. (2004). Processing of primary microRNAs by the Microprocessor complex. Nature *432*, 231-235.
Diaz-Cano, S.J. (2008). General morphological and biological features of neoplasms: integration of molecular findings. Histopathology *53*, 1-19.
Dickerson, E.B., Blackburn, W.H., Smith, M.H., Kapa, L.B., Lyon, L.A., and McDonald, J.F. (2010). Chemosensitization of cancer cells by siRNA using targeted nanogel delivery. BMC Cancer *10*, 10.
Didiano, D., and Hobert, O. (2008). Molecular architecture of a miRNA-regulated 3' UTR. RNA *14*, 1297-1317.

Djuranovic, S., Nahvi, A., and Green, R. (2011). A parsimonious model for gene regulation by miRNAs. Science *331*, 550-553.
Doench, J.G., and Sharp, P.A. (2004). Specificity of microRNA target selection in translational repression. Genes Dev *18*, 504-511.
Doolittle, W.F., and Sapienza, C. (1980). Selfish genes, the phenotype paradigm and genome evolution. Nature *284*, 601-603.
Duursma, A.M., Kedde, M., Schrier, M., le Sage, C., and Agami, R. (2008). miR-148 targets human DNMT3b protein coding region. RNA *14*, 872-877.
Ebert, M.S., Neilson, J.R., and Sharp, P.A. (2007). MicroRNA sponges: competitive inhibitors of small RNAs in mammalian cells. Nat Methods *4*, 721-726.
Eddy, S.R. (2001). Non-coding RNA genes and the modern RNA world. Nat Rev Genet *2*, 919-929.
Eitan, R., Kushnir, M., Lithwick-Yanai, G., David, M.B., Hoshen, M., Glezerman, M., Hod, M., Sabah, G., Rosenwald, S., and Levavi, H. (2009). Tumor microRNA expression patterns associated with resistance to platinum based chemotherapy and survival in ovarian cancer patients. Gynecol Oncol *114*, 253-259.
Elcheva, I., Goswami, S., Noubissi, F.K., and Spiegelman, V.S. (2009). CRD-BP protects the coding region of betaTrCP1 mRNA from miR-183-mediated degradation. Mol Cell *35*, 240-246.
Enright, A.J., John, B., Gaul, U., Tuschl, T., Sander, C., and Marks, D.S. (2003). MicroRNA targets in Drosophila. Genome Biol *5*, R1.
Esau, C.C., and Monia, B.P. (2007). Therapeutic potential for microRNAs. Adv Drug Deliv Rev *59*, 101-114.
Esquela-Kerscher, A., and Slack, F.J. (2006). Oncomirs - microRNAs with a role in cancer. Nat Rev Cancer *6*, 259-269.
Eulalio, A., Huntzinger, E., and Izaurralde, E. (2008). Getting to the root of miRNA-mediated gene silencing. Cell *132*, 9-14.
Evangelisti, C., Florian, M.C., Massimi, I., Dominici, C., Giannini, G., Galardi, S., Bue, M.C., Massalini, S., McDowell, H.P., Messi, E.*, et al.* (2009). MiR-128 up-regulation inhibits Reelin and DCX expression and reduces neuroblastoma cell motility and invasiveness. FASEB J *23*, 4276-4287.
Fabian, M.R., Mathonnet, G., Sundermeier, T., Mathys, H., Zipprich, J.T., Svitkin, Y.V., Rivas, F., Jinek, M., Wohlschlegel, J., Doudna, J.A.*, et al.* (2009). Mammalian miRNA RISC recruits CAF1 and PABP to affect PABP-dependent deadenylation. Mol Cell *35*, 868-880.
Fabian, M.R., Sonenberg, N., and Filipowicz, W. (2010). Regulation of mRNA translation and stability by microRNAs. Annu Rev Biochem *79*, 351-379.
Farazi, T.A., Spitzer, J.I., Morozov, P., and Tuschl, T. (2011). miRNAs in human cancer. J Pathol *223*, 102-115.
Feng, Z., Zhang, C., Wu, R., and Hu, W. (2011). Tumor suppressor p53 meets microRNAs. J Mol Cell Biol *3*, 44-50.
Fillman, C., and Lykke-Andersen, J. (2005). RNA decapping inside and outside of processing bodies. Curr Opin Cell Biol *17*, 326-331.
Foekens, J.A., Sieuwerts, A.M., Smid, M., Look, M.P., de Weerd, V., Boersma, A.W., Klijn, J.G., Wiemer, E.A., and Martens, J.W. (2008). Four miRNAs associated

with aggressiveness of lymph node-negative, estrogen receptor-positive human breast cancer. Proc Natl Acad Sci U S A *105*, 13021-13026.
Forman, J.J., Legesse-Miller, A., and Coller, H.A. (2008). A search for conserved sequences in coding regions reveals that the let-7 microRNA targets Dicer within its coding sequence. Proc Natl Acad Sci U S A *105*, 14879-14884.
Friedman, J.M., and Jones, P.A. (2009). MicroRNAs: critical mediators of differentiation, development and disease. Swiss Med Wkly *139*, 466-472.
Friedman, R.C., Farh, K.K., Burge, C.B., and Bartel, D.P. (2009). Most mammalian mRNAs are conserved targets of microRNAs. Genome Res *19*, 92-105.
Fujita, S., and Iba, H. (2008). Putative promoter regions of miRNA genes involved in evolutionarily conserved regulatory systems among vertebrates. Bioinformatics *24*, 303-308.
Fukuda, T., Yamagata, K., Fujiyama, S., Matsumoto, T., Koshida, I., Yoshimura, K., Mihara, M., Naitou, M., Endoh, H., Nakamura, T.*, et al.* (2007). DEAD-box RNA helicase subunits of the Drosha complex are required for processing of rRNA and a subset of microRNAs. Nat Cell Biol *9*, 604-611.
Furuta, M., Kozaki, K.I., Tanaka, S., Arii, S., Imoto, I., and Inazawa, J. (2010). miR-124 and miR-203 are epigenetically silenced tumor-suppressive microRNAs in hepatocellular carcinoma. Carcinogenesis *31*, 766-776.
Gallagher, M.F., Flavin, R.J., Elbaruni, S.A., McInerney, J.K., Smyth, P.C., Salley, Y.M., Vencken, S.F., O'Toole, S.A., Laios, A., Lee, M.Y.*, et al.* (2009). Regulation of microRNA biosynthesis and expression in 2102Ep embryonal carcinoma stem cells is mirrored in ovarian serous adenocarcinoma patients. J Ovarian Res *2*, 19.
Gao, C., Zhang, Z., Liu, W., Xiao, S., Gu, W., and Lu, H. (2010). Reduced microRNA-218 expression is associated with high nuclear factor kappa B activation in gastric cancer. Cancer *116*, 41-49.
Garofalo, M., and Croce, C.M. (2011). microRNAs: Master regulators as potential therapeutics in cancer. Annu Rev Pharmacol Toxicol *51*, 25-43.
Ge, H., and Manley, J.L. (1990). A protein factor, ASF, controls cell-specific alternative splicing of SV40 early pre-mRNA in vitro. Cell *62*, 25-34.
Godlewski, J., Nowicki, M.O., Bronisz, A., Williams, S., Otsuki, A., Nuovo, G., Raychaudhury, A., Newton, H.B., Chiocca, E.A., and Lawler, S. (2008). Targeting of the Bmi-1 oncogene/stem cell renewal factor by microRNA-128 inhibits glioma proliferation and self-renewal. Cancer Res *68*, 9125-9130.
Goh, A.M., Coffill, C.R., and Lane, D.P. (2011). The role of mutant p53 in human cancer. J Pathol *223*, 116-126.
Goto, M., Katayama, K.I., Shirakawa, F., and Tanaka, I. (1999). Involvement of NF-kappaB p50/p65 heterodimer in activation of the human pro-interleukin-1beta gene at two subregions of the upstream enhancer element. Cytokine *11*, 16-28.
Gregory, P.A., Bert, A.G., Paterson, E.L., Barry, S.C., Tsykin, A., Farshid, G., Vadas, M.A., Khew-Goodall, Y., and Goodall, G.J. (2008). The miR-200 family and miR-205 regulate epithelial to mesenchymal transition by targeting ZEB1 and SIP1. Nat Cell Biol *10*, 593-601.
Gregory, R.I., Yan, K.P., Amuthan, G., Chendrimada, T., Doratotaj, B., Cooch, N., and Shiekhattar, R. (2004). The Microprocessor complex mediates the genesis of microRNAs. Nature *432*, 235-240.

Griffiths-Jones, S. (2004). The microRNA Registry. Nucleic Acids Res *32*, D109-111.
Griffiths-Jones, S., Grocock, R.J., van Dongen, S., Bateman, A., and Enright, A.J. (2006). miRBase: microRNA sequences, targets and gene nomenclature. Nucleic Acids Res *34*, D140-144.
Griffiths-Jones, S., Saini, H.K., van Dongen, S., and Enright, A.J. (2008). miRBase: tools for microRNA genomics. Nucleic Acids Res *36*, D154-158.
Grimson, A., Farh, K.K., Johnston, W.K., Garrett-Engele, P., Lim, L.P., and Bartel, D.P. (2007). MicroRNA targeting specificity in mammals: determinants beyond seed pairing. Mol Cell *27*, 91-105.
Gruber, J.J., Zatechka, D.S., Sabin, L.R., Yong, J., Lum, J.J., Kong, M., Zong, W.X., Zhang, Z., Lau, C.K., Rawlings, J.*, et al.* (2009). Ars2 links the nuclear cap-binding complex to RNA interference and cell proliferation. Cell *138*, 328-339.
Grun, D., Wang, Y.L., Langenberger, D., Gunsalus, K.C., and Rajewsky, N. (2005). microRNA target predictions across seven Drosophila species and comparison to mammalian targets. PLoS Comput Biol *1*, e13.
Gu, S., Jin, L., Zhang, F., Sarnow, P., and Kay, M.A. (2009). Biological basis for restriction of microRNA targets to the 3' untranslated region in mammalian mRNAs. Nat Struct Mol Biol *16*, 144-150.
Guidi, M., Muinos-Gimeno, M., Kagerbauer, B., Marti, E., Estivill, X., and Espinosa-Parrilla, Y. (2010). Overexpression of miR-128 specifically inhibits the truncated isoform of NTRK3 and upregulates BCL2 in SH-SY5Y neuroblastoma cells. BMC Mol Biol *11*, 95.
Guimbellot, J.S., Erickson, S.W., Mehta, T., Wen, H., Page, G.P., Sorscher, E.J., and Hong, J.S. (2009). Correlation of microRNA levels during hypoxia with predicted target mRNAs through genome-wide microarray analysis. BMC Med Genomics *2*, 15.
Gumireddy, K., Young, D.D., Xiong, X., Hogenesch, J.B., Huang, Q., and Deiters, A. (2008). Small-molecule inhibitors of microrna miR-21 function. Angew Chem Int Ed Engl *47*, 7482-7484.
Guo, H., Ingolia, N.T., Weissman, J.S., and Bartel, D.P. (2010). Mammalian microRNAs predominantly act to decrease target mRNA levels. Nature *466*, 835-840.
Haase, A.D., Jaskiewicz, L., Zhang, H., Laine, S., Sack, R., Gatignol, A., and Filipowicz, W. (2005). TRBP, a regulator of cellular PKR and HIV-1 virus expression, interacts with Dicer and functions in RNA silencing. EMBO Rep *6*, 961-967.
Hammond, S.M. (2006). MicroRNA therapeutics: a new niche for antisense nucleic acids. Trends Mol Med *12*, 99-101.
Han, J., Pedersen, J.S., Kwon, S.C., Belair, C.D., Kim, Y.K., Yeom, K.H., Yang, W.Y., Haussler, D., Blelloch, R., and Kim, V.N. (2009). Posttranscriptional crossregulation between Drosha and DGCR8. Cell *136*, 75-84.
Han, L., Witmer, P.D., Casey, E., Valle, D., and Sukumar, S. (2007). DNA methylation regulates MicroRNA expression. Cancer Biol Ther *6*, 1284-1288.
Hanahan, D., and Weinberg, R.A. (2011). Hallmarks of cancer: the next generation. Cell *144*, 646-674.
Hatley, M.E., Patrick, D.M., Garcia, M.R., Richardson, J.A., Bassel-Duby, R., van Rooij, E., and Olson, E.N. (2010). Modulation of K-Ras-dependent lung tumorigenesis by MicroRNA-21. Cancer Cell *18*, 282-293.

Hausler, S.F., Keller, A., Chandran, P.A., Ziegler, K., Zipp, K., Heuer, S., Krockenberger, M., Engel, J.B., Honig, A., Scheffler, M.*, et al.* (2010). Whole blood-derived miRNA profiles as potential new tools for ovarian cancer screening. Br J Cancer *103*, 693-700.

He, G., and Karin, M. (2011). NF-kappaB and STAT3 - key players in liver inflammation and cancer. Cell Res *21*, 159-168.

He, J., Zhang, J.F., Yi, C., Lv, Q., Xie, W.D., Li, J.N., Wan, G., Cui, K., Kung, H.F., Yang, J.*, et al.* (2010). miRNA-mediated functional changes through co-regulating function related genes. PLoS One *5*, e13558.

He, L., He, X., Lim, L.P., de Stanchina, E., Xuan, Z., Liang, Y., Xue, W., Zender, L., Magnus, J., Ridzon, D.*, et al.* (2007a). A microRNA component of the p53 tumour suppressor network. Nature *447*, 1130-1134.

He, L., He, X., Lowe, S.W., and Hannon, G.J. (2007b). microRNAs join the p53 network--another piece in the tumour-suppression puzzle. Nat Rev Cancer *7*, 819-822.

He, L., Thomson, J.M., Hemann, M.T., Hernando-Monge, E., Mu, D., Goodson, S., Powers, S., Cordon-Cardo, C., Lowe, S.W., Hannon, G.J.*, et al.* (2005). A microRNA polycistron as a potential human oncogene. Nature *435*, 828-833.

Heale, B.S., Keegan, L.P., McGurk, L., Michlewski, G., Brindle, J., Stanton, C.M., Caceres, J.F., and O'Connell, M.A. (2009). Editing independent effects of ADARs on the miRNA/siRNA pathways. EMBO J *28*, 3145-3156.

Henke, J.I., Goergen, D., Zheng, J., Song, Y., Schuttler, C.G., Fehr, C., Junemann, C., and Niepmann, M. (2008). microRNA-122 stimulates translation of hepatitis C virus RNA. EMBO J *27*, 3300-3310.

Heo, I., Joo, C., Cho, J., Ha, M., Han, J., and Kim, V.N. (2008). Lin28 mediates the terminal uridylation of let-7 precursor MicroRNA. Mol Cell *32*, 276-284.

Hevir, N., Sinkovec, J., and Rizner, T.L. (2011). Disturbed expression of phase I and phase II estrogen-metabolizing enzymes in endometrial cancer: lower levels of CYP1B1 and increased expression of S-COMT. Mol Cell Endocrinol *331*, 158-167.

Hon, L.S., and Zhang, Z. (2007). The roles of binding site arrangement and combinatorial targeting in microRNA repression of gene expression. Genome Biol *8*, R166.

Hu, H.Y., Yan, Z., Xu, Y., Hu, H., Menzel, C., Zhou, Y.H., Chen, W., and Khaitovich, P. (2009). Sequence features associated with microRNA strand selection in humans and flies. BMC Genomics *10*, 413.

Huang, T.H., Wu, F., Loeb, G.B., Hsu, R., Heidersbach, A., Brincat, A., Horiuchi, D., Lebbink, R.J., Mo, Y.Y., Goga, A.*, et al.* (2009). Up-regulation of miR-21 by HER2/neu signaling promotes cell invasion. J Biol Chem *284*, 18515-18524.

Huang, X., Gschweng, E., Van Handel, B., Cheng, D., Mikkola, H.K., and Witte, O.N. (2011). Regulated expression of microRNAs-126/126* inhibits erythropoiesis from human embryonic stem cells. Blood *117*, 2157-2165.

Huber, W., von Heydebreck, A., Sultmann, H., Poustka, A., and Vingron, M. (2002). Variance stabilization applied to microarray data calibration and to the quantification of differential expression. Bioinformatics *18 Suppl 1*, S96-104.

Hynes, N.E., and MacDonald, G. (2009). ErbB receptors and signaling pathways in cancer. Curr Opin Cell Biol *21*, 177-184.

Iorio, M.V., Visone, R., Di Leva, G., Donati, V., Petrocca, F., Casalini, P., Taccioli, C., Volinia, S., Liu, C.G., Alder, H.*, et al.* (2007). MicroRNA signatures in human ovarian cancer. Cancer Res *67*, 8699-8707.

Jemal, A., Siegel, R., Ward, E., Hao, Y., Xu, J., Murray, T., and Thun, M.J. (2008). Cancer statistics, 2008. CA Cancer J Clin *58*, 71-96.

Jiang, L., Liu, X., Chen, Z., Jin, Y., Heidbreder, C.E., Kolokythas, A., Wang, A., Dai, Y., and Zhou, X. (2010). MicroRNA-7 targets IGF1R (insulin-like growth factor 1 receptor) in tongue squamous cell carcinoma cells. Biochem J *432*, 199-205.

John, B., Enright, A.J., Aravin, A., Tuschl, T., Sander, C., and Marks, D.S. (2004). Human MicroRNA targets. PLoS Biol *2*, e363.

Jones, S., Zhang, X., Parsons, D.W., Lin, J.C., Leary, R.J., Angenendt, P., Mankoo, P., Carter, H., Kamiyama, H., Jimeno, A.*, et al.* (2008). Core signaling pathways in human pancreatic cancers revealed by global genomic analyses. Science *321*, 1801-1806.

Jopling, C.L., Yi, M., Lancaster, A.M., Lemon, S.M., and Sarnow, P. (2005). Modulation of hepatitis C virus RNA abundance by a liver-specific MicroRNA. Science *309*, 1577-1581.

Jung, M., Schaefer, A., Steiner, I., Kempkensteffen, C., Stephan, C., Erbersdobler, A., and Jung, K. (2010). Robust microRNA stability in degraded RNA preparations from human tissue and cell samples. Clin Chem *56*, 998-1006.

Karin, M., and Greten, F.R. (2005). NF-kappaB: linking inflammation and immunity to cancer development and progression. Nat Rev Immunol *5*, 749-759.

Katoh, T., Sakaguchi, Y., Miyauchi, K., Suzuki, T., Kashiwabara, S., and Baba, T. (2009). Selective stabilization of mammalian microRNAs by 3' adenylation mediated by the cytoplasmic poly(A) polymerase GLD-2. Genes Dev *23*, 433-438.

Kawahara, Y., Megraw, M., Kreider, E., Iizasa, H., Valente, L., Hatzigeorgiou, A.G., and Nishikura, K. (2008). Frequency and fate of microRNA editing in human brain. Nucleic Acids Res *36*, 5270-5280.

Kawahara, Y., Zinshteyn, B., Chendrimada, T.P., Shiekhattar, R., and Nishikura, K. (2007). RNA editing of the microRNA-151 precursor blocks cleavage by the Dicer-TRBP complex. EMBO Rep *8*, 763-769.

Kefas, B., Godlewski, J., Comeau, L., Li, Y., Abounader, R., Hawkinson, M., Lee, J., Fine, H., Chiocca, E.A., Lawler, S.*, et al.* (2008). microRNA-7 inhibits the epidermal growth factor receptor and the Akt pathway and is down-regulated in glioblastoma. Cancer Res *68*, 3566-3572.

Khan, A.A., Betel, D., Miller, M.L., Sander, C., Leslie, C.S., and Marks, D.S. (2009). Transfection of small RNAs globally perturbs gene regulation by endogenous microRNAs. Nat Biotechnol *27*, 549-555.

Khan, A.P., Poisson, L.M., Bhat, V.B., Fermin, D., Zhao, R., Kalyana-Sundaram, S., Michailidis, G., Nesvizhskii, A.I., Omenn, G.S., Chinnaiyan, A.M.*, et al.* (2010). Quantitative proteomic profiling of prostate cancer reveals a role for miR-128 in prostate cancer. Mol Cell Proteomics *9*, 298-312.

Kim, D.H., Saetrom, P., Snove, O., Jr., and Rossi, J.J. (2008). MicroRNA-directed transcriptional gene silencing in mammalian cells. Proc Natl Acad Sci U S A *105*, 16230-16235.

Kim, V.N., and Nam, J.W. (2006). Genomics of microRNA. Trends Genet *22*, 165-173.
Kiriakidou, M., Nelson, P.T., Kouranov, A., Fitziev, P., Bouyioukos, C., Mourelatos, Z., and Hatzigeorgiou, A. (2004). A combined computational-experimental approach predicts human microRNA targets. Genes Dev *18*, 1165-1178.
Kiriakidou, M., Tan, G.S., Lamprinaki, S., De Planell-Saguer, M., Nelson, P.T., and Mourelatos, Z. (2007). An mRNA m7G cap binding-like motif within human Ago2 represses translation. Cell *129*, 1141-1151.
Kluiver, J., van den Berg, A., de Jong, D., Blokzijl, T., Harms, G., Bouwman, E., Jacobs, S., Poppema, S., and Kroesen, B.J. (2007). Regulation of pri-microRNA BIC transcription and processing in Burkitt lymphoma. Oncogene *26*, 3769-3776.
Koppelstaetter, C., Jennings, P., Hochegger, K., Perco, P., Ischia, R., Karkoszka, H., and Mayer, G. (2005). Effect of tissue fixatives on telomere length determination by quantitative PCR. Mech Ageing Dev *126*, 1331-1333.
Kota, J., Chivukula, R.R., O'Donnell, K.A., Wentzel, E.A., Montgomery, C.L., Hwang, H.W., Chang, T.C., Vivekanandan, P., Torbenson, M., Clark, K.R.*, et al.* (2009). Therapeutic microRNA delivery suppresses tumorigenesis in a murine liver cancer model. Cell *137*, 1005-1017.
Krainer, A.R., Conway, G.C., and Kozak, D. (1990). Purification and characterization of pre-mRNA splicing factor SF2 from HeLa cells. Genes Dev *4*, 1158-1171.
Krek, A., Grun, D., Poy, M.N., Wolf, R., Rosenberg, L., Epstein, E.J., MacMenamin, P., da Piedade, I., Gunsalus, K.C., Stoffel, M.*, et al.* (2005). Combinatorial microRNA target predictions. Nat Genet *37*, 495-500.
Krol, J., Loedige, I., and Filipowicz, W. (2010). The widespread regulation of microRNA biogenesis, function and decay. Nat Rev Genet *11*, 597-610.
Krutovskikh, V.A., and Herceg, Z. (2010). Oncogenic microRNAs (OncomiRs) as a new class of cancer biomarkers. Bioessays *32*, 894-904.
Krutzfeldt, J., Rajewsky, N., Braich, R., Rajeev, K.G., Tuschl, T., Manoharan, M., and Stoffel, M. (2005). Silencing of microRNAs in vivo with 'antagomirs'. Nature *438*, 685-689.
Kuhn, D.E., Martin, M.M., Feldman, D.S., Terry, A.V., Jr., Nuovo, G.J., and Elton, T.S. (2008). Experimental validation of miRNA targets. Methods *44*, 47-54.
Lagos-Quintana, M., Rauhut, R., Lendeckel, W., and Tuschl, T. (2001). Identification of novel genes coding for small expressed RNAs. Science *294*, 853-858.
Laios, A., O'Toole, S., Flavin, R., Martin, C., Kelly, L., Ring, M., Finn, S.P., Barrett, C., Loda, M., Gleeson, N.*, et al.* (2008). Potential role of miR-9 and miR-223 in recurrent ovarian cancer. Mol Cancer *7*, 35.
Lal, A., Kim, H.H., Abdelmohsen, K., Kuwano, Y., Pullmann, R., Jr., Srikantan, S., Subrahmanyam, R., Martindale, J.L., Yang, X., Ahmed, F.*, et al.* (2008). p16(INK4a) translation suppressed by miR-24. PLoS ONE *3*, e1864.
Lall, S., Grun, D., Krek, A., Chen, K., Wang, Y.L., Dewey, C.N., Sood, P., Colombo, T., Bray, N., Macmenamin, P.*, et al.* (2006). A genome-wide map of conserved microRNA targets in C. elegans. Curr Biol *16*, 460-471.
Landthaler, M., Gaidatzis, D., Rothballer, A., Chen, P.Y., Soll, S.J., Dinic, L., Ojo, T., Hafner, M., Zavolan, M., and Tuschl, T. (2008). Molecular characterization of human Argonaute-containing ribonucleoprotein complexes and their bound target mRNAs. RNA *14*, 2580-2596.

Lau, N.C., Lim, L.P., Weinstein, E.G., and Bartel, D.P. (2001). An abundant class of tiny RNAs with probable regulatory roles in Caenorhabditis elegans. Science *294*, 858-862.

Lee, C.H., Subramanian, S., Beck, A.H., Espinosa, I., Senz, J., Zhu, S.X., Huntsman, D., van de Rijn, M., and Gilks, C.B. (2009). MicroRNA profiling of BRCA1/2 mutation-carrying and non-mutation-carrying high-grade serous carcinomas of ovary. PLoS ONE *4*, e7314.

Lee, R.C., and Ambros, V. (2001). An extensive class of small RNAs in Caenorhabditis elegans. Science *294*, 862-864.

Lee, R.C., Feinbaum, R.L., and Ambros, V. (1993). The C. elegans heterochronic gene lin-4 encodes small RNAs with antisense complementarity to lin-14. Cell *75*, 843-854.

Lee, Y., Kim, M., Han, J., Yeom, K.H., Lee, S., Baek, S.H., and Kim, V.N. (2004). MicroRNA genes are transcribed by RNA polymerase II. EMBO J *23*, 4051-4060.

Lee, Y.S., and Dutta, A. (2009). MicroRNAs in cancer. Annu Rev Pathol *4*, 199-227.

Lehrbach, N.J., Armisen, J., Lightfoot, H.L., Murfitt, K.J., Bugaut, A., Balasubramanian, S., and Miska, E.A. (2009). LIN-28 and the poly(U) polymerase PUP-2 regulate let-7 microRNA processing in Caenorhabditis elegans. Nat Struct Mol Biol *16*, 1016-1020.

Lewis, B.P., Burge, C.B., and Bartel, D.P. (2005). Conserved seed pairing, often flanked by adenosines, indicates that thousands of human genes are microRNA targets. Cell *120*, 15-20.

Li, S.D., Zhang, J.R., Wang, Y.Q., and Wan, X.P. (2010). The role of microRNAs in ovarian cancer initiation and progression. J Cell Mol Med *14*, 2240-2249.

Liang, Y., Ridzon, D., Wong, L., and Chen, C. (2007). Characterization of microRNA expression profiles in normal human tissues. BMC Genomics *8*, 166.

Lim, L.P., Lau, N.C., Garrett-Engele, P., Grimson, A., Schelter, J.M., Castle, J., Bartel, D.P., Linsley, P.S., and Johnson, J.M. (2005). Microarray analysis shows that some microRNAs downregulate large numbers of target mRNAs. Nature *433*, 769-773.

Liu, X.Q., Song, W.J., Sun, T.M., Zhang, P.Z., and Wang, J. (2011). Targeted delivery of antisense inhibitor of miRNA for antiangiogenesis therapy using cRGD-functionalized nanoparticles. Mol Pharm *8*, 250-259.

Lossos, I.S., Czerwinski, D.K., Alizadeh, A.A., Wechser, M.A., Tibshirani, R., Botstein, D., and Levy, R. (2004). Prediction of survival in diffuse large-B-cell lymphoma based on the expression of six genes. N Engl J Med *350*, 1828-1837.

Lu, J., Getz, G., Miska, E.A., Alvarez-Saavedra, E., Lamb, J., Peck, D., Sweet-Cordero, A., Ebert, B.L., Mak, R.H., Ferrando, A.A.*, et al.* (2005). MicroRNA expression profiles classify human cancers. Nature *435*, 834-838.

Lubling, Y., and Segal, E. Genomica. Available at http://genomica.weizmann.ac.il/. Accessed on July 7, 2010.

Majid, S., Dar, A.A., Saini, S., Yamamura, S., Hirata, H., Tanaka, Y., Deng, G., and Dahiya, R. (2010). MicroRNA-205-directed transcriptional activation of tumor suppressor genes in prostate cancer. Cancer *116*, 5637-5649.

Majumder, S. (2006). REST in good times and bad: roles in tumor suppressor and oncogenic activities. Cell Cycle *5*, 1929-1935.

Marks, P., Rifkind, R.A., Richon, V.M., Breslow, R., Miller, T., and Kelly, W.K. (2001). Histone deacetylases and cancer: causes and therapies. Nat Rev Cancer *1*, 194-202.

Maroney, P.A., Yu, Y., Fisher, J., and Nilsen, T.W. (2006). Evidence that microRNAs are associated with translating messenger RNAs in human cells. Nat Struct Mol Biol *13*, 1102-1107.

Martin, G., Schouest, K., Kovvuru, P., and Spillane, C. (2007). Prediction and validation of microRNA targets in animal genomes. J Biosci *32*, 1049-1052.

Mattick, J.S. (2007). A new paradigm for developmental biology. J Exp Biol *210*, 1526-1547.

McDonald, J.F. (in press). Cancer systems biology: current progress and future promise. Future Oncology.

Metias, S.M., Lianidou, E., and Yousef, G.M. (2009). MicroRNAs in clinical oncology: at the crossroads between promises and problems. J Clin Pathol *62*, 771-776.

Mezzanzanica, D., Bagnoli, M., De Cecco, L., Valeri, B., and Canevari, S. (2010). Role of microRNAs in ovarian cancer pathogenesis and potential clinical implications. Int J Biochem Cell Biol *42*, 1262-1272.

Micallef, J., Taccone, M., Mukherjee, J., Croul, S., Busby, J., Moran, M.F., and Guha, A. (2009). Epidermal growth factor receptor variant III-induced glioma invasion is mediated through myristoylated alanine-rich protein kinase C substrate overexpression. Cancer Res *69*, 7548-7556.

Michlewski, G., Guil, S., Semple, C.A., and Caceres, J.F. (2008). Posttranscriptional regulation of miRNAs harboring conserved terminal loops. Mol Cell *32*, 383-393.

Mieczkowski, J., Tyburczy, M.E., Dabrowski, M., and Pokarowski, P. (2010). Probeset filtering increases correlation between Affymetrix GeneChip and qRT-PCR expression measurements. BMC Bioinformatics *11*, 104.

Min, H., and Yoon, S. (2010). Got target? Computational methods for microRNA target prediction and their extension. Exp Mol Med *42*, 233-244.

Mishra, P.J., and Merlino, G. (2009). MicroRNA reexpression as differentiation therapy in cancer. J Clin Invest *119*, 2119-2123.

Mitchell, P.S., Parkin, R.K., Kroh, E.M., Fritz, B.R., Wyman, S.K., Pogosova-Agadjanyan, E.L., Peterson, A., Noteboom, J., O'Briant, K.C., Allen, A.*, et al.* (2008). Circulating microRNAs as stable blood-based markers for cancer detection. Proc Natl Acad Sci U S A *105*, 10513-10518.

Monteys, A.M., Spengler, R.M., Wan, J., Tecedor, L., Lennox, K.A., Xing, Y., and Davidson, B.L. (2010). Structure and activity of putative intronic miRNA promoters. RNA *16*, 495-505.

Moretti, F., Thermann, R., and Hentze, M.W. (2010). Mechanism of translational regulation by miR-2 from sites in the 5' untranslated region or the open reading frame. RNA *16*, 2493-2502.

Mott, J.L., Kurita, S., Cazanave, S.C., Bronk, S.F., Werneburg, N.W., and Fernandez-Zapico, M.E. (2010). Transcriptional suppression of mir-29b-1/mir-29a promoter by c-Myc, hedgehog, and NF-kappaB. J Cell Biochem *110*, 1155-1164.

Nam, E.J., Yoon, H., Kim, S.W., Kim, H., Kim, Y.T., Kim, J.H., Kim, J.W., and Kim, S. (2008). MicroRNA expression profiles in serous ovarian carcinoma. Clin Cancer Res *14*, 2690-2695.

Nam, S., Li, M., Choi, K., Balch, C., Kim, S., and Nephew, K.P. (2009). MicroRNA and mRNA integrated analysis (MMIA): a web tool for examining biological functions of microRNA expression. Nucleic Acids Res *37*, W356-362.

Naora, H. (2007). The heterogeneity of epithelial ovarian cancers: reconciling old and new paradigms. Expert Rev Mol Med *9*, 1-12.

Napoli, C., Lemieux, C., and Jorgensen, R. (1990). Introduction of a Chimeric Chalcone Synthase Gene into Petunia Results in Reversible Co-Suppression of Homologous Genes in trans. Plant Cell *2*, 279-289.

Newman, M.A., Thomson, J.M., and Hammond, S.M. (2008). Lin-28 interaction with the Let-7 precursor loop mediates regulated microRNA processing. RNA *14*, 1539-1549.

Normanno, N., De Luca, A., Bianco, C., Strizzi, L., Mancino, M., Maiello, M.R., Carotenuto, A., De Feo, G., Caponigro, F., and Salomon, D.S. (2006). Epidermal growth factor receptor (EGFR) signaling in cancer. Gene *366*, 2-16.

Nottrott, S., Simard, M.J., and Richter, J.D. (2006). Human let-7a miRNA blocks protein production on actively translating polyribosomes. Nat Struct Mol Biol *13*, 1108-1114.

O'Donnell, K.A., Wentzel, E.A., Zeller, K.I., Dang, C.V., and Mendell, J.T. (2005). c-Myc-regulated microRNAs modulate E2F1 expression. Nature *435*, 839-843.

Olsen, P.H., and Ambros, V. (1999). The lin-4 regulatory RNA controls developmental timing in Caenorhabditis elegans by blocking LIN-14 protein synthesis after the initiation of translation. Dev Biol *216*, 671-680.

Orgel, L.E., and Crick, F.H. (1980). Selfish DNA: the ultimate parasite. Nature *284*, 604-607.

Orom, U.A., Nielsen, F.C., and Lund, A.H. (2008). MicroRNA-10a binds the 5'UTR of ribosomal protein mRNAs and enhances their translation. Mol Cell *30*, 460-471.

Ozsolak, F., Poling, L.L., Wang, Z., Liu, H., Liu, X.S., Roeder, R.G., Zhang, X., Song, J.S., and Fisher, D.E. (2008). Chromatin structure analyses identify miRNA promoters. Genes Dev *22*, 3172-3183.

Pacifico, F., Crescenzi, E., Mellone, S., Iannetti, A., Porrino, N., Liguoro, D., Moscato, F., Grieco, M., Formisano, S., and Leonardi, A. (2010). Nuclear factor-{kappa}B contributes to anaplastic thyroid carcinomas through up-regulation of miR-146a. J Clin Endocrinol Metab *95*, 1421-1430.

Pardee, A.B. (2006). Regulatory molecular biology. Cell Cycle *5*, 846-852.

Parker, R., and Sheth, U. (2007). P bodies and the control of mRNA translation and degradation. Mol Cell *25*, 635-646.

Parsons, D.W., Jones, S., Zhang, X., Lin, J.C., Leary, R.J., Angenendt, P., Mankoo, P., Carter, H., Siu, I.M., Gallia, G.L.*, et al.* (2008). An integrated genomic analysis of human glioblastoma multiforme. Science *321*, 1807-1812.

Pasquinelli, A.E., Reinhart, B.J., Slack, F., Martindale, M.Q., Kuroda, M.I., Maller, B., Hayward, D.C., Ball, E.E., Degnan, B., Muller, P.*, et al.* (2000). Conservation of the sequence and temporal expression of let-7 heterochronic regulatory RNA. Nature *408*, 86-89.

Pattyn, F., Speleman, F., De Paepe, A., and Vandesompele, J. (2003). RTPrimerDB: the real-time PCR primer and probe database. Nucleic Acids Res *31*, 122-123.

Pawlicki, J.M., and Steitz, J.A. (2010). Nuclear networking fashions pre-messenger RNA and primary microRNA transcripts for function. Trends Cell Biol *20*, 52-61.
Peter, M.E. (2009). Let-7 and miR-200 microRNAs: guardians against pluripotency and cancer progression. Cell Cycle *8*, 843-852.
Petersen, C.P., Bordeleau, M.E., Pelletier, J., and Sharp, P.A. (2006). Short RNAs repress translation after initiation in mammalian cells. Mol Cell *21*, 533-542.
Pfaffl, M.W., Horgan, G.W., and Dempfle, L. (2002). Relative expression software tool (REST) for group-wise comparison and statistical analysis of relative expression results in real-time PCR. Nucleic Acids Res *30*, e36.
Phalon, C., Rao, D.D., and Nemunaitis, J. (2010). Potential use of RNA interference in cancer therapy. Expert Rev Mol Med *12*, e26.
Pillai, R.S., Bhattacharyya, S.N., and Filipowicz, W. (2007). Repression of protein synthesis by miRNAs: how many mechanisms? Trends Cell Biol *17*, 118-126.
Place, R.F., Li, L.C., Pookot, D., Noonan, E.J., and Dahiya, R. (2008). MicroRNA-373 induces expression of genes with complementary promoter sequences. Proc Natl Acad Sci U S A *105*, 1608-1613.
Rajewsky, N. (2006). microRNA target predictions in animals. Nat Genet *38 Suppl*, S8-13.
Raver-Shapira, N., Marciano, E., Meiri, E., Spector, Y., Rosenfeld, N., Moskovits, N., Bentwich, Z., and Oren, M. (2007). Transcriptional activation of miR-34a contributes to p53-mediated apoptosis. Mol Cell *26*, 731-743.
Razani, B., Zhang, X.L., Bitzer, M., von Gersdorff, G., Bottinger, E.P., and Lisanti, M.P. (2001). Caveolin-1 regulates transforming growth factor (TGF)-beta/SMAD signaling through an interaction with the TGF-beta type I receptor. J Biol Chem *276*, 6727-6738.
Rearick, D., Prakash, A., McSweeny, A., Shepard, S.S., Fedorova, L., and Fedorov, A. (2010). Critical association of ncRNA with introns. Nucleic Acids Res.
Reddy, S.D., Ohshiro, K., Rayala, S.K., and Kumar, R. (2008). MicroRNA-7, a homeobox D10 target, inhibits p21-activated kinase 1 and regulates its functions. Cancer Res *68*, 8195-8200.
Reinhart, B.J., Weinstein, E.G., Rhoades, M.W., Bartel, B., and Bartel, D.P. (2002). MicroRNAs in plants. Genes Dev *16*, 1616-1626.
Ritchie, W., Rajasekhar, M., Flamant, S., and Rasko, J.E. (2009). Conserved expression patterns predict microRNA targets. PLoS Comput Biol *5*, e1000513.
Rodriguez, A., Griffiths-Jones, S., Ashurst, J.L., and Bradley, A. (2004). Identification of mammalian microRNA host genes and transcription units. Genome Res *14*, 1902-1910.
Ruike, Y., Ichimura, A., Tsuchiya, S., Shimizu, K., Kunimoto, R., Okuno, Y., and Tsujimoto, G. (2008). Global correlation analysis for micro-RNA and mRNA expression profiles in human cell lines. J Hum Genet *53*, 515-523.
Sabin, L.R., Zhou, R., Gruber, J.J., Lukinova, N., Bambina, S., Berman, A., Lau, C.K., Thompson, C.B., and Cherry, S. (2009). Ars2 regulates both miRNA- and siRNA-dependent silencing and suppresses RNA virus infection in Drosophila. Cell *138*, 340-351.
Saini, H.K., Griffiths-Jones, S., and Enright, A.J. (2007). Genomic analysis of human microRNA transcripts. Proc Natl Acad Sci U S A *104*, 17719-17724.

Saito, T., and Saetrom, P. (2010). MicroRNAs--targeting and target prediction. N Biotechnol *27*, 243-249.
Sakamoto, S., Aoki, K., Higuchi, T., Todaka, H., Morisawa, K., Tamaki, N., Hatano, E., Fukushima, A., Taniguchi, T., and Agata, Y. (2009). The NF90-NF45 complex functions as a negative regulator in the microRNA processing pathway. Mol Cell Biol *29*, 3754-3769.
Sanford, J.R., Wang, X., Mort, M., Vanduyn, N., Cooper, D.N., Mooney, S.D., Edenberg, H.J., and Liu, Y. (2009). Splicing factor SFRS1 recognizes a functionally diverse landscape of RNA transcripts. Genome Res *19*, 381-394.
Saydam, O., Senol, O., Wurdinger, T., Mizrak, A., Ozdener, G.B., Stemmer-Rachamimov, A.O., Yi, M., Stephens, R.M., Krichevsky, A.M., Saydam, N.*, et al.* (2010). miRNA-7 Attenuation in Schwannoma Tumors Stimulates Growth by Upregulating Three Oncogenic Signaling Pathways. Cancer Res.
Scadden, A.D. (2005). The RISC subunit Tudor-SN binds to hyper-edited double-stranded RNA and promotes its cleavage. Nat Struct Mol Biol *12*, 489-496.
Schaar, D.G., Medina, D.J., Moore, D.F., Strair, R.K., and Ting, Y. (2009). miR-320 targets transferrin receptor 1 (CD71) and inhibits cell proliferation. Exp Hematol *37*, 245-255.
Scully, R.E., Clement, P.B., and Young, R.H. (2004). Ovarian Surface Epithelial-Stromal Tumors, 4th edn (Philadelphia, PA, Lippincott Williams and Wilkins).
Selbach, M., Schwanhausser, B., Thierfelder, N., Fang, Z., Khanin, R., and Rajewsky, N. (2008). Widespread changes in protein synthesis induced by microRNAs. Nature *455*, 58-63.
Seo, C.H., Kim, J.R., Kim, M.S., and Cho, K.H. (2009). Hub genes with positive feedbacks function as master switches in developmental gene regulatory networks. Bioinformatics *25*, 1898-1904.
Sethupathy, P., Megraw, M., and Hatzigeorgiou, A.G. (2006). A guide through present computational approaches for the identification of mammalian microRNA targets. Nat Methods *3*, 881-886.
Shabalina, S.A., and Koonin, E.V. (2008). Origins and evolution of eukaryotic RNA interference. Trends Ecol Evol *23*, 578-587.
Shalgi, R., Brosh, R., Oren, M., Pilpel, Y., and Rotter, V. (2009). Coupling transcriptional and post-transcriptional miRNA regulation in the control of cell fate. Aging (Albany NY) *1*, 762-770.
Shalgi, R., Lieber, D., Oren, M., and Pilpel, Y. (2007). Global and local architecture of the mammalian microRNA-transcription factor regulatory network. PLoS Comput Biol *3*, e131.
Shibata, M., Nakao, H., Kiyonari, H., Abe, T., and Aizawa, S. (2011). MicroRNA-9 regulates neurogenesis in mouse telencephalon by targeting multiple transcription factors. J Neurosci *31*, 3407-3422.
Silber, J., Lim, D.A., Petritsch, C., Persson, A.I., Maunakea, A.K., Yu, M., Vandenberg, S.R., Ginzinger, D.G., James, C.D., Costello, J.F.*, et al.* (2008). miR-124 and miR-137 inhibit proliferation of glioblastoma multiforme cells and induce differentiation of brain tumor stem cells. BMC Med *6*, 14.
Small, E.M., Frost, R.J., and Olson, E.N. (2010). MicroRNAs add a new dimension to cardiovascular disease. Circulation *121*, 1022-1032.

Somervaille, T.C., and Cleary, M.L. (2006). PU.1 and Junb: suppressing the formation of acute myeloid leukemia stem cells. Cancer Cell *10*, 456-457.

Sood, P., Krek, A., Zavolan, M., Macino, G., and Rajewsky, N. (2006). Cell-type-specific signatures of microRNAs on target mRNA expression. Proc Natl Acad Sci U S A *103*, 2746-2751.

Sorrentino, A., Liu, C.G., Addario, A., Peschle, C., Scambia, G., and Ferlini, C. (2008). Role of microRNAs in drug-resistant ovarian cancer cells. Gynecol Oncol *111*, 478-486.

Stark, A., Lin, M.F., Kheradpour, P., Pedersen, J.S., Parts, L., Carlson, J.W., Crosby, M.A., Rasmussen, M.D., Roy, S., Deoras, A.N*., et al.* (2007). Discovery of functional elements in 12 Drosophila genomes using evolutionary signatures. Nature *450*, 219-232.

Surveillance, Epidemiology, and End Results (SEER) Program (www.seer.cancer.gov) Research Data (1973-2007), National Cancer Institute, DCCPS, Surveillance Research Program, Cancer Statistics Branch, released April 2010, based on the November 2009 submission.

Tang, F., Hajkova, P., O'Carroll, D., Lee, C., Tarakhovsky, A., Lao, K., and Surani, M.A. (2008a). MicroRNAs are tightly associated with RNA-induced gene silencing complexes in vivo. Biochem Biophys Res Commun *372*, 24-29.

Tang, G., Tang, X., Mendu, V., Jia, X., Chen, Q.J., and He, L. (2008b). The art of microRNA: various strategies leading to gene silencing via an ancient pathway. Biochim Biophys Acta *1779*, 655-662.

Tang, R., and Zen, K. (2011). Gold glitters everywhere: nucleus microRNAs and their functions. Frontiers in Biology *6*, 69-75.

Tavazoie, S.F., Alarcon, C., Oskarsson, T., Padua, D., Wang, Q., Bos, P.D., Gerald, W.L., and Massague, J. (2008). Endogenous human microRNAs that suppress breast cancer metastasis. Nature *451*, 147-152.

Tay, Y., Zhang, J., Thomson, A.M., Lim, B., and Rigoutsos, I. (2008). MicroRNAs to Nanog, Oct4 and Sox2 coding regions modulate embryonic stem cell differentiation. Nature *455*, 1124-1128.

Thaker, P.H., Yazici, S., Nilsson, M.B., Yokoi, K., Tsan, R.Z., He, J., Kim, S.J., Fidler, I.J., and Sood, A.K. (2005). Antivascular therapy for orthotopic human ovarian carcinoma through blockade of the vascular endothelial growth factor and epidermal growth factor receptors. Clin Cancer Res *11*, 4923-4933.

Thomas, M., Lieberman, J., and Lal, A. (2010). Desperately seeking microRNA targets. Nat Struct Mol Biol *17*, 1169-1174.

Tong, A.W., and Nemunaitis, J. (2008). Modulation of miRNA activity in human cancer: a new paradigm for cancer gene therapy? Cancer Gene Ther *15*, 341-355.

Trabucchi, M., Briata, P., Garcia-Mayoral, M., Haase, A.D., Filipowicz, W., Ramos, A., Gherzi, R., and Rosenfeld, M.G. (2009). The RNA-binding protein KSRP promotes the biogenesis of a subset of microRNAs. Nature *459*, 1010-1014.

Trang, P., Wiggins, J.F., Daige, C.L., Cho, C., Omotola, M., Brown, D., Weidhaas, J.B., Bader, A.G., and Slack, F.J. (2011). Systemic Delivery of Tumor Suppressor microRNA Mimics Using a Neutral Lipid Emulsion Inhibits Lung Tumors in Mice. Mol Ther.

Tritschler, F., Huntzinger, E., and Izaurralde, E. (2010). Role of GW182 proteins and PABPC1 in the miRNA pathway: a sense of deja vu. Nat Rev Mol Cell Biol *11*, 379-384.

Tsai, N.P., Lin, Y.L., and Wei, L.N. (2009). MicroRNA mir-346 targets the 5'-untranslated region of receptor-interacting protein 140 (RIP140) mRNA and up-regulates its protein expression. Biochem J *424*, 411-418.

Tsuda, N., Ishiyama, S., Li, Y., Ioannides, C.G., Abbruzzese, J.L., and Chang, D.Z. (2006). Synthetic microRNA designed to target glioma-associated antigen 1 transcription factor inhibits division and induces late apoptosis in pancreatic tumor cells. Clin Cancer Res *12*, 6557-6564.

Tusher, V.G., Tibshirani, R., and Chu, G. (2001). Significance analysis of microarrays applied to the ionizing radiation response. Proc Natl Acad Sci U S A *98*, 5116-5121.

Valencia-Sanchez, M.A., Liu, J., Hannon, G.J., and Parker, R. (2006). Control of translation and mRNA degradation by miRNAs and siRNAs. Genes Dev *20*, 515-524.

van Jaarsveld, M.T., Helleman, J., Berns, E.M., and Wiemer, E.A. (2010). MicroRNAs in ovarian cancer biology and therapy resistance. Int J Biochem Cell Biol *42*, 1282-1290.

Vasudevan, S., Tong, Y., and Steitz, J.A. (2007). Switching from repression to activation: microRNAs can up-regulate translation. Science *318*, 1931-1934.

Veerla, S., Lindgren, D., Kvist, A., Frigyesi, A., Staaf, J., Persson, H., Liedberg, F., Chebil, G., Gudjonsson, S., Borg, A.*, et al.* (2009). MiRNA expression in urothelial carcinomas: important roles of miR-10a, miR-222, miR-125b, miR-7 and miR-452 for tumor stage and metastasis, and frequent homozygous losses of miR-31. Int J Cancer *124*, 2236-2242.

Ventura, A., and Jacks, T. (2009). MicroRNAs and cancer: short RNAs go a long way. Cell *136*, 586-591.

Visone, R., and Croce, C.M. (2009). MiRNAs and cancer. Am J Pathol *174*, 1131-1138.

Viswanathan, S.R., Daley, G.Q., and Gregory, R.I. (2008). Selective blockade of microRNA processing by Lin28. Science *320*, 97-100.

Volinia, S., Galasso, M., Costinean, S., Tagliavini, L., Gamberoni, G., Drusco, A., Marchesini, J., Mascellani, N., Sana, M.E., Abu Jarour, R.*, et al.* (2010). Reprogramming of miRNA networks in cancer and leukemia. Genome Res *20*, 589-599.

Wahid, F., Shehzad, A., Khan, T., and Kim, Y.Y. (2010). MicroRNAs: synthesis, mechanism, function, and recent clinical trials. Biochim Biophys Acta *1803*, 1231-1243.

Wakiyama, M., Takimoto, K., Ohara, O., and Yokoyama, S. (2007). Let-7 microRNA-mediated mRNA deadenylation and translational repression in a mammalian cell-free system. Genes Dev *21*, 1857-1862.

Wang, B., Majumder, S., Nuovo, G., Kutay, H., Volinia, S., Patel, T., Schmittgen, T.D., Croce, C., Ghoshal, K., and Jacob, S.T. (2009). Role of microRNA-155 at early stages of hepatocarcinogenesis induced by choline-deficient and amino acid-defined diet in C57BL/6 mice. Hepatology *50*, 1152-1161.

Wang, B., Yanez, A., and Novina, C.D. (2008). MicroRNA-repressed mRNAs contain 40S but not 60S components. Proc Natl Acad Sci U S A *105*, 5343-5348.
Wang, B.D., Kline, C.L., Pastor, D.M., Olson, T.L., Frank, B., Luu, T., Sharma, A.K., Robertson, G., Weirauch, M.T., Patierno, S.R.*, et al.* (2010). Prostate apoptosis response protein 4 sensitizes human colon cancer cells to chemotherapeutic 5-FU through mediation of an NF kappaB and microRNA network. Mol Cancer *9*, 98.
Wang, E., Lenferink, A., and O'Connor-McCourt, M. (2007). Cancer systems biology: exploring cancer-associated genes on cellular networks. Cell Mol Life Sci *64*, 1752-1762.
Wang, Y.P., and Li, K.B. (2009). Correlation of expression profiles between microRNAs and mRNA targets using NCI-60 data. BMC Genomics *10*, 218.
Webster, R.J., Giles, K.M., Price, K.J., Zhang, P.M., Mattick, J.S., and Leedman, P.J. (2009). Regulation of epidermal growth factor receptor signaling in human cancer cells by microRNA-7. J Biol Chem *284*, 5731-5741.
Weiss, G.J., Bemis, L.T., Nakajima, E., Sugita, M., Birks, D.K., Robinson, W.A., Varella-Garcia, M., Bunn, P.A., Jr., Haney, J., Helfrich, B.A.*, et al.* (2008). EGFR regulation by microRNA in lung cancer: correlation with clinical response and survival to gefitinib and EGFR expression in cell lines. Ann Oncol *19*, 1053-1059.
Wiemer, E.A. (2007). The role of microRNAs in cancer: no small matter. Eur J Cancer *43*, 1529-1544.
Wightman, B., Ha, I., and Ruvkun, G. (1993). Posttranscriptional regulation of the heterochronic gene lin-14 by lin-4 mediates temporal pattern formation in C. elegans. Cell *75*, 855-862.
Williams, T.M., and Lisanti, M.P. (2005). Caveolin-1 in oncogenic transformation, cancer, and metastasis. Am J Physiol Cell Physiol *288*, C494-506.
Wilson, J.A., Zhang, C., Huys, A., and Richardson, C.D. (2011). Human Ago2 is required for efficient microRNA 122 regulation of hepatitis C virus RNA accumulation and translation. J Virol *85*, 2342-2350.
Wu, H., Sun, S., Tu, K., Gao, Y., Xie, B., Krainer, A.R., and Zhu, J. (2010a). A splicing-independent function of SF2/ASF in microRNA processing. Mol Cell *38*, 67-77.
Wu, S., Huang, S., Ding, J., Zhao, Y., Liang, L., Liu, T., Zhan, R., and He, X. (2010b). Multiple microRNAs modulate p21Cip1/Waf1 expression by directly targeting its 3' untranslated region. Oncogene *29*, 2302-2308.
Wyman, S.K., Parkin, R.K., Mitchell, P.S., Fritz, B.R., O'Briant, K., Godwin, A.K., Urban, N., Drescher, C.W., Knudsen, B.S., and Tewari, M. (2009). Repertoire of microRNAs in epithelial ovarian cancer as determined by next generation sequencing of small RNA cDNA libraries. PLoS ONE *4*, e5311.
Xiao, J., Yang, B., Lin, H., Lu, Y., Luo, X., and Wang, Z. (2007). Novel approaches for gene-specific interference via manipulating actions of microRNAs: examination on the pacemaker channel genes HCN2 and HCN4. J Cell Physiol *212*, 285-292.
Xie, X., Lu, J., Kulbokas, E.J., Golub, T.R., Mootha, V., Lindblad-Toh, K., Lander, E.S., and Kellis, M. (2005). Systematic discovery of regulatory motifs in human promoters and 3' UTRs by comparison of several mammals. Nature *434*, 338-345.
Xin, F., Li, M., Balch, C., Thomson, M., Fan, M., Liu, Y., Hammond, S.M., Kim, S., and Nephew, K.P. (2009). Computational analysis of microRNA profiles and their

target genes suggests significant involvement in breast cancer antiestrogen resistance. Bioinformatics *25*, 430-434.

Xu, J., Li, C.X., Li, Y.S., Lv, J.Y., Ma, Y., Shao, T.T., Xu, L.D., Wang, Y.Y., Du, L., Zhang, Y.P.*, et al.* (2011). MiRNA-miRNA synergistic network: construction via co-regulating functional modules and disease miRNA topological features. Nucleic Acids Res *39*, 825-836.

Yamagata, K., Fujiyama, S., Ito, S., Ueda, T., Murata, T., Naitou, M., Takeyama, K., Minami, Y., O'Malley, B.W., and Kato, S. (2009). Maturation of microRNA is hormonally regulated by a nuclear receptor. Mol Cell *36*, 340-347.

Yang, H., Kong, W., He, L., Zhao, J.J., O'Donnell, J.D., Wang, J., Wenham, R.M., Coppola, D., Kruk, P.A., Nicosia, S.V.*, et al.* (2008). MicroRNA expression profiling in human ovarian cancer: miR-214 induces cell survival and cisplatin resistance by targeting PTEN. Cancer Res *68*, 425-433.

Yang, J., and Weinberg, R.A. (2008). Epithelial-mesenchymal transition: at the crossroads of development and tumor metastasis. Dev Cell *14*, 818-829.

Yang, J.S., Phillips, M.D., Betel, D., Mu, P., Ventura, A., Siepel, A.C., Chen, K.C., and Lai, E.C. (2011). Widespread regulatory activity of vertebrate microRNA* species. RNA *17*, 312-326.

Ye, W., Lv, Q., Wong, C.K., Hu, S., Fu, C., Hua, Z., Cai, G., Li, G., Yang, B.B., and Zhang, Y. (2008). The effect of central loops in miRNA:MRE duplexes on the efficiency of miRNA-mediated gene regulation. PLoS ONE *3*, e1719.

Yi, R., Qin, Y., Macara, I.G., and Cullen, B.R. (2003). Exportin-5 mediates the nuclear export of pre-microRNAs and short hairpin RNAs. Genes Dev *17*, 3011-3016.

Yu, B., Bi, L., Zheng, B., Ji, L., Chevalier, D., Agarwal, M., Ramachandran, V., Li, W., Lagrange, T., Walker, J.C.*, et al.* (2008). The FHA domain proteins DAWDLE in Arabidopsis and SNIP1 in humans act in small RNA biogenesis. Proc Natl Acad Sci U S A *105*, 10073-10078.

Zeineldin, R., Muller, C.Y., Stack, M.S., and Hudson, L.G. (2010). Targeting the EGF receptor for ovarian cancer therapy. J Oncol *2010*, 414676.

Zhang, C., Wang, C., Chen, X., Yang, C., Li, K., Wang, J., Dai, J., Hu, Z., Zhou, X., Chen, L.*, et al.* (2010). Expression profile of microRNAs in serum: a fingerprint for esophageal squamous cell carcinoma. Clin Chem *56*, 1871-1879.

Zhang, L., Huang, J., Yang, N., Greshock, J., Megraw, M.S., Giannakakis, A., Liang, S., Naylor, T.L., Barchetti, A., Ward, M.R.*, et al.* (2006). microRNAs exhibit high frequency genomic alterations in human cancer. Proc Natl Acad Sci U S A *103*, 9136-9141.

Zhang, L., Volinia, S., Bonome, T., Calin, G.A., Greshock, J., Yang, N., Liu, C.G., Giannakakis, A., Alexiou, P., Hasegawa, K.*, et al.* (2008). Genomic and epigenetic alterations deregulate microRNA expression in human epithelial ovarian cancer. Proc Natl Acad Sci U S A *105*, 7004-7009.

Zhang, Y., Chao, T., Li, R., Liu, W., Chen, Y., Yan, X., Gong, Y., Yin, B., Qiang, B., Zhao, J.*, et al.* (2009). MicroRNA-128 inhibits glioma cells proliferation by targeting transcription factor E2F3a. J Mol Med *87*, 43-51.

Zhao, H., Shen, J., Medico, L., Wang, D., Ambrosone, C.B., and Liu, S. (2010). A pilot study of circulating miRNAs as potential biomarkers of early stage breast cancer. PLoS ONE *5*, e13735.

Zhao, T., Li, G., Mi, S., Li, S., Hannon, G.J., Wang, X.J., and Qi, Y. (2007). A complex system of small RNAs in the unicellular green alga Chlamydomonas reinhardtii. Genes Dev *21*, 1190-1203.

Zhou, R., Hu, G., Liu, J., Gong, A.Y., Drescher, K.M., and Chen, X.M. (2009). NF-kappaB p65-dependent transactivation of miRNA genes following Cryptosporidium parvum infection stimulates epithelial cell immune responses. PLoS Pathog *5*, e1000681.

Zhou, X., Ruan, J., Wang, G., and Zhang, W. (2007). Characterization and identification of microRNA core promoters in four model species. PLoS Comput Biol *3*, e37.

Zhou, Z., Licklider, L.J., Gygi, S.P., and Reed, R. (2002). Comprehensive proteomic analysis of the human spliceosome. Nature *419*, 182-185.

Zorn, K.K., Jazaeri, A.A., Awtrey, C.S., Gardner, G.J., Mok, S.C., Boyd, J., and Birrer, M.J. (2003). Choice of normal ovarian control influences determination of differentially expressed genes in ovarian cancer expression profiling studies. Clin Cancer Res *9*, 4811-4818.